“Open Quantum Systems Beyond the Markovian Regime”

by

Gerardo Suárez

Submitted in Partial Fulfillment of the Requirements for the Degree
Doctor of Philosophy, in Physics
Advisor:
Prof. dr hab. Michał Horodecki

December 1, 2025

Abstract

The dynamics of a quantum system that is not isolated are generally hard to obtain, either numerically or analytically. Usually, many approximations need to be employed. The most popular set of approximations leads to what is known as the Gorini-Kossakowski-Lindblad-Sudarshan (GKLS) equation, a Markovian master equation that is the cornerstone of open quantum systems theory. It is the most popular method despite of its known limitations, it is not a good approximation of transient dynamics, and if the coupling is not weak enough, it does not describe the steady state correctly either. Other popular methods are numerically exact, however, they rely on enlarging the Hilbert space of the system, which makes the simulation unfeasible for many-body systems.

In this thesis, we provide an overview of the most common techniques to simulate open systems beyond the Markovian regime, with special emphasis on Non-Markovian master equations such as the cumulant equation and the time-convolutionless equation. We provide a novel way to simulate them faster by approximating the environment in a way analogous to that used in numerically exact techniques. We show the potential of these equations and their superiority to the GKLS equation in several examples, showing that Non-Markovian equations are needed for a good description of finite-time thermodynamics.

Keywords: Open Quantum systems, Non-Markovianity, HEOM, Pseudomodes, Heat Transport

Abstrakt

Dynamika układu kwantowego, który nie jest izolowany, jest zwykle trudna do uzyskania, zarówno numerycznie, jak i analitycznie. Zazwyczaj wymaga zastosowania wielu przybliżeń. Najpopularniejszy zestaw przybliżeń prowadzi do tak zwanego równania Goriniego-Kossakowskiego-Lindblada-Sudarshana (GKLS), markowskiego równania mistrza, które jest kamieniem węgielnym teorii otwartych układów kwantowych. Ograniczenia tej popularnej metody są znane: nie przybliża dobrze dynamiki przejściowej, a jeśli sprzężenie nie jest wystarczająco słabe, nie opisuje prawidłowo również stanu stacjonarnego. Inne popularne metody są numerycznie dokładne, jednak opierają się na powiększaniu przestrzeni Hilberta układu, co czyni symulację niewykonalną dla układów wielociałowych.

W niniejszej pracy przedstawiamy przegląd najczęściej stosowanych technik symulacji układów otwartych poza reżimem markowskim, ze szczególnym naciskiem na niemarkowskie równania mistrza, takie jak równanie kumulantowe i równanie bez konwolucji czasowej. Przedstawiamy nową metodę ich szybszej symulacji poprzez przybliżenie otoczenia w sposób analogiczny do tego stosowanego w technikach numerycznie dokładnych. Pokazujemy potencjał tych równań i ich wyższość nad równaniem GKLS na kilku przykładach, dowodząc, że niemarkowskie równania są niezbędne do dobrego opisu termodynamiki w skończonym czasie.

Słowa kluczowe: Otwarte układy kwantowe, Niemarkowskość, HEOM, Pseudomody, Transport ciepła

Acknowledgements

No list does justice to the people who have helped me in my journey. First of all I would like to thank my parents, whose love and support made me the person I am today. Next I would like to thank Alfredo Mejia who was the person who helped me the most to pursue science at a hard point in my life, without his support and advice, I would not be here today. I would also like to thank Karina Castillo, my life partner during this journey and my best friend.

Thanks to Neill Lambert for allowing me to contribute to QuTiP and for his mentoring and support. Thanks to Paul Menczel for his mentoring and patience when reviewing my code and to Franco Nori for hosting me in RIKEN, the visits to his group are unforgettable memories where I got new skills, and made important connections. I would also like to thank all my colleagues and collaborators.

I would like to thank all of the administrative staff in UG and ICTQT, their support made my life easier all of these years, special thanks to Ewa Kaszewska, even though she was always busy, she always made time to help PhD students with a smile on her face. Last but not least I would like to thank my PhD advisor Michal Horodecki, who is not only a great scientist but a great mentor, the kind that lets you pursue your ideas and is willing to sacrifice his time even on weekends or midnights to make sure he can help you achieve your goals, his comprehension, and friendliness made my PhD journey a lot easier.

Contents

Gdansk
May 2025

Gerardo Suarez
gerardo.suarez@phdstud.edu.ug.pl

List of Publications

The thesis is related to the following works

1. Neill Lambert, Eric Giguère, Paul Menczel, Boxi Li, Patrick Hopf, **Gerardo Suárez**, Marc Gali, Jake Lishman, Rushiraj Gadhvi, Rochisha Agarwal, Asier Galicia, Nathan Shammah, Paul Nation, J.R. Johansson, Shahnawaz Ahmed, Simon Cross, Alexander Pitchford, and Franco Nori. "QuTiP 5: The Quantum Toolbox in Python". In: *Physics Reports* 1153 (2026), pp. 1–62. ISSN: 0370-1573. DOI: https://doi.org/10.1016/j.physrep.2025.10.001

2. Marcin Łobejko, Marek Winczewski, **Suárez, Gerardo**, Robert Alicki, and Michał Horodecki. "Corrections to the Hamiltonian induced by finite-strength coupling to the environment". In: *Phys. Rev. E* 110 (1 2024), p. 014144. DOI: 10.1103/PhysRevE.110.014144

3. **Suárez, Gerardo**, Marcin Łobejko, and Michał Horodecki. "Dynamics of the nonequilibrium spin-boson model: A benchmark of master equations and their validity". In: *Phys. Rev. A* 110 (4 2024), p. 042428. DOI: 10.1103/PhysRevA.110.042428

4. Marek Winczewski, Antonio Mandarino, **Suárez, Gerardo**, Robert Alicki, and Michał Horodecki. "Intermediate-times dilemma for open quantum system: Filtered approximation to the refined weak-coupling limit". In: *Phys. Rev. E* 110 (2 2024), p. 024110. DOI: 10.1103/PhysRevE.110.024110

5. **Suárez, Gerardo** and Michał Horodecki. *Making Non-Markovian master equations accessible with approximate environments*. 2025. arXiv: 2506.22346 [quant-ph]

The following works were produced during the PhD but are not directly related to the thesis

1. Robert Alicki, Michał Horodecki, Alejandro Jenkins, Marcin Łobejko, and **Suárez, Gerardo**. "The Josephson junction as a quantum engine". en. In: *New J. Phys.* 25.11 (2023). Publisher: IOP Publishing, p. 113013. ISSN: 1367-2630. DOI: 10.1088/1367-2630/ad06d8

2. R. R. Rodríguez, B. Ahmadi, **Suárez, G.**, P. Mazurek, S. Barzanjeh, and P. Horodecki. "Optimal quantum control of charging quantum batteries". en. In: *New J. Phys.* 26.4 (2024). Publisher: IOP Publishing, p. 043004. ISSN: 1367-2630. DOI: 10.1088/1367-2630/ad3843

Introduction

This thesis consists of two parts, the first part is an overview of methods to model open quantum systems beyond the Markovian regime. While the material there is not an original contribution, the way it is presented is, since these methods are rarely in the same notation, much less in the same document, different conventions differ by the definition of spectral densities and Fourier transform normalization. This makes comparison among different methods complicated, as the final formulas do not usually indicate what convention is used, and a coupling constant that corresponds to the weak coupling limit in one convention may be moderate or strong in another. This part is basically a review on recent developments in the field, clarifying a few key points that make some methods that are closely related (pseudomodes, dampf, pseudolindblad, mesoscopic leads) appear different. It provides the reader with a clear picture of how they differ, their limitations, and when to use one or another. Part of this review is based on work done for QuTiP.

Neill Lambert, Eric Giguère, Paul Menczel, Boxi Li, Patrick Hopf, **Gerardo Suárez**, Marc Gali, Jake Lishman, Rushiraj Gadhvi, Rochisha Agarwal, Asier Galicia, Nathan Shammah, Paul Nation, J.R. Johansson, Shahnawaz Ahmed, Simon Cross, Alexander Pitchford, and Franco Nori. "QuTiP 5: The Quantum Toolbox in Python". In: *Physics Reports* 1153 (2026), pp. 1–62. ISSN: 0370-1573. DOI: https://doi.org/10.1016/j.physrep.2025.10.001

The second part of the thesis consists of original contributions by the author and collaborators. These contributions can be subdivided into two. The first subpart addresses the steady state of open quantum systems beyond the weak coupling regime. It builds on the work published as

Marcin Łobejko, Marek Winczewski, **Suárez, Gerardo**, Robert Alicki, and Michał Horodecki. "Corrections to the Hamiltonian induced by finite-strength coupling to the environment". In: *Phys. Rev. E* 110 (1 2024), p. 014144. DOI: 10.1103/PhysRevE.110.014144

We explain how the perturbative approach in that work can be misleading, as well as how to deal with the deviations from the steady state in practice and we'll deviate a little from the content in that paper to include a discussion as to whether or not these deviations are relevant in heat transport scenarios, and their connection to the ongoing local vs global debate in open quantum systems.

The second subpart consists of comparisons of the different methods to model open quantum systems, focusing on their advantages and disadvantages. This section also includes our recently proposed approach to accelerate Non-Markoviann descriptions in a way that makes them more similar to GKLS equations. We hope this makes their usage widespread as it allows for significantly faster simulations, especially when the number of jump operators is not too high, or a GPU is used. The theory was included in part one to keep the narrative. In this part, we show its usefulness by studying original examples, using Redfield, HEOM, Cumulant, and the other descriptions beyond GKLS descriptions, emphasizing how they differ from the typ-

ical description, and whether going beyond the standard open quantum systems description is relevant in these examples. Here we will also argue for the inclusion of Lamb-shift and the necessity of using Non-Markovian equations when dealing with properties that depend on the dynamics generator such as heat and work. This part is based on

Suárez, Gerardo, Marcin Łobejko, and Michał Horodecki. "Dynamics of the nonequilibrium spin-boson model: A benchmark of master equations and their validity". In: *Phys. Rev. A* 110 (4 2024), p. 042428. DOI: 10.1103/PhysRevA.110.042428

Marek Winczewski, Antonio Mandarino, **Suárez, Gerardo**, Robert Alicki, and Michał Horodecki. "Intermediate-times dilemma for open quantum system: Filtered approximation to the refined weak-coupling limit". In: *Phys. Rev. E* 110 (2 2024), p. 024110. DOI: 10.1103/PhysRevE.110.024110

Suárez, Gerardo and Michał Horodecki. *Making Non-Markovian master equations accessible with approximate environments*. 2025. arXiv: 2506.22346 [quant-ph]

and works in preparation.

Part I

Preliminaries

Chapter 1

The Free Correlation Function

The free correlation function or two time correlation function is the most important quantity in open quantum systems. The interaction with the environment is completely determined by the two time free correlation function of the environment and its temperature for Gaussian environments with linear coupling (instead of the free correlation function, one may equivalently use the power spectrum or spectral density). Typically, dealing with the full dynamics of the open system is too complex, so often approximations are employed to facilitate it. In this thesis, we will often approximate the free correlation function with damped sinusoidals in a Fourier-like expansion [1], which makes the dynamics tractable.

In this section, we will review the definitions of correlation function and power spectrum for both Bosonic and Fermionic systems. Then we will discuss how to approximate them as a sum of damped sinusoids. We will give a brief overview of some of the modern techniques to do so, and finally, we will compare the different approximation techniques and provide brief advice about when to use them.

1.1 The Bath's two time Free Correlation Function

A key quantity in characterizing the environment in an open quantum system setup is the **free** evolution of the two time correlation function, which we will call $C(t)$. Here we will only discuss the correlation function of environments in a thermal state, meaning that the environment is in the canonical equilibrium state (usually called Gibbs' state)

$$\rho_B = \frac{e^{-\beta H_B}}{Z}, \tag{1.1}$$

where Z is the partition function, which is just the normalization factor of the state and $\beta = \frac{1}{T}$ is the inverse temperature. We have set the Boltzmann constant $k_B = 1$. Notice that this state does not evolve due to the free evolution of the environment $U_B = e^{iH_B t}$, because $[U_B, \rho_B] = 0$

$$\rho_B = \frac{e^{-\beta H_B}}{Z} = U_B(t)\frac{e^{-\beta H_B}}{Z}U_B^\dagger(t). \tag{1.2}$$

The two time correlation of operators in this state are given by

$$C(t,t') = \mathrm{Tr}\Big[A(t)B(t')\rho_B\Big]. \tag{1.3}$$

[1] Though other expansions are possible, for example in terms of Bessel functions [2, 3]

where A and B are just two operators. Notice that this can be rewritten as

$$\begin{aligned} C(t,t') &= \mathrm{Tr}\Big[U_B^\dagger(t)AU_B(t)U_B^\dagger(t')BU_B(t')\rho_B\Big], \\ &= \mathrm{Tr}\Big[U_B(t')U_B^\dagger(t)AU_B(t)U_B^\dagger(t')B\rho_B\Big], \end{aligned} \tag{1.4}$$

where we used the fact that $U_B(t)$ commutes with ρ_B and the cyclic property of the trace. Notice that

$$U_B(t')U_B^\dagger(t) = e^{-iH_B(t-t')} = U_B^\dagger(t-t'), \tag{1.5}$$

so that we can write Eq. (1.4)

$$\begin{aligned} C(t,t') = C(t-t') &= \mathrm{Tr}\Big[U_B^\dagger(t-t')AU_B(t-t')B\rho_B\Big], \\ &= \mathrm{Tr}\Big[A(t-t')B\rho_B\Big], \end{aligned} \tag{1.6}$$

the two time correlation function depends only on the difference of times rather than each time individually.

1.2 The free correlation function for Bosonic Baths

In this thesis, our primary focus is on Bosonic environments. Such environments are often represented as an infinite collection of harmonic oscillators. These oscillators tend to couple to the system of interest via their position and do not interact with each other. This setup involving such environments are usually referred to as Caldeira-Leggett models [4–6]. The Hamiltonian considered in our analysis will typically take the form

$$H = H_S + S \otimes \sum_k g_k X_k + \sum_k \omega_k a_k^\dagger a_k. \tag{1.7}$$

Here H_S is the Hamiltonian of our system of interest, S is an arbitrary system operator, g_k is a coupling constant, while ω_k is the energy of the k^{th} harmonic oscillator, a_k is the annihilation operator of the k^{th} oscillator, and X_k is the position of the k^{th} harmonic oscillator from the environment. Since this is the usual setup we will be interested in, a two time correlation function of interest is that of the position of the harmonic oscillators at different times, in a thermal reservoir:

$$C(t) = \mathrm{Tr}\Big[X(t-t')X\rho_B\Big], \tag{1.8}$$

where

$$X = \sum_k g_k X_k = \sum_k \frac{g_k}{\sqrt{2\omega_k}}(a_k^\dagger + a_k). \tag{1.9}$$

As mentioned before, the environment is made up of non interacting harmonic oscillators, as such, their Hamiltonian is given by

$$H_B = \sum_k \omega_k a_k^\dagger a_k. \tag{1.10}$$

When we consider this Hamiltonian the free evolution of position is given by

$$X(t) = U_B(t) X U_B^\dagger(t) = \sum_k \frac{g_k}{\sqrt{2\omega_k}} (e^{i\omega_k t} a_k^\dagger + a_k e^{-i\omega_k t}). \tag{1.11}$$

Notice that for a thermal state

$$\langle a_k a_{k'} \rangle = 0, \tag{1.12}$$
$$\langle a_k^\dagger a_{k'}^\dagger \rangle = 0, \tag{1.13}$$
$$\langle a_k^\dagger a_{k'} \rangle = \delta_{k,k'} n(\omega_k, \beta), \tag{1.14}$$
$$\langle a_k a_{k'}^\dagger \rangle = \delta_{k,k'} (n(\omega_k, \beta) + 1). \tag{1.15}$$

Where $n(\omega_k, \beta)$ is the Bose-Einstein distribution of the k^{th} mode

$$n(\omega_k, \beta) = \frac{1}{e^{\beta\omega_k} - 1}. \tag{1.16}$$

So in the product $X(t)X$ we only need to keep the terms that contain one creation and one annihilation operator

$$C(t) = \langle X(t) X \rangle_B = \sum_{k,k'} \frac{g_k g_{k'}}{2\sqrt{\omega_k \omega_{k'}}} \mathrm{Tr}\Big[(e^{i\omega_k t} a_k^\dagger + a_k e^{-i\omega_k t})(a_k^\dagger + a_k) \rho_B \Big], \tag{1.17}$$
$$= \sum_{k,k'} \frac{g_k g_{k'}}{2\sqrt{\omega_k \omega_{k'}}} \left(\mathrm{Tr}\Big[e^{i\omega_k t} a_k^\dagger a_{k'} \rho_B \Big] + \mathrm{Tr}\Big[e^{-i\omega_k t} a_k a_{k'}^\dagger \rho_B \Big] \right), \tag{1.18}$$
$$= \sum_k \frac{g_k^2}{2\omega_k} \Big(e^{i\omega_k t} n(\omega_k, \beta) + e^{-i\omega_k t} (n(\omega_k, \beta) + 1) \Big), \tag{1.19}$$
$$= \sum_k \frac{g_k^2}{2\omega_k} \Big(\cos(\omega_k t) \underbrace{(2n(\omega_k, \beta) + 1)}_{\coth\left(\frac{\beta\omega_k}{2}\right)} - i \sin(\omega_k t) \Big). \tag{1.20}$$

Usually, we express the coupling coefficients in terms of the spectral density, unfortunately the community has equivalent different ways of expressing this quantity [B1, B2, 7, 8] which sometimes make comparison between different approaches cumbersome. In this thesis we will adapt the notation from [A1], however we would like to remark that often the literature uses other conventions that differ by a factor of π or 2π. We will use the following convention for the spectral density [B1, 9],

$$J(\omega) = \pi \sum_k \frac{g_k^2}{2\omega_k} \delta(\omega - \omega_k), \tag{1.21}$$

another common convention is [B3, 10]

$$\sigma(\omega) = \frac{J(\omega)}{\pi}. \tag{1.22}$$

While the difference is a simple multiplicative factor, it can make comparison between different approaches hard, specially when they are close to the limits their validity. QuTiP's enviroment class aims at setting a standard for this convention

[A1] and it has been one of the contributions of the author to the QuTiP library, while in some papers we used the $\sigma(\omega)$ convention, in this thesis, we will follow the $J(\omega)$. If we then go into the continuous limit, we obtain

$$C(t) = \frac{1}{\pi}\int_0^\infty d\omega J(\omega)\Big(\cos(\omega t)\coth\Big(\frac{\beta\omega}{2}\Big) - i\sin(\omega t)\Big), \tag{1.23}$$

which is the correlation function we will use for the remainder of the thesis. For later convenience, let us remark an important property of the correlation function

$$C(-t) = \overline{C}(|t|). \tag{1.24}$$

While this function is sometimes defined for positive times only, a complete description requires considering the negative case. To make this explicit, the non-equilibrium Green's function community typically incorporates step functions and splits positive and negative times into two different functions [8]

$$C(t) = \theta(t)C^{Adv}(t) + \theta(-t)C^{Ret}(t), \tag{1.25}$$

where

$$C^{Adv}(t) = \frac{1}{\pi}\int_0^\infty d\omega J(\omega)\Big(\cos(\omega t)\coth\Big(\frac{\beta\omega}{2}\Big) - i\sin(\omega t)\Big), \tag{1.26}$$

$$C^{Ret}(t) = \frac{1}{\pi}\int_0^\infty d\omega J(\omega)\Big(\cos(\omega t)\coth\Big(\frac{\beta\omega}{2}\Big) + i\sin(\omega t)\Big). \tag{1.27}$$

and consider them to be separate, individual objects. In this thesis, we will use the former, less explicit notation, and simply be aware of Eq. (1.24).

1.3 The free power spectrum for Bosonic Baths

While the correlation function provides a picture of the environment's effects in the time domain, the power spectrum offers a complementary and often more intuitive view in the frequency domain. Obtained by taking the Fourier transform of the correlation function, the power spectrum decomposes the complex system-environment interaction into the fundamental frequencies that drive it.

In the power spectrum, peaks correspond to the characteristic frequencies of the system, such as the transition energies between quantum states. The shape of these peaks is associated with the timescales of those transitions. Therefore, the power spectrum serves as a direct bridge between theoretical models and experimental measurements, such as optical absorption and emission spectra [11, B4], making it an indispensable tool for characterizing the behavior of open quantum systems. To evaluate the physicality of an approximation to the correlation function, one can compute its power spectrum [4, 12–16] and see that it satisfies the expected properties.

The power spectrum is defined as the Fourier transform of the correlation function, namely

$$S(\omega) = \int_{-\infty}^{\infty} dt C(t) e^{i\omega t}. \tag{1.28}$$

By inserting Eq. (1.23) one can write

$$S(\omega) = \frac{1}{\pi}\int_{-\infty}^{\infty} dt e^{i\omega t}\int_{0}^{\infty} d\omega' J(\omega')\Big(\cos(\omega' t)\coth\left(\frac{\beta\omega'}{2}\right) - i\sin(\omega' t)\Big). \tag{1.29}$$

Assuming that the integrand is an integrable function that is

$$\iint |f(x,y)|d(x,y) < \infty. \tag{1.30}$$

Then we are free to exchange the order of integration since

$$\int_X \left(\int_Y f(x,y)dy\right)dx = \int_Y \left(\int_X f(x,y)dx\right)dy = \iint f(x,y)d(x,y). \tag{1.31}$$

Which is known as Fubini's theorem [B5]. What this implies in terms of physical quantities is that the spectral density must vanish as $\omega \to \infty$. In other words, our system-environment interaction happens in a finite range of energy scales. This allows us to write

$$S(\omega) = \frac{1}{\pi}\int_{0}^{\infty} d\omega' \int_{-\infty}^{\infty} dt e^{i\omega t} J(\omega')\Big(\cos(\omega' t)\coth\left(\frac{\beta\omega'}{2}\right) - i\sin(\omega' t)\Big). \tag{1.32}$$

The only time dependent terms are sines and cosines, so it suffices to find their Fourier transforms

$$\mathcal{F}(\cos(\omega' t)) = \int_{\infty}^{\infty} dt\cos(\omega' t)e^{i\omega t} = \pi\left(\delta(\omega-\omega') + \delta(\omega+\omega')\right), \tag{1.33}$$

$$\mathcal{F}(\sin(\omega' t)) = \int_{\infty}^{\infty} dt\sin(\omega' t)e^{i\omega t} = \frac{\pi}{i}\left(\delta(\omega+\omega') - \delta(\omega-\omega')\right). \tag{1.34}$$

By substituting Eq. (1.33) into Eq. (1.29) we obtain

$$\begin{aligned} S(\omega) = \int_0^{\infty} d\omega' J(\omega')\Big(&\left(\delta(\omega-\omega') + \delta(\omega+\omega')\right)\coth\left(\frac{\beta\omega'}{2}\right) \\ &- \left(\delta(\omega+\omega') - \delta(\omega-\omega')\right)\Big). \end{aligned} \tag{1.35}$$

Notice $\coth(-x) = -\coth(x)$ so that

$$S(\omega) = \left(J(\omega) - J(-\omega)\right)\coth\left(\frac{\beta\omega}{2}\right) - \pi\left(J(-\omega) - J(\omega)\right) \tag{1.36}$$

$$= \left(J(\omega) - J(-\omega)\right)\left(\underbrace{\coth\left(\frac{\beta\omega}{2}\right)}_{2n(\omega)+1} + 1\right) \tag{1.37}$$

$$= 2\left(J(\omega) - J(-\omega)\right)\left(n(\omega)+1\right). \tag{1.38}$$

We can further simplify this by using the spectral density definition in Eq. (1.21) such that

$$J(\omega) - J(-\omega) = \sum_k \frac{g_k^2}{2\omega_k}\left(\delta(\omega-\omega_k) - \delta(-\omega-\omega_k)\right) \tag{1.39}$$

$$= \sum_k \frac{g_k^2}{2\omega_k}\operatorname{sign}(\omega)\delta(|\omega| - \omega_k) \tag{1.40}$$

$$= \operatorname{sign}(\omega)J(|\omega|), \tag{1.41}$$

so we finally obtain

$$S(\omega) = 2\,\mathrm{sign}(\omega) J(|\omega|)\,(n(\omega,\beta)+1)\,, \tag{1.42}$$

which is the expression often encountered in books and articles [B3, 15, B6]. Regardless of the convention, this shows that these quantities (the correlation function and power spectrum) contain information about both spectral density and temperature, but that neither can be recovered from them individually, as they are merged together. However, they fully determine the dynamics of an open quantum system when combined with the system Hamiltonian and the operator that describes the coupling to the environment [B1, B2]. At last an important condition the power spectrum must satisfy is the detailed balance condition, which reads

$$S(\omega) = e^{\beta\omega} S(-\omega), \tag{1.43}$$

and can be obtained from Eq. 1.42 by direct substitution. Approximations often struggle to satisfy Eq. (1.43) when β is big with respect to ω.

1.4 The free correlation function for Fermionic Baths

For Fermionic baths, the interaction to the bath is more akin to the rotating wave approximation (RWA) in Bosonic systems [B1, B7] . Their Hamiltonian can be written as

$$H = H_S + H_B + H_I, \tag{1.44}$$

where $H_B = \sum_k \omega_k c_k^\dagger c_k$ and the interaction Hamiltonian is given by

$$H_I = \sum_k g_k (S c_k^\dagger + c_k S^\dagger), \tag{1.45}$$

where S is a Fermionic operator with odd parity with support on the system, This is because we expect the physical system to have even parity ($Sc_k^\dagger$ is even). Again the bath is in thermal equilibrium. However, for Fermionic systems the equilibrium state is different and given by

$$\rho_{eq} = \frac{e^{\sum_k \beta(\omega_k-\mu)c_k^\dagger c_k}}{Z_{eq}}, \tag{1.46}$$

where μ is the chemical potential. Usually we want to express the interaction as

$$H_I = S^\dagger B + S B^\dagger, \tag{1.47}$$

where

$$B = \sum_k g_k c_k. \tag{1.48}$$

In the interaction picture we have

$$B(t) = \sum_k g_k c_k e^{i\omega_k t}. \tag{1.49}$$

Due to the coupling form the correlation function relations are different from the Bosonic case. Let us consider all the possible combinations of the bath operator B

- $B(t)B(0)$,
- $B^\dagger(t)B(0)$,
- $B(t)B^\dagger(0)$,
- $B^\dagger(t)B^\dagger(0)$.

We use centralized Fermionic operators, namely

$$\langle c_k\rangle = \mathrm{Tr}[c_k\rho_{eq}] = \sum_i \langle i|\, c_k \frac{e^{\beta\sum_k(\omega_k-\omega)c_k^\dagger c_k}}{Z_{eq}}\, |i\rangle = 0. \tag{1.50}$$

And that due to their Fermionic nature

$$\langle c_k^2\rangle = 0. \tag{1.51}$$

We then analyze the thermal average of each of the terms individually to obtain

$$\langle B(t)B(0)\rangle = 0, \tag{1.52}$$
$$\langle B^\dagger(t)B(0)\rangle = \sum_k g_k^2 n_F(\beta(\omega-\mu))e^{i\omega_k t}, \tag{1.53}$$
$$\langle B(t)B^\dagger(0)\rangle = \sum_k g_k^2 (1-n_F(\beta(\omega-\mu)))e^{-i\omega_k t}, \tag{1.54}$$
$$\langle B^\dagger(t)B^\dagger(0)\rangle = 0, \tag{1.55}$$

where μ is the chemical potential and n_F is the Fermi-Dirac distribution

$$n_F(\beta(\omega-\mu)) = \frac{1}{e^{\beta(\omega-\mu)}+1}. \tag{1.56}$$

Then going into the continuum limit, we may write the correlation functions

$$C^{(+)}(t) = \frac{1}{2\pi}\int_{-\infty}^{\infty} J(\omega)n_F(\beta(\omega-\mu))e^{i\omega t}d\omega, \tag{1.57}$$
$$C^{(-)}(t) = \frac{1}{2\pi}\int_{-\infty}^{\infty} J(\omega)\left(1-n_F(\beta(\omega-\mu))\right)e^{-i\omega t}d\omega, \tag{1.58}$$

where we used

$$J(\omega) = 2\pi\sum_k g_k^2\delta(\omega-\omega_k). \tag{1.59}$$

Notice that a different convention with respect to the Bosonic case was used to be consistent with the literature and the current definitions in [A1]. Unlike in the Bosonic case Eq. (1.25), we have two different correlation functions due to B and $B^\dagger$ being coupled differently to the bath. It is often convenient to use the fact that

$$1-n_F(\beta(\omega-\mu)) = 1-\frac{1}{e^{\beta(\omega-\mu)}+1} = \frac{e^{\beta(\omega-\mu)}}{e^{\beta(\omega-\mu)}+1} \tag{1.60}$$
$$= \frac{1}{e^{-\beta(\omega-\mu)}+1} = n_F(-\beta(\omega-\mu)). \tag{1.61}$$

to write (with $\sigma=\pm$)

$$C^{(\sigma)}(t) = \frac{1}{2\pi}\int_{-\infty}^{\infty} J(\omega)n_F(\sigma\beta(\omega-\mu))e^{i\sigma\omega t}d\omega. \tag{1.62}$$

1.5 The Power Spectrum for Fermionic Baths

Since Fermionic environments have two correlation functions, they have two power spectrums as well, each correspoding to one of the correlation functions. Just as in the previous case one can relate the spectral density to one of the power spectrums via the fluctuation dissipation relation. If we follow the same steps as in section 1.3 we get

$$S^{(\sigma)}(\omega) = \int_{-\infty}^{\infty} dt C^{(\sigma)}(t) e^{-i\sigma\omega t} \tag{1.63}$$

$$= \frac{1}{2\pi} \int_{-\infty}^{\infty} dt e^{-i\sigma\omega t} \int_{-\infty}^{\infty} J(\omega') n_F(\sigma\beta(\omega' - \mu)) e^{i\sigma\omega' t} d\omega' \tag{1.64}$$

$$= \frac{1}{2\pi} \int_{-\infty}^{\infty} J(\omega') n_F(\sigma\beta(\omega' - \mu)) d\omega' \int_{-\infty}^{\infty} dt e^{-i\sigma(\omega-\omega')t}. \tag{1.65}$$

If we now use

$$\int_{-\infty}^{\infty} dt e^{-i\sigma(\omega-\omega')t} = 2\pi\delta(\omega - \omega'), \tag{1.66}$$

we obtain

$$S^{(\sigma)}(\omega) = J(\omega) n_F(\sigma\beta(\omega - \mu)). \tag{1.67}$$

Notice from Eq. 1.60 that $n_F(x) + n_F(-x) = 1$ thus we have

$$S^{(+)}(\omega) + S^{(-)}(\omega) = J(\omega). \tag{1.68}$$

And from Eq. 1.67 and 1.60 we can derive that the detailed balance condition for the power spectrum which reads

$$S^{(+)}(\omega) = e^{-\beta(\omega-\mu)} S^{(-)}(\omega). \tag{1.69}$$

1.6 Approximating the Correlation function

Whether we have Bosonic or Fermionic environments, obtaining analytical expressions for the bath correlation function can be difficult, and even when achievable, it might lead to complicated functions that will be part of the integrals required to obtain the dynamics of the system [5, B1, 17–19]. Many numerical methods require the correlation function to be decomposed in terms of simple functions whose integrals can be easily computed [4, 16, 20–26]. Figure 1.1 illustrates this idea. In this thesis we decompose the correlation function using a Fourier-like series, decomposing the signal into damped sinusoidals. The main methods in this thesis do not require such a decomposition but greatly benefit from it. There exists many methods to achieve this decomposition. They can roughly be broken down into two categories

- Analytical decompositions
- Numerical decompositions

We will now give a brief overview of how they work and indicate their limitations. All the numerical methods in this section were added by the author and collaborators to QuTiP's environment class, a QuTiP feature developed largely by the author, Paul Menczel and Neill Lambert.

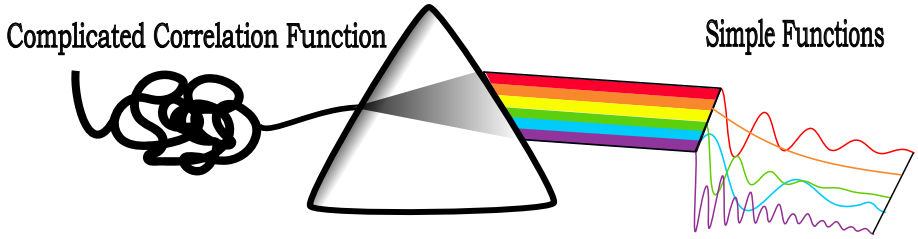

Figure 1.1: Illustration of the decomposition of the correlation function, the idea is to take a complicated function and decompose it somehow as the sum of simple functions

1.6.1 Analytical Decompositions

In rare cases, we are able to obtain an expression for the correlation function in terms of simple functions analytically. However, this only applies to a handful of spectral densities. The way to obtain analytical expressions is to notice that in the correlation function expression we have infinitely many poles which we can use to perform contour integration. Specifically those poles come from $\coth\left(\frac{\beta\omega}{2}\right)$ and are called Matsubara poles (or Matsubara frequencies) [22, 27, 28]. In the case of bosons, the expansion can be achieved when using an underdamped or Drude-Lorentz (also referred to as overdamped) spectral density. We will focus on the underdamped case to illustrate the technique, as the Drude-Lorentz introduces slight physical issues [29]

$$J_U(\omega) = \frac{\alpha^2\Gamma\omega}{[(\omega_c^2-\omega^2)^2+\Gamma^2\omega^2]}. \tag{1.70}$$

Performing contour integration [12, 20] (see appendix D) one finds the correlation function to be

$$C(\tau) = \sum_{k=0}^{\infty} c_k e^{-\nu_k t}, \tag{1.71}$$

where

$$c_k = \begin{cases} \left(\alpha^2\coth(\beta(\Omega+i\Gamma/2)/2)+i\alpha^2\right)/4\Omega & k=0 \\ \left(\alpha^2\coth(\beta(\Omega-i\Gamma/2)/2)-i\alpha^2\right)/4\Omega & k=1 \\ \frac{-4\alpha^2\Gamma\pi k}{\beta^2[(\Omega+i\Gamma/2)^2+(\frac{2\pi k}{\beta})^2)][(\Omega-i\Gamma/2)^2+(\frac{2\pi k}{\beta})^2]} & k\geq 2, \end{cases} \tag{1.72}$$

$$\nu_k = \begin{cases} -i\Omega+\Gamma/2 & k=0 \\ i\Omega+\Gamma/2 & k=1 \\ 2\pi kT & k\geq 2. \end{cases} \tag{1.73}$$

Where we used $\Omega = \sqrt{\omega_c^2-\left(\frac{\Gamma}{2}\right)^2}$. The usefulness of this expansion (known as Matsubara expansion [21, 27, 28]) is largely due to three simple reasons.

1. The sum converges quickly when the $T \gg \frac{\hbar\omega_c}{2\pi k_b}$, where $\hbar$ is Planck's reduced constant and k_b is Boltzman's contant, both are set to one throughout the manuscript. Whenever this is satisfied, we can express the correlation function as a sum of a small number of decaying exponents

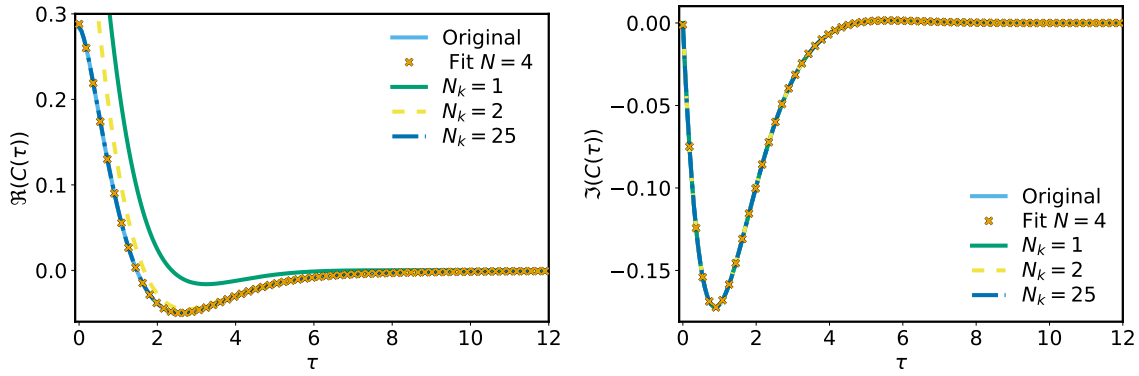

Figure 1.2: Real and imaginary part of the correlation function of an underdamped spectral density, the convergence of the Matsubara expansion is shown, the parameters used for the plot where $T = 0.05$, $\omega_c = 1.2$, $\alpha = 1$, $\Gamma = 2$. For an underdamped spectral density only one exponent is needed for the imaginary part of the correlation, while the real part converges slowly

2. The correlation function expressed this way, has simple derivatives that allows for the derivation of useful dynamical equations such as HEOM
3. It is an analytical answer, so no matter what the parameters are it just requires evaluation of the expression, and no other information to recover the correlation function.

while its main drawbacks are

1. In the regime where $T \to 0$, the expansion converges slowly, needing many exponents to correctly describe the correlation function as figure 1.2 shows
2. Only a handful of spectral densities allow for such a nice, analytical expansion.

The typical methods for which this sort of decomposition is required, put an emphasis on approximating the environment with the least number of exponents possible, while still maintaining the detailed balance condition Eq. (1.43) which can be challenging in practice. In approximate descriptions like master equations, we do not need to concern ourselves with requiring the least number of exponents possible, however, we do care about achieving detailed balance approximately. Another analytical decomposition that is worth mentioning is the Padé decomposition. It relies on using the Padé approximation for the Bose-Einstein or Fermi-Dirac distributions for the integration instead of the Matsubara poles. While the method has better convergence, it suffers the same shortcomings as the Matsubara decomposition.

1.6.2 Numerical Decompositions

Numerical decompositions of the correlation function have recently attracted significant interest in the HEOM community [12, 15, 16, 20, 30, 31]. In this section, we will briefly overview different ways to numerically obtain a decaying exponential decomposition for the correlation function. Building on the discussion in [16], we broaden the comparison by including a few extra methods. All the methods described here are now available in QuTiP for Bosonic environments as part of the contributions of the author to QuTiP [A1], while Fermionic environments are a work in progress.

1.6.3 Approximation via Non-Linear Least squares

Nonlinear least squares fitting (NLSQ) is a mathematical optimization technique used to model data by finding the best-fit parameters of a nonlinear function. This approach minimizes the sum of the squared differences (residuals) between the observed data points and the corresponding values predicted by the model. It is a powerful tool for analyzing experimental data and is widely applied in fields such as physics, chemistry, biology, engineering, and finance.

The goal is to find the set of parameters θ that minimizes the residual sum of squares (RSS):

$$RSS = \sum_{i=1}^{N} (y_i - f(x_i, \theta))^2, \tag{1.74}$$

where y_i is the data to be fitted, x_i the independent variable in our case time, $f(x_i, \theta)$ the function we wish to use to explain the data, and N is the number of data points. We express our correlation function as

$$C(t) = C_R(t) + iC_I(t), \tag{1.75}$$

where we have separated the real and imaginary part, and perform a different fit for each one as outlined in [20]. The real and imaginary parts are given by

$$C_R(t, c^R, \nu^R, \nu^I) = \sum_{k=1}^{m} c_k^R e^{-\nu_k^R} \cos\left(\nu_k^I\right), \tag{1.76}$$

$$C_I(t, c^I, \nu^R, \nu^I) = \sum_{k=1}^{m} c_k^I e^{-\nu_k^R} \sin\left(\nu_k^I\right), \tag{1.77}$$

where the superscript R, I refers to real and imaginary parts respectively and no subscript refers to a vector of the m parameters. The main advantange of this approach with respect to the others is that it allows to constraint c_k and ν_k, which can often help make numerically exact solutions more stable, but the fitting is less robust than the other methods. We observe no relevant advantage for master equations, where we are not limited by the number of exponents used. Nevertheless, for a small number of exponents, it's often the best approximation. We use the implementation in scipy [32]. NLSQ is flexible, we can also fit our spectral density to be a combination of underdamped spectral densities for which we know the Matsubara decomposition [33], in this sense the model we fit our spectral density to is [A1, 20]

$$J_{approx}(\omega; a, b, c) = \sum_{i=1}^{m} \frac{2a_i b_i w}{((w + c_i)^2 + b_i^2)((w - c_i)^2 + b_i^2)}. \tag{1.78}$$

We then generate the set of exponents for each of the m spectral densities using the Matsubara expansion. Unfortunately, we need to set the number of Matsubara exponents to appropriately describe the correlation function. Inspired by this method and the AAA method, the author instead proposes fitting the power spectrum using the model function

$$S(\omega) = \sum_{k=1}^{N} \frac{2(a_k c_k + b_k(d_k - \omega))}{(\omega - d_k)^2 + c_k^2}. \tag{1.79}$$

This allows for using NLSQ in the frequency domain without relying on the Matsubara expansion unlike previous methods based on the spectral density [20, 33, 34]. It is a massive improvement on the spectral density fitting method [33, 34] as this is not limited by Matsubara exponents in the zero temperature limit. One recovers the correlation function by realizing that the inverse Fourier transform of each individual k component is given by

$$C_k(t) = (a_k + ib_k)e^{-(c_k+id_k)} \qquad \text{for } t > 0. \tag{1.80}$$

1.6.4 The AAA method

The Adaptive Antoulas Anderson algorithm (AAA) is a method for the approximation of a function in terms of a rational function [15, 16, 35]

$$f(z) \approx \frac{q(z)}{p(z)} = \frac{\sum_{j=1}^{m} \frac{\text{weight}_j f_j}{z-z_j}}{\sum_{j=1}^{m} \frac{\text{weight}_j}{z-z_j}} = \sum_{j=1}^{m} \frac{residues}{z - poles}, \tag{1.81}$$

where the z_j are called support points and the f_j are the values of the function at support points. These sort of expressions are called rational barycentric approximations [35]. One does not use this method on the correlation function directly, but on the power spectrum which we obtain via Eq. (1.42) [15, 36]. After obtaining this rational polynomial form of the power spectrum one can recover the correlation function by noticing that

$$S(\omega) = \int_{-\infty}^{\infty} dt e^{i\omega t} C(t) = 2\,\text{Re}\left(\sum_k \frac{c_k}{\nu_k - i\omega}\right). \tag{1.82}$$

Which allows us to identify

$$\nu_k = i \times poles, \tag{1.83}$$
$$c_k = -i \times residues. \tag{1.84}$$

For a detailed discussion of how this method works see [35], while for its application on open quantum systems see [15, 16, 36]. Here we provide a brief overview of the main steps

1. Supply the sample set $Z = (Z_1, \ldots, Z_N)$
2. Start the Loop and repeat until $|F(Z) - r(z)| < tol$ where F is the original function, r its rational approximation and tol the numerical tolerance to use.
3. Initialize the rational approximation r, support points z, and a vector f to be vectors of zeros.
4. Find the k for which $|F(Z_k) - r(Z_k)|$ is maximum and add Z_k to the support points z, add the value of the function at the support point to the vector f.
5. Compute the Cauchy and matrices for Z and z (substraction via outer product)

$$C = \frac{1}{Z - z}. \tag{1.85}$$

6. Compute the Loewner Matrix

$$L = \frac{F - f}{Z - z}. \tag{1.86}$$

7. Perform SVD on the Loewner matrix $L = UDW$ and keep the matrix w which denotes the weights of the approximation.

8. We get the rational approximation of the function $r(z) = \frac{q(z)}{r(z)}$ by computing the numerator and denominator as

$$q(z) = C(wF), \qquad p(z) = Cw. \tag{1.87}$$

9. We check if our rational approximation satisfies our required tolerance, it does we break the Loop $|f(Z) - r(Z)| < tol$.

10. The Loop ran $2N + 1$ times before breaking, compute the $2N$, poles and residues. residues are obtained via the simple quotient rule on r

$$residues = -\frac{C(wf)}{C^2 w}, \tag{1.88}$$

while poles correspond to the eigenvalues of the generalized eigenvalue problem

$$\begin{pmatrix} 0 & w_1 & w_2 & \cdots & w_m \\ 1 & z_1 & & & \\ 1 & & z_2 & & \\ \vdots & & & \ddots & \\ 1 & & & & z_m \end{pmatrix} = \lambda \begin{pmatrix} 0 & & & & \\ & 1 & & & \\ & & 1 & & \\ & & & \ddots & \\ & & & & 1 \end{pmatrix}. \tag{1.89}$$

11. From Eq. 1.82 we see that c_k and $\nu_k - i\omega$ come in complex conjugate pairs. to find them. We filter the poles in the lower half on the complex plane, and identify the c_k and ν_k with Eq. 1.83.

1.6.5 Prony Polynomial based methods

The Prony polynomial forms the mathematical foundation for many spectral analysis techniques that estimate frequencies, damping factors, and amplitudes of signals. These methods work by interpreting a given signal as a sum of complex exponents and deriving a polynomial whose roots correspond to the frequencies or poles of the system.

The methods consider M samples a linearly spaced signal

$$(f(t_0), f(t_0 + \delta t), \ldots f(t_0 + (M-1)\delta t), \tag{1.90}$$

and assume that this signal comes from a sum of complex exponents

$$f(t) = \sum_{k=0}^{N-1} c_k e^{-\nu_k t} = \sum_{k=0}^{N-1} c_k z_k^t. \tag{1.91}$$

The Prony polynomial based methods estimate the phases z_k^t from which we can obtain the ν_k and the amplitudes c_k. The z_k can be seen as the generalized eigenvalues of the matrix pencil [2][37]

$$z_j \mathbf{H}_{M-N,N}(0) - \mathbf{H}_{M-N,N}(1) = \mathbf{V}_{M-N,N}(\mathbf{z}) \text{diag}\Big(((z_j - z_k)\gamma_k)_{k=1}^N \Big) \mathbf{V}_{N,N}(\mathbf{z})^T, \quad (1.92)$$

where $\mathbf{H}$ denotes a Hankel matrix built from the signal, the subscripts indicating the sampling points in the first column and last row respectively, the argument of the Hankel matrix denotes how many shifts to apply to the signal. For example

$$\mathbf{H}_{3,2}(0) = \begin{pmatrix} f(t_0) & f(t_0+\delta t) & f(t_0+2\delta t) \\ f(t_0+\delta t) & f(t_0+2\delta t) & f(t_0+3\delta t) \end{pmatrix}. \quad (1.93)$$

The amplitudes (c_k) can later be obtained by solving the least-squares Vandermonde system given by

$$V_{N,M}(z)c = f, \quad (1.94)$$

where $V_{N,M}(z)$ is the Vandermonde matrix given by

$$V_{M,N}(z) = \begin{pmatrix} 1 & 1 & \dots & 1 \\ z_1 & z_2 & \dots & z_N \\ z_1^2 & z_2^2 & \dots & z_N^2 \\ \vdots & \vdots & \ddots & \vdots \\ z_1^M & z_2^M & \dots & z_N^M \end{pmatrix}, \quad (1.95)$$

M is the length of the signal, N the number of exponents, and $f = f(t_{sample})$ is the signal evaluated in the sampling points, while $c = (c_1, \dots, c_N)$ is a vector containing the amplitudes. The main difference between the Prony and the Estimation of Signal Parameters via Rotational Invariance Techniques (ESPRIT) methods is the way one obtains the roots of the polynomial, typically whether this system is solved or a low rank approximation is found for the polynomial [37].

For the Prony method we obtain those eigenvalues directly (typically by using the least squares solution of the left hand side of Eq. (1.92)), while for ESPRIT we perform the singular value decomposition on $H(0)$ then

$$\mathbf{H}_{M-N,N}(0) = U_{M-N,M-N} D_{M-N,N} W_{N,N}, \quad (1.96)$$

where U is a unitary matrix, D is diagonal and W is a square matrix. The phases z_k can be obtained from the eigenvalues of the matrix [16, 37]

$$A = (W(0)^T)^+ W(1), \quad (1.97)$$

where $^+$ denotes the Penrose pseudoinverse. The c_k are obtained by least squares on the Vandermonde system

[2]Typically there is another dimension involved in the matrix pencil an upper bound on the number of exponents, and the number of exponents is treated as an unknown, we omitted this for simplicity

1.6.6 Estimation of Signal Parameters by Iterative Rational Approximation (ESPIRA)

ESPIRA exploits the connection between parameter estimation (Prony like methods estimate amplitude and phase) and the rational approximation of functions. In our context it exploits the fact that the correlation function and power spectrum are fourier transforms of each other

$$C(\tau) = \sum_k c_k e^{\nu_k t} \longleftrightarrow S(\omega) = 2\,\mathrm{Re}\left(\sum_k \frac{c_k}{\nu_k - i\omega}\right). \tag{1.98}$$

Intuitively, though not strictly true, one can think of it as ESPRIT on the correlation function and AAA on the power spectrum merged together. As such it provides the best of both worlds providing good fits on both quantities as Figure 1.3 shows. For further information about how the methods works see [37]. We recommend it when using master equations as it is the method we find most flexible, and it is relatively straightforward to obtain a desired accuracy, whereas other methods might not improve with more exponents. The method steps are (taken from Algorithm 3 [37]):

1. Supply $\mathbf{f} = (f_k)_{k=0}^{2N-1}$ equidistant samples of the signal, and the required tolerance for the rational approximation.
2. Compute the Discrete Fourier transform vector $\hat{\mathbf{f}} = (\hat{f}_k)_{k=0}^{2N-1}$ with $\hat{f}_k = \sum_{j=0}^{2N-1} f_j \omega_{2N}^{kj}$ of $\mathbf{f}$ (with $\omega_{2N} := e^{-2\pi i/2N}$).
3. Use AAA to compute a rational function $r_M(z)$ of (smallest possible) type $(M-1, M)$ $(M \leq N)$, such that
$$|r_M(\omega_{2N}^{-k}) - \omega_{2N}^{-k}\hat{f}_k| < tol, \quad k = 0, \ldots, 2N-1.$$
4. Compute the rational function representation of $r_M(z)$,
$$r_M(z) = \sum_{k=1}^{M} \frac{a_k}{z - z_k}.$$
5. Obtain the amplitudes by $c_k := \frac{a_k}{1 - z_k^2}$, $k = 1, \ldots, M$.

The main advantage of this method over the AAA method is its reduced sensitivity to the support points selected. The AAA scheme relies heavily on the chosen sampling points, although this usually isn't an issue when using logarithmically distributed rather than linearly spaced points [15, 36]. Achieving a good fit often requires significantly more sampling points with AAA than with ESPIRA. Increasing the number of sampling points can be both memory- and time-intensive.

1.7 Which method should I use to approximate my correlation function?

Which method to use depends largely on the spectral density considered and the temperature of the environment (or alternatively its power spectrum or correlation

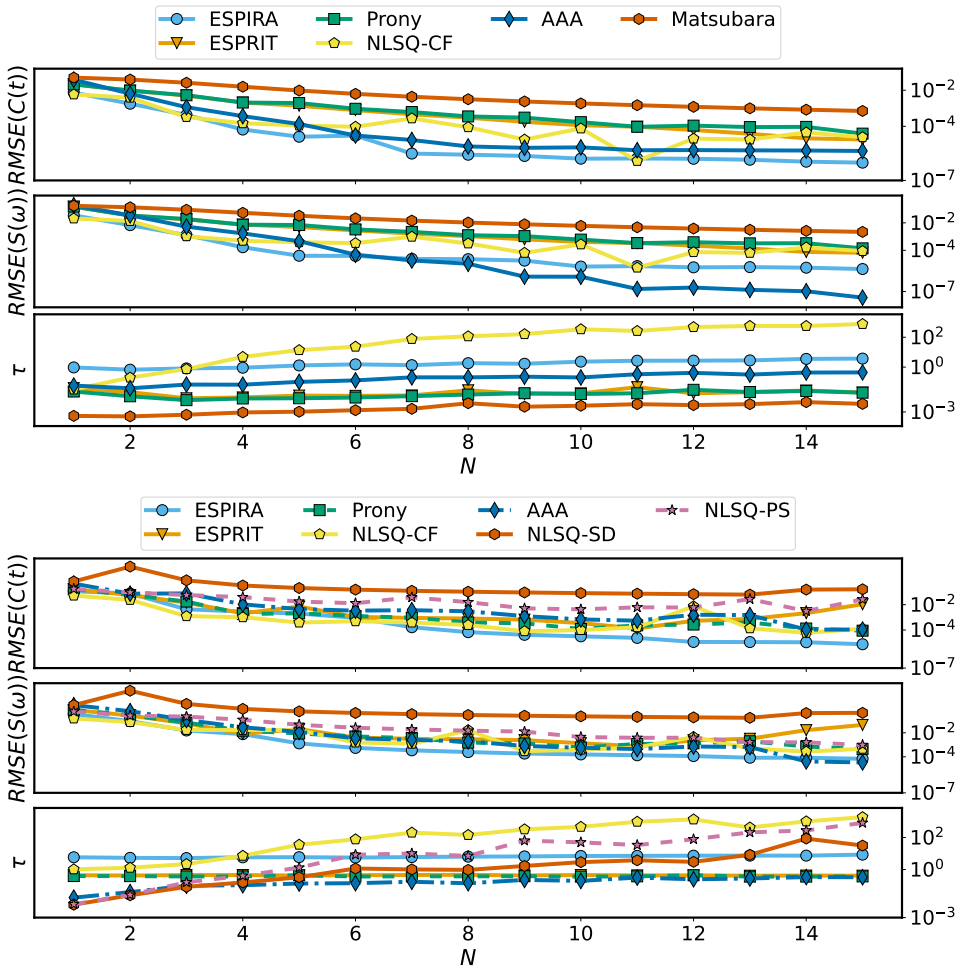

Figure 1.3: a) An underdamped spectral density with parameters $T = 0.05$, $\omega_0 = 1.2$, $\alpha = 1$, $\gamma = 2$. b)An Ohmic spectral density with parameters $T = 0.5, \alpha = 1$, $s = 1$, $\omega_c = 5$. The figure shows the number of exponents needed to achieve a certain root mean squared error (RMSE). We show the error for several methods to obtain the exponents. The top image shows the RMSE on the correlation function, the middle one the RMSE on the power spectrum and the bottom one the time it takes each method to obtain the exponents. Where PS stands for Power spectrum, SD for spectral density and CF for correlation function.

function). In this section, we provide a comparison of the different methods, summarizing their main advantages and disadvantages in table 1.1.

In Figure 1.3 a), we can see the accuracy of each method for a fixed number of exponents. We chose an underdamped spectral density because we know a lot about the structure of its exponents [12]. Thus NLSQ methods shine here as they dot not get stuck in local minima (we have good guesses and bounds), even though, we see that after a certain number of exponents they are outperformed by ESPIRA and AAA. In this figure we neglected the spectral density fitting because the underdamped spectral density is our fitting function and therefore it would just coincide with Matsubara.

The reason Matsubara does so poorly compared to other methods is the low temperature considered in this example. One can then realize how the other methods

enable low temperature simulations with numerically exact methods where reducing the number of exponents is extremely important [A1, 15, 20]. In figure 1.3 b) we used the spectral density

$$J(\omega) = \alpha \frac{\omega^s}{\omega_c^{s-1}} e^{-\omega/\omega_c}, \tag{1.99}$$

its behaviour depends on the "Ohmicity" parameter s, when $s = 1$ its behaviour is Ohmic, while for $s > 1$ and $s < 1$ it is super-Ohmic or sub-Ohmic respectively. For lack of a better name we will refer the spectral density dependent on s is called Ohmic [A1].

Unfortunately, in this case, we do not have good knowledge about the structure of the exponents. Results show that NLSQ methods perform slightly worse overall. In both figures, for a low number of exponents, NLSQ typically outperforms other methods. Therefore, we recommend NLSQ for applications like HEOM and Pseudomodes where the simulation is limited by the number of exponents. If NLSQ gives divergent solutions or fails to approximately satisfy detailed balance (or results in a poor correlation fit when using NLSQ-PS), consider using ESPIRA for transient dynamics or AAA for steady-state analysis.

For Non-Markovian master equations, reducing the number of exponents is less important than ensuring a fit that satisfies the detailed balance condition. This is why, for such simulations, we recommend using ESPIRA and AAA, as these methods are more reliable in upholding this condition. In some examples presented in the Thesis, we use NLSQ to match the effective environment with Pseudomodes or HEOM simulations. The rationale here is to enable direct comparisons across different simulation approaches. A short summary of all methods is provided in table 1.2.

It is also noted that, while the discussion here is aimed at Bosonic environments, these techniques are applicable to Fermionic environments as well. They are being added to the QuTiP Fermionic environments developed by the author and collaborators.

Table 1.1: Comparison of Methods to approximate the correlation function

Method	Advantages	Disadvantages
ESPIRA	• Generally provides a good fit on both the correlation function and the power spectrum. • Works well on noisy data. • Reasonably fast. • One can fit the real and imaginary parts of the correlation function jointly or separately. • Works on arbitrary spectral densities.	• Sensitive to the support points used for the approximation. • Not widely available. • Obtaining the exponents can require relatively high computer memory. • Obtaining the exponents for the real and imaginary part separately, often leads to nondesirable errors on the imaginary part.
ESPRIT	• Works well on noisy data. • Reasonably fast. • One can fit the real and imaginary parts of the correlation function jointly or separately. • Works on arbitrary spectral densities. • Its implementation is simple.	• Sensitive to the support points used for the approximation. • Not widely available. • If the support points are too dense it can lose accuracy due to numerical overflow or underflow.
Prony's Method	• Reasonably fast. • One can fit the real and imaginary parts of the correlation function jointly or separately. • Works on arbitrary spectral densities. • Its implementation is simple.	• Sensitive to the support points used for the approximation. • If the support points are too dense it can lose accuracy due to numerical overflow or underflow. • Too sensitive to noisy data.

Continued on next page

Table 1.1 – continued from previous page

Method	Advantages	Disadvantages
NLSQ	• Often leads to good fits with a low number of exponents. • Works on arbitrary spectral densities. • It's widely available.	• Sensitive to the support points. • Can get stuck in local minima providing suboptimal fits. • Too sensitive to noisy data. • Requires knowledge about the function. • Often leads to problems with the detailed balance condition.
AAA	• Best for calculations of the steady state. • Widely available. • Allows flexibility to find thermal and spectral contributions separately or jointly.	• Sensitive to the support points. • Can get stuck in local minima. • Too sensitive to noisy data. • Requires knowledge about the function. • Often leads to problems with the detailed balance condition.
Matsubara	• Analytical, optimal for high temperature. • Clear interpretation. • Insensitive to support points.	• Only available for specific spectral densities. • Does not converge well for low temperatures.

Table 1.2: Visual Comparison of the methods

Method	Works on Arbitrary Functions	Allows for constraints	Does not Require Extra input	Does not require optimization	Not Sensitive to sampling points	Works at arbitrary Temperatures	Works on Noisy data	Recommended when...
NLSQ	✓	✓	✗	✗	✗	✓	✓	You have an idea about which exponents should be included [12]
AAA	✓	✗	✓	✓	✗	✓	✓	The steady-state is most important and spectral density is not too structured
Prony	✓	✗	✓	✓	✗	✓	✗	The correlation function is noiseless and long lived.
Matsubara	✗	✗	✓	✓	✓	✗	✗	Doing high temperature simulations using the specific spectral densities it is available for.
ESPIRA	✓	✗	✓	✓	✗	✓	✓	A general-purpose method is required. It is the main method we recommend.
ESPRIT	✓	✗	✓	✓	✗	✓	✓	The correlation function is long lived.

Chapter 2

Dynamics of closed quantum systems

Before starting with the basics of the evolution of open quantum systems, a review of the dynamics of closed quantum systems might be helpful. Throughout all of this manuscript we set $\hbar = 1$. The reason for this review, is that eventhough this is standard, the steps taken to obtain time ordered products and the associated change of integration limits, are used multiple times in multiple derivations in the rest of the thesis, so we want to remind the reader about these steps and introduce the notation used.

2.1 The Time evolution operator

According to the basic formulation of quantum mechanics, the evolution of the wave function is governed by the Schrodinger equation

$$i\frac{\partial \left|\psi(t)\right\rangle}{\partial t} = H(t)\left|\psi(t)\right\rangle . \tag{2.1}$$

As it is a first order linear differential equation, given the initial conditions $|\psi(0)\rangle$, we can express the solution by means of the operator $U(t, t_0)$ such that

$$\left|\psi(t)\right\rangle = U(t, t_0)\left|\psi(t_0)\right\rangle . \tag{2.2}$$

From this point on we will call U the time evolution operator. If we now substitute equation Eq. (2.2) into Eq. (2.1), we obtain

$$i\frac{\partial \left(U(t, t_0)\left|\psi(t_0)\right\rangle\right)}{\partial t} = H(t)U(t, t_0)\left|\psi(t_0)\right\rangle . \rightarrow \boxed{\text{Must be valid for any initial state.}} \tag{2.3}$$

Since the equation must be valid for any initial state we have:

$$i\frac{\partial U(t, t_0)}{\partial t} = H(t)U(t, t_0). \rightarrow \boxed{\text{Subjected to the initial condition } U(t_0, t_0) = \mathbb{I}.} \tag{2.4}$$

From here we can find that the adjoint is given by

$$-i\frac{\partial U(t, t_0)^\dagger}{\partial t} = U(t, t_0)^\dagger H(t). \tag{2.5}$$

Now let us consider the product $U^\dagger(t,t_0)U(t,t_0) = \mathbb{I}$. Then it's derivative obeys:

$$\frac{\partial U^\dagger(t,t_0)U(t,t_0)}{\partial t} = \frac{\partial U^\dagger(t,t_0)}{\partial t}U(t,t_0) + U^\dagger(t,t_0)\frac{\partial U(t,t_0)}{\partial t} \tag{2.6}$$

$$= \frac{\partial U^\dagger(t,t_0)}{\partial t}U(t,t_0) + \frac{\partial U(t,t_0)}{\partial t}U^\dagger(t,t_0) \tag{2.7}$$

$$iU^\dagger(t,t_0)(H(t) - H(t))U(t,t_0) = 0. \tag{2.8}$$

So the operator U is always unitary. If the Hamiltonian is time independent then we can easily integrate Eq. (2.4). To obtain

$$U(t,t_0) = \mathbb{I} - i\int_{t_0}^{t} H(t')U(t',t_0)dt'. \tag{2.9}$$

As $U(t,t_0)$ appears on both sides of the equation, it can be solved iteratively, we use a subindex i to denote the number of iterations. The way it works is that we make increasingly good approximations on the right hand side, As a first step we make $U(t,t_0) = \mathbb{I}$ on the right hand side:

$$U_1(t,t_0) = \mathbb{I} - i\int_{t_0}^{t} H(t')dt', \tag{2.10}$$

in the next iteration we approximate $U(t,t_0) = U_1(t,t_0)$

$$U_2(t,t_0) = \mathbb{I} - i\int_{t_0}^{t} H(t')dt' - \int_{t_0}^{t} H(t')dt' \int_{t_0}^{t'} H(t'')dt''. \tag{2.11}$$

If we follow the same procedure N times we well finally obtain

$$U_N(t,t_0) = \mathbb{I} + \sum_{n=1}^{N}(i)^n \int_{t_0}^{t} dt_1 \int_{t_0}^{t_1} dt_2 \int_{t_0}^{t_2} dt_3 \cdots \int_{t_0}^{t_{n-1}} dt_n H(t_1)H(t_2)\dots H(t_n). \tag{2.12}$$

In the limit of $N \to \infty$, this would represent the exact solution for the evolution operator. Eq. (2.12) is known as the Dyson series. If the Hamiltonian commutes at different times ($[H(t_j), H(t_i)]$) then the series reduces to

$$U(t,t_0) = e^{-i\int_{t_0}^{t} H(t)dt}. \tag{2.13}$$

To rewrite Eq. (2.12) in a similar way to Eq. (2.13), we introduce the time ordering operator

$$\mathcal{T}[H(t_1)H(t_2)\dots H(t_n)] = H(t_{j1})H(t_{j2})\dots H(t_{jn}), \tag{2.14}$$

$$\text{where} \quad t_{j1} > t_{j2} > \cdots > t_{jn}. \tag{2.15}$$

The time ordering is simply an instruction to reorder the Hamiltonians in such a way that the time arguments of the corresponding Hamiltonians decrease as one goes from left to right. The largest time appears in the argument of the first operator while the smallest one in the last. In order to provide a clear picture on how to use

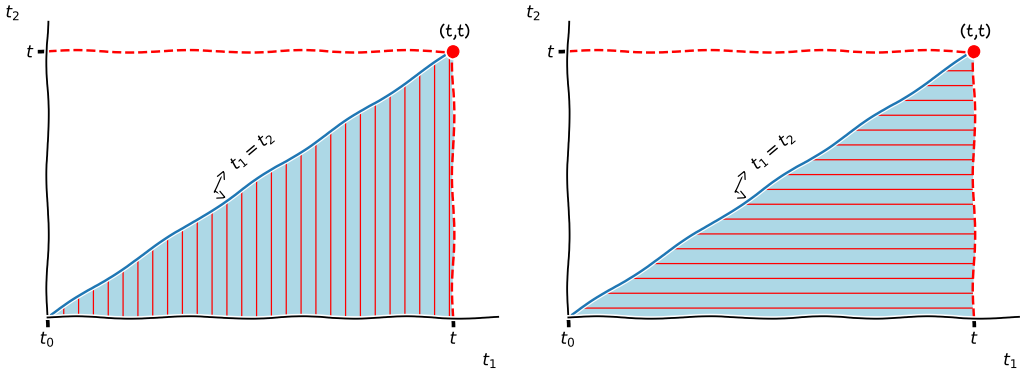

(a) $t_1 \geq t_2$ **(b)** After change of integration order

Figure 2.1: Integration region for Eq. (2.16) and the same integration region when the order of integration is exchanged,

time ordering to take Eq. (2.12) into Eq. (2.13) using the time ordering operator, let us illustrate the procedure with

$$J = \int_{t_0}^{t} dt_1 \int_{t_0}^{t_1} dt_2 H(t_1)H(t_2) = \int_{t_0}^{t} dt_1 \int_{t_0}^{t_1} dt_2 \mathcal{T}(H(t_1)H(t_2)). \tag{2.16}$$

The integration region of interest is given by the region, which we can visualize in Figure 2.1

$$t_0 \leq t_1 \leq t, \quad t_0 \leq t_2 \leq t, \quad t_2 \leq t_1. \tag{2.17}$$

As t_1 is always greater we can write

$$J = \int_{t_0}^{t} dt_1 \int_{t_0}^{t_1} dt_2 H(t_1)H(t_2) = \int_{t_0}^{t} dt_1 \int_{t_0}^{t_1} dt_2 \mathcal{T}(H(t_1)H(t_2)). \tag{2.18}$$

Notice that if we exchange the integration order in Eq. (2.16), the value of the integral does not change, to find the new integration limits it suffices to look at Fig. 2.1, so that now we obtain

$$J = \int_{t_0}^{t} dt_2 \int_{t_2}^{t} dt_1 H(t_1)H(t_2) \tag{2.19}$$

$$= \int_{t_0}^{t} dt_1 \int_{t_0}^{t_1} dt_2 H(t_1)H(t_2) = \int_{t_0}^{t} dt_1 \int_{t_0}^{t_1} dt_2 \mathcal{T}(H(t_1)H(t_2)). \tag{2.20}$$

We are allowed to use the time ordering operator because the integration area is the triangle above the diagonal $t_2 \geq t_1$. Thus

$$J = \int_{t_0}^{t} dt_1 \int_{t_1}^{t} dt_2 \mathcal{T}(H(t_1)H(t_2)) = \int_{t_0}^{t} dt_1 \int_{t_0}^{t_1} dt_2 \mathcal{T}(H(t_1)H(t_2)). \tag{2.21}$$

As time ordering will take care of the ordering for us, given the integration region. Remarkably this can be rewritten as

$$J = \frac{1}{2} \int_{t_0}^{t} dt_1 \int_{t_0}^{t} dt_2 \mathcal{T}(H(t_1)H(t_2)), \tag{2.22}$$

so that the integration limits are now decoupled. The same procedure can be generalized to all higher orders using a hypervolume (a high dimensional cube) bounded by $0 \leq t_1, t_2, t_3, \ldots, t_n \leq t$ such that $t_1 \geq t_2 \geq t_3 \geq \cdots \geq t_n$. Just as the region we just studied is $\frac{1}{2!} = \frac{1}{2}$ of a square. The bounded region in our hypervolume will represent $\frac{1}{n!}$ of the volume of the hypercube. using this we may finally rewrite Eq. (2.12) as

$$U(t, t_0) = \mathbb{I} + \mathcal{T} \sum_{n=1}^{\infty} \frac{1}{n!} \left(\int_{t_0}^{t} dt_1 H(t_1) \right)^n \tag{2.23}$$

$$= \mathcal{T} e^{-i \int_{t_0}^{t} dt_1 H(t_1)}. \tag{2.24}$$

2.2 The Evolution of Mixed states

In open quantum systems, a system of interest is coupled to an external environment. This interaction leads to correlations between the system and the environment.

If we only describe the system itself, ignoring the state of the environment, our knowledge of the system becomes "incomplete". The system can no longer be described by a single, well-defined quantum state (a "pure state"). Instead, it must be represented as a statistical mixture of different possible pure states, which is known as a mixed state. Mixed states are characterized by the density matrix

$$\rho(t_0) = \sum_{\alpha} \lambda_\alpha \left| \psi_\alpha(t_0) \right\rangle \left\langle \psi_\alpha(t_0) \right|. \tag{2.25}$$

We already know how kets evolve, they evolve according to the Schrodinger equation. In the same way we can obtain the evolution of bras by taking the adjoint in the same spirit as in the last subsection. Using the evolution operator one may write

$$\rho(t) = \sum_{\alpha} \lambda_\alpha U(t, t_0) \left| \psi_\alpha(t) \right\rangle \left\langle \psi_\alpha(t) \right| U^\dagger(t, t_0) = U(t, t_0) \rho(t_0) U^\dagger(t, t_0). \tag{2.26}$$

If we now take the derivative of Eq. (2.26) one obtains:

$$\frac{\partial \rho(t)}{\partial t} = \frac{\partial U(t, t_0)}{\partial t} \rho(t_0) U^\dagger(t, t_0) + U(t, t_0) \rho(t_0) \frac{\partial U^\dagger(t, t_0)}{\partial t} \tag{2.27}$$

$$= -iH(t) U(t, t_0) \rho(t_0) U^\dagger(t, t_0) + iU(t, t_0) \rho(t_0) U^\dagger(t, t_0) H(t) \tag{2.28}$$

$$= -i[H(t), \rho(t)]. \tag{2.29}$$

This equation is known as the Von-Neumann equation. Usually one might want to define the superoperator $\mathcal{L}(t)[\bullet] = -i[H(t), \bullet]$ so that one may write this equation as

$$\frac{\partial \rho(t)}{\partial t} = \mathcal{L}(t) \rho(t). \tag{2.30}$$

If we follow the same procedure we did to obtain Eq. (2.23) we obtain a formal solution for this equation in terms of the time ordering operator

$$\rho(t) = \mathcal{T} e^{\int_{t_0}^{t} \mathcal{L}(t_1) dt_1} \rho(t_0). \tag{2.31}$$

Chapter 3

Dynamical Pictures: Heisenberg and Interaction

In the previous sections we were working in the Schrodinger picture, meaning that states evolve in time while operators remain constant. In some situations, it may be beneficial to consider other reference frames (usually called pictures), where operators are changing in time, while states may or may not. In open quantum systems derivations are carried out almost exclusively in the Interaction or Heisenberg pictures. To go from the Schrodinger picture to any other, one assumes that at some fixed initial time (t_0) observables in both pictures coincide, that is $\rho(t_0) = \rho^P(t_0)$ where the superscript P denotes the other frame of reference and no superscript denotes the Schrodinger picture. The expectation value of an observable is given by

$$\langle A(t)\rangle = \mathrm{Tr}\left[A(t)U(t,t_0)\rho(t_0)U^\dagger(t,t_0)\right], \tag{3.1}$$

We will use this, to derive the equations of motion in other pictures.

3.1 The Heisenberg Picture

The Heisenberg picture of quantum mechanics is the one where states remain constant but operators evolve in time, kind of the opposite to the Schrodinger picture. In this sense, using the cyclic property of the trace it is easy to see that

$$\langle A(t)\rangle = \mathrm{Tr}\left[A(t)U(t,t_0)\rho(t_0)U^\dagger(t,t_0)\right] = \mathrm{Tr}\left[U^\dagger(t,t_0)A(t)U(t,t_0)\rho(t_0)\right] \tag{3.2}$$

$$= \mathrm{Tr}\left[A^H(t)\rho(t_0)\right]. \tag{3.3}$$

So the operators in the Heisenberg and Schrodinger pictures are related by

$$A^H(t) = U^\dagger(t,t_0)A(t)U(t,t_0), \tag{3.4}$$

Using this, it is easy to obtain the equation of motion for a given operator, we simply take the derivative of Eq. (3.4)

$$\frac{dA^H(t)}{dt} = \frac{\partial U^\dagger(t,t_0)}{\partial t}A(t)U(t,t_0) + U^\dagger(t,t_0)\frac{\partial A(t)}{\partial t}U(t,t_0) + U^\dagger(t,t_0)A(t)\frac{\partial U(t,t_0)}{\partial t}. \tag{3.5}$$

We already determined the derivative of the evolution operator Eq. (2.4), substituting we obtain

$$\frac{dA^H(t)}{dt} = i\left(U^\dagger(t,t_0)H(t)A(t)U(t,t_0) - U^\dagger(t,t_0)A(t)H(t)U(t,t_0)\right) + \underbrace{\frac{\partial A_H(t)}{\partial t}}_{\frac{\partial A_H(t)}{\partial t}=U^\dagger(t,t_0)\frac{\partial A(t)}{\partial t}U(t,t_0)}. \tag{3.6}$$

Notice that the product of operators in the Schrodinger picture becomes the product of operators in the Heisenberg picture:

$$AB \xrightarrow{Heisenberg\ \ Picture} U^\dagger(t,t_0)ABU(t,t_0) \tag{3.7}$$

$$= U^\dagger(t,t_0)A\underbrace{U(t,t_0)U^\dagger(t,t_0)}_{\mathbb{I}}BU(t,t_0) \tag{3.8}$$

$$= A^H B^H. \tag{3.9}$$

So we can write our equation of motion as

$$\frac{dA^H(t)}{dt} = i[H^H(t)A^H(t) - A^H(t)H^H(t)] + \frac{\partial A_H(t)}{\partial t} \tag{3.10}$$

$$= i[H^H(t), A^H(t)] + \frac{\partial A_H(t)}{\partial t}. \tag{3.11}$$

3.2 The Interaction Picture

There is one more dynamical picture we will consider, namely, the interaction picture. Let us begin by the interaction picture. Let us begin by splitting our Hamiltonian into two terms namely

$$H = H_0 + H_I(t), \tag{3.12}$$

where H_0 is time independent. Let us introduce the operators

$$U_0(t,t_0) = e^{-iH_0(t-t_0)}, \tag{3.13}$$

and

$$U_I(t,t_0) = U_0^\dagger(t,t_0)U(t,t_0). \tag{3.14}$$

Then the expectation value of an observable may be rewritten as:

$$\langle A(t)\rangle = \mathrm{Tr}\left[A(t)U_0(t,t_0)U_I(t,t_0)\rho(t_0)U_I^\dagger(t,t_0)U^\dagger(t,t_0)\right] \tag{3.15}$$

$$= \mathrm{Tr}\left[U^\dagger(t,t_0)A(t)U_0(t,t_0)U_I(t,t_0)\rho(t_0)U_I^\dagger(t,t_0)\right] \tag{3.16}$$

$$= \mathrm{Tr}\left[A^I(t)\rho^I(t)\right]. \tag{3.17}$$

Here we have used

$$A^I(t) = U^\dagger(t,t_0)A(t)U_0(t,t_0), \tag{3.18}$$
$$\rho^I(t) = U_I(t,t_0)\rho(t_0)U_I^\dagger(t,t_0). \tag{3.19}$$

Notice that when we substitute the $U_0(t,t_0)U_I(t,t_0) = U(t,t_0)$ into Eq. (2.4) we get

$$i\frac{\partial U_0(t,t_0)U_I(t,t_0)}{\partial t} = (H_I(t) + H_0)U_0(t,t_0)U_I(t,t_0). \tag{3.20}$$

Then

$$i\frac{\partial U_0(t,t_0)U_I(t,t_0)}{\partial t} = iU_0(t,t_0)\frac{\partial U_I(t,t_0)}{\partial t} + i\frac{\partial U_0(t,t_0)}{\partial t}U_I(t,t_0) \tag{3.21}$$
$$= iU_0(t,t_0)\frac{\partial U_I(t,t_0)}{\partial t} + H_0U_0(t,t_0)U_I(t,t_0), \tag{3.22}$$

and substituting this into Eq. (3.20) we may write

$$iU_0(t,t_0)\frac{\partial U_I(t,t_0)}{\partial t} = H_I(t)U_0(t,t_0)U_I(t,t_0) \tag{3.23}$$
$$i\frac{\partial U_I(t,t_0)}{\partial t} = U_0^\dagger(t,t_0)H_I(t)U_0(t,t_0)U_I(t,t_0) \tag{3.24}$$
$$i\frac{\partial U_I(t,t_0)}{\partial t} = H_I^I(t)U_I(t,t_0), \tag{3.25}$$

subjected to the initial condition $U_I(t_0,t_0) = \mathbb{I}$. Then following the same procedure we used to derive Eq. (2.27) we obtain the evolution in the interaction picture as

$$\frac{\partial \rho^I(t)}{\partial t} = -i[H^I(t), \rho^I(t)]. \tag{3.26}$$

Most of our derivations will be done in this picture. As a consequence most of the dynamics in this thesis are obtained in this picture. At times, we need to interpret results in the Schrodinger picture, in those cases we simply perform the appropriate rotation on the density matrices. Figures throughout the thesis are in the Schrodinger picture.

Part II

Dynamics of open quantum systems

Chapter 4

The general Coarse-Graining Idea

In general terms, an open quantum system is simply a system we are interested in (system S). There is also a larger quantum system, which we call B, that acts as an effective environment to our system S. Each system represents a subsystem in the larger $S + B$ space. The dynamics of system S will be a mixture of its own internal dynamics and the effect the system B has on it. If we are not willing to keep all relevant degrees of freedom from system B, we will need to devise an effective way to incorporate the effect of B into S. This is what coarse-graining is in a nutshell: to come up with a simplified model of a complex system by smoothing out some of the details, in this case, the environment's degrees of freedom. In general, such an effective description will no longer be represented by unitary Hamiltonian dynamics. Instead, it is usually modeled by some effective reduced dynamics, which is typically dissipative. Figure 4.1, illustrates this concept

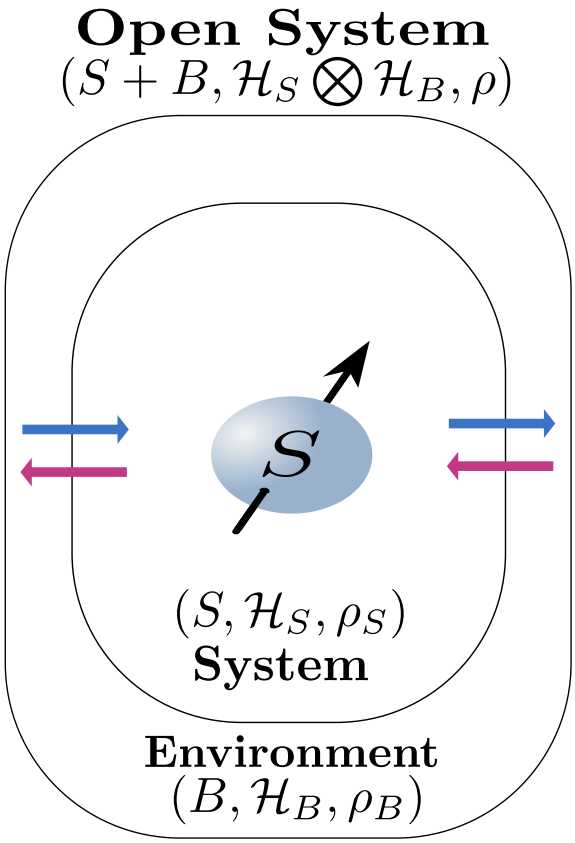

Figure 4.1: An illustration of an open system: we basically partition everything into a subsystem we care about —the system —and the rest —the environment. The idea of coarse-graining is to model the interaction between the system and environment with as little information about the environment as possible.

We may write our Hamiltonian as:

$$H(t) = H_S + H_B + H_{SB}(t). \tag{4.1}$$

Typically, our system B is what we call a bath, reservoir, or environment. A reservoir is a system with an infinite number of degrees of freedom such that one might consider that its frequencies (basically its energy) form a continuum [B1, B2, B7], which is important from the point of view of irreversibility because otherwise we would have Poincare recurrences [B1, 38, 39]. Since we are only interested in the behavior of the system and not the bath, we will trace out the information of the bath to obtain our system observables, that is, we will define our system observables by

$$\langle A \rangle = \mathrm{Tr}[A\rho_S(t)], \tag{4.2}$$

where

$$\rho_S(t) = \mathrm{Tr}_B\Big[\rho(t)\Big]. \tag{4.3}$$

The dynamics of our system of interest lost unitarity as we took a partial trace. Our $\rho(t)$ evolves unitarily according to Eq. (2.27) by taking the partial trace, we obtain:

$$\frac{\mathrm{d}\rho_S(t)}{\mathrm{d}t} = -i\mathrm{Tr}_B\Big[[H(t), \rho(t)]\Big]. \tag{4.4}$$

Even though it looks like a simple equation, finding an adequate approximation of this equation, in a way that it can be solved with efficient computer methods, is the main task when working in open quantum systems theory.

Chapter 5

Feynman Vernon Influence Functional

5.1 Introduction

In this section, we will examine the exact evolution of open quantum systems using the Feynman Vernon influence functional. Our derivation is based on [4, 14, 24]. While we won't use this technique for simulation directly, we will derive most other methods from it, providing a new way to derive them that makes the connection between the Redfield and cumulant equations easy to understand. The derivation in this manuscript is done for Bosonic environments, for a derivation in the Fermionic case see [14]. We start with the total Hamiltonian, of the system and environment given by

$$H = H_S(t) + H_B + H_{SB}. \tag{5.1}$$

When going into the interaction picture (see chapter 3.2), the dynamics is described in terms of

$$H_{SB}(t) = \mathcal{T} \exp^{\frac{i}{\hbar}\int_0^t H_S(\tau)+H_B d\tau} H_{SB} \mathcal{T} \exp^{\frac{-i}{\hbar}\int_0^t H_S(\tau)+H_B d\tau}, \tag{5.2}$$

while the density matrix of the system reads

$$\rho^I(t) = \mathcal{T} \exp^{-\frac{i}{\hbar}\int_0^t H_S(\tau)+H_B d\tau} \rho \mathcal{T} \exp^{\frac{i}{\hbar}\int_0^t H_S(\tau)+H_B d\tau}. \tag{5.3}$$

The density matrix evolves according to the Von-Neumann equation

$$\frac{\partial \rho^I(t)}{\partial t} = -\frac{i}{\hbar}[H_{SB}(t), \rho^I(t)]. \tag{5.4}$$

The Von-Neumann equation has the formal solution Eq. (2.31)

$$\rho^I(t) = \mathcal{T} e^{\int_0^t -\frac{i}{\hbar}[H_{SB}(\tau),\ \bullet] d\tau} \rho^I(0), \tag{5.5}$$

where $\bullet$ denotes the operator it acts on, so that

$$[H_{SB}(\tau),\ \bullet]\rho = [H_{SB}(\tau),\ \rho]. \tag{5.6}$$

In this section, we will derive the Feynman-Vernon Influence Functional formulation for Gaussian Bosonic environments. We will make the following assumptions

1. The system is initially in a product state

   $\rho(0) = \rho_S(0) \otimes \rho_B(0)$.

2. The system is linearly coupled to the environment[1]; the interaction Hamiltonian can be written as

   $$H_{SB}(t) = A(t) \otimes B(t). \tag{5.7}$$

[1] Meaning the coupling is linear in creation and annihilation operators of the environment

3. The bath is Gaussian, meaning we can get a full description of the bath using its first and second moments.

4. The derivations in this and subsequent chapters holds for arbitrary Gaussian Bosonic environments, but whenever we explicitly calculate the coefficients (Γ, S, ξ) we assumed the bath to be in thermal equilibrium

$$\rho_B^I(0) = \frac{e^{-\beta H_B}}{Tr[e^{-\beta H_B}]}. \tag{5.8}$$

5. The coupling operators to the bath have been centralized

$$\langle B(0) \rangle = 0, \tag{5.9}$$

so that we may describe the bath in terms of its second moment (the free correlation function only) [2]

6. Throughout the rest of this thesis we will assume the environment is Bosonic.

Box 5.1.1: Is centralization a viable assumption?

For an arbitrary initial state, this must always be satisfied which means

$$\mathrm{Tr}_B \Big[H_{SB}(t) \rho_B^I \Big] = 0 \tag{5.10}$$

Notice this doesn't seem very general, as one might guess most Hamiltonians won't satisfy this. However, one can always shift the interaction hamiltonian such that this is fullfilled by making the change

$$H_{SB}^{'} = H_{SB} - \mathrm{Tr}_B \Big[H_{SB} \rho_B \Big] \otimes \mathbb{I}_B \tag{5.11}$$

$$H_S^{'} = H_S + \mathrm{Tr}_B \Big[H_{SB} \rho_B \Big] \otimes \mathbb{I}_B \tag{5.12}$$

which follow the same dynamics, since we only substracted and added a constant. Even when this can be an issue (for example time dependent Hamiltonians), thermal environments fulfill Eq. (5.10).

5.2 First steps in the Derivation of the influence functional

Without loss of generality (apart from the constraints by the above assumptions), one may write

$$B(t) = \sum_k \left(\xi_k c_k^\dagger(t) + \overline{\xi_k} c_k(t) \right), \tag{5.13}$$

where the c_k are ladder operators either Fermionic or Bosonic, depending on the nature of the bath. Now if substitute the first assumption into Eq. (2.31) and take

[2] Gaussian systems are fully described by their covariance matrix, and the free evolution of the environment preserves Gaussianity [7]

a partial trace with respect to the bath we obtain

$$\rho_S^I(t) = Tr_B\left[\mathcal{T} e^{\int_0^t -\frac{i}{\hbar}[H_{SB}(\tau),\ \bullet]d\tau}\left(\rho_S^I(0)\otimes\rho_B^I(0)\right)\right]. \tag{5.14}$$

If we now Taylor expand the exponential we obtain

$$\rho_S^I(t) = \sum_{n=0}^{\infty}\frac{1}{n!}Tr_B\left[\mathcal{T}\left(\int_0^t -\frac{i}{\hbar}[H_{SB}(\tau),\ \bullet]d\tau\right)^n\left(\rho_S^I(0)\otimes\rho_B^I(0)\right)\right]. \tag{5.15}$$

By conveniently defining

$$\rho_n^I(t) = \frac{1}{n!}Tr_B\left[\mathcal{T}\left(\int_0^t -\frac{i}{\hbar}[H_{SB}(\tau),\ \bullet]d\tau\right)^n\left(\rho_S^I(0)\otimes\rho_B^I(0)\right)\right]. \tag{5.16}$$

We may express the evolution of the system as

$$\rho_S^I(t) = \sum_{n=0}^{\infty}\rho_n^I(t). \tag{5.17}$$

Since we assumed that the bath operators are centralized, then we have

$$\langle c_k\rangle = Tr_B[c_k\rho_B^I(0)] = 0, \tag{5.18}$$

using this, immediately we find that

$$\rho_1^I = \rho_{2n+1}^I = 0. \tag{5.19}$$

This means that in order to obtain the evolution, we only need to be concerned with the even powers.

5.3 The second order term

We can obtain all correlators from the second order correlator by using Wick's theorem [B8]. We begin by exploring the first non-zero term of our evolution Eq. (5.17)

$$\rho_2^I(t) = -\frac{1}{2\hbar^2}Tr_B\left[\mathcal{T}\int_0^t dt_2\int_0^t dt_1\,[H_{SB}(t_2),\bullet]\,[H_{SB}(t_1),\bullet]\,\rho_S^I(0)\otimes\rho_B^I\right]. \tag{5.20}$$

This can be rewritten as

$$\rho_2^I(t) = -\frac{1}{2\hbar^2}Tr_B\left[\mathcal{T}\int_0^t dt_2\int_0^t dt_1\Big[H_{SB}(t_2),\Big[H_{SB}(t_1),\rho_S^I(0)\otimes\rho_B^I\Big]\Big]\right]. \tag{5.21}$$

Let us substitute H_{SB} explicitly and take a closer look at the double commutator

$$C = \Big[H_{SB}(t_2),\Big[H_{SB}(t_1),\rho_S^I(0)\otimes\rho_B^I\Big]\Big] \tag{5.22}$$

$$= \Big[B(t_2)\otimes A(t_2),\Big[B(t_1)\otimes A(t_1),\rho_S^I(0)\otimes\rho_B^I\Big]\Big] \tag{5.23}$$

$$\begin{aligned}
&= A(t_1)A(t_2)\rho_S^I(0)\otimes B(t_1)B(t_2)\rho_B^I(0)\\
&- A(t_1)\rho_S^I(0)A(t_2)\otimes B(t_1)\rho_B^I(0)B(t_2)\\
&+ \rho_S^I(0)A(t_1)A(t_2)\otimes\rho_B^I(0)B(t_1)B(t_2)\\
&- A(t_2)\rho_S^I(0)A(t_1)\otimes B(t_2)\rho_B^I(0)B(t_1).
\end{aligned} \tag{5.24}$$

From this point on we will no longer write the tensor product explicitly, but it is always there between operators that belong to the Hilbert space of the system $\mathcal{H}_S$ and operators belonging to the Hilbert space of the bath $\mathcal{H}_B$. If we now trace out the bath from Eq. (5.22), and introduce the short hand notations $A_i = A(t_i)$,$\langle A\rangle = Tr_B[A\rho_B^I(0)]$ and $C(t_1,t_2) = \langle B(t_1)B(t_2)\rangle$, then we may rewrite the double commutator as

$$\begin{aligned} O(t_1,t_2) = Tr_B[C] = A_2A_1\rho_S^I(0)C(t_2,t_1) - A_1\rho_S^I(0)A_2C(t_2,t_1) \\ + \rho_S^I(0)A_1A_2C(t_1,t_2) - A_2\rho_S^I(0)A_1C(t_1,t_2). \end{aligned} \tag{5.25}$$

Notice the time ordering operator from Eq. (5.21) only acts on Eq. (5.25). By applying it explicitly, one may write

$$\rho_2^I(t) = -\frac{1}{2\hbar^2}\int_0^t dt_2 \int_0^t dt_1 \left(\theta(t_2-t_1)O(t_1,t_2) + \theta(t_1-t_2)O(t_2,t_1)\right), \tag{5.26}$$

where θ is the Heaviside-theta function given by:

$$\theta(x) = \begin{cases} 1, & \text{for } x \geq 0 \\ 0, & \text{for } x < 0 \end{cases} \tag{5.27}$$

Now if we exchange the times in the second part of the integral and apply the Heaviside-theta function to simplify the integral we obtain

$$\rho_2^I(t) = -\frac{1}{2\hbar^2}\int_0^t dt_2 \int_0^t dt_1 \left(\theta(t_2-t_1)O(t_1,t_2) + \theta(t_1-t_2)O(t_2,t_1)\right) \tag{5.28}$$

$$= -\frac{1}{2\hbar^2}\int_0^t dt_2 \int_0^t dt_1 \left(\theta(t_2-t_1)O(t_1,t_2) + \theta(t_2-t_1)O(t_1,t_2)\right) \tag{5.29}$$

$$= -\frac{1}{\hbar^2}\int_0^t dt_2 \int_0^t dt_1 \theta(t_2-t_1)O(t_1,t_2) \tag{5.30}$$

$$= -\frac{1}{\hbar^2}\int_0^t dt_2 \int_0^{t_2} dt_1 O(t_1,t_2). \tag{5.31}$$

Notice that

$$C(t_1,t_2) = \langle B(t_1)B(t_2)\rangle = \overline{\langle (B(t_1)B(t_2))^\dagger\rangle} = \overline{C(t_1,t_2)}, \tag{5.32}$$

where we used the cyclic property of the trace and $Tr[A] = \overline{Tr[A^\dagger]}$ for a matrix A. We may split the correlators $C(t_i,t_j)$ into its real and imaginary parts and using the fact that $C(t_i,t_j) = \overline{C(t_j,t_i)}$, we also adopt the notation

$$Re(C(t_i,t_j)) = \Gamma_{i,j}, \tag{5.33}$$

$$Im(C(t_i,t_j)) = S_{i,j}. \tag{5.34}$$

Using all of the above one may write Eq. (5.21) as

$$\rho_2^I(t) = -\frac{1}{\hbar^2}\int_0^t dt_2 \int_0^{t_2} dt_1 \Big(\left(A_2A_1\rho_S^I(0) - A_1\rho_S^I(0)A_2\right)\overline{C(t_1,t_2)} + \left(\rho_S^I(0)A_1A_2 - A_2\rho_S^I(0)A_1\right)C(t_1,t_2)\Big) \tag{5.35}$$

$$= -\frac{1}{\hbar^2}\int_0^t dt_2 \int_0^{t_2} dt_1 \Big[\Gamma_{1,2}\left(A_2A_1\rho_S^I(0) - A_1\rho_S^I(0)A_2 + \rho_S^I(0)A_1A_2 - A_2\rho_S^I(0)A_1\right) + iS_{1,2}\left(A_1\rho_S^I(0)A_2 - A_2A_1\rho_S^I(0) + \rho_S^I(0)A_1A_2 - A_2\rho_S^I(0)A_1\right)\Big]. \tag{5.36}$$

Then notice that

$$[A_2,[A_1,\rho_S^I(0)]] = A_2A_1\rho_S^I(0) - A_1\rho_S^I(0)A_2 + \rho_S^I(0)A_1A_2 - A_2\rho_S^I(0)A_1, \tag{5.37}$$

$$[A_2,\{A_1,\rho_S^I(0)\}] = A_1\rho_S^I(0)A_2 - A_2A_1\rho_S^I(0) + \rho_S^I(0)A_1A_2 - A_2\rho_S^I(0)A_1. \tag{5.38}$$

Thus finally, one may write Eq. (5.21) as

$$\rho_2^I(t) = -\frac{1}{\hbar^2}\int_0^t dt_2 \int_0^{t_2} dt_1 \Big(\Gamma_{1,2}[A_2,[A_1,\rho_S^I(0)]] + iS_{1,2}[A_2,\{A_1,\rho_S^I(0)\}]\Big) \tag{5.39}$$

$$= -\frac{1}{\hbar^2}\int_0^t dt_2 \int_0^{t_2} dt_1 \Big(\Gamma_{1,2}[A_2,[A_1,\bullet]] + iS_{1,2}[A_2,\{A_1,\bullet\}]\Big)\rho_S^I(0). \tag{5.40}$$

5.4 The Fourth Order term

Even though it is not necessary, deriving the fourth order term gives intuition on how to derive the higher order $2nth$ order terms, for that reason let us derive it here for completeness

$$\rho_4^I(t) = \frac{1}{4!\hbar^4}\int_0^t dt_4 \int_0^t dt_3 \int_0^t dt_2 \int_0^t dt_1 Tr_B\Big[\mathcal{T}\left[H_{SB}(t_4),\bullet\right]\left[H_{SB}(t_3),\bullet\right] \left[H_{SB}(t_2),\bullet\right]\left[H_{SB}(t_1),\bullet\right]\rho_S^I(0)\otimes\rho_B^I\Big]. \tag{5.41}$$

Before splitting into system and bath operators, let us state Wick's Theorem

Box 5.4.1: Wick's Theorem for Bosonic environments

Wick's Theorem [B8] states that the product of creation and annihilation operators ABCDEF ... can be expressed as

$$ABCDEF\ldots =: ABCDEF\cdots : + \sum_{singles} : A^{\bullet}B^{\bullet}CDEF\cdots : + \sum_{doubles} : A^{\bullet}B^{\bullet\bullet}C^{\bullet\bullet}D^{\bullet}EF\cdots : + \ldots \tag{5.42}$$

Where :: denotes normal ordering and $\bullet$ denotes contractions which are given by

$$A^{\bullet}B^{\bullet} \equiv AB - : AB : \tag{5.43}$$

$\bullet\bullet$ just denotes a second different contraction and so on. In other words, a string of creation and annihilation operators can be rewritten as the normal-ordered product of the string, plus the normal-ordered product after all single contractions among operator pairs, plus all double contractions, etc., plus all full contractions.
In terms of fields what this means is that[a]

$$\langle \phi_{2n}\phi_{2n-1}\phi_{2n-2}\ldots\phi_1\rangle = \sum_{a.p.p}\prod_{k,l}\langle\phi_k\phi_l\rangle \tag{5.44}$$

Where a.p.p means all possible ways of picking pairs. Which allows us to obtain all 2n correlators from the second order correlator.

[a] Our B operators are similar to the free fields in QFT but discrete

Now for higher orders, it is convenient to use the notation

$$L_A^{(1)} = A\bullet \quad L_A^{(2)} = \bullet A. \tag{5.45}$$

Then we can write commutators as

$$[A\otimes B, \rho_S^I\otimes\rho_B^I] = A\rho_S^I B\rho_B^I - \rho_S^I A\rho_B^I B \tag{5.46}$$
$$= L_A^{(1)}\rho_S^I L_B^{(1)}\rho_B^I + L_A^{(2)}\rho_S^I L_B^{(2)}\rho_B^I \tag{5.47}$$
$$= \sum_i^2 L_A^{(i)}\rho_S^I \otimes L_B^{(i)}\rho_B^I. \tag{5.48}$$

This allows us to rewrite Eq. (5.41) as

$$\rho_4^I(t) = \frac{1}{4!\hbar^4}\int_0^t dt_4\int_0^t dt_3\int_0^t dt_2\int_0^t dt_1 \sum_{i,j,k,l}^2 \mathcal{T}L_{A_4}^{(i)}L_{A_3}^{(j)}L_{A_2}^{(k)}L_{A_1}^{(l)}\rho_S^I(0) \otimes Tr_B\left[\mathcal{T}L_{B_4}^{(i)}L_{B_3}^{(j)}L_{B_2}^{(k)}L_{B_1}^{(l)}\rho_B^I\right]. \tag{5.49}$$

Where we used

$$\mathcal{T}\sum_i^2 L_A^{(i)}\rho_S^I\otimes L_B^{(i)}\rho_B^I = \sum_i^2 \mathcal{T}L_A^{(i)}\rho_S^I\otimes\mathcal{T}L_B^{(i)}\rho_B^I. \tag{5.50}$$

If we now focus on the term that depends only on bath operators and apply Wick's Theorem we may write

$$\langle \mathcal{T} L^{(i)}_{B_4} L^{(j)}_{B_3} L^{(k)}_{B_2} L^{(l)}_{B_1} \rangle = \overbrace{\langle \mathcal{T} L^{(i)}_{B_4} L^{(j)}_{B_3} \rangle \langle \mathcal{T} L^{(k)}_{B_2} L^{(l)}_{B_1} \rangle}^{O_1} + \overbrace{\langle \mathcal{T} L^{(i)}_{B_4} L^{(k)}_{B_2} \rangle \langle \mathcal{T} L^{(j)}_{B_3} L^{(l)}_{B_1} \rangle}^{O_2} + \underbrace{\langle \mathcal{T} L^{(i)}_{B_4} L^{(l)}_{B_1} \rangle \langle \mathcal{T} L^{(j)}_{B_3} L^{(k)}_{B_2} \rangle}_{O_3}. \tag{5.51}$$

Let us now add the part containing system operators to each of the three individual terms

$$Z_m = \mathcal{T}\Big(\sum_{i,j}^{2} \mathcal{T} L^{(i)}_{A_4} L^{(j)}_{A_3} \sum_{k,l}^{2} L^{(k)}_{A_2} L^{(l)}_{A_1} \Big) O_m. \tag{5.52}$$

where the sum was split this way for future convenience, then evaluating each of the terms individually we find

$$Z_1 = \mathcal{T}\Big(\sum_{i,j}^{2} \mathcal{T} L^{(i)}_{A_4} L^{(j)}_{A_3} \sum_{k,l}^{2} L^{(k)}_{A_2} L^{(l)}_{A_1} \Big) O_1 \tag{5.53}$$

$$= \mathcal{T}\Big(\sum_{i,j}^{2} L^{(i)}_{A_4} L^{(j)}_{A_3} \langle \mathcal{T} L^{(i)}_{B_4} L^{(j)}_{B_3} \rangle \sum_{k,l}^{2} L^{(k)}_{A_2} L^{(l)}_{A_1} \langle \mathcal{T} L^{(k)}_{B_2} L^{(l)}_{B_1} \rangle \Big). \tag{5.54}$$

Then

$$Z_2 = \mathcal{T}\Big(\sum_{i,j}^{2} \mathcal{T} L^{(i)}_{A_4} L^{(j)}_{A_3} \sum_{k,l}^{2} L^{(k)}_{A_2} L^{(l)}_{A_1} \Big) O_2 \tag{5.55}$$

$$= \mathcal{T}\Big(\sum_{i,j}^{2} L^{(i)}_{A_4} L^{(j)}_{A_3} \langle \mathcal{T} L^{(i)}_{B_4} L^{(k)}_{B_2} \rangle \sum_{k,l}^{2} L^{(k)}_{A_2} L^{(l)}_{A_1} \langle \mathcal{T} L^{(j)}_{B_3} L^{(l)}_{B_1} \rangle \Big). \tag{5.56}$$

Since time ordering will be applied on the system operators, we may switch $L^{(l)}_{A_3}$ and $L^{(l)}_{A_3}$, as they will be arranged accordingly after the time ordering operation, we also rearrange the splitting of the sums to obtain

$$Z_2 = \mathcal{T}\Big(\sum_{i,k}^{2} L^{(i)}_{A_4} L^{(k)}_{A_2} \langle \mathcal{T} L^{(i)}_{B_4} L^{(k)}_{B_2} \rangle \sum_{j,l}^{2} L^{(j)}_{A_3} L^{(l)}_{A_1} \langle \mathcal{T} L^{(j)}_{B_3} L^{(l)}_{B_1} \rangle \Big). \tag{5.57}$$

Similarly we may write

$$Z_3 = \mathcal{T}\Big(\sum_{i,l}^{2} L^{(i)}_{A_4} L^{(l)}_{A_1} \langle \mathcal{T} L^{(i)}_{B_4} L^{(l)}_{B_1} \rangle \sum_{j,k}^{2} L^{(j)}_{A_3} L^{(k)}_{A_2} \langle \mathcal{T} L^{(j)}_{B_3} L^{(k)}_{B_2} \rangle \Big). \tag{5.58}$$

Now notice that they all differ only by the dummy variables for integration, exchanging the t_i accordingly in each Z_m one finds that

$$Z_1 = Z_2 = Z_3, \tag{5.59}$$

so then one may write Eq. (5.41) as

$$\rho_4^I(t) = \frac{3}{4!\hbar^4}\int_0^t dt_4\int_0^t dt_3\int_0^t dt_2\int_0^t dt_1 \mathcal{T}\Big(\sum_{i,j}^{2} L_{A_4}^{(i)}L_{A_3}^{(j)}\langle \mathcal{T} L_{B_4}^{(i)}L_{B_3}^{(j)}\rangle \times \sum_{k,l}^{2} L_{A_2}^{(k)}L_{A_1}^{(l)}\langle \mathcal{T} L_{B_2}^{(k)}L_{B_1}^{(l)}\rangle\Big). \tag{5.60}$$

Before continuing, notice

$$Z = \mathcal{T}\Big(\sum_{i,j}^{2} L_{A_4}^{(i)}L_{A_3}^{(j)}\langle \mathcal{T} L_{B_4}^{(i)}L_{B_3}^{(j)}\rangle \sum_{k,l}^{2} L_{A_2}^{(k)}L_{A_1}^{(l)}\langle \mathcal{T} L_{B_2}^{(k)}L_{B_1}^{(l)}\rangle\Big) \tag{5.61}$$

$$= \mathcal{T}\Big(\sum_{i,j,k,l}^{2} L_{A_4}^{(i)}L_{A_3}^{(j)}L_{A_2}^{(k)}L_{A_1}^{(l)}\langle \mathcal{T} L_{B_4}^{(i)}L_{B_3}^{(j)}\rangle\langle \mathcal{T} L_{B_2}^{(k)}L_{B_1}^{(l)}\rangle\Big) \tag{5.62}$$

$$= \sum_{i,j,k,l}^{2}\langle \mathcal{T} L_{B_4}^{(i)}L_{B_3}^{(j)}\rangle\langle \mathcal{T} L_{B_2}^{(k)}L_{B_1}^{(l)}\rangle \mathcal{T}\Big(L_{A_4}^{(i)}L_{A_3}^{(j)}L_{A_2}^{(k)}L_{A_1}^{(l)}\Big). \tag{5.63}$$

Now let us do the time ordering on the bath operators by making use of Eq. (5.50)

$$\begin{aligned} Z = &\sum_{i,j,k,l}^{2}\Big(\theta(t_4-t_3)\langle L_{B_4}^{(i)}L_{B_3}^{(j)}\rangle + \theta(t_3-t_4)\langle L_{B_3}^{(j)}L_{B_4}^{(i)}\rangle\Big) \\ &\times\Big(\theta(t_2-t_1)\langle L_{B_2}^{(k)}L_{B_1}^{(l)}\rangle + \theta(t_1-t_2)\langle L_{B_1}^{(l)}L_{B_2}^{(k)}\rangle\Big)\,\mathcal{T}\Big(L_{A_4}^{(i)}L_{A_3}^{(j)}L_{A_2}^{(k)}L_{A_1}^{(l)}\Big) \qquad (5.64)\\ = &\sum_{i,j,k,l}^{2}\Big(\theta(t_4-t_3)\theta(t_2-t_1)\langle L_{B_4}^{(i)}L_{B_3}^{(j)}\rangle\langle L_{B_2}^{(k)}L_{B_1}^{(l)}\rangle \\ &+\theta(t_4-t_3)\theta(t_1-t_2)\langle L_{B_4}^{(i)}L_{B_3}^{(j)}\rangle\langle L_{B_1}^{(I)}L_{B_2}^{(k)}\rangle \\ &+\theta(t_3-t_4)\theta(t_2-t_1)\langle L_{B_3}^{(j)}L_{B_4}^{(i)}\rangle\langle L_{B_2}^{(k)}L_{B_1}^{(l)}\rangle \\ &+\theta(t_3-t_4)\theta(t_1-t_2)\langle L_{B_3}^{(j)}L_{B_4}^{(i)}\rangle\langle L_{B_1}^{(I)}L_{B_2}^{(k)}\rangle\Big)\mathcal{T}\left(L_{A_4}^{(i)}L_{A_3}^{(j)}L_{A_2}^{(k)}L_{A_1}^{(l)}\right). \qquad (5.65)\end{aligned}$$

Directly substituting into Eq. (5.60) and directly applying the theta Heaviside functions on the integration limits we obtain

$$\begin{aligned}\rho_4^I(t) = \frac{1}{8\hbar^4}\sum_{i,j,k,l}^{2}\Bigg(&\int_0^t dt_4\int_0^{t_4} dt_3\int_0^t dt_2\int_0^{t_2} dt_1\langle L_{B_4}^{(i)}L_{B_3}^{(j)}\rangle\langle L_{B_2}^{(k)}L_{B_1}^{(l)}\rangle\mathcal{T}\left(L_{A_4}^{(i)}L_{A_3}^{(j)}L_{A_2}^{(k)}L_{A_1}^{(l)}\right) \\ &+\int_0^t dt_4\int_0^{t_4} dt_3\int_0^t dt_1\int_0^{t_1} dt_2\langle L_{B_4}^{(i)}L_{B_3}^{(j)}\rangle\langle L_{B_1}^{(I)}L_{B_2}^{(k)}\rangle\mathcal{T}\left(L_{A_4}^{(i)}L_{A_3}^{(j)}L_{A_1}^{(l)}L_{A_2}^{(k)}\right) \\ &+\int_0^t dt_3\int_0^{t_3} dt_4\int_0^t dt_2\int_0^{t_2} dt_1\langle L_{B_3}^{(j)}L_{B_4}^{(i)}\rangle\langle L_{B_2}^{(k)}L_{B_1}^{(l)}\rangle\mathcal{T}\left(L_{A_3}^{(j)}L_{A_4}^{(i)}L_{A_2}^{(k)}L_{A_1}^{(l)}\right) \\ &+\int_0^t dt_3\int_0^{t_3} dt_4\int_0^t dt\int_0^{t_1} dt_2\langle L_{B_3}^{(j)}L_{B_4}^{(i)}\rangle\langle L_{B_1}^{(I)}L_{B_2}^{(k)}\rangle\mathcal{T}\left(L_{A_3}^{(j)}L_{A_4}^{(j)}L_{A_1}^{(l)}L_{A_2}^{(k)}\right)\Bigg), \qquad (5.66)\end{aligned}$$

and we used the fact that we can freely swap the ordering of the operators inside the time ordering as

$$\mathcal{T}\left(L^{(i)}_{A_r}L^{(j)}_{A_s}L^{(k)}_{A_q}L^{(l)}_{A_p}\right)=\mathcal{T}\left(L^{(i)}_{A_s}L^{(j)}_{A_r}L^{(k)}_{A_p}L^{(l)}_{A_q}\right). \tag{5.67}$$

Using this one may notice that all the integrals are the same, since their only differences are their mute indices t_i. The four integrals or 2^n for our $n=2$ are all the same. So that one may finally write

$$\rho^I_4(t)=\frac{1}{2\hbar^4}\sum_{i,j,k,l}^{2}\int_0^t dt_4\int_0^{t_4}dt_3\int_0^t dt_2\int_0^{t_2}dt_1\langle L^{(i)}_{B_4}L^{(j)}_{B_3}\rangle\langle L^{(k)}_{B_2}L^{(l)}_{B_1}\rangle\mathcal{T}\left(L^{(i)}_{A_4}L^{(j)}_{A_3}L^{(k)}_{A_2}L^{(l)}_{A_1}\right) \tag{5.68}$$

$$=\frac{\mathcal{T}}{2\hbar^4}\int_0^t dt_4\int_0^{t_4}dt_3\sum_{i,j}^{2}L^{(i)}_{A_4}L^{(j)}_{A_3}\langle L^{(i)}_{B_4}L^{(j)}_{B_3}\rangle\int_0^t dt_2\int_0^{t_2}dt_1\sum_{k,l}^{2}L^{(k)}_{A_2}L^{(l)}_{A_1}\langle L^{(k)}_{B_2}L^{(l)}_{B_1}\rangle. \tag{5.69}$$

Now using Eq. (5.22), Eq. (5.25), and Eq. (5.46), gives us by direct substitution that

$$\sum_{i,j}^{2}L^{(k)}_{A_2}L^{(l)}_{A_1}\langle L^{(k)}_{B_2}L^{(l)}_{B_1}\rangle=O(t_1,t_2). \tag{5.70}$$

Then using the results from the previous section we obtain

$$\rho^I_4(t)=\frac{\mathcal{T}}{2\hbar^4}\int_0^t dt_4\int_0^{t_4}dt_3\Big(\Gamma_{3,4}[A_4,[A_3,\bullet]]+iS_{3,4}[A_4,\{A_3,\bullet\}]\Big)$$
$$\times\int_0^t dt_2\int_0^{t_2}dt_1\Big(\Gamma_{1,2}[A_2,[A_1,\bullet]]+iS_{1,2}[A_2,\{A_1,\bullet\}]\Big)\rho^I_S(0). \tag{5.71}$$

Again, the only difference are the mute indices in integration, so by renaming them we may finally write

$$\rho^I_4(t)=\frac{\mathcal{T}}{2\hbar^4}\left(\int_0^t dt_2\int_0^{t_2}dt_1\Big(\Gamma_{1,2}[A_2,[A_1,\bullet]]+iS_{1,2}[A_2,\{A_1,\bullet\}]\Big)\right)^2\rho^I_S(0). \tag{5.72}$$

5.5 The $2n^{th}$ order terms

We follow the exact same procedure as in the previous section, only this time we do so in general. We can write the $2n^{th}$ order contribution as

$$\rho^I_{2n}(t)=\frac{(-1)^n}{2n!\hbar^{2n}}\int_0^t dt_{2n}\cdots\int_0^t dt_1\sum_{i,j,k,l,\ldots}^{2}\mathcal{T}L^{(i)}_{A_{2n}}L^{(j)}_{A_{2n-1}}\ldots L^{(k)}_{A_2}L^{(l)}_{A_1}\rho^I_S(0)$$
$$\otimes Tr_B\Big[\mathcal{T}L^{(i)}_{B_{2n}}L^{(j)}_{B_{2n-1}}\ldots L^{(k)}_{B_2}L^{(l)}_{B_1}\rho^I_B\Big], \tag{5.73}$$

and just like we did before we now want simplify this by rewriting the pair-wise partitions of the bath operators,for the 4^{th} we had three partitions, however for the

$2n^{th}$ order we have M terms, which correspond to the unique pair combinations of $2n$ elements.[14, 24, B8]

$$M = (2n-1)!! = \frac{2n!}{2^n n!}. \tag{5.74}$$

Just like before we can make up something analogous to the Z_i for each of the M terms, and just like in the previous case the M terms will be equal to each other so that one then has

$$\rho^I_{2n}(t) = \frac{(-1)^n M\mathcal{T}}{2n!\hbar^{2n}}\left(\int_0^t dt_{2n}\int_0^t dt_{2n-1}\int_0^t dt_{2n-2}\int_0^t dt_{2n-3}Z_{2n-3}\times\dots \right.$$
$$\left.\times\cdots\times\int_0^t dt_4\int_0^t dt_3\int_0^t dt_2\int_0^t dt_1 Z_1\right) \tag{5.75}$$

If we now apply the time ordering explicitly on the correlators we will obtain n multiplications by two just like in the last subsection

$$\rho^I_{2n}(t) = \frac{(-1)^n 2^n M\mathcal{T}}{2n!\hbar^{2n}}\int_0^t dt_{2n}\int_0^{t_{2n}} dt_{2n-1}O(t_{2n-1},t_{2n})\cdots\int_0^t dt_2\int_0^{t_2} dt_1 O(t_1,t_2). \tag{5.76}$$

Now finally by substituting M explicitly and renaming the mute indices we obtain

$$\rho^I_{2n}(t) = \frac{(-1)^n\mathcal{T}}{n!\hbar^{2n}}\left(\int_0^t dt_2\int_0^{t_2} dt_1\left(\Gamma_{1,2}[A_2,[A_1,\bullet]] + iS_{1,2}[A_2,\{A_1,\bullet\}]\right)\right)^n\rho^I_S(0). \tag{5.77}$$

5.6 Exact time evolution as a Time ordered exponential

Using the results of the previous sections, we can now substitute them into Eq. (2.31) and under the assumptions considered, obtain exact evolution of the system by

$$\rho^I(t) = \sum_{n=0}^{\infty}\rho^I_{2n}(t) = \mathcal{T}e^{\frac{-1}{\hbar^2}\int_0^t dt_2\int_0^{t_2} dt_1\left(\Gamma_{1,2}[A_2,[A_1,\bullet]]+iS_{1,2}[A_2,\{A_1,\bullet\}]\right)}\rho^I_S(0). \tag{5.78}$$

This is usually rewritten in terms of the second order Cumulant [40–42]

$$W(t_2) = -\frac{1}{\hbar^2}\int_0^{t_2} dt_1\left(\Gamma_{1,2}[A_2,[A_1,\bullet]] + iS_{1,2}[A_2,\{A_1,\bullet\}]\right), \tag{5.79}$$

so that the exact evolution can be written as

$$\rho^I_S(t) = \mathcal{T}e^{\int_0^t dt_2 W(t_2)}\rho^I_S(0). \tag{5.80}$$

It will be convenient to denote

$$\mathcal{K}_2(t) = \int_0^t dt_2 W(t_2), \tag{5.81}$$

so finally we have

$$\rho_S^I(t) = \mathcal{T} e^{\mathcal{K}_2(t)} \rho_S^I(0). \tag{5.82}$$

Let us remark that

$$\frac{\partial \mathcal{K}_2(t)}{\partial t} = W(t). \tag{5.83}$$

While seemingly trivial it will make the connection between the cumulant and Redfield generators, first mentioned in [A2], easier to understand as we obtain that result from a deeper connection. Note that while this chapter contains $\hbar$ explicitly, in all other sections we work in natural units so $\hbar = 1$.

Chapter 6

The Redfield Equation

The Redfield equation is a quantum master equation that describes the dynamics of a system's reduced density matrix under the assumption of weak coupling to an environment. Usually derived using a second-order Dyson expansion [B1], it provides a fundamental description of the system's evolution.

A defining feature of the Redfield equation is that it is time-local, meaning the derivative of the density matrix at time t depends only on the state at that same time. However, the rates within the equation are time-dependent and incorporate memory of the bath's correlation functions, making the resulting dynamics generally Non-Markovian. While powerful the Redfield equation is not completely positive and may lead to unphysical solutions [A3, B1, 43], however, in its range of validity this is rarely a concern.

6.1 Derivation from the Feynman Vernon Influence Functional

This derivation is an original contribution, it is analogous to the derivation of the "Redfield Plus" equation from HEOM [44, 45] . We would like to remark that "Redfield Plus" is just the Nakajima-Zwanzig equation at second order (see B.27). We start from Eq. (5.82) and use the fact that the derivative of the exponential map is given by

$$\frac{d}{dt}e^{X(t)} = \int_0^1 e^{(1-s)X(t)}\frac{dX(t)}{dt}e^{sX(t)}. \tag{6.1}$$

Then we have

$$\frac{\partial \rho_S^I(t)}{\partial t} = \mathcal{T}\left(\int_0^1 e^{(1-s)\mathcal{K}_2(t)}\frac{d\mathcal{K}_2(t)}{dt}e^{s\mathcal{K}_2(t)}\rho_S^I(0)ds\right) \tag{6.2}$$

$$= \mathcal{T}\left(\int_0^1 e^{(1-s)\mathcal{K}_2(t)}W(t)e^{s\mathcal{K}_2(t)}\underbrace{\mathcal{T}e^{-\mathcal{K}_2(t_1)}\mathcal{T}e^{\mathcal{K}_2(t_1)}}_{\mathbb{I}}\rho_S^I(0)ds\right) \tag{6.3}$$

$$= \mathcal{T}\left(\int_0^1 e^{(1-s)\mathcal{K}_2(t)}W(t)e^{s\mathcal{K}_2(t)}\mathcal{T}e^{-\mathcal{K}_2(t_1)}\rho_S^I(t_1)ds\right), \tag{6.4}$$

where we used t_1 the dummy time label in Eq. (5.79) to keep everything inside the parentheses "time-ordered" [1]. Now in order to get the lowest non tirivial order

[1] Not strictly time ordered, but the expression after the approximation will be time ordered.

we truncate the product of the operators in such a way that we only keep second order in system enviroment coupling (remember all $W(t)$ and $\mathcal{K}_2(t)$ are second order quantities in the coupling constant). Expanding the exponentials into their Taylor series and keeping the lowest order in the coupling [2] we obtain

$$\frac{\partial \rho_S^I(t)}{\partial t} = \mathcal{T}\left(\int_0^1 W(t)\rho_S^I(t_1)ds \right) = W(t)\rho_S^I(t_1), \tag{6.5}$$

where we used the fact that the product was already time ordered. Substituting Eq. (5.79) we obtain

$$\frac{\partial \rho_S^I(t)}{\partial t} = -\frac{1}{\hbar^2}\int_0^{t_2} dt_1 \left(\Gamma_{1,2}[A_2,[A_1,\rho_S^I(t_1)]] + iS_{1,2}[A_2,\{A_1,\rho_S^I(t_1)\}] \right), \tag{6.6}$$

which is the second order Nakajima-Zwanzig equation [A2, B1, B2]. This expression might be unfamiliar to the reader, so if we take a step back and use Eqs. Eq. (5.21),Eq. (5.28),Eq. (5.35),Eq. (5.39) and Eq. (5.79) we can see by direct substitution that

$$\begin{aligned} W(t_2) &= -\frac{1}{\hbar^2}\int_0^{t_2} dt_1 \left(\Gamma_{1,2}[A_2,[A_1,\bullet]] + iS_{1,2}[A_2,\{A_1,\bullet\}] \right) && (6.7)\\ &= -\frac{1}{\hbar^2}\int_0^{t_2} dt_1 \Big((A_2A_1\bullet - A_1\bullet A_2)\,\overline{C(t_1-t_2)} \\ &+ (\bullet A_1A_2 - A_2\bullet A_1)\,C(t_1-t_2)\Big) && (6.8)\\ &= -\frac{1}{\hbar^2}\int_0^{t_2} dt_1 Tr_B\left[\left[H_{SB}(t_2),\left[H_{SB}(t_1),\bullet\otimes\rho_B^I\right]\right]\right]. && (6.9) \end{aligned}$$

Using this the second order Nakajima-Zwanzig equation reads (See Eq. (B.27))

$$\frac{\partial \rho_S^I(t)}{\partial t} = -\frac{1}{\hbar^2}\int_0^{t} dt_1 Tr_B\left[\left[H_{SB}(t),\left[H_{SB}(t_1),\rho_S^I(t_1)\otimes\rho_B^I\right]\right]\right]. \tag{6.10}$$

If we now perform the Markov approximation, that is we assume the evolution of the system only depends on the current state, which means $\rho_S^I(s)\approx\rho_S^I(t)$ we obtain

$$\frac{\partial \rho_S^I(t)}{\partial t} = -\int_0^{t} dt_1 \mathrm{Tr}_B\Big[[H_{SB}^I(t),[H_{SB}^I(t_1),\rho_S^I(t)\otimes\rho_B^I]]\Big], \tag{6.11}$$

which is the Redfield equation[B1, B9]. For simplicity, let us make the change of variable $t_1 = t-s$, then

$$\frac{\partial \rho_S^I(t)}{\partial t} = -\int_0^{t} ds \mathrm{Tr}_B\Big[[H_{SB}^I(t),[H_{SB}^I(t-s),\rho_S^I(t)\otimes\rho_B^I]]\Big]. \tag{6.12}$$

Substituting the jump operator representation of the system operators (see appendix A) into Eq. (6.7) we obtain

$$\begin{aligned} \frac{\partial \rho_S^I(t)}{\partial t} &= -\sum_{\omega,\omega'}\int_0^t ds C(s)e^{i\omega' t}e^{-i\omega(t-s)}\left(A^\dagger(\omega')A(\omega)\rho_S^I(t) - A(\omega)\rho_S^I(t)A^\dagger(\omega')\right) \\ &-\sum_{\omega,\omega'}\int_0^t ds\overline{C}(s)e^{-i\omega' t}e^{i\omega(t-s)}\left(\rho_S^I(t)A^\dagger(\omega)A(\omega') - A(\omega')\rho_S^I(t)A^\dagger(\omega)\right). \end{aligned} \tag{6.13}$$

[2] Basically substituting all exponentials by Identity

We define

$$\Gamma(\omega,t)=\int_0^t ds e^{i\omega s}\langle B^\dagger(t)B(t-s)\rangle_B, \tag{6.14}$$

and

$$\Gamma(\omega,\omega',t)=e^{i(\omega'-\omega)t}\int_0^t ds e^{i\omega s}\langle B^\dagger(t)B(t-s)\rangle_B=e^{i(\omega'-\omega)t}\Gamma(\omega,t). \tag{6.15}$$

One might finally write

$$\begin{aligned}\frac{\partial\rho_S^I(t)}{\partial t}&=\sum_{\omega,\omega'}\Gamma(\omega,\omega',t)\left(A(\omega)\rho_S^I(t)A^\dagger(\omega')-A^\dagger(\omega')A(\omega)\rho_S^I(t)\right)\\&+\sum_{\omega,\omega'}\overline{\Gamma}(\omega,\omega',t)\left(A(\omega')\rho_S^I(t)A^\dagger(\omega)-\rho_S^I(t)A^\dagger(\omega)A(\omega')\right),\end{aligned} \tag{6.16}$$

or in a simpler way

$$\frac{\partial\rho_S^I(t)}{\partial t}=\sum_{\omega,\omega'}\Gamma(\omega,\omega',t)\left(A(\omega)\rho_S^I(t)A^\dagger(\omega')-A^\dagger(\omega')A(\omega)\rho_S^I(t)\right)+H.C, \tag{6.17}$$

where H.C means Hermitian conjugate. It is convenient to split the integral of correlation functions into its real and imaginary parts. This allows for the separation of the coherent dynamics (Lamb-shift) and the dissipation induced by the environment (Decay). In this spirit we define

$$\Gamma(\omega,\omega',t)=\frac{\gamma(\omega,\omega',t)}{2}+iS(\omega,\omega',t), \tag{6.18}$$

so that

$$\gamma(\omega,\omega',t)=\Gamma(\omega,\omega',t)+\overline{\Gamma}(\omega,\omega',t), \tag{6.19}$$

$$S(\omega,\omega',t)=\frac{\Gamma(\omega,\omega',t)-\overline{\Gamma}(\omega,\omega',t)}{i}. \tag{6.20}$$

Now we can rewrite Eq. (6.16), in terms of γ and S as

$$\begin{aligned}\frac{\partial\rho_S^I(t)}{\partial t}&=\sum_{\omega,\omega'}\left(\frac{\gamma(\omega,\omega',t)}{2}+iS(\omega,\omega',t)\right)\left(A(\omega)\rho_S^I(t)A^\dagger(\omega')-A^\dagger(\omega')A(\omega)\rho_S^I(t)\right)\\&+\sum_{\omega,\omega'}\left(\frac{\gamma(\omega,\omega',t)}{2}-iS(\omega,\omega',t)\right)\left(A(\omega')\rho_S^I(t)A^\dagger(\omega)-\rho_S^I(t)A^\dagger(\omega)A(\omega')\right).\end{aligned} \tag{6.21}$$

Notice that we are free to rename the mute indices in each of the independent terms in the sum. Using this we rewrite Eq. (6.21) as

$$\begin{aligned}\frac{\partial\rho_S^I(t)}{\partial t}&=\sum_{\omega,\omega'}\left(\frac{\gamma(\omega,\omega',t)}{2}+iS(\omega,\omega',t)\right)\left(A(\omega)\rho_S^I(t)A^\dagger(\omega')-A^\dagger(\omega')A(\omega)\rho_S^I(t)\right)\\&+\sum_{\omega,\omega'}\left(\frac{\gamma(\omega,\omega',t)}{2}-iS(\omega,\omega',t)\right)\left(A(\omega')\rho_S^I(t)A^\dagger(\omega)-\rho_S^I(t)A^\dagger(\omega)A(\omega')\right)\end{aligned} \tag{6.22}$$

$$\begin{aligned}&=\sum_{\omega,\omega'}\frac{\gamma(\omega,\omega',t)}{2}\left(2A(\omega')\rho_S^I(t)A^\dagger(\omega)-\rho_S^I(t)A^\dagger(\omega)A(\omega')-A^\dagger(\omega')A(\omega)\rho_S^I(t)\right)\\&+i\sum_{\omega,\omega'}S(\omega,\omega',t)\left(\rho_S^I(t)A^\dagger(\omega)A(\omega')-A^\dagger(\omega')A(\omega)\rho_S^I(t)\right),\end{aligned} \tag{6.23}$$

which we can finally write in a way similar to the Gorini-Kossakowski-Lindblad-Sudarshan (GKLS) form[3]

$$\frac{\partial \rho_S^I(t)}{\partial t} = \sum_{\omega,\omega'} \gamma(\omega,\omega',t)\left(A(\omega')\rho_S^I(t)A^\dagger(\omega) - \frac{\{A^\dagger(\omega)A(\omega'),\rho_S^I(t)\}}{2}\right) + i\sum_{\omega,\omega'} S(\omega,\omega',t)\Big[\rho_S^I(t), A^\dagger(\omega)A(\omega')\Big]. \tag{6.24}$$

Reverting to Eq. (6.15) and defining

$$\tilde{\gamma}(\omega,t) = \Gamma(\omega,t) + \overline{\Gamma}(\omega,t), \tag{6.25}$$

$$\tilde{S}(\omega,t) = \frac{\Gamma(\omega,t) - \overline{\Gamma}(\omega,t)}{i}, \tag{6.26}$$

we may write it in the Schrodinger picture as

$$\frac{\partial \rho_S(t)}{\partial t} = \sum_{\omega,\omega'} \tilde{\gamma}(\omega,t)\left(A(\omega')\rho_S(t)A^\dagger(\omega) - \frac{\{A^\dagger(\omega)A(\omega'),\rho_S(t)\}}{2}\right) + i\Big[\rho_S(t), H_S + \sum_{\omega,\omega'} \tilde{S}(\omega,t)A^\dagger(\omega)A(\omega')\Big]. \tag{6.27}$$

6.2 Decay rates and Lamb-shift from decaying exponentials

At this point, if we wanted to simulate the Redfield equation, we would need to perform numerical integration to compute both the Lamb-shift and the decay rates, and we need to do that for each t, which makes the simulation of the Redfield equation relatively costly, when compared to the standard GKLS equation. Recently, we proposed a method to compute these decay rates and the Lamb shift algebraically [1]. As we will see in section 15, this greatly reduces the simulation time of the Redfield equation without sacrificing accuracy. Typically one would substitute Eq. (1.23) into Eq. (6.25) to obtain

$$\Gamma(\omega,t) = \int_0^t ds e^{i\omega s} C(s) \tag{6.28}$$

$$= \frac{1}{\pi}\int_0^t ds e^{i\omega s}\int_0^\infty d\omega' J(\omega')\left(\cos(\omega' s)\coth\left(\frac{\beta\omega'}{2}\right) - i\sin(\omega' s)\right) \tag{6.29}$$

$$= \frac{1}{\pi}\int_0^\infty d\omega' J(\omega')\left(A(\omega,\omega')\coth\left(\frac{\beta\omega'}{2}\right) - B(\omega,\omega')\right), \tag{6.30}$$

where

$$A(\omega,\omega') = \frac{i\left(\omega + e^{i\omega t}(-\omega\cos(\omega' t) + i\omega'\sin(\omega' t))\right)}{(\omega-\omega')(\omega+\omega')}, \tag{6.31}$$

$$B(\omega,\omega') = \frac{i\left(\omega' + e^{i\omega t}(-\omega'\cos(\omega' t) + i\omega\sin(\omega' t))\right)}{(\omega-\omega')(\omega+\omega')}, \tag{6.32}$$

[3] It is not in GKLS form because the matrix $\gamma = (\gamma(i,j,t))_{i=\omega,j=\omega'}$ is not necessarily positive semidefinite for every t

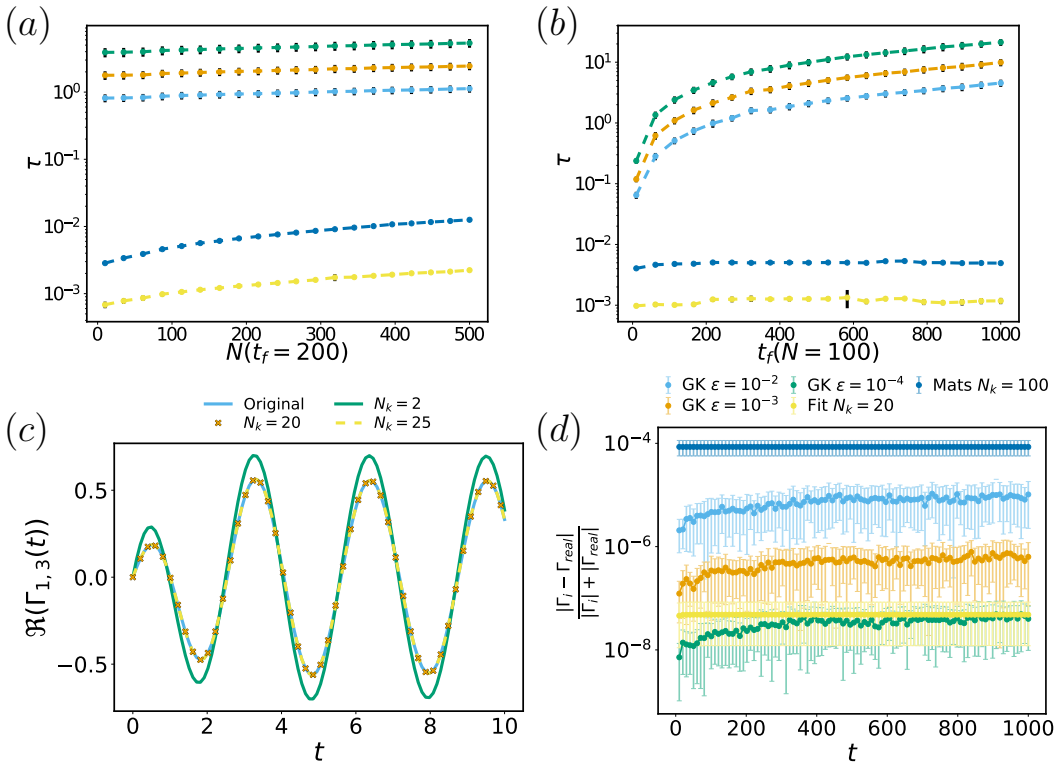

Figure 6.1: The plots show how the approximation of the decay rates affects their computation time and precision, In these plots, "GK" stands for the Gauss-Kronrod method for integration with 21 points, and ϵ is the tolerance required during the numerical integration procedure. These plots are aggregate from 50 randomly chosen ω, ω'. a) The time it takes to compute the decay rate with a fixed final time $t_f = 200$ using N time steps, measured in seconds. We see for this particular example one gets a speed up of around 3 orders of magnitude. b)Time taken to obtain decay rates as time increases with $N = 100$ points, measured in seconds. c) Example of a decay rate computed with the decaying exponential representation d) Average symmetric mean absolute percentage error of the approximation of the decay rates. For these plots we used an underdamped spectral density Eq. (1.78) with $T = 0.05$, $\omega_c = 1.2$, $\alpha = 1$ and $\Gamma = 2$.

and perform numerical integration. However, we can avoid numerical integration by using the decaying exponential representation of the environment. Using it, one has

$$\Gamma(\omega, t) = \sum kc_k \int_0^t ds e^{-(\nu_k - i\omega)s} = \sum_k c_k \frac{1 - e^{-(\nu_k - i\omega)t}}{(\nu_k - i\omega)}. \tag{6.33}$$

Those expressions allow us to obtain both the decay rate and the Lamb-Shift of the Redfield equation easily.

In Fig. 6.1 a) and b) as they are around three orders of magnitude faster than computing the integrals. We see how it becomes advantageous to use the decaying exponential representation of the environment. This speed up is specially important for high dimensional systems where the number of decay rates grows quickly with the number of transitions. Furthermore, it helps us construct the Lamb-Shift easily by directly avoiding the poles in integration that lead to principal value integrals [A2, 46, 47]. In Fig. 6.1 d) we see the average symmetric mean absolute percentage error of the approximation of the decay rates. We used this instead of relative error

because as 6.1 c) shows, the decay rate can be zero at multiple moments in time (when $\omega \neq \omega'$). How much precision we need in our decay rates is not straightforward to answer, but in practice when computing examples we find that errors lower than $10^{-3}|\omega - \omega'|$ do not typically affect the dynamics.

The approximation also helps us to avoid numerical integration problems due to the rapidly oscillating functions [48, 49], which often are computationally costly and can induce large errors when using standard quadrature techniques, unlike in most methods that use this sort of approximation [4, 12, 15, 21–23, 25, 30, 50]. The simulation is not limited by the number of exponents; in fact the cost of estimating either the decay rates of Lamb-shift is $O(m)$, where m is the number of exponents used in the approximation.

6.3 The Bloch-Redfield equation

The Redfield equation Eq. (6.24), while compact and time local is still a set of non-autonomous differential equations, which is in general difficult to solve, and is usually approximated to the Bloch-Redfield equation [A3, B1, 51, 52]. The first step to do this is to assume that the bath correlation function decays fast and the memory effects are short lived, in such a way that $s \gg \tau_B$ where τ_B is the time that it takes the correlation function to decay. This approximation is valid provided that the time scale of evolution of the system τ_S (the time it takes the system to relax to equilibrium) is much greater than τ_B, namely $\tau_S \gg \tau_B$. What this achieves in practice is to make out integrals independent of time (since we assumed all relevant time scales to be much greater than τ_B we may take $t \to \infty$ in Eq. (6.14)) such it becomes "the one-sided Fourier Transform" [4]

$$\Gamma(\omega, \infty) = \Gamma(\omega) = \int_0^\infty ds e^{i\omega s} \langle B^\dagger(t) B^\dagger(t-s) \rangle_B \tag{6.34}$$

$$= \int_0^\infty ds e^{i\omega s} \langle B^\dagger(s) B^\dagger(0) \rangle_B. \tag{6.35}$$

The same notation will follow all other coefficients, so that now equation Eq. (6.24) becomes

$$\frac{\partial \rho_S(t)}{\partial t} = \sum_{\omega,\omega'} \tilde{\gamma}(\omega) \left(A(\omega') \rho_S(t) A^\dagger(\omega) - \frac{\{A^\dagger(\omega) A(\omega'), \rho_S(t)\}}{2} \right)$$
$$+ i \Big[\rho_S(t), H_S + \sum_{\omega,\omega'} \tilde{S}_{LS}(\omega) A^\dagger(\omega) A(\omega') \Big], \tag{6.36}$$

where

$$\tilde{\gamma}(\omega) = \lim_{t\to\infty} \tilde{\gamma}(\omega, t), \tag{6.37}$$

$$\tilde{A}(\omega) = \lim_{t\to\infty} \tilde{S}(\omega, t). \tag{6.38}$$

[4] Though it is usually called this way in physics, it is just a particular case of a Laplace transformation

Notice that $\tilde{\gamma}$ is just the power spectrum of the environment Eq. (6.34);

$$\begin{aligned}
\tilde{\gamma}(\omega) &= \Gamma(\omega) + \overline{\Gamma}(\omega) && (6.39)\\
&= \int_0^\infty ds e^{i\omega s}\langle B^\dagger(s)B(0)\rangle_B + \int_0^\infty ds e^{-i\omega s}\overline{\langle B^\dagger(s)B(0)\rangle_B} && (6.40)\\
&= \int_0^\infty ds e^{i\omega s}\langle B^\dagger(s)B(0)\rangle_B + \int_{-\infty}^0 ds e^{i\omega s}\overline{\langle B^\dagger(-s)B(0)\rangle_B} && (6.41)\\
&= \int_{-\infty}^\infty ds e^{i\omega s}\langle B^\dagger(s)B(0)\rangle_B && (6.42)\\
&= S(\omega), && (6.43)
\end{aligned}$$

where we used Eq. (1.24). In the literature, usually this is written in terms of the Redfield Tensor [53], however this is not relevant for the purposes of this thesis.

6.4 The GKLS Davies Equation

As mentioned before, when we passed from the Redfield to the Bloch-Redfield equation, we consider the regime where the correlation function of the bath must decay fast over the time scale τ_B of the evolution of the bath which is small compared to the relaxation time of our system τ_S. It is important to note that the decay of the correlations can only be strictly valid for an environment with an extremely large number of degrees of freedom such that it contains a continuum of frequencies. Let τ_I be the time scale change of our system defined by the eigenvalues of the system, specifically it roughly goes as $|\omega - \omega'|^{-1}$ where $\omega \neq \omega'$. If τ_S is large with respect to τ_I, one can neglect terms associated with $\omega \neq \omega'$, since they evolve very rapidly compared to the relaxation time and will tend to be averaged out. This means that terms with $\omega' \neq \omega$ are negligeable with respect to those where $\omega' = \omega$ (They are fast oscillating terms in comparison), and we may ignore them as an approximation.

This is usually called the secular approximation [B1]. If we neglect the terms with different frequencies (the different frequencies present in Eq. (6.36)). We finally obtain

$$\begin{aligned}
\frac{\partial \rho_S^I(t)}{\partial t} = &\sum_\omega S(\omega)\left(A(\omega)\rho_S(t)A^\dagger(\omega) - \frac{\{A^\dagger(\omega)A(\omega), \rho_S(t)\}}{2}\right)\\
&+ i\Big[\rho_S(t), H_S + \sum_\omega S_{LS}(\omega)A^\dagger(\omega)A(\omega)\Big]. \qquad (6.44)
\end{aligned}$$

This equation should be taken as a long time limit approximation [B1, B7]. It is the one most used in the literature of quantum thermodynamics due to its ease of simulation. The fact that we sum only over one Bohr frequency, greatly reduces the number of matrix operations that need to be perform, furthermore the decay rates can be obtained directly unlike in the case of Non-Markovian master equations.

Chapter 7

A CPTP map for Non Markovian Dynamics

In this section, we will describe the main method studies during the PhD, namely the cumulant equation (aka refined weak coupling limit), which was first proposed in 1989 by Alicki [54] and later rediscovered and developed by Rivas [55]. As pointed out by Rivas it is closely related to the coarse grained master equation [51, 56–58] due to having the form of the Schaller-Brandais exponent [59]. The cumulant or refined weak coupling has no extra coarse grained time parameter though, and generally performs better.

In this section we will derive it from the Feynman Vernon Influence functional, unlike the published derivations out there [A2, A4, 54, 55]. This new derivation allows for an easier interpretation of the equation as well as the relation between the Redfield and Cumulant generators. It also provides a straightforward path to obtain higher order approximations, and hopefully helps to clarify the misconception that the cumulant equation should be exact for Gaussian systems [1].

7.1 Cumulant from Feynman-Vernon

Let us begin by considering Eq. (5.82) namely

$$\rho^I(t) = \mathcal{T} e^{\int_0^t dt_2 W(t_2)} \rho_S^I(0). \tag{7.1}$$

By using the Magnus expansion [61] namely

$$\mathcal{T} e^{\int_0^t dt_2 W(t_2)} = \mathcal{T} e^{\mathcal{K}_2(t)} = e^{\Omega(t)}. \tag{7.2}$$

Where Ω is expressed in terms of an infinite series

$$\Omega(t) = \sum_k^\infty \Omega_k(t). \tag{7.3}$$

The first few terms of the series are given by

$$\Omega_1(t) = \int_0^t dt_2 W(t_2), \tag{7.4}$$

$$\Omega_2(t) = \frac{1}{2!} \int_0^t dt_2 \int_0^t dt_3 [W(t_2), W(t_3)], \tag{7.5}$$

$$\Omega_3(t) = \frac{1}{3!} \int_0^t dt_4 \int_0^t dt_2 \int_0^t dt_3 \left([W(t_2), [W(t_3), W(t_4)]] + [W(t_4), [W(t_3), W(t_2)]] \right). \tag{7.6}$$

[1] The misconception is due to the fact that since the system is Gaussian, second order moments are enough to describe it fully, so the second order Van Kampen expansion should fully contain it. This is false [60, 61]

The first order coincides with the case of scalar equations [62], it implies $[W(t_2), W(t_3)] = 0$ which is rarely the case, and from a practical point of view would be equivalent to neglecting the time ordering operator. Even when this is rarely the case we see that it can be a good approximation of open quantum system dynamics later in the text. **The cumulant equation corresponds to the first non trivial term in the Magnus expansion of the Feynman Vernon generator**. This result allows us to justify the so called conundrum of exact solutions [63] later on as in the pure dephasing case

$$\Omega_2(t) = 0. \tag{7.7}$$

Since the cumulant is the first order Magnus expansion we can now directly understand the fact that the cumulant equation is the integral of the Redfield generator Eq. (5.83)

$$\frac{\partial \mathcal{K}_2(t)}{\partial t} = W(t), \tag{5.83}$$

This relationship is useful when it comes to calculating heat currents in the weak coupling limit (See Eq. (11.20)). Now let us derive the usual form of the cumulat equation Eq. (6.7)

$$\begin{aligned}\mathcal{K}_2(t) = -\int_0^t dt_2 \int_0^{t_2} dt_1 \Big(&(A_2 A_1 \bullet - A_1 \bullet A_2)\, \overline{C(t_1 - t_2)} \\ &+ (\bullet A_1 A_2 - A_2 \bullet A_1)\, C(t_1 - t_2)\Big).\end{aligned} \tag{7.8}$$

Inspired by section 2.1 we know that we could have written this time ordering as two double integrals from zero to t, we do something analogous here. First lets separate the correlation function for positive and negative time differences. Let us rewrite this as

$$\begin{aligned}\mathcal{K}_2(t) = &-\int_0^t dt_2 \int_0^{t_2} dt_1\, (A_2 A_1 \bullet - A_1 \bullet A_2)\, C(t_2 - t_1) \\ &- \int_0^t dt_2 \int_0^{t_2} dt_1\, (\bullet A_1 A_2 - A_2 \bullet A_1)\, C(t_1 - t_2).\end{aligned} \tag{7.9}$$

We can change the limits of integration by using the theta heaviside function as

$$\begin{aligned}\mathcal{K}_2(t) = &-\int_0^t dt_2 \int_0^{t} dt_1\, (A_2 A_1 \bullet - A_1 \bullet A_2)\, C(t_2 - t_1)\theta(t_1 - t_2) \\ &- \int_0^t dt_2 \int_0^{t} dt_1\, (\bullet A_1 A_2 - A_2 \bullet A_1)\, C(t_1 - t_2)\theta(t_1 - t_2).\end{aligned} \tag{7.10}$$

We can make a change of variables in the first term so that $t_1 \leftrightarrow t_2$

$$\begin{aligned}\mathcal{K}_2(t) = &-\int_0^t dt_2 \int_0^{t} dt_1\, (A_1 A_2 \bullet - A_2 \bullet A_1)\, C(t_1 - t_2)\theta(t_2 - t_1) \\ &- \int_0^t dt_2 \int_0^{t} dt_1\, (\bullet A_1 A_2 - A_2 \bullet A_1)\, C(t_1 - t_2)\theta(t_1 - t_2).\end{aligned} \tag{7.11}$$

Then we can substitute the Heaviside theta θ by

$$\theta(x) = \frac{1+\text{sign}(x)}{2}. \tag{7.12}$$

So then we obtain

$$\begin{aligned}\mathcal{K}_2(t) = &-\int_0^t dt_2 \int_0^t dt_1 \left(A_1A_2 \bullet - A_2 \bullet A_1 + \bullet A_1A_2 - A_2 \bullet A_1\right) C(t_1-t_2) \\ &-\int_0^t dt_2 \int_0^t dt_1 \left(A_1A_2 \bullet - A_2 \bullet A_1 - \bullet A_1A_2 + A_2 \bullet A_1\right) C(t_1-t_2)\,\text{sign}(t_1-t_2).\end{aligned} \tag{7.13}$$

We can then rewrite this as

$$\begin{aligned}\mathcal{K}_2(t) = &\int_0^t dt_2 \int_0^t dt_1 \left(A_2 \bullet A_1 - \frac{\{A_1A_2, \bullet\}}{2}\right) C(t_1-t_2) \\ &-\int_0^t dt_2 \int_0^t dt_1 [A_1A_2, \bullet] C(t_1-t_2)\,\text{sign}(t_1-t_2),\end{aligned} \tag{7.14}$$

where

$$A_1 = \sum_\omega e^{i\omega t_1} A^\dagger(\omega), \tag{7.15}$$

$$A_2 = \sum_{\omega'} e^{-i\omega' t_2} A(\omega'), \tag{7.16}$$

so that

$$\begin{aligned}\mathcal{K}_2(t) = &\sum_{\omega',\omega} \int_0^t dt_2 \int_0^t dt_1 e^{i(\omega t_1 - \omega' t_2)} \left(A(\omega') \bullet A^\dagger(\omega) - \frac{\{A^\dagger(\omega)A(\omega'), \bullet\}}{2}\right) C(t_1-t_2) \\ &-\sum_{\omega',\omega} \int_0^t dt_2 \int_0^t dt_1 e^{i(\omega t_1 - \omega' t_2)} [A^\dagger(\omega)A(\omega'), \bullet] C(t_2-t_1)\,\text{sign}(t_2-t_1).\end{aligned} \tag{7.17}$$

Let us define

$$\Gamma(\omega,\omega',t) = \int_0^t dt_1 \int_0^t dt_2 e^{i(wt_1 - w't_2)} C(t_1-t_2), \tag{7.18}$$

$$\xi(\omega,\omega',t) = \iint_0^t \frac{dt_1}{2i} dt_2\,\text{sign}(t_1-t_2) e^{i(\omega t_1 - \omega' t_2)} C(t_1-t_2). \tag{7.19}$$

Then, for a Gaussian environment, the equation can be written as

$$\begin{aligned}\mathcal{K}_2(t) = &\sum_{\omega',\omega} \Gamma(\omega,\omega',t) \left(A(\omega) \bullet A^\dagger(\omega') - \frac{\{A^\dagger(\omega')A(\omega), \bullet\}}{2}\right) \\ &+ i\xi(\omega,\omega',t)[A^\dagger(\omega')A(\omega), \bullet].\end{aligned} \tag{7.20}$$

The last step to have the cumulant equation as it is often presented in the literature [A2–A4, 55, 64] is to write the Lamb-shift and decay rates in terms of the spectral density. We start from Eq. (7.18) and substitute Eq. (1.23) but first let us rewrite the latter as

$$C(t) = \frac{1}{\pi} \int_0^\infty d\omega J(\omega) \Big(\cos(\omega t)(2n(\beta,\omega)+1) - i\sin(\omega t)\Big) \tag{7.21}$$

$$= \frac{1}{\pi} \int_0^\infty d\omega J(\omega) \Big(e^{-i\omega t}(n(\beta,\omega)+1) + e^{i\omega t} n(\beta,\omega)\Big). \tag{7.22}$$

Substituting into Eq. (7.18) results in

$$\Gamma(\omega,\omega',t)=\frac{1}{\pi}\int_0^\infty d\nu J(\nu)\iint_0^t dt_1dt_2e^{i(wt_1-w't_2)}\Big(e^{-i\nu(t_1-t_2)}(n(\beta,\nu)+1) + e^{i\nu(t_1-t_2)}n(\beta,\nu)\Big). \tag{7.23}$$

We then proceed to do the time integrals for $\Gamma(\omega,\omega',t)$ using

$$e^{i(\omega t_1-\omega' t_2)}e^{\pm i\nu(t_1-t_2)}=e^{i(\omega\pm\nu)t_1}e^{i(\omega'\pm\nu)t_2} \tag{7.24}$$

$$\int_0^t e^{\pm ixs}=t\,\mathrm{sinc}\left(\frac{xt}{2}\right)e^{\pm i\frac{xt}{2}}. \tag{7.25}$$

We obtain

$$\Gamma(\omega,\omega',t)=\frac{t^2}{\pi}e^{i\frac{\omega-\omega'}{2}t}\int_0^\infty d\nu J(\nu)\left[(n(\nu,\beta)+1)\,\mathrm{sinc}\left(\frac{(\omega-\nu)t}{2}\right)\mathrm{sinc}\left(\frac{(\omega'-\nu)t}{2}\right) + n(\nu,\beta)\,\mathrm{sinc}\left(\frac{(\omega+\nu)t}{2}\right)\mathrm{sinc}\left(\frac{(\omega'+\nu)t}{2}\right)\right], \tag{7.26}$$

which is the expression often encountered in the literature [A3, A4, 64, 65]. However, using Eq. (1.42) we may recast it as

$$\Gamma(\omega,\omega',t)=\frac{t^2}{2\pi}e^{i\frac{\omega-\omega'}{2}t}\int_0^\infty d\nu\left[S(\nu)\,\mathrm{sinc}\left(\frac{(\omega-\nu)t}{2}\right) \times\mathrm{sinc}\left(\frac{(\omega'-\nu)t}{2}\right)+S(-\nu)\,\mathrm{sinc}\left(\frac{(\omega+\nu)t}{2}\right)\mathrm{sinc}\left(\frac{(\omega'+\nu)t}{2}\right)\right] \tag{7.27}$$

$$=\frac{t^2}{2\pi}e^{i\frac{\omega-\omega'}{2}t}\int_{-\infty}^\infty d\nu S(\nu)\,\mathrm{sinc}\left(\frac{(\omega-\nu)t}{2}\right)\mathrm{sinc}\left(\frac{(\omega'-\nu)t}{2}\right). \tag{7.28}$$

Notice the factor $\frac{1}{\pi}$ difference which comes from the spectral density convention difference with Eq. (1.21)[2] [55, 64]. For the Lamb-shift, writing an expression in the frequency domain is slightly more involved. Let us consider

$$\mathrm{sign}(\tau)C(\tau)=\frac{1}{2\pi}\int_{-\infty}^\infty d\nu\,\mathrm{sign}(\tau)e^{-i\nu\tau}S(\nu), \tag{7.29}$$

where we express the correlation by means of an inverse Fourier transform on Eq. (1.28)

$$\int_{-\infty}^\infty d\tau e^{i\phi\tau}\,\mathrm{sign}(\tau)C(\tau)=\frac{1}{2\pi}\int_{-\infty}^\infty d\tau\int_{-\infty}^\infty d\nu\,\mathrm{sign}(\tau)e^{-i(\nu-\phi)\tau}S(\nu). \tag{7.30}$$

But the Fourier transform of a sign function is a Principal value [66, B10]

$$\int_{-\infty}^\infty d\tau\,\mathrm{sign}(\tau)e^{-i(\nu-\phi)\tau}=2iP.V.\frac{1}{\phi-\nu}, \tag{7.31}$$

so we have

$$\int_{-\infty}^\infty d\tau e^{i\phi\tau}\,\mathrm{sign}(\tau)C(\tau)=\frac{i}{\pi}P.V.\int_{-\infty}^\infty d\nu\frac{S(\nu)}{\phi-\nu}. \tag{7.32}$$

[2]Equivalently a different convention for the correlation function without the $\frac{1}{\pi}$ factor

If we now take an inverse Fourier transform with respect to ϕ we have

$$\int_{-\infty}^{\infty}\frac{d\phi}{2\pi}e^{-i\phi\tau}\int_{-\infty}^{\infty}d\tau' e^{i\phi\tau'}\,\mathrm{sign}(\tau')C(\tau')=\int_{-\infty}^{\infty}\frac{id\phi}{2\pi^2}e^{-i\phi\tau}P.V\int_{-\infty}^{\infty}d\nu\frac{S(\nu)}{\phi-\nu}. \tag{7.33}$$

using

$$2\pi\delta(x-\alpha)=\int_{-\infty}^{\infty}dte^{i(x-\alpha)t}. \tag{7.34}$$

We finally obtain

$$\begin{aligned}\mathrm{sign}(\tau)C(\tau)&=\frac{i}{2\pi^2}\int_{-\infty}^{\infty}d\phi e^{-i\phi\tau}P.V\int_{-\infty}^{\infty}d\nu\frac{S(\nu)}{\phi-\nu} &(7.35)\\ &=\frac{i}{2\pi^2}\int_{-\infty}^{\infty}d\phi e^{-i\phi\tau}P.V\int_{0}^{\infty}d\nu\left(\frac{S(\nu)}{\phi-\nu}+\frac{S(-\nu)}{\phi+\nu}\right) &(7.36)\\ &=\frac{i}{\pi^2}\int_{-\infty}^{\infty}d\phi e^{-i\phi\tau}P.V\int_{0}^{\infty}d\nu J(\nu)\left(\frac{n(\nu,\beta)+1}{\phi-\nu}+\frac{n(\nu,\beta)}{\phi+\nu}\right). &(7.37)\end{aligned}$$

Where again we have a $\frac{1}{\pi}$ factor difference for the same reason. Substituting into Eq. (7.18) we obtain

$$\begin{aligned}\xi(\omega,\omega',t)=&\iint_0^t\frac{dt_1}{2\pi^2}dt_2e^{i(\omega t_1-\omega' t_2)}\int_{-\infty}^{\infty}d\phi e^{-i\phi(t_1-t_2)}\\ &\times P.V\int_0^{\infty}d\nu J(\nu)\left(\frac{n(\nu,\beta)+1}{\phi-\nu}+\frac{n(\nu,\beta)}{\phi+\nu}\right),\end{aligned} \tag{7.38}$$

using Eq. (7.24) we obtain

$$\begin{aligned}\xi(\omega,\omega',t)=&\frac{t^2}{2\pi^2}\int_{-\infty}^{\infty}d\phi\,\mathrm{sinc}\left(\frac{(\omega-\phi)t}{2}\right)\mathrm{sinc}\left(\frac{(\omega'-\phi)t}{2}\right)\\ &\times P.V\int_0^{\infty}d\nu J(\nu)\left(\frac{n(\nu,\beta)+1}{\phi-\nu}+\frac{n(\nu,\beta)}{\phi+\nu}\right).\end{aligned} \tag{7.39}$$

Concluding the derivation of the cumulant equation, we would like to remark that differences of $\pi, 2\pi$ and other factors are too common in the literature making it hard to compare different methods [3] which typically differ in the convention used for the derivation. The environment class in QuTiP aims at providing a standard convention to avoid these issues [A1], that convention is the one used throughout this thesis.

7.2 The Filtered Approximation for the cumulant equation

The cumulant equation from the previous sections has a structure that resembles the GKLS equation, it's completely positive and relaxes to the GKLS equation in the

[3] See the derivation for the Lamb-shift in [65] where while the results seem to agree another 2π factor needs to be taken into account due to different convention of the Fourier transform

long time limit, all desirable features. However, due to the integrals in the decay rates and Lamb-shift coefficient, it is not only unfriendly to analytical solutions, but also costly to simulate compared to the GKLS equation. We proposed an approximation of the decay rates [A4] that allow for a simpler description, while retaining, all these desirable features.

The Filtered Approximation for the cumulant equation is a different attempt at simplifying the decay rates of the cumulant equation to obtain an equation that is easier to simulate. The main idea lies in the approximation of the sinc function. for long times. In FA the decay rates of the cumulant equation are approximated by [A4]:

$$\begin{aligned}\gamma(\omega,\omega',t) &\approx \gamma^{\star}(\omega,\omega',t)\\ &= 2te^{i\frac{\omega'-\omega}{2}t}\mathrm{sinc}\left(\frac{\omega'-\omega}{2}t\right)S^{\frac{1}{2}}(\omega')S^{\frac{1}{2}}(\omega),\end{aligned} \tag{7.40}$$

One remarkable thing about FA is that it's an approximation that keeps the cumulant completely positive. It makes the cumulant easy to simulate, however, accuracy is lost in populations [A4]. Nevertheless is an useful approximation akin to the Bloch-Redfield equation.

7.3 Decay rates and Lambshift from decaying exponentials

Inspired by FA, we developed an approximation that does not compromise in accuracy and allows to calculate the decay rates from an algebraic expression. The approximation is based on the decaying exponential approximation for the correlation function described in section 1.1.

7.3.1 Approximation of the Decay rates

We start from Eq. (7.18) taking into account that the correlation function satisfies

$$C(-t) = \overline{C}(t). \tag{7.41}$$

It is convenient to split the integral into the regions with $t_1 > t_2$,$t_2 > t_1$, as follows

$$\begin{aligned}\Gamma(\omega,\omega',t) = &\int_0^t dt_1 \int_0^{t_1} dt_2 e^{i(wt_1 - w't_2)}C(t_1-t_2)\\ &+ \int_0^t dt_2 \int_0^{t_2} dt_1 e^{i(wt_1 - w't_2)}C(t_1-t_2).\end{aligned} \tag{7.42}$$

Then we make the change of labels in the second integral to incorporate Eq. (7.41)

$$\Gamma(\omega,\omega',t) = \int_0^t dt_1 \int_0^{t_1} dt_2 e^{i(wt_1 - w't_2)} C(t_1 - t_2) \tag{7.43}$$

$$+ \int_0^t dt_1 \int_0^{t_1} dt_2 e^{i(wt_2 - w't_1)} C(t_2 - t_1) \tag{7.44}$$

$$= \int_0^t dt_1 \int_0^{t_1} dt_2 e^{i(wt_1 - w't_2)} C(t_1 - t_2) \tag{7.45}$$

$$+ \int_0^t dt_1 \int_0^{t_1} dt_2 e^{i(wt_2 - w't_1)} \overline{C(t_1 - t_2)}. \tag{7.46}$$

By substituting the exponential representation of the correlation function Eq. (1.71) and separating the terms in the sum one might write

$$\Gamma(\omega,\omega',t) = \sum_k \Gamma_k(\omega,\omega',t) = \sum_k c_k \int_0^t dt_1 \int_0^{t_1} dt_2 e^{i(\omega t_1 - \omega' t_2)} e^{-\nu_k (t_1 - t_2)}$$

$$+ \sum_k \overline{c_k} \int_0^t dt_1 \int_0^{t_1} dt_2 e^{i(\omega t_2 - \omega' t_1)} e^{-\overline{\nu_k}(t_1 - t_2)}, \tag{7.47}$$

Thanks to the exponential representation of the correlation function the integrals are straight-forward, carrying up the integration yields

$$\Gamma_k(\omega,\omega',t) = \frac{c_k e^{-(\nu_k - i\omega)t}}{(\nu_k - i\omega)(\nu_k - i\omega')} + \frac{\overline{c_k} e^{-(\overline{\nu_k} + i\omega')t}}{(\overline{\nu_k} + i\omega)(\overline{\nu_k} + i\omega')}$$

$$+ \frac{i c_k}{\omega - \omega'} \left(\frac{1}{(\nu_k - i\omega)} - \frac{e^{i(\omega - \omega')t}}{(\nu_k - i\omega')} \right)$$

$$+ \frac{i \overline{c_k}}{\omega - \omega'} \left(\frac{1}{(\overline{\nu_k} + i\omega')} - \frac{e^{i(\omega - \omega')t}}{(\overline{\nu_k} + i\omega)} \right) \tag{7.48}$$

Let us define

$$\chi_k(\omega,\omega',t) = \frac{c_k e^{-(\nu_k - i\omega)t}}{(\nu_k - i\omega)(\nu_k - i\omega')} + \frac{i c_k}{\omega - \omega'} \left(\frac{1}{(\nu_k - i\omega)} - \frac{e^{i(\omega - \omega')t}}{(\nu_k - i\omega')} \right), \tag{7.49}$$

then we can write the decay rates as

$$\Gamma_k(\omega,\omega,t) = \overline{\chi_k}(\omega',\omega,t) + \chi_k(\omega,\omega',t) \tag{7.50}$$

We then take the limit $\omega \to \omega'$

$$\Gamma_k(\omega,\omega,t) = \lim_{\omega \to \omega'} \Gamma_k(\omega,\omega',t) = 2\,\mathrm{Re}\left(\frac{c_k \left((\nu_k t - i\omega t - 1) + e^{-(\nu_k - i\omega)t} \right)}{(\nu_k - i\omega)^2} \right). \tag{7.51}$$

These expressions substitute Eq. 7.18, bypassing numerical integration . Notice that even when the integral is one-dimensional, it needs to be computed for every value of t, thus having an algebraic expression such as Eq. (7.48) and Eq. (7.51) is beneficial, especially when high accuracy in integration is needed. Figure 7.1 shows how it is advantageous to obtain decay rates using exponential decompositions of the environment[4].

[4]Relative error is undefined because the true value is zero at multiple instances in time, there are many alternatives for relative error in this situation, out of the possible alternatives we chose the symmetric mean absolute error.

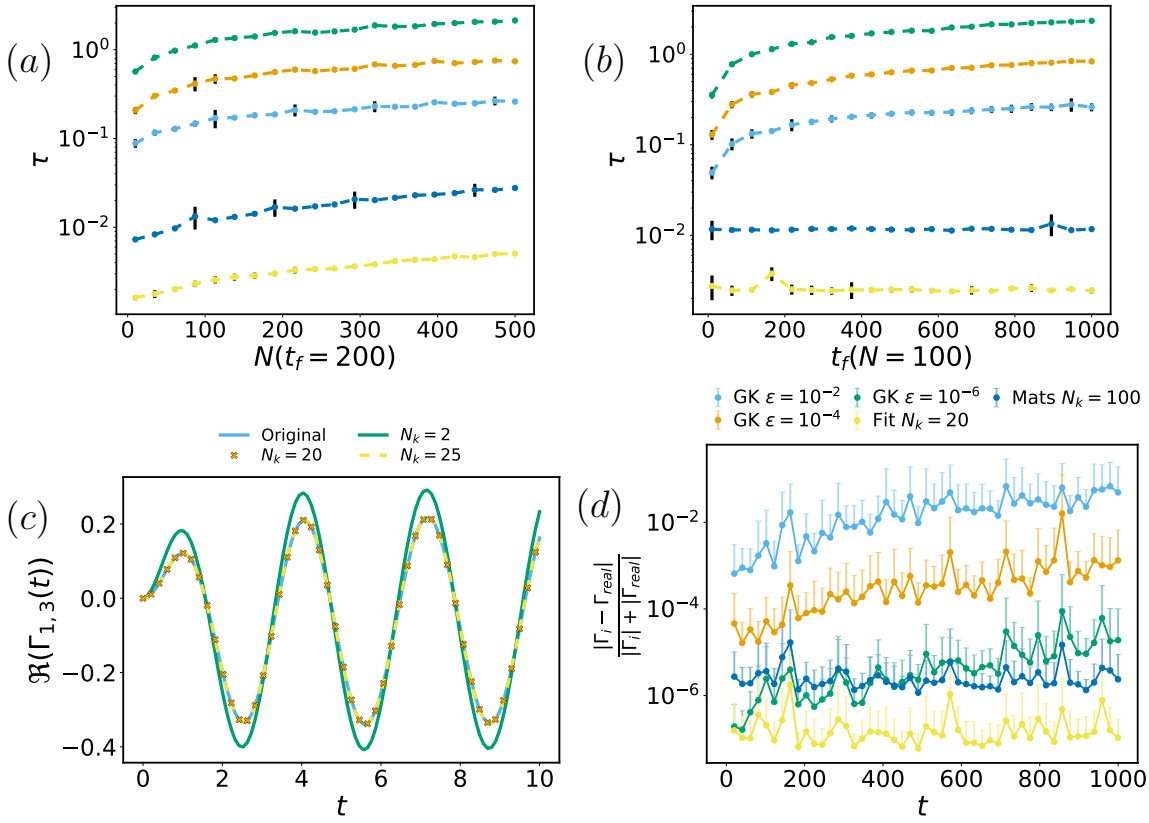

Figure 7.1: The plots show how the approximation of the decay rates affects its computation time and precision. In these plots, "GK" stands for the Gauss-Kronrod method for integration with 21 points, and ϵ is the tolerance required during the numerical integration procedure. These plots are aggregated from 50 randomly chosen ω, ω'. a) The time it takes to compute the decay rate with a fixed final time $t_f = 200$ using N time steps, we see for this particular example one gets a speed up of around 3 orders of magnitude. b)Time taken to obtain decay rates as time increases with $N = 100$ points, c) Example of a decay rate computed with the decaying exponential representation d) Average symmetric mean absolute error of the approximation of the decay rates at time t. For these plots we used an underdamped spectral density Eq. (1.78) with $T = 0.05$, $\omega_c = 1.2$, $\alpha = 1$ and $\Gamma = 2$.

7.3.2 Approximation of the Lambshift

Let us start by considering Eq. (7.19) and the fact that the sign function can be written as

$$\text{sign}(x) = 2\theta(x) - 1, \tag{7.52}$$

so that

$$\xi(\omega, \omega', t) = \int_0^t dt_1 \int_0^t dt_2 \frac{(2\theta(t_1 - t_2) - 1)}{2i} e^{i(\omega t_1 - \omega' t_2)} C(t_1 - t_2) \tag{7.53}$$

$$= \frac{1}{i} \int_0^t dt_1 \int_0^t dt_2 \theta(t_1 - t_2) e^{i(\omega t_1 - \omega' t_2)} C(t_1 - t_2)$$

$$- \frac{1}{2i} \int_0^t dt_1 \int_0^t dt_2 e^{i(\omega t_1 - \omega' t_2)} C(t_1 - t_2). \tag{7.54}$$

However, notice that for the cumulant equation

$$\Gamma(\omega,\omega',t)=\int_0^t dt_1\int_0^t dt_2 e^{i(\omega t_1-\omega' t_2)}C(t_1-t_2). \tag{7.55}$$

So we have

$$\xi(\omega,\omega',t)=\frac{1}{2i}\int_0^t dt_1\int_0^t dt_2(2\theta(t_1-t_2)-1)e^{i(\omega t_1-\omega' t_2)}C(t_1-t_2) \tag{7.56}$$

$$=\frac{1}{i}\int_0^t dt_1\int_0^t dt_2\theta(t_1-t_2)e^{i(\omega t_1-\omega' t_2)}C(t_1-t_2)-\frac{\Gamma(\omega,\omega',t)}{2i}. \tag{7.57}$$

Since the Heaviside theta forces $t_1>t_2$ then

$$\xi(\omega,\omega',t)=\frac{1}{i}\int_0^t dt_1\int_0^{t_1} dt_2 e^{i(\omega t_1-\omega' t_2)}C(t_1-t_2)-\frac{\Gamma(\omega,\omega',t)}{2i}. \tag{7.58}$$

Futher notice

$$\begin{aligned}\Gamma(\omega,\omega',t)=&\int_0^t dt_1\int_0^{t_1} dt_2 e^{i(wt_1-w' t_2)}C(t_1-t_2)\\&+\int_0^t dt_2\int_0^{t_2} dt_1 e^{i(wt_1-w' t_2)}C(t_1-t_2),\end{aligned} \tag{7.59}$$

hence

$$\begin{aligned}\xi(\omega,\omega',t)=&\frac{1}{i}\int_0^t dt_1\int_0^{t_1} dt_2 e^{i(\omega t_1-\omega' t_2)}C(t_1-t_2)\\&-\frac{1}{2i}\left(\int_0^t dt_1\int_0^{t_1} dt_2 e^{i(wt_1-w' t_2)}C(t_1-t_2)+\int_0^t dt_2\int_0^{t_2} dt_1 e^{i(wt_1-w' t_2)}C(t_1-t_2)\right)\end{aligned} \tag{7.60}$$

$$=\frac{1}{2i}\left(\int_0^t dt_1\int_0^{t_1} dt_2 e^{i(\omega t_1-\omega' t_2)}C(t_1-t_2)-\int_0^t dt_2\int_0^{t_2} dt_1 e^{i(wt_1-w' t_2)}C(t_1-t_2)\right). \tag{7.61}$$

At this point notice that this expression contains the same integrals as Eq. (7.43) with difference instead of a sum. This should not come as a surprise as the decay and Lamb-Shift are associated to the real and imaginary part of the correlation function [B1, B9]. After integration the Lamb-Shift can be written as

$$\xi(\omega,\omega',t)=\sum_k \xi^k(\omega,\omega',t)=\frac{1}{2i}\sum_k(\chi_k(\omega,\omega',t)-\overline{\chi_k}(\omega',\omega,t)). \tag{7.62}$$

We then take the limit $\omega\to\omega'$

$$\begin{aligned}\xi_k(\omega,\omega,t)=&\lim_{\omega\to\omega'}\xi_k(\omega,\omega',t)\\=&\,\mathrm{Im}\left(\frac{c_k\left((\nu_k t-i\omega t-1)+e^{-(\nu_k-i\omega)t}\right)}{(\nu_k-i\omega)^2}\right).\end{aligned} \tag{7.63}$$

Let us recall that the usual expression used to calculate the Lamb-shift is [5]

$$\xi(\omega,\omega',t) = \frac{t^2}{2\pi^2}\int_{-\infty}^{\infty} d\phi\,\mathrm{sinc}\left(\frac{(\omega-\phi)t}{2}\right)\mathrm{sinc}\left(\frac{(\omega'-\phi)t}{2}\right) \times P.V\int_0^{\infty} d\nu J(\nu)\left(\frac{n(\nu,\beta)+1}{\phi-\nu}+\frac{n(\nu,\beta)}{\phi+\nu}\right). \tag{7.64}$$

Compared to the standard way Eq. (7.56) and Eq. (7.63) are remarkably simple. The main advantages of these expressions are three, namely

- The same algebraic expressions can be used to obtain both the decay rates and the Lamb-Shift term
- The calculation of Lamb-shift is simple, and lifts the requirement of special integration methods for Cauchy's principal value integrals, which are often expensive, noisy and requires special integration methods [68]
- It puts the Lamb-shift corrections and the decay rates back in the same footing, as the imaginary and real parts of the same quantity, a fact that is not so straightforward to see from Eq. (7.26) and Eq. (7.39) where the latter seems more complex.

[5] The principal value's presence makes this computation non-trivial [67]

Chapter 8

Hierarchical Equations of Motion (HEOM)

8.1 Introduction

The Hierarchical equations of motion [2, 20–22, 40, 69] are a powerful numerically exact technique for the simulation of open quantum systems. The basic idea behinds them lies in the use of auxiliary density matrices (ADOS) will encode the role of the environment. The system plus the ADOS now play the role of the new system, which now has a larger Hilbert space. While the system plus ADOS is a finite-dimensional system, it does not undergo Poincaré recurrences because the equations of motion are not unitary [38, 39] [1]. Figure 8.1 shows a cartoon of the normal and system plus ADO configuration. The states of the ADOS are not usually needed once the simulation is done, since we only care about the state of our system, however, if we want to obtain information about thermodynamical quantities like heat (see section 11.4) we will have to store them. This poses a problem because the amount of memory needed to store all the ADOS states of the first hierarchy [21, 69] can quickly become an issue.

An intuitive way to think about them is that we are removing the contribution of each exponent (which is a Lorentzian Eq. (1.82)) to the power spectrum. That is, after adding each ADO to our system we are dealing with a less structured weaker environment, Figure 8.1 b) illustrates this idea. This way of interpreting it makes it easy to connect HEOM with other methods where the same kind on interpretation can be applied, such as pseudomode methods and the reaction coordinate methods [2].

[1] We make this point to remark that this is different from modeling the environment with a finite set of harmonic oscillators.

[2] This intuitive way of thinking about it is not too accurate, because certain exponent contribu-

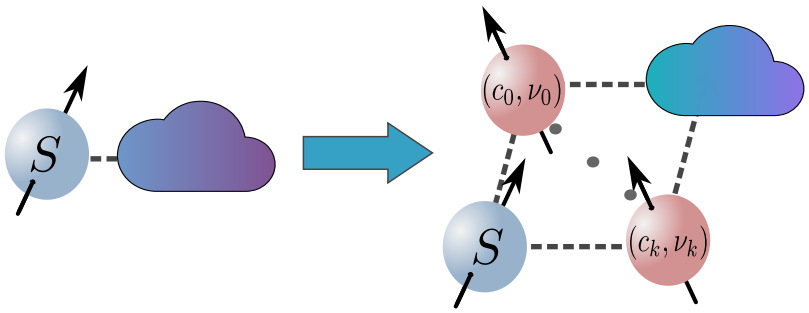

Figure 8.1: An illustration of the HEOM idea, we start with the system interacting with an environment, but rewrite it in such a way that we have the system interacting with fictitious particles (The ADOS) that undergo dissipative dynamics

The hierarchical equations of motion are a controlled approximation in the sense that any desired accuracy can be obtained by increasing its "two knobs". Those knobs are the hierarchy n and the number of exponents used to describe the correlation function m. In the next section we will derive HEOM from the Feynman Vernon Influence functional.

8.2 Derivation

To derive the hierarchy we will assume our bath correlation functions obey a certain profile

$$C(\tau) = \sum_k (c_k^R + i c_k^I) e^{-\nu_k \tau}, \tag{8.1}$$

where the ν_k are complex numbers. In section 1.6, we show that this assumption is not really restrictive, as numerical methods in the later years have made this possible regardless of the spectral density (see section 1.6). This is a huge improvement as when the method first came up [22] when it was rather restrictive as we needed the Matsubara decomposition of the environment. Substituting this into the second order cumulant (Eq. (5.79)) we obtain

$$W(t_2) = -\sum_k \int_0^{t_2} dt_1 c_k^R [A_2, [A_1, \bullet]] + i c_k^I [A_2, \{A_1, \bullet\}] e^{-\nu_k (t_2 - t_1)}. \tag{8.2}$$

Now let us define the superoperators

$$\Phi(t) = i[A(t), \bullet], \tag{8.3}$$

$$\theta_k(t) = i \left(c_k^R [A(t), \bullet] + i c_k^I \{A(t), \bullet\} \right). \tag{8.4}$$

We would like to emphasize that $\theta_i(t)$ denotes the super operator above, and $\theta(t)$ with no subscript denotes the theta Heaviside function. Then the second order cumulant may be written in terms of these superoperators as

$$W(t) = \sum_n \Phi(t) \int_0^t dt' e^{-\nu_n (t - t')} \theta_n(t'). \tag{8.5}$$

We now take the derivative with respect to time of Eq. (5.82)

$$\frac{\partial \rho_S^I(t)}{\partial t} = \mathcal{T} \left(W(t) e^{\int_0^t dt' W(t')} \rho_S^I(0) \right) = \mathcal{T} \left(W(t) \rho_S^I(t) \right). \tag{8.6}$$

Let us denote

$$U_0 = \mathcal{T} e^{\frac{-i}{\hbar} \int_0^t H_S(t') dt'}. \tag{8.7}$$

Then transforming Eq. (8.6) into the Schrodinger picture yields

$$\frac{\partial \rho_S^I(t)}{\partial t} = \underbrace{-i[H_S(t), \rho_S(t)]}_{-\mathcal{L}_S} + \overbrace{U_0^\dagger(t) \mathcal{T} \left(W(t) \rho_S^I(t) \right) U_0}^{X}. \tag{8.8}$$

tions thought about this way would make the power spectrum negative, nevertheless is an useful way to think about it.

8.3 ADOS of the first hierarchy tier

Let us now concentrate on the second term of Eq. (8.8)

$$X = U_0^\dagger \mathcal{T} \Phi(t) \sum_n \int_0^t dt' e^{-\nu_n (t-t')} \theta_n(t') \rho_S^I(t) U_0 \tag{8.9}$$

$$= U_0^\dagger \Phi(t) \mathcal{T} \underbrace{U_0 U_0^\dagger}_{\mathbb{I}} \mathcal{T} \sum_n \int_0^t dt' e^{-\nu_n (t-t')} \theta_n(t') \rho_S^I(t) U_0 \tag{8.10}$$

$$= \phi \sum_n U_0^\dagger \mathcal{T} \int_0^t dt' e^{-\nu_n (t-t')} \theta_n(t) \rho_S^I(t) U_0, \tag{8.11}$$

where we used $\phi = U_0^\dagger \Phi(t) U_0$, and moved ϕ out of time ordering because $t \geq t'$. So far we haven't discussed how we expressed the correlation function as a series of decaying exponentials - different methods are discussed in section 1.6-. Suppose we managed to do it using the Matsubara formalism, then for high enough n the Matsubara frequencies are larger than system time scales meaning that

$$\nu_n \approx \frac{2\pi n}{\beta} \gg \omega_s. \tag{8.12}$$

For high enough n the exponent behaves as

$$e^{-\nu_n t} \approx \frac{\delta(t)}{\nu_n}. \tag{8.13}$$

Which n is high enough depends on the parameters of the problem (Eq. (8.13) allows us to account for the contribution of exponents beyond m in a simple way, doing so leads to the so called terminator[3]). Let us split the sum at m so we have

$$X = \phi \sum_n^m U_0^\dagger \mathcal{T} \int_0^t dt' e^{-\nu_n (t-t')} \theta_n(t') \rho_S^I(t) U_0 + \phi \sum_{n=m+1}^\infty U_0^\dagger \frac{\theta_n(t)}{\nu_n} \underbrace{U_0 U_0^\dagger}_{\mathbb{I}} \rho_S^I(t) U_0 \tag{8.14}$$

$$= \phi \sum_n^m U_0^\dagger \mathcal{T} \int_0^t dt' e^{-\nu_n (t-t')} \theta_n(t') \rho_S^I(t) U_0 + \phi \sum_{n=m+1}^\infty \frac{\theta_n}{\nu_n} \rho_S(t). \tag{8.15}$$

Here we used $\theta_n = U_0^\dagger \theta_n(t) U_0$ then we can write

$$\frac{\partial \rho_S(t)}{\partial t} = -\mathcal{L}_S \rho_S(t) + \phi(t) \sum_n^m U_0^\dagger \mathcal{T} \int_0^t dt' e^{-\nu_n (t-t')} \theta_n(t') \rho_S^I(t) U_0 + \phi \sum_{n=m+1}^\infty \frac{\theta_n}{\nu_n} \rho_S(t). \tag{8.16}$$

Now let us define

$$\sigma^{(1)}_{(0,\dots,1_n,0,\dots)} = U_0^\dagger \mathcal{T} \int_0^t dt' e^{-\nu_n (t-t')} \theta_n(t') \rho_S^I(t) U_0, \tag{8.17}$$

[3]The terminator is mainly used for the Drude-Lorentz spectral density, whenever using methods other than Matsubara we simply truncate the sum at m instead of doing this split

where the subscript $(0,\dots,1_n,0,\dots)$ indicates a m-tuple, in which a 1 is positioned at the index $n=1,\dots,m$, indicating that the object corresponds to the n^{th} exponent. So there is a 1 in the n^{th} position and the rest of the items in the list are zero, such that the sum of the elements in this list is 1. We may rewrite our equation for the dynamics of the system as

$$\frac{\partial\rho_S(t)}{\partial t}=-\left(\mathcal{L}_S-\phi\sum_{n=m+1}^{\infty}\frac{\theta_n}{\nu_n}\right)\rho_S(t)+\phi\sum_{n}^{m}\sigma^{(1)}_{(0,\dots,1_n,0,\dots)}. \tag{8.18}$$

To fully obtain the dynamics of our system we need to find the equation of motion of σ_1. We start by taking the time derivative of Eq. (8.17)

$$\begin{aligned}\frac{\mathrm{d}\sigma^{(1)}_{(0,\dots,1_n,0,\dots)}}{\mathrm{d}t}&=\frac{\mathrm{d}U_0^\dagger}{\mathrm{d}t}\mathcal{T}\int_0^t dt' e^{-\nu_n(t-t')}\theta_n(t')\rho_S^I(t)U_0\\&\quad+U_0^\dagger\frac{\mathrm{d}\Big(\mathcal{T}\int_0^t dt' e^{-\nu_n(t-t')}\theta_n(t')\rho_S^I(t)\Big)}{\mathrm{d}t}U_0\\&\quad+U_0^\dagger\mathcal{T}\int_0^t dt' e^{-\nu_n(t-t')}\theta_n(t')\rho_S^I(t)\frac{\mathrm{d}U_0}{\mathrm{d}t}.\end{aligned} \tag{8.19}$$

Consider

$$F=\mathcal{T}\Big(\int_0^t dt' e^{-\nu_n(t-t')}\theta_n(t')\rho_S^I(t)\Big). \tag{8.20}$$

We can then obtain its time derivative using the Leibniz Integral rule, namely

$$\frac{\mathrm{d}(\int_0^t f(t,t')dt')}{\mathrm{d}t}=f(t,t)+\int_0^t\frac{\partial f(t,t')}{\partial t}dt', \tag{8.21}$$

which results in

$$\frac{\mathrm{d}F}{\mathrm{d}t}=\theta_n(t)\rho_S^I(t)+\mathcal{T}\Big(\int_0^t dt'\frac{\mathrm{d}\big(e^{-\nu_n(t-t')}\theta_n(t')\rho_S^I(t)\big)}{\mathrm{d}t}\Big) \tag{8.22}$$

$$=\theta_n(t)\rho_S^I(t)+\mathcal{T}\Big(\int_0^t dt' e^{-\nu_n(t-t')}\theta_n(t')\big(W(t)\rho_S^I(t)-\nu_n\rho_S^I(t)\big)\Big), \tag{8.23}$$

where we used Eq. (8.6) and the fact the time ordering operator acts as the identity on time ordered products. Then we may write

$$\begin{aligned}&\frac{\mathrm{d}\sigma^{(1)}_{(0,\dots,1_n,0,\dots)}}{\mathrm{d}t}=-\mathcal{L}_S\sigma^{(1)}_{(0,\dots,1_n,0,\dots)}\\&+U_0^\dagger\left(\theta_n(t)\rho_S^I(t)+\mathcal{T}\Big(\int_0^t dt' e^{-\nu_n(t-t')}\theta_n(t')\big(W(t)\rho_S^I(t)-\nu_n\rho_S^I(t)\big)\Big)\right)U_0.\end{aligned} \tag{8.24}$$

Notice that one of the terms is $\sigma^{(1)}_{(0,\dots,1_n,0,\dots)}$. By substituting Eq. (8.5) and rearranging inside the time ordering operator one obtains

$$\begin{aligned}\frac{\mathrm{d}\sigma^{(1)}_{(0,\dots,1_n,0,\dots)}}{\mathrm{d}t}&=-\mathcal{L}_S\sigma^{(1)}_{(0,\dots,1_n,0,\dots)}-\nu_n\sigma^{(1)}_{(0,\dots,1_n,0,\dots)}+U_0^\dagger\theta_n(t)\underbrace{U_0U_0^\dagger}_{\mathbb{I}}\rho_S^I(t)U_0\\&+\sum_{n'}\phi U_0^\dagger\,\mathcal{T}\Big(\iint_0^t dt_1dt_2e^{-\nu_n(t-t_1)}e^{-\nu_{n'}(t-t_2)}\theta_n(t_1)\theta_{n'}(t_2)\rho_S^I(t)\Big)U_0,\end{aligned} \tag{8.25}$$

by defining

$$\sigma^{(2)}_{(\dots,1_{n'},\dots,1_n,\dots)} = U_0^\dagger\,\mathcal{T}\Big(\iint_0^t dt_1 dt_2 e^{-\nu_n(t-t_1)}e^{-\nu_{n'}(t-t_2)}\theta_n(t_1)\theta_{n'}(t_2)\rho_S^I(t)\Big)U_0, \quad (8.26)$$

where again the subscript $(\dots,1_{n'},\dots,1_n,\dots) = (\dots,1_{n'},0,\dots)+(\dots,1_n,0,\dots)$ indicates a list of m indices, if $n\neq n'$ there is a 1 in the n^{th} and n'^{th} positions and the rest of the items in the list are zero, if $n=n'$ then there is a 2 in that position, such that the sum of the elements of this list is 2. We can now rewrite the equation as

$$\frac{\mathrm{d}\sigma^{(1)}_{(0,\dots,1_n,0,\dots)}}{\mathrm{d}t} = -\Big(\mathcal{L}_S+\nu_n\Big)\sigma^{(1)}_{(0,\dots,1_n,0,\dots)} + \theta_n\rho_S(t) \quad +\phi\sum_{n'}\sigma^{(2)}_{(\dots,1_{n'},\dots,1_n,\dots)}. \quad (8.27)$$

Once again we want to divide the sum into two contributions using Eq. (8.13) so that we obtain

$$\begin{aligned}\frac{\mathrm{d}\sigma^{(1)}_{(0,\dots,1_n,\dots,0)}}{\mathrm{d}t} &= -\Big(\mathcal{L}_S+\nu_n-\phi\sum_{n'=m+1}^{\infty}\frac{\theta_{n'}}{\nu_{n'}}\Big)\sigma^{(1)}_{(0,\dots,1_n,0,\dots)}+\theta_n\rho_S(t)\\ &\quad+\phi\sum_{n'}^{m}\sigma^{(2)}_{(\dots,1_{n'},\dots,1_n,\dots)}. \end{aligned}\quad (8.28)$$

Now for convenience let us define $\sigma^0(0,\dots,0)=\rho_S$, then one can rewrite this equation as

$$\begin{aligned}\frac{\mathrm{d}\sigma^{(1)}_{(0,\dots,1_n,0,\dots)}}{\mathrm{d}t} &= -\Big(\mathcal{L}_S+\nu_n-\phi\sum_{n'=K+1}^{\infty}\frac{\theta_{n'}}{\nu_{n'}}\Big)\sigma^{(1)}_{(0,\dots,1_n,0,\dots)}+\theta_n\sigma^{(1-1)}_{(0,\dots,1_n-1,0)}\\ &\quad+\phi\sum_{n'=0}^{K}\sigma^{(1+1)}_{(0,\dots,1_n,\dots,0_{n'}+1,\dots)}\end{aligned}\quad (8.29)$$

8.4 Higher Tiers and Truncation

To find the equation of motion of $\sigma^{(2)}$ we follow the same procedure

$$\begin{aligned}\frac{d}{dt}\sigma^{(2)}_{(1_n,\dots,1_{n'})} &= -\mathcal{L}_S\sigma^{(2)}_{(1_n,\dots,1_{n'})}+\theta_n\sigma^{(1)}_{(0,\dots,1_{n'})}+\theta_{n'}\sigma^{(1)}_{(0,\dots,1_n)}-(\nu_n+\nu_{n'})\sigma^{(2)}_{(1_n,\dots,1_{n'})}\\ &+U_0^\dagger\mathcal{T}\int_0^t dt_1 e^{-\nu_n(t-t_1)}\theta_n(t_1)\int_0^t dt_2 e^{-\nu_{n'}(t-t_2)}\theta_{n'}(t_2)W(t)\rho_S^I(t)U_0,\end{aligned}\quad (8.30)$$

using the definition

$$\begin{aligned}\sigma^{(3)}_{(1_{n''},1_{n'},\dots,1_n,\dots)} &= U_0^\dagger\mathcal{T}\Big(\iiint_0^t dt_1dt_2dt_3 e^{-\nu_n(t-t_1)}e^{-\nu_{n'}(t-t_2)}e^{-\nu_{n''}(t-t_3)}\\ &\quad\times\theta_n(t_1)\theta_{n'}(t_2)\theta_{n''}(t_3)\rho_S^I(t)\Big)U_0.\end{aligned}\quad (8.31)$$

And using the same procedure for $W(t)$ where we split the number of exponents we finally obtain

$$\frac{d}{dt}\sigma^{(2)}_{(1_n,\dots,1_{n'})} = -\left(\mathcal{L}_S + \nu_n + \nu_{n'} - \phi \sum_{n'=K+1}^{\infty} \frac{\theta_{n'}}{\nu_{n'}}\right)\sigma^{(2)}_{(1_n,\dots,1_{n'})} + \theta_n \sigma^{(2-1)}_{(0,\dots,1_{n'})} + \theta_{n'}\sigma^{(2-1)}_{(0,\dots,1_n)} + \phi \sum_{n''=0}^{K} \sigma^{(2+1)}_{(1_{n'},\dots,1_n,\dots,0_{n''}+1,\dots)}. \tag{8.32}$$

At this point, we can stop to appreciate the similarity between Eq. (8.29) and Eq. (8.32). We start to see the pattern emerging. By following the same procedure and finding the equations of motion for each $\sigma^{(n)}_{(0,\dots,1_n,0,\dots)}$, one obtains

$$\frac{\mathrm{d}\sigma^{(n)}_{(j_0,\dots,j_m)}}{\mathrm{d}t} = \left(\mathcal{L}_S - \sum_{k}^{m} j_k\nu_k + \phi \sum_{k=m+1}^{\infty} \frac{\theta_k}{\nu_k}\right)\frac{\mathrm{d}\sigma^{(n)}_{(j_0,\dots,j_m)}}{\mathrm{d}t} + \sum_{k}^{m} j_k\theta_k\sigma^{(n-1)}_{(j_0,\dots,j_k-1,\dots,j_m)} + \phi\sum_{k}^{m}\sigma^{(n+1)}_{(j_0,\dots,j_k+1,\dots,j_m)}, \tag{8.33}$$

where $\sum_k j_k = n$. We eventually truncate at a given hierarchy, meaning we stop at $\sigma^{(n)}$ and solve the system of coupled differential equations to obtain the dynamics of our system.

Chapter 9

Pseudomodes

Pseudomode methods [4, 12, 23, 25, 31, 50, 70–72] are a useful tool to study open quantum systems; their main advantage lies in the fact that the exact dynamics can be written down as a so-called **Local** GKLS master equation on a dilated space [70]. The mention of a dilated space should make us connect this to HEOM as indicated in figure 8.1. The relationship between both methods is explored in more detail in [73].

From the point of view of open quantum systems, different Gaussian environments with identical correlation functions are equivalent. The core idea of the pseudomode method is to dilate our Hilbert space to one where the extra space undergoes GKLS dynamics [70], in such a way that the two-time correlation function of the particles in this dilated space is the same as our original correlation function. By doing this, we can simulate our exact dynamics by a local GKLS master equation in this extended space and later trace out the dilation. The name pseudomodes comes from the fact that originally, the dilated Hilbert space was comprised of the original space plus harmonic oscillators, those extra oscillators we add to the Hilbert space are the pseudomodes.

9.1 Equivalence between Unitary and Non-unitary environments

Consider the dilated Hilbert space consisting of the system and the pseudomodes that undergo GKLS evolution. The state ρ (system+pseudomodes) obeys

$$\frac{\mathrm{d}\rho(t)}{\mathrm{d}t} = -i\Big[H_S, \rho(t)\Big] + \sum_n L_n\rho(t) - i\lambda_n\Big[A(t)X_n, \rho(t)\Big], \tag{9.1}$$

where L_n is

$$\begin{aligned} L_n\rho(t) = &-i\Omega_n\Big[b_n^\dagger b_n, \rho\Big] + \Gamma_n N_n\left(b_n^\dagger\rho b_n - \frac{\{b_n b_n^\dagger, \rho\}}{2}\right) \\ &+ \Gamma_n(N_n+1)\left(b_n\rho b_n^\dagger - \frac{\{b_n^\dagger b_n, \rho\}}{2}\right), \end{aligned} \tag{9.2}$$

and Ω_n, Γ_n and N_n are coefficients we will need to adjust, to make sure the evolution using Eq. (9.2) reproduces the original dynamics [4, 70]. This generator has the following properties:

- It is trace preserving, meaning

$$Tr[L_n\rho] = 0 \tag{9.3}$$

- it has a Gaussian stationary state, such that it obeys Wick's theorem 5.4
- The evolution preserves canonical commutation relations

Futhermore

- We impose that the original system and environment before dilation are in a product state $\rho_{SB}(0) = \rho_S(0) \otimes \rho_B(0)$ [70].

To obtain the dynamics of our system, we simply trace out the pseudomode subsystems

$$\rho_S(t) = Tr_{pm}\left[\rho(t)\right]. \tag{9.4}$$

The position operator for these pseudomodes is given by:

$$X_n^\mu = b_n^{\mu\dagger} + b_n^\mu. \tag{9.5}$$

The steady state of the generator L_n^μ is given by

$$\rho_{B,n}^\mu = \frac{e^{-\eta b_n^{\mu\dagger} b_n^\mu}}{z_n^\mu}, \tag{9.6}$$

where $\eta = -\log\left(\frac{N_n^\mu+1}{N_n^\mu}\right)$, and μ is a label for the environment in the case where there is more than one. Now, that we have established our non unitary evolution, we can see the contribution of each pseudomode $b_n^{\mu\dagger}$ to the correlation function. For this evolution to be equivalent to the exact dynamics, the correlation function of the pseudomodes needs to be the same as for the original unitary environment [70]. Thus, we need to reproduce the components associated with both positive and negative times (sometimes called advanced and retarded components)[1]) as given by Eq. (1.26) or by Eq. (1.24). In order to compute the contribution of each mode, notice that for the non-unitary evolution, the Heisenberg picture evolution is obtained by the adjoint generator.

$$\langle X_n^\mu(t)\rangle_B = \mathrm{Tr}\left[X_n^\mu e^{L_n^\mu}(\rho_B)\right] = \mathrm{Tr}\left[e^{L_n^{\mu\dagger}}(X_n^\mu)\rho_B\right] = \mathrm{Tr}[X_n^\mu(t)\rho_B]. \tag{9.7}$$

Such that

$$X_n^\mu(t) = e^{L_n^{\mu\dagger} t}(X_n^\mu). \tag{9.8}$$

Since the superoperator $L_n^{\mu\dagger}$ acts linearly if suffices to compute its action on b_n^μ

$$L_n^{\mu\dagger} b_n^\mu = -\left(\frac{\Gamma_n^\mu}{2} + i\Omega_n^\mu\right) b_n^\mu. \tag{9.9}$$

Using this we may compute the Heisenberg Picture operator as

$$b_n^\mu(t) = e^{-\left(\frac{\Gamma_n^\mu}{2} + i\Omega_n^\mu\right)t} b_n^\mu. \tag{9.10}$$

[1]Remember though we are only using one parameter and referring to it as time, this is the difference of two times so there is nothing mysterious about being negative

Let us again notice, the remark from section 1.1. where we simply see that the only remaining terms will be the product of $b_n^\mu(t)$ and its adjoint. For $t > 0$

$$C_n^\mu(t) = \mathrm{Tr}\left[X_n^\mu(t) X_n^\mu \rho_{B,n}^\mu\right] \tag{9.11}$$

$$= \mathrm{Tr}\left[\left(e^{-\left(\frac{\Gamma_n^\mu}{2} - i\Omega_n^\mu\right)t} b_n^{\mu\dagger} + b_n^\mu e^{-\left(\frac{\Gamma_n^\mu}{2} + i\Omega_n^\mu\right)t}\right)(b_n^{\mu\dagger} + b_n^\mu)\rho_{B,n}^\mu\right] \tag{9.12}$$

$$= e^{-\left(\frac{\Gamma_n^\mu}{2} - i\Omega_n^\mu\right)t} \mathrm{Tr}\left[b_n^{\mu\dagger} b_n^\mu \rho_{B,n}^\mu\right] + e^{-\left(\frac{\Gamma_n^\mu}{2} + i\Omega_n^\mu\right)t} \mathrm{Tr}\left[b_n^\mu b_n^{\mu\dagger} \rho_{B,n}^\mu\right] \tag{9.13}$$

$$= e^{-\left(\frac{\Gamma_n^\mu}{2} - i\Omega_n^\mu\right)t} N_n^\mu + e^{-\left(\frac{\Gamma_n^\mu}{2} + i\Omega_n^\mu\right)t}\left(N_n^\mu + 1\right), \tag{9.14}$$

while for $t < 0$

$$C_n^\mu(-t) = \mathrm{Tr}\left[X_n^\mu X(t) \rho_{B,n}^\mu\right] \tag{9.15}$$

$$= e^{-\left(\frac{\Gamma_n^\mu}{2} + i\Omega_n^\mu\right)t} N_n^\mu + e^{-\left(\frac{\Gamma_n^\mu}{2} - i\Omega_n^\mu\right)t}\left(N_n^\mu + 1\right). \tag{9.16}$$

To obtain an appropriate dilation we must satisfy the following requirement

$$C(\tau) = \sum_n C_n(\tau). \tag{9.17}$$

As established in [70] as long as this is satisfied, Eq. (9.2) is equivalent to Eq. (5.82). The bad news at this point is that a finite number of modes can only exactly reproduce a sum of complex exponentials. On the other hand, we can approximate it really closely using the methods from section 1.6. We will however, need to be careful to satisfy Eq. (1.24) as we show in the next section.

9.2 A Simple case

To illustrate how to construct a dilation appropriately from an approximation of the correlation function, we need to consider the contribution of each pseudomode to the total correlation function. We consider the simplest case, namely, the case $C(t) = \theta(t) a e^{-\nu t} + \theta(-t) a e^{\overline{\nu} t}$ for $a \in \mathcal{R}$. Since we want the least number of pseudomodes that can reproduce the correlation function for both $t > 0$ and $t < 0$, we need both contributions to be complex conjugates of each other (however we only need to be careful about the exponents, as we can put the coefficient in the coupling). Inspired by this we can see that this is easily achievable if we set $N_n^\mu = 0$ such that the contributions are given by

$$C_n^\mu(t) = e^{-\left(\frac{\Gamma_n^\mu}{2} + i\Omega_n^\mu\right)t}, \qquad C_n^\mu(-t) = e^{-\left(\frac{\Gamma_n^\mu}{2} - i\Omega_n^\mu\right)t}. \tag{9.18}$$

By direct comparison one can conclude

$$\mathrm{Re}(\nu) = \frac{\Gamma_n^\mu}{2}, \qquad \mathrm{Im}(\nu) = \Omega_n^\mu. \tag{9.19}$$

Since $a \in \mathcal{R}$ we don't need to worry about the conjugation from positive to negative times, as such, one can simply assign it to the coupling such that $a = (\lambda_n^\mu)^2$. Following a similar kind of reasoning one can obtain the results in the table 9.1

Table 9.1: Pseudomode Representation of Different Exponential Terms, reproduced from [4], FCF stands for free correlation function, while PMs stands for the number of pseudomodes needed.

FCF Term	**Conditions**	**PMs**	**Parameters**		
			$\boldsymbol{\Omega}$	$\boldsymbol{\Gamma}$	$\boldsymbol{\lambda^2}$
$ae^{-\nu t}$	$a \in \mathcal{R}$	1	$\mathrm{Im}(\nu)$	$2\,\mathrm{Re}(\nu)$	a
$ae^{-\nu_1 t} + \bar{a}e^{-\nu_2 t}$	None	2	$\begin{pmatrix} \frac{1}{2i}(\nu_1 - \bar{\nu}_2) \\ \frac{1}{2i}(\nu_2 - \bar{\nu}_1) \end{pmatrix}$	$\begin{pmatrix} \nu_1 + \bar{\nu}_2 \\ \nu_2 + \bar{\nu}_1 \end{pmatrix}$	$\begin{pmatrix} \bar{a} \\ a \end{pmatrix}$
$ae^{-\nu_1 t} - ae^{\nu_2 t}$	None	3	$\begin{pmatrix} \mathrm{Im}(\nu_1) \\ \mathrm{Im}(\nu_2) \\ \frac{1}{2i}(\nu_1 - \bar{\nu}_2) \end{pmatrix}$	$\begin{pmatrix} 2\,\mathrm{Re}(\nu_1) \\ 2\,\mathrm{Re}(\nu_2) \\ \nu_1 + \bar{\nu}_2 \end{pmatrix}$	$\begin{pmatrix} \bar{a} \\ -a \\ a - \bar{a} \end{pmatrix}$
$a_1 e^{-\nu t}$ $+a_2 e^{-\bar{\nu} t}$	$a_1 + a_2 \in \mathcal{R}$ $\lvert\mathrm{Re}(a_1)\rvert > \lvert\mathrm{Re}(a_2)\rvert$	2	$\begin{pmatrix} \mathrm{Im}(\nu) \\ 0 \end{pmatrix}$	$\begin{pmatrix} 2\,\mathrm{Re}(\nu) \\ 0 \end{pmatrix}$	$\begin{pmatrix} a_1 - \bar{a}_2 \\ a_1 - \bar{a}_1 \end{pmatrix}$
$ae^{-\nu t}$	$a \notin \mathcal{R}$	Should be treated as $ae^{-\nu_1 t} + \bar{a}e^{-\nu_2 t}$ for $\frac{\nu_2}{\nu_1} \gg 1$			

9.3 Comment on related Methods

Unfortunately, the literature is full of pseudomode methods under different names, a fact that can be overwhelming for newcomers. For example, "Dissipative-Assisted Matrix product factorization (DAMPF)" is a pseudomode method where we encode Eq. (9.2) using matrix product states. Pseudofermion and mesoscopic leads are the same method applied to Fermionic reservoirs [72, 74]. Dissipatons are pure pseudomodes [71], non-hermitian pseudomodes typically refers to pseudomodes for which Ω_n may be complex and γ_n may be negative. Quasi-Lindblad pseudomodes, Pseudolindblad, GKLS master equation in the ultrastrong coupling, and other related acronyms, also refer to pseudomode techniques and their main difference tends to be the way the correlation function is approximated (see section 1.6)[50, 75]

Something similar happens for HEOM, to a lesser extend, where fortunately the word HEOM is usually kept, and letters are added at the beginning, for example, eHEOM uses spectral density fitting[34] (section 1.6.3), FP-HEOM uses the AAA algorithm[15][2] (section 1.6.4), HOPS is HEOM for product states [76] ... etc.

Having said all of this, we would just like to remark that the methods themselves are the same even if they have a different name, and their difference are mostly details related to their implementation rather than differences in the theory. We hope the reader finds this comment useful, as navigating through these methods can be a complex challenge at first.

[2] It is also suppose to use matrix product states, but often AAA alone will be referred to as FP-HEOM

Chapter 10

Reaction Coordinate Mapping

10.1 General Idea

The idea of the method is to enlarge the Hilbert space of the system, and at the same time putting most of the interaction with the bath into the coherent dynamics of the new enlarged system. This procedure changes the spectral density and its dynamics can then be explored with any of the methods mentioned before. The idea is that after the mapping, the residual interaction to the bath is weak enough that we can use a Bloch-Redfield or GKLS equation [9, 12, 77, 78] to describe the system accurately. The discussion in this section largely follows [78]. Figure 10.1 illustrates this concept; we take one oscillator out of the environment, make it part of the system, and now this oscillator that is part of our system is coupled to a simpler environment.

10.2 Hamiltonian Mapping

Consider an arbitrary system coupled linearly to a bath of harmonic oscillators

$$H = H_S(t) + \frac{1}{2}\sum_k \left(p_k^2 + \omega_k^2 \left(x_k - \frac{c_k}{w_k^2} S \right)^2 \right). \tag{10.1}$$

Where S is an system operator and ω_k (x_k) denotes the angular frequency (position) of the k^{th} oscillator. As discussed previously, the effect of the bath can be encoded in the correlation function, which in turn is fixed once we set T and the spectral density (Eq. (1.21)). The spirit of the Reaction Coordinate methods (RC) is to define the interaction with the collective degrees of freedom of the bath as a new mode, or new coordinate which we will denote with X_1. Basically we want a map that satisfies

$$\sum_k c_k x_k = \lambda_0 X_1. \tag{10.2}$$

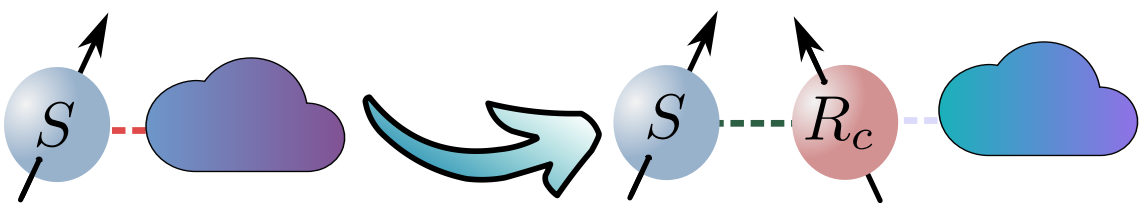

Figure 10.1: An illustration of the reaction coordinate mapping

In order to achieve this formally we just perform a Bogoliubov transformation such that

$$\vec{X} = \Lambda\vec{x}; \quad \vec{P} = \Lambda\vec{p}, \tag{10.3}$$

where mayus denotes new variables, while minus denotes the old ones. The map Λ must preserve canonical commutation relations, in order to do so it must be an orthogonal matrix, meaning $\Lambda^{-1} = \Lambda^T$. This means it has $N(N+1)/2$ independent components. Those components are fixed once we require that the residual bath (the $N-1$ modes that do not correspond to the RC) are normal modes, meaning

$$\sum_k \omega_k \Lambda_{1,k}\Lambda_{m,k} = \delta_{l,m}\Omega_l^2 \quad l,k > 1. \tag{10.4}$$

Then the Hamiltonian can be written as

$$H = H_S(t) + \frac{1}{2}\sum_k \left(p_k + \omega_k^2\left(x_k^2 - \frac{c_k^2}{w_k^4}S^2 - 2\frac{c_k}{w_k^2}x_k S\right)\right). \tag{10.5}$$

If we now take out the first mode (our RC, the one not normal) and apply the transformation, we obtain

$$\begin{aligned} H = H_S(t) + \frac{P_1^2 + \Omega_1^2 X_1^2}{2} + \sum_{k=2}^{\infty}\frac{P_k^2 + \Omega_k^2 X_k^2}{2} - \sum_k^{\infty}\frac{c_k^2}{2\omega_k^2}S^2 - \lambda_0 X_1 S \\ - X_1\sum_{k=2} C_k X_k, \end{aligned} \tag{10.6}$$

where the sum starts from 2 because we have $N-1$ modes. To rewrite the Hamiltonian this way, we have used

$$\vec{x}\cdot\vec{x} = X_1\sum_{n=2} X_n \sum_k \Lambda_{nk}\lambda_{k1}\omega_k^2 + X_1^2\Lambda_{1k}\Lambda_{1k}\omega_k^2. \tag{10.7}$$

Then defining

$$C_k = -\sum_l \omega_l^2 \Lambda_{kl}\lambda_{k1}, \tag{10.8}$$

we may write

$$\vec{x}\cdot\vec{x} = X_1\sum_{n=2} C_n X_n + X_1^2\Omega_1^2. \tag{10.9}$$

where we've defined $\Omega_1^2 = \sum_k \omega_k^2\Lambda_{1k}^2$ and $\delta\Omega_0^2 = \sum_k(\frac{C_k}{\omega_k})^2$. We finally write

$$\begin{aligned} H_{RC} = H_S(t) + \frac{P_1^2 + \Omega_1^2 X_1^2}{2} + \sum_{k=2}\frac{P_k^2 + \Omega_k^2 X_k^2}{2} - \delta\Omega_0^2 S^2 \\ - \lambda_0 X_1 S - X_1\sum_{k=2} C_k X_k. \end{aligned} \tag{10.10}$$

Notice, that the only coefficients affected by the change of the bath parameters (c_k and ω_k) are λ_0 and $\delta\Omega_0$. They encode the information about the coupling strength. **The key point here is that the mode we choose as the reaction coordinate does not matter**, as all information will be contained in the spectral density when going into the continuum limit. Once we go into the continuous limit we have

$$\delta\Omega_0^2 = \frac{2}{\pi}\int_0^\infty d\omega \frac{J(\omega)}{\omega}, \tag{10.11}$$

$$\lambda_0^2 = \frac{2}{\pi}\int_0^\infty d\omega\omega J(\omega), \tag{10.12}$$

where the second relation comes from the fact that the transformation preserves canonical commutation relations

$$[X_1, P_1] = i = \sum_k [\frac{c_k}{\lambda_0} x_k, \sum_{k'} \lambda_{k'1} p_{k'}] \tag{10.13}$$

$$= i\sum_k \frac{c_k}{\lambda_0}\Lambda_{1k}. \tag{10.14}$$

This implies that

$$\lambda_0 = \sum_k c_k \Lambda_{1k}. \tag{10.15}$$

At the same time we have

$$\sum_k c_k x_k = \lambda_0 X_1 = \lambda_0 \sum_k \Lambda_{1k} x_k, \tag{10.16}$$

which must be satisfied for all indices, thus

$$c_k = \lambda_{1k}\lambda_0. \tag{10.17}$$

By substituting in Eq. (10.15) we obtain

$$\lambda_0^2 = \sum_k c_k^2 \to \frac{2}{\pi}\int_0^\infty d\omega\omega J(\omega). \tag{10.18}$$

Similarly

$$\Omega_1^2 = \sum_k \left(\omega_k \frac{c_k}{\lambda_0}\right)^2 \to \frac{2}{\lambda_0^2\pi}\int_0^\infty d\omega\omega^3 J(\omega). \tag{10.19}$$

On the other hand the spectral densitity asociated to the residual bath takes the form

$$J_1(\omega) = \frac{\pi}{2}\sum_{k\neq 1}\frac{C_k^2}{\Omega_k^2}\delta(w - \Omega_k). \tag{10.20}$$

The only remaining step to finish this mapping is to provide a relationship between the original spectral density and the new one. In order to relate them we follow the prescription developed in [79].

We would like to remark that the coefficient $\delta\Omega_0^2$ is what is known in the literature as the reorganisation energy [40, 78, 80] (up to a multiplicative constant due to convention). Adding the term $\delta\Omega_0^2 S^2$ to the Hamiltonian may compensate for the so-called mean force correction as indicated in [80], in a similar way as the reaction coordinate mapping does.

To simulate open systems using the reaction coordinate we simply start our simulation as if Eq. (10.10) was our original Hamiltonian, and trace out the RC after simulation. Notice that the RC is the one in contact with the environment, so decay rates, Lamb-shift RC are typically calculated using RC operators [1]. One of the main advantages of the RC mapping is that it is a mapping on the Hamiltonian, and we can obtain the "dressed" steady state simply by

$$\rho_S = tr_{rc}\left[\frac{e^{-\beta H_{RC}}}{Z}\right]. \tag{10.21}$$

Futhermore the map is precise for every temperature. The reaction coordinate mapping is useful to check the correct thermalization of other methods such as pseudomodes, or HEOM for this precise reason [A2, 12, 81]

10.3 Relating the spectral densities

So far, we have introduced the reaction coordinate mapping, but we have no way to find the spectral density that would correspond to the new Hamiltonian (System + RC + Environment) in terms of the original spectral density (System + Environment). Without knowledge about how the residual environment interacts with the new system, we cannot proceed further with calculations. To use this mapping for simulations, we need a way to relate them, which is what we will find in this section.

Without loss of generality, consider a particle with position q and momentum p as the system coupled to the environment via position and moving in a potential $V(q)$. In other words, we take Eq. (10.1) and make $S = q$ and $H_S = \frac{p}{2} + V(q)$. Then the equations of motion of the system in the Heisenberg picture according to the original Hamiltonian are given by

$$\dot{q} = p, \tag{10.22}$$

$$\dot{p} = -\frac{\partial V(q)}{\partial q} + \sum_k \frac{c_k^2}{\omega_k^2} q + \sum_k c_k x_k. \tag{10.23}$$

While for the bath one has

$$\ddot{x_k} = -\omega_k^2 x_k + c_k q. \tag{10.24}$$

The system of coupled differential equations can easily be solved via a Fourier transform. After a Fourier transform we obtain (Here we use z as the Fourier transform

[1] Usually a local master equation is used, if one uses a Redfield or Global master equation, the system operators are also involved in these calculations.

variables and $\hat{}$ for the transformed variables)

$$-z^2\hat{q} = -\frac{\partial \hat{V}(q)}{\partial \hat{q}} + \sum_k c_k \hat{x}_k - \sum_k \frac{c_k^2}{\omega_k^2}\hat{q}, \tag{10.25}$$

$$-z^2\hat{x}_k = -\omega_k^2 \hat{x}_k + c_k \hat{q}. \tag{10.26}$$

Solving the algebraic system we can get rid of x_k

$$\hat{x}_k = \frac{c_k}{\omega_k^2 - z^2}\hat{q}. \tag{10.27}$$

Which allows one to write the evolution of q as

$$\frac{\partial \hat{V}(q)}{\partial q} = -L_0(z)\hat{q}, \tag{10.28}$$

where

$$L_0(z) = -z^2 - W_0(z) + \delta\Omega_0^2, \tag{10.29}$$

$$W_0(z) = \sum_k \frac{c_k^2}{\omega_k^2 - z^2}. \tag{10.30}$$

Let us take a closer look at $W_0(z)$ which is sometimes known as the Cauchy transform of the spectral density [B10, 79]

$$W_0(z) = \sum_k \frac{c_k^2}{\omega_k^2 - z^2} \to \frac{2}{\pi}\int_0^\infty \frac{\omega J(\omega)}{\omega^2 - z^2}. \tag{10.31}$$

Using partial fraction decomposition we may write

$$\frac{\omega}{(\omega + z)(\omega - z)} = \frac{1}{2(\omega + z)} + \frac{1}{2(\omega - z)} \tag{10.32}$$

$$W_0(z) = \frac{1}{\pi}\int_0^\infty d\omega \left(\frac{J(\omega)}{\omega - z} + \frac{J(\omega)}{\omega + z}\right). \tag{10.33}$$

Now, in many cases, it is useful to assume the spectral density is an antisymmetric function $J(\omega) = -J(-\omega)$. If we do we may write

$$W_0(z) = \frac{1}{\pi}\int_{-\infty}^\infty d\omega \frac{J(\omega)}{\omega - z}, \tag{10.34}$$

which is the definition of a Cauchy transform. Now let us remark an important point of this propagator [5, 6, 82], namely that if we consider $z = \omega + i\epsilon$ in the limit of $\epsilon \to 0$ we can relate the propagator with the spectral density directly

$$\lim_{\epsilon\to 0} L_0(\omega + i\epsilon) = \lim_{\epsilon\to 0}\left(-(\omega + i\epsilon)^2 - W_0(\omega + i\epsilon) + \delta\Omega_0^2\right). \tag{10.35}$$

Now we assume the dominated convergence theorem holds [B5], meaning both the limit and the function are integrable. Then one may exchange the order of the limit

and the integral such that

$$\pi \lim_{\epsilon\to 0} W_0(\omega + i\epsilon) = \int_{-\infty}^{\infty} d\omega' \lim_{\epsilon\to 0}\left(\frac{J(\omega')}{\omega' - \omega + i\epsilon}\right) \tag{10.36}$$

$$= \int_{-\infty}^{\infty} d\omega' J(\omega') \lim_{\epsilon\to 0}\left(\frac{\omega' - \omega - i\epsilon}{(\omega' - \omega)^2 + \epsilon^2}\right) \tag{10.37}$$

$$= \int_{-\infty}^{\infty} d\omega' \frac{J(\omega')}{(\omega' - \omega)} - i\int_{-\infty}^{\infty} d\omega' J(\omega') \lim_{\epsilon\to 0}\left(\frac{\epsilon}{(\omega' - \omega)^2 + \epsilon^2}\right). \tag{10.38}$$

Notice however that

$$\delta(x) = \lim_{\epsilon\to 0}\frac{1}{\pi}\left(\frac{\epsilon}{(x)^2 + \epsilon^2}\right), \tag{10.39}$$

So finally we obtain

$$\pi \lim_{\epsilon\to 0} W_0(\omega + i\epsilon) = \int_{-\infty}^{\infty} d\omega' \frac{J(\omega')}{(\omega' - \omega)} - i\pi\int_{-\infty}^{\infty} d\omega' J(\omega')\delta(\omega' - \omega) \tag{10.40}$$

$$= \int_{-\infty}^{\infty} d\omega' \frac{J(\omega')}{(\omega' - \omega)} - i\pi J(\omega), \tag{10.41}$$

if we substitute this back into Eq. (10.35) then we obtain

$$\lim_{\epsilon\to 0} L_0 = \left(-\omega^2 - \frac{1}{\pi}\int_{-\infty}^{\infty} d\omega' \frac{J(\omega')}{(\omega' - \omega)} - iJ(\omega) + \delta\Omega_0^2\right). \tag{10.42}$$

Notice the imaginary part is directly proportional to the spectral density, Because of this we have found a relationship between the Fourier propagator and the spectral density

$$\mathrm{Im}(\lim_{\epsilon\to 0} L_0(\omega + i\epsilon)) = -J(\omega), \tag{10.43}$$

As a next step we follow the same procedure with the transformed Hamiltonian. As we want the dynamics to be the same before and after the mapping their propagators must be equal, which will allow us to relate the spectral densities. The equations of motion for the transformed Hamiltonian are

$$\ddot{q} = -\frac{\partial V(q)}{\partial q} - q\delta\Omega_0^2 + \lambda_0 X_1, \tag{10.44}$$

$$\ddot{X}_1 = \lambda_0 q - \Omega_1^2 X_1 + \sum_k C_k X_k, \tag{10.45}$$

$$\ddot{X}_k = \Omega_k^2 X_k + C_k X_1. \tag{10.46}$$

Once again we turn this into an algebraic system of equations using the Fourier transformation

$$-z^2\hat{q} = -\frac{\partial V(q)}{\partial q} - \hat{q}\delta\Omega_0^2 + \lambda_0\hat{X}_1, \tag{10.47}$$

$$-z^2\hat{X}_1 = \lambda_0\hat{q} - \Omega_1^2\hat{X}_1 + \sum_k C_k\hat{X}_k, \tag{10.48}$$

$$-z^2\hat{X}_k = \Omega_k^2\hat{X}_k + C_k\hat{X}_1. \tag{10.49}$$

This allows one to find the relations

$$\hat{X}_k = \frac{C_k}{\Omega_k^2 - z^2}\hat{X}_1, \tag{10.50}$$

$$\hat{X}_1 = -\frac{\lambda_0}{z^2 + W_1(z) - \Omega_1^2}\hat{q}. \tag{10.51}$$

where analogously to Eq. (10.31) we have defined

$$W_1(z) = \sum_k \frac{C_k}{\Omega_k^2 - z^2} \to \frac{1}{\pi}\int_{-\infty}^{\infty} d\omega \frac{J_1(\omega)}{\omega - z}. \tag{10.52}$$

Finally, we may write the propagator of the transformed Hamiltonian as

$$-\frac{\partial \hat{V}(q)}{\partial q} = -L_1(z)\hat{q}, \tag{10.53}$$

where

$$L_1(z) = -z^2 + \delta\Omega_0^2 + \frac{\lambda_0}{z^2 + W_1(z) - \Omega_1^2}, \tag{10.54}$$

Since both propagators must be equal then

$$L_1(z) = L_0(z), \tag{10.55}$$

$$-z^2 + \delta\Omega_0^2 + \frac{\lambda_0}{z^2 + W_1(z) - \Omega_1^2} = -z^2 - W_0(z) + \delta\Omega_0^2. \tag{10.56}$$

This allows us to write one Cauchy transform in terms of the other as

$$W_1(z) = \Omega_1^2 - z^2 - \frac{\lambda_0^2}{W_0(z)}. \tag{10.57}$$

If we now again consider the analytical continuation we have

$$\mathrm{Im}(\lim_{\epsilon\to 0} W_1(\omega + i\epsilon)) = \mathrm{Im}(\lim_{\epsilon\to 0}\left(\Omega_1^2 - (\omega + i\epsilon)^2 - \frac{\lambda_0^2}{W_0(\omega + i\epsilon)}\right)) \tag{10.58}$$

$$-J_1(\omega) = \mathrm{Im}(\lim_{\epsilon\to 0}\frac{\lambda_0^2}{W_0(\omega + i\epsilon)}) \tag{10.59}$$

$$= \mathrm{Im}(\lim_{\epsilon\to 0}\frac{\lambda_0^2 W_0(\omega + i\epsilon)}{W_0(\omega + i\epsilon)W_0(\omega - i\epsilon)}) \tag{10.60}$$

$$= -\frac{\lambda_0^2 J(\omega)}{|W_0(\omega)|}. \tag{10.61}$$

Thus we finally found a relationship between the original and transformed spectral densities

$$J_1(\omega) = \frac{\lambda_0^2 J(\omega)}{|W_0(\omega)|}. \tag{10.62}$$

10.3.1 Iterative nature of the mapping and Markovianization

Once we have obtained a relationship between the new and old spectral density, one might wonder what would happen if we decided to repeat the procedure with the system and RC as our new system and find a new reaction coordinate. We may also wonder whether many iterations of the mapping reach a terminal spectral density. We will address both of these questions in this section.

Let us define

$$\delta\Omega_1^2 = \sum_k \frac{C_k^2}{\Omega_k^2} \to \frac{2}{\pi}\int_0^\infty d\omega \frac{J_1(\omega)}{\omega}. \tag{10.63}$$

Then notice that by definition

$$W_0(0) = \sum_k \frac{c_k^2}{\omega_k^2} = \delta\Omega_0^2, \tag{10.64}$$

$$W_1(0) = \sum_k \frac{C_k^2}{\Omega_k^2} = \delta\Omega_1^2, \tag{10.65}$$

by substituting this into Eq. (10.57), we obtain

$$\delta\Omega_1^2 + \frac{\lambda_0^2}{\delta\Omega_0^2} = \Omega_1^2. \tag{10.66}$$

For convenience let us rewrite the Hamiltonian of Eq. (10.10)

$$\begin{aligned} H = H_S(t) + \frac{P_1^2 + \Omega_1^2 X_1^2}{2} + \sum_{k=2} \frac{P_k^2 + \Omega_k^2 X_k^2}{2} \\ - \delta\Omega_0^2 S^2 - \lambda_0 X_1 S - X_1 \sum_{k=2} C_k X_k. \end{aligned} \tag{10.67}$$

Substituting Eq. (10.66) we get

$$\begin{aligned} H = H_S(t) + \frac{P_1^2 + \left(\delta\Omega_1^2 + \frac{\lambda_0^2}{\delta\Omega_0^2}\right) X_1^2}{2} + \sum_{k=2} \frac{P_k^2 + \Omega_k^2 X_k^2}{2} \\ - \frac{\delta\Omega_0^2}{2} S^2 - \lambda_0 X_1 S - X_1 \sum_{k=2} C_k X_k. \end{aligned} \tag{10.68}$$

However, notice that

$$\frac{\lambda_0}{2\delta\Omega_0^2} X_1^2 - \lambda_0 X_1 S + \frac{\delta\Omega_0^2}{2} S^2 = \frac{\lambda_0}{2\delta\Omega_0^2}\left(X_1^2 - 2\frac{\delta\Omega_0^2}{\lambda_0} S X_1 + (\frac{\delta\Omega_0^2}{\lambda_0})^2 S^2 \right) \tag{10.69}$$

$$= \frac{\lambda_0}{2\delta\Omega_0^2}\left(X_1^2 - \frac{\delta\Omega_0}{2} S \right)^2, \tag{10.70}$$

and by substituting Eq. (10.63)

$$\sum_k \frac{\Omega_k}{2} X_k^2 - C_k X_1 X_k + \frac{C_k^2}{2\Omega_k^2} X_1^2 = \frac{\Omega_k^2}{2}\left(X_k - \frac{C_k}{\Omega_k^2} X_1 \right)^2. \tag{10.71}$$

so that the Hamiltonian can be written as

$$H = H_S(t) + \frac{P_1^2}{2} + \sum_{k=2} \frac{P_k^2}{2} + \frac{\Omega_k^2}{2}\left(X_k - \frac{C_k}{\Omega_k^2}X_1\right)^2 + \frac{\lambda_0}{2\delta\Omega_0^2}\left(X_1^2 - \frac{\delta\Omega_0}{2}S\right)^2. \tag{10.72}$$

Notice that this makes thermodynamic stability evident as everything depends only on the initial parameters. At the same time notice that this has the same form as the original Hamiltonian if the Reaction Coordinate mode X_1 is considered part of the system. So one might just apply the procedure once again. In practice adding harmonic oscillators to the system is undesirable, and it's preferred to use a better approximation for the dynamics or another transformation like polaron to reduce the effective coupling [9, 77]

One may wonder whether succesive applications of the mapping reach a fixed point. Since the Hamiltonian is in the same form, the same procedure would follow in each iteration. In particular it is clear that

$$W_{n+1}(z) = \Omega_{n+1}^2 - z^2 - \frac{\lambda_n^2}{W_n(z)}. \tag{10.73}$$

Provided the limit $n \to \infty$ exists, this would lead us to

$$W(z) = \Omega^2 - z^2 - \frac{\lambda^2}{W(z)}, \tag{10.74}$$

where $W(z) = \lim_{n\to\infty} W_n(z)$, $\Omega = \lim_{n\to\infty} \Omega_n$ and $\lambda = \lim_{n\to\infty} \lambda_n$. The spectral density

$$J'(\omega) = -\lim_{\epsilon\to 0^+} \mathrm{Im}(W(\omega + i\epsilon)) \tag{10.75}$$

is the limiting case. We expect this spectral density to be analytic in all of the complex plane except in its support points on the real axis. Using Eq. (10.74) we have

$$W(z)^2 - (\Omega^2 - z^2)^2 W(z) - \lambda^2 = 0, \tag{10.76}$$

from which we obtain

$$J'(\omega) = \frac{\sqrt{4\lambda^2 - (\Omega^2 - \omega^2)^2}}{2} \quad for \;\; 4\lambda^2 > (\Omega^2 - \omega^2)^2 \tag{10.77}$$

This spectral density that terminates the chain must obey $J'(\omega) > 0 \;\; for \;\; \omega > 0$. This indicates it has a non-vanishing value for

$$\omega^2 \in [max(\Omega^2 - 2\lambda, 0), \Omega^2 + 2\lambda], \tag{10.78}$$

and must be zero everywhere else, as all other modes have been taken out. This is made clearer if we rewrite it as

$$J'(\omega) = \frac{\sqrt{(\omega^2 - \omega_L^2)(\omega_R^2 - \omega^2)}}{2} \quad \omega_L \leq \omega \leq \omega_R, \tag{10.79}$$

where

$$\omega_R^2 = \Omega^2 + 2\lambda \quad \omega_L^2 = max(\Omega^2 - 2\lambda, 0). \tag{10.80}$$

Since we require $J(\omega) > 0$ this fixes $\Omega^2 = 2\lambda$ then

$$J'(\omega) = \frac{\sqrt{\omega^2(\omega_R^2 - \omega^2)}}{2} \quad 0 \leq \omega \leq \omega_R, \tag{10.81}$$

$$= \frac{\omega\omega_R}{2}\sqrt{1 - \frac{\omega^2}{\omega_R^2}}\theta(\omega_R - \omega). \tag{10.82}$$

This is the Rubin model for dissipation, while this is argued to be Markovian [79] and it's generally claimed to be the markovian fixed point of the RC [78, 79], this is still colored noise. Another remark is that this procedure fails if there are gaps in the spectral density as well as when there are low frequency cutoffs. However, this does not mean that RC is a bad description, but rather means that the prescription does not necessarily converge to the real spectral density/correlation function, thus being an approximate solution at best in those cases, and this is due to the assumptions related to the Cauchy transform.

10.4 Mappings for typical spectral densities

$J(\omega)$	λ^2	Ω	$J_1(\omega)$
$\frac{8\delta^4\epsilon\omega(\omega^2+\delta^2+\epsilon^2)}{[\delta^2+(\omega-\epsilon)^2]^2[\delta^2+(\omega+\epsilon)^2]^2}$	$\delta\epsilon$	$\sqrt{3\delta^2+\epsilon^2}$	$\frac{8\delta^3\omega(\delta^2+\omega^2+\epsilon^2)}{\omega^4+2\omega^2(5\delta^2-\epsilon^2)+(3\delta^2+\epsilon^2)^2}$
$\frac{4\delta^5\omega^3}{[\delta^2+(\omega-\epsilon)^2]^2[\delta^2+(\omega+\epsilon)^2]^2}$	$\frac{\delta^2}{4}$	$\sqrt{5\delta^2+\epsilon^2}$	$\frac{16\delta^3\omega^3}{\omega^4+2\omega^2(7\delta^2-\epsilon^2)+(\delta^2+\epsilon^2)^2}$
$\frac{\omega}{\omega_m}\Theta(\omega_m-\omega)$	$\frac{2\omega_m^2}{3\pi}$	$\sqrt{\frac{3}{5}}\omega_m$	$\frac{\pi\omega\omega_m^3}{6(\omega_m-\omega\,\mathrm{arctanh}(\frac{\omega_m}{w}))(\omega_m-\omega\overline{\mathrm{arctanh}(\frac{\omega_m}{w})})}$

Table 10.1: Reaction coordinate mapping for selected spectral densities. Unfortunately the number of spectral densities for which the reaction coordinate is available is limited. However, notice the underdamped spectral density is here. One could in principle express other spectral densities as the sum of an underdamped one using the methods in section 1.6

Chapter 11

Defining Heat and Work

Open quantum systems are an essential part of quantum thermodynamics. While we have been mainly concerned with equations for the density matrix we may now wonder how to obtain thermodynamic quantities from it. This section follows and unifies [4, 69]. Consider the energy of the system at time t [83, 84]

$$E(t) = \mathrm{Tr}[H(t)\rho(t)]. \tag{11.1}$$

If we now take a time derivative

$$\dot{E}(t) = \mathrm{Tr}\Big[\dot{H(t)}\rho(t)\Big] + \mathrm{Tr}[H(t)\dot{\rho}(t)]. \tag{11.2}$$

From thermodynamics [84] we know that the energy change of the internal energy of the system is due to heat and work, we then associate work to the changes we can control, in this case our time dependent Hamiltonian. Since this is per unit time, the term in the right hand side is asociated with power, the time derivative of work

$$\dot{E}(t) = P(t) + \dot{Q}(t), \tag{11.3}$$

$$P(t) = \mathrm{Tr}\Big[\dot{H(t)}\rho(t)\Big], \tag{11.4}$$

$$\dot{Q}(t) = \mathrm{Tr}[H(t)\dot{\rho}(t)] = \sum_k J_k(t). \tag{11.5}$$

$\dot{Q}(t)$ is the sum of net heat currents supplied by individual baths. The J_k are the heat currents associated with each bath. While this is general, more specific formulas can be applied to more specific situations, which we will explore in the next sections. The formula for power on the other hand, remains the same for the different approaches.

11.1 Heat for a GKLS or Redfield Master equation

Let us remember that the GKLS master equation is given by

$$\begin{aligned}\frac{\partial \rho_S^I(t)}{\partial t} &= \sum_{\omega,\alpha,\beta} \gamma(\omega)\left(A(\omega)\rho_S^I(t)A^\dagger(\omega) - \frac{\{A^\dagger(\omega)A(\omega), \rho_S^I(t)\}}{2}\right) \\ &\quad + i\sum_{\omega,\alpha,\beta} S_{LS}(\omega)\Big[\rho_S^I(t), A^\dagger(\omega)A(\omega)\Big] \qquad (11.6)\\ &= i\sum_{\omega,\alpha,\beta} S_{LS}(\omega)\Big[\rho_S^I(t), A^\dagger(\omega)A(\omega)\Big] + D(\rho), \qquad (11.7)\end{aligned}$$

where D describes the dissipative part of the generator. By substituting $\dot{\rho}(t)$ into Eq. (11.5)

$$Q(t) = \mathrm{Tr}\left[H\left(D(\rho) + i\sum_{\omega,\alpha,\beta} S_{LS}(\omega)\Big[\rho_S^I(t), A^\dagger(\omega)A(\omega)\Big]\right)\right]. \tag{11.8}$$

Now let us notice that

$$\mathrm{Tr}\{A[B,C]\} = \mathrm{Tr}\{A(BC-CB)\} = \mathrm{Tr}\{ABC - BAC\} \tag{11.9}$$
$$= \mathrm{Tr}\{[A,B]C\}, \tag{11.10}$$

using Eq. (A.12) we see that only the dissipative part contributes to heat for a GKLS master equation. On the other hand notice that for the Redfield equation the Lamb-shift depends on two Bohr frequencies so that

$$[H_S, A^\dagger(\omega')A(\omega)] = [H_S, A^\dagger(\omega')]A(\omega) + A^\dagger(\omega')[H_S, A(\omega)] \tag{11.11}$$
$$= \omega' A^\dagger(\omega')A(\omega) - \omega A^\dagger(\omega')A(\omega) \tag{11.12}$$
$$= (\omega' - \omega)A^\dagger(\omega')A(\omega), \tag{11.13}$$

which is nonzero in general. Thus let us define

$$D_{GKLS}(\rho) = D(\rho), \tag{11.14}$$

$$D_{Redfield}(\rho) = \sum_{\omega,\omega'}\left(\gamma(\omega,\omega',t)\left(A(\omega')\rho A^\dagger(\omega) - \frac{\{A^\dagger(\omega)A(\omega'),\rho\}}{2}\right)\right.$$
$$\left. + iS(\omega,\omega',t)\Big[\rho(t), A^\dagger(\omega)A(\omega')\Big]\right). \tag{11.15}$$

Then

$$\dot{Q}(t) = \mathrm{Tr}\Big[HD_i(\rho)\Big]. \tag{11.16}$$

where i indicates the GKLS or Redfield generator respectively. Each bath has a dissipator associated to it. To find the individual heat currents we simply consider the contribution of each to the k environments to $D_i = \sum_k D_i^k$ such that

$$J_k = \mathrm{Tr}\Big[HD_i^k(\rho)\Big]. \tag{11.17}$$

Now, we would like to remark the two main differences between the Redfield and GKLS generator, at least for the computation of heat currents

- The Redfield Lamb-Shift does not necessarily commute with the Hamiltonian of the system, while the GKLS one does; this means that for the GKLS it is merely an energy shift while for Redfield it can induce non trivial changes. We find in chapter 16 that the inclusion of Lamb-shift is necessary to study heat
- The GKLS master equation is time independent, and the generator does not depend on any information about the state. This often leads to non-zero currents at time zero, which should not be the case.

11.2 Heat for dynamical maps

The cumulant equation presented in section 7.1 is a dynamical map rather than a differential equation, for that reason finding the time derivative of the generator might be non-trivial. Doing it analytically is particularly challenging as the derivative of a time dependent exponential yields

$$\frac{d}{dt}e^{X(t)} = \int_0^1 ds e^{(1-s)X(t)} \frac{d}{dt}X(t) e^{sX(t)}. \tag{11.18}$$

In the weak coupling limit we may ignore powers of the operator $X(t)$ to approximate this as

$$\frac{d}{dt}e^{X(t)}\rho(0) \approx \frac{d}{dt}X(t)\rho(t), \tag{11.19}$$

with a similar justification as in section 6.1. Equation Eq. (11.18) makes it hard to obtain an expression for the heat current, except in some particular cases where the general expression might simplify. In practice, however, Eq. (11.18) can be obtained numerically fairly cheaply via automatic differentiation [85, 86] or via numerical differentiation; in this thesis we use the latter. Once we are able to get this sort of expressions we consider

$$\rho_S(t) = \Lambda(t)\rho_S(0). \tag{11.20}$$
$$\dot{\rho_S}(t) = \dot{\Lambda}(t)\rho_S(0) \tag{11.21}$$

We can then simply substitute this in the definition of heat to obtain

$$\dot{Q}(t) = \mathrm{Tr}\left[H\dot{\Lambda}(t)\rho_S(0)\right]. \tag{11.22}$$

Then the heat currents can be isolated from the individual bath contributions

$$J_k = \mathrm{Tr}\left[H\dot{\Lambda}^k(t)\rho_S(0)\right]. \tag{11.23}$$

11.3 Heat for Pseudomode methods

A pseudomode equation is after all a master equation of the GKLS form, on an extended Hilbert space space, so one can expect the same expression as the GKLS expression would apply namely

$$\dot{Q}(t) = \mathrm{Tr}\left[HD(\rho)\right]. \tag{11.24}$$

However, one needs to be careful, in pseudomodes, the system is not dissipating directly, the pseudomodes are. Thus the Hamiltonian to be used is the Hamiltonian of the pseudomode and its interaction to the system, we can extract it from Eq. (9.2), and it reads

$$H_I^k = \Omega_k b_k^\dagger b_k + \lambda_k A(t) X_k, \tag{11.25}$$

Finally the heat current is given by

$$\dot{Q}(t) = \sum_{k=1}^{M} \mathrm{Tr}\left[H_I^k D^k(\rho)\right]. \tag{11.26}$$

Other than that it is a direct analogy to the GKLS equation, this same expression is usually defined via more complicated arguments [4] but the procedure is equivalent to the simple derivations we have outlined so far. In the case of the Reaction Coordinate it can be thought of as a special kind of pseudomode and the same equation applies.

11.4 Heat for the Hierarchical equations of motion

When using HEOM we need to be aware of the fact that heat will depend on the states of the ADOS of the first tier [20, 44, 69] which will need to be stored during the simulation. To define heat for this approach, let us recall that from the hierarchical equations of motion we have

$$\frac{\partial \rho_S(t)}{\partial t} = -\left(i\mathcal{L}_S - \phi \sum_{n=k+1}^{\infty} \frac{\theta_n}{\nu_k}\right)\rho_S(t) + \phi \sum_{n}^{k} \sigma^{(1)}_{(0,\dots,1_n,0,\dots)}. \tag{11.27}$$

where k is the number of exponents used to approximate our correlation function using the methods from section 1.6. Just as before the coherent part will commute with the Hamiltonian, so that if we identify

$$D_{HEOM}(\rho) = \left(\phi \sum_{n=k+1}^{\infty} \frac{\theta_n}{\nu_k}\right)\rho(t) + \phi \sum_{n}^{k} \sigma^{(1)}_{(0,\dots,1_n,0,\dots)} \left[\rho^I(t), A^\dagger(\omega)A(\omega)\right], \tag{11.28}$$

where the first term is associated to the terminator and typically only used for the Drude-Lorentz spectral Density (typically one considers enough exponents or Eq. (8.13)). Using this we may write the heat for HEOM in terms of the first tier of ADOS as

$$\dot{Q}(t) = \mathrm{Tr}\left[H D_{HEOM}(\rho)\right]. \tag{11.29}$$

To conclude this section we would like to remark that even though these are the accepted definitions of heat currents in the literature, the results from 16 seem to suggest that this cannot be interpreted as heat currents in the Non Markovian case. Further study in this direction is required, as there seems to be heat flow from cold to hot reservoirs.

Chapter 12

Projection operator techniques

Projector operator techniques are techniques inherited from Non-equilibrium statistical mechanics [B1, 87, 88]. The basic idea behind these techniques is to separate the complex system which we want to study into the "relevant" (to us), and irrelevant degrees of freedom by means of some projector operator.

12.1 Projection operators

A projection operator is a map

$$\mathcal{P}\rho \mapsto \rho'. \tag{12.1}$$

The projector operators obeys the following properties:

- It is a linear i.e. $\mathcal{P}(a\rho + b\sigma) = a\rho' + b\sigma'$.
- It is idempotent meaning $\mathcal{P}^2 = \mathcal{P}$.
- It is a completely positive and trace preserving map (CPTP).

We need to keep in mind that our Hilbert space of interest will typically be $\mathcal{H} = \mathcal{H}_S \otimes \mathcal{H}_{IR}$, where IR is our subscript for the "irrelevant part"of the system. With that in mind our projectors of interest are of the form

$$\mathcal{P} = \mathbb{I} \otimes \Lambda, \tag{12.2}$$

where Λ is a CPTP idempotent map on $\mathcal{H}_{IR}$. This form is chosen because product states are mapped to products states, this way we do not create artificial correlations between subsystems. Then for pure states we can write:

$$\rho_S = \mathcal{P}\rho = (\mathbb{I} \otimes \Lambda)\, \rho_S \otimes \rho_{IR} = \rho_S \otimes \Lambda\rho_{IR}. \tag{12.3}$$

We then realize than in order for the the expression to make sense we need $\Lambda\rho_{IR} \mapsto \mathbb{I}$. A sensible choice then seems to be the partial trace on $\mathcal{H}_{IR}$. Then

$$\mathcal{P}\rho = \mathbb{I} \otimes \mathrm{Tr}_{IR}[\rho], \tag{12.4}$$

Box 12.1.1: Theorem: Valid Projection operators

A projector operator that obeys the desired properties can be written as

$$\mathcal{P}\rho = \sum_i \mathrm{Tr}_{IR}[A_i\rho] \otimes B_i \tag{12.5}$$

Where $\{A_i\}, \{B_i\}$ are linearly independent sets of observables, that satisfy

- $\mathrm{Tr}_{IR}[A_iB_i] = \delta_{ij}$
- $\sum_i \mathrm{Tr}_{IR}[B_i]A_i = \mathbb{I}_{IR}$
- $\sum_i A_i^T \otimes B_i \geq 0$

However in practice it is standard to pick $A = \mathbb{I}_{IR}$,$B = \rho_{IR}$ it is useful to know that there exist infinitely many choices

12.2 The Nakajima-Zwanzig equation

Based on the projection operator technique outlined above, one can derive the Nakajima-Zwanzig equation, which is an exact equation for the dynamics of the system of interest. It is given by (see appendix B for the derivation)

$$\frac{d}{dt}\rho_s(t) = \int_0^t dt_1 \mathcal{K}_S(t,t_1)\rho_s(t_1). \tag{12.6}$$

Where we applied the projector operator $\mathcal{P}$ and traced out the environment from Eq. (B.20). Here $\mathcal{K}_S(t,t_1)$ is the memory kernel superoperator given by

$$\mathcal{K}_S(t,t_1) = \mathcal{P}\mathcal{L}(t)G(t,t_1)Q\mathcal{L}(t_1), \tag{12.7}$$

and

$$G(t,t_1) = \mathcal{T}e^{\int_{t_1}^t dt_2 Q\mathcal{L}(t_2)}. \tag{12.8}$$

While the Nakajima-Zwanzig equation is formally exact, it is generally too complex to solve. A common simplification involves approximating the Green's function, which yields an approximate memory kernel. For greater computational tractability, however even then, a time-local formulation is desirable. This motivates the development of the time-convolutionless equation, which is discussed in the next section.

12.3 The Time-Convolutionless (TCL) equation

As mentioned previously we would like to have a time local description of open quantum systems. To do so one can begin by realizing that one can write (see appendix B)

$$\rho(s) = G_R(t,s)\rho(t) = G_R(t,s)(\mathcal{P}+\mathcal{Q})\rho(t), \tag{12.9}$$

where $G_R(t,s)$ is the backward propagator of the full evolution

$$G_R(t,s) = \mathcal{T}_{\leftarrow} e^{-\int_s^t dt_2 \mathcal{L}(t_2)}, \tag{12.10}$$

and $\mathcal{T}_{\leftarrow}$ denotes anti-chronological time ordering. Using these (see appendix B for the derivation) we obtain the time local equation

$$\frac{d}{dt}\rho_s(t) = \mathcal{K}(t)\rho_s(t). \tag{12.11}$$

Here we assumed an initial product state. $\mathcal{K}(t)$ is a complex object that contains the Green functions mentioned above. But one can obtain $\mathcal{K}(t)$ perturbatively using

$$\mathcal{K}(t) = \alpha \sum_{n=0}^{\infty} \mathcal{P}\mathcal{L}(t)\Sigma(t)^n = \sum_{n=1}^{\infty} \alpha^n \mathcal{K}_n(t), \tag{12.12}$$

where α is our parameter for the perturbative expansion i.e. the coupling constant, and

$$\Sigma(t) = \int_{t_0}^{t} ds G(t,s) Q\mathcal{L}(s)\mathcal{P}G_R(t,s). \tag{12.13}$$

When talking about baths that have been centralized 5.1, the first non trivial order TCL_2 corresponds to the Redfield equation 6.1, while the next order reads

$$\mathcal{K}_{\triangle}(t) = \int_0^t dt_1 \int_0^{t_1} dt_2 \int_0^{t_2} dt_3 \Bigg(\mathcal{P}\mathcal{L}(t)\mathcal{L}(t_1)\mathcal{L}(t_2)\mathcal{L}(t_3)\mathcal{P} \tag{12.14}$$

$$- \mathcal{P}\mathcal{L}(t)\mathcal{L}(t_1)\mathcal{P}\mathcal{L}(t_2)\mathcal{L}(t_3)\mathcal{P} - \mathcal{P}\mathcal{L}(t)\mathcal{L}(t_2)\mathcal{P}\mathcal{L}(t_1)\mathcal{L}(t_3)\mathcal{P} \tag{12.15}$$

$$\mathcal{P}\mathcal{L}(t)\mathcal{L}(t_3)\mathcal{P}\mathcal{L}(t_1)\mathcal{L}(t_2)\mathcal{P} \Bigg). \tag{12.16}$$

In general the n^{th} order contribution is given by

$$\mathcal{K}_n(t) = \int_0^t dt_1 \int_0^{t_1} dt_2 \cdots \int_0^{t_{n-2}} dt_{n-1} \langle \mathcal{L}(t)\mathcal{L}(t_1)\mathcal{L}(t_2)\ldots\mathcal{L}(t_{n-1})\rangle_{oc}, \tag{12.17}$$

where the subscript oc stands for ordered cumulant [41, 42] (See appendix B). The TCL equation gives us a systematic way of obtaining higher-order approximations to the open system dynamics. Furthermore, these approximations are time local. On the downside, there are problems with invertibility of $\Sigma(t)$, which is required for the derivation to hold, though, some claim it might not be an issue after all [89]. A problem that has prevented its mass adoption is that the TCL generator depends on $n-1$ dimensional integrals which often need to be computed numerically. This often makes the simulation too expensive for practical purposes. This problem can be overcome by solving some of the integrals analytically when possible [18, 90]. However, that is not always the case, and it involves a considerable amount of work. In the next section, we show that we can obtain these integrals easily using a decaying exponential approximation of the correlation function, regardless of the order of the approximation.

12.4 Using the decaying exponential approximation in TCL

Whatever the order of the approximation is, when considering Gaussian environments, the ordered cumulants will be composed of a combination of the system operators at different times, which we can write in terms of jump operators, and the product of $n-1$ correlation functions that come from the bath operators. The decay rates and Lamb-shift can always be written down in terms of expressions like

$$\int_0^t dt_1 \int_0^{t_1} dt_2 \int_0^{t_2} dt_3 \cdots \int_0^{t_{2n-2}} dt_{2n-1} C(t-t_2)\ldots C(t_1-t_{2n-1}) \times e^{i\omega_1 t \pm i\omega_2 t_2 \pm \cdots \pm i\omega_{n-1} t_1 \pm i\omega_n t_{n-1}}. \quad (12.18)$$

Although complicated, notice that if we use the approximations outlined in section 1.6 then this is just a high dimensional integral of an exponential function.

$$\sum_{\vec{k}} \int_0^t dt_1 \int_0^{t_1} dt_2 \cdots \int_0^{t_{2n-2}} dt_{2n-1} c_{k_1} e^{-\nu_{k_1}(t-t_2)} \ldots c_{k_n} e^{-\nu_{k_n}(t_1-t_{n-1})} \times e^{i\omega_1 t \pm i\omega_2 t_2 \pm \cdots \pm i\omega_{n-1} t_1 \pm i\omega_n t_{n-1}}. \quad (12.19)$$

By doing the integral analytically we will turn this high dimensional integral into a multi-index sum. Notice that the decay rates in previous sections, were approximated by a sum of m elements, where m is the number of exponents we used to describe our two time correlation function, as the sum was over only one index is computational cost was $O(m)$. However, from the TCL_{2n} expansion with ordered cumulants, we see that after approximation we will have $O(m^n)$ indices in the summation (as it will be an integral of the product of n correlation functions), increasing the computational cost, thus for higher order master equations, reducing the number of exponents used has significant impact on the computational cost of the simulation. However, the approximation of the high dimensional integrals to this form will remain possible regardless of the order of the truncation (n). While the idea seems a bit abstract in this section, we will have a practical example in section 14.2.

Part III

Open Quantum systems II: Steady state

Chapter 13

The Mean Force Hamiltonian

13.1 Introduction

Usually in the theory of open quantum systems, the weak coupling limit is used. Typically this limit leads to descriptions that are second order in its coupling strength. In these descriptions, it is assumed that a system interacting **with a single** quantum environment will thermalize to the Gibbs state of the system at the temperature of the environment. That is, assume our Hamiltonian is

$$H = H_S + \alpha H_{SB} + H_B. \tag{13.1}$$

Then the thermal equilibrium state of our system is given by its Gibbs state.

$$\rho_S = \frac{e^{-\beta H_S}}{\mathrm{Tr}_S[e^{-\beta H_S}]}. \tag{13.2}$$

However, the real equilibrium state of the full Hamiltonian is given by [A2, 46, 47, 91, 92]

$$\rho_{eq} = \frac{e^{-\beta H}}{\mathrm{Tr}[e^{-\beta H}]}. \tag{13.3}$$

As we only want the information about the system, we now take a partial trace

$$\rho_S^{eq} = \mathrm{Tr}_B\Big[\rho_{eq}\Big] = \frac{\mathrm{Tr}_B\Big[e^{-\beta H}\Big]}{\mathrm{Tr}[e^{-\beta H}]} \equiv \frac{e^{-\beta H_{MF}}}{\mathrm{Tr}_S[e^{-\beta H_{MF}}]}. \tag{13.4}$$

The state ρ_S^{eq} is called the mean force Gibbs state. We can also appreciate from Eq. (13.4) that any finite α modifies equilibrium Gibbs state, which has led to different naming conventions for the different coupling regimes in statics and dynamics, as figure 13.2 shows. The ground state if the Mean Force Hamiltonian H_{MF} is not uniquely specified by Eq. (13.4), as it is invariant under the transformation $H_{MF} \to H_{MF} + \delta$ for an arbitrary real constant δ. Commonly, this constant is fixed by using the gauge [A2, 47, 92, 93]

$$\mathrm{Tr}\big[e^{-\beta H}\big] = \mathrm{Tr}_S[e^{-\beta H_{MF}}]\,\mathrm{Tr}_B[e^{-\beta H_R}]. \tag{13.5}$$

The figure 13.1 illustrates the difference between the state in Eq. (13.2) and Eq. (13.4). Using the gauge Eq. (13.5) we can write

$$\frac{\mathrm{Tr}_B\Big[e^{-\beta H}\Big]}{\mathrm{Tr}_S[e^{-\beta H_{MF}}]\,\mathrm{Tr}_B[e^{-\beta H_R}]} = \frac{e^{-\beta H_{MF}}}{\mathrm{Tr}_S[e^{-\beta H_{MF}}]}, \tag{13.6}$$

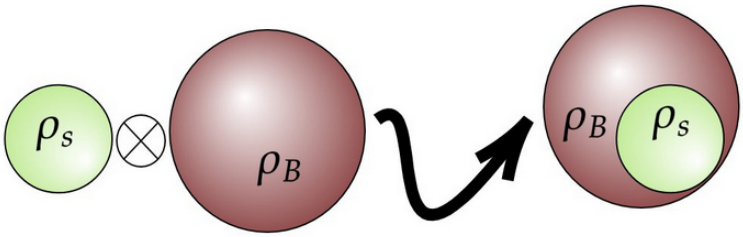

Figure 13.1: Illustration of the thermalization process, the system thermalizes to the joint Gibbs state on the right rather than the product of local Gibbs states on the left

therefore

$$e^{-\beta H_{MF}} = \frac{\mathrm{Tr}_B\left[e^{-\beta H}\right]}{\mathrm{Tr}_B[e^{-\beta H_R}]} \tag{13.7}$$

Thus, the Mean Force Hamiltonian is then given by

$$H_{MF}(\beta) = \frac{-1}{\beta} \ln\left(\frac{\mathrm{Tr}_B[e^{\beta H}]}{\mathrm{Tr}_B[e^{-\beta H_R}]}\right), \tag{13.8}$$

which determines the Hamiltonian up to a 'gauge"[1]. We see the expression involves the full Hamiltonian, thus it is challenging to compute a quantity such as its exponential. In practice one can use approximate techniques to estimate the Mean Force Hamiltonian. While the literature mainly focuses on the state [91], we will focus on the Hamiltonian following [A2], our main reason to do this, is that the Hamiltonian correction can be used to "dress" our system in a similar way that the reaction coordinate (see chapter 10) but without increasing the size of our Hilbert space, akin to more recent efforts in this direction using the reorganisation energy Eq. (10.11) [80].

13.2 The mean force Hamiltonian calculated perturbatively

To calculate the mean force correction perturbatively we may perform a Dyson series in imaginary time [A2, 27, 28, 91]. In the following section, we use the notation

[1] A gauge is needed because the state determines the Hamiltonian up to a term proportional to the identity. This constant is not relevant for the physics, but we need to keep track of it to obtain the correction from a given quantum state.

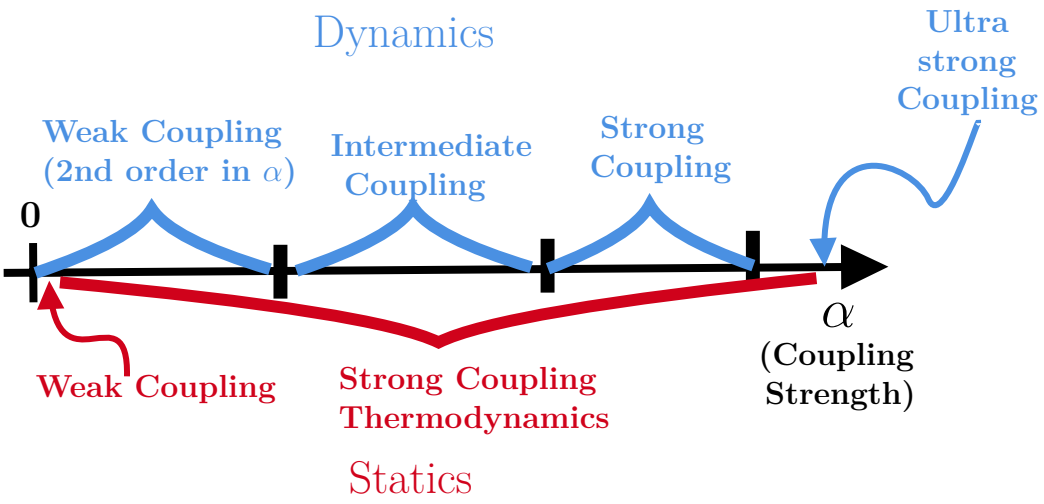

Figure 13.2: Naming convention of the coupling regimes in dynamics and statics. In statics, any coupling for which the mean force correction is non-negligeable is strong coupling. This figure is reproduced from [91]

$\hat{A}(t) = e^{t(H_0+H_R)}Ae^{-t(H_0+H_R)}$. We start with the LHS of the Eq. (13.6), which we represent by the formal expansion Dyson form:

$$e^{-\beta H_{\rm mf}} = e^{-\beta H_0}e^{\beta H_0}e^{-\beta H_{MF}} = e^{-\beta H_0}\mathcal{T}e^{-\int_0^\beta dt\ \delta\hat{H}_{\rm mf}(t)}, \tag{13.9}$$

where

$$\delta\hat{H}_{\rm mf} = \hat{H}_{\rm mf} - H_0, \tag{13.10}$$

which gives us the series expansion:

$$\mathcal{T}e^{-\int_0^\beta dt\ \delta\hat{H}_{\rm mf}(t)} = \mathbb{I} - \int_0^\beta dt_1\ \delta\hat{H}_{\rm mf}(t_1) + \int_0^\beta dt_1 \int_0^{t_1} dt_2\ \delta\hat{H}_{\rm mf}(t_1)\ \delta\hat{H}_{\rm mf}(t_2) + \dots \tag{13.11}$$

Similarly, for the RHS, we have

$$e^{-\beta H} = e^{-\beta H_0}\mathcal{T}e^{-\alpha\int_0^\beta dt\ \hat{H}_{SB}(t)}, \tag{13.12}$$

so that

$$\mathcal{T}e^{-\alpha\int_0^\beta dt\hat{H}_{SB}(t)} = \mathbb{I} - \alpha\int_0^\beta dt_1\hat{H}_{SB}(t_1) + \alpha^2\int_0^\beta dt_1\int_0^{t_1} dt_2\ \hat{H}_{SB}(t_1)\ \hat{H}_{SB}(t_2) + \dots \tag{13.13}$$

Finally, one can write

$$\frac{\mathrm{Tr}_B[e^{-\beta H}]}{\mathrm{Tr}_B[e^{-\beta H_R}]} = \frac{\mathrm{Tr}_B[e^{-\beta H_0}\mathcal{T}e^{-\alpha\int_0^\beta dt\ \hat{H}_{SB}(t)}]}{\mathrm{Tr}_B[e^{-\beta H_R}]} = e^{-\beta H_0}\,\mathrm{Tr}_B[\mathcal{T}e^{-\alpha\int_0^\beta dt\ \hat{H}_{SB}(t)}\rho_B], \tag{13.14}$$

where $\rho_B = \frac{e^{-\beta\hat{H}_B}}{\mathrm{Tr}_B[e^{-\beta H_R}]}$ is the Gibbs state of the bath. Substituting Eq. (13.14) into Eq. (13.6), we have:

$$e^{-\beta H_{\rm mf}} = e^{-\beta H_0}\,\mathrm{Tr}_B[\mathcal{T}e^{-\int_0^\beta dt\ \delta\hat{H}_{\rm mf}(t)}\rho_B], \tag{13.15}$$

so that Eq. (13.6) can be written as:

$$\mathrm{Tr}_B\left[\mathcal{T}\left(e^{-\int_0^\beta dt\ \delta\hat{H}_{\mathrm{mf}}(t)} - e^{-\alpha\int_0^\beta dt\ \hat{H}_{SB}(t)}\right)\rho_B\right] = 0, \tag{13.16}$$

or in the series form as:

$$\sum_{k=1}^{\infty}(-1)^k\int_0^\beta dt_1\int_0^{t_1} dt_2\cdots\int_0^{t_{k-1}} dt_k\Bigg(\delta\hat{H}_{MF}(t_1)\ \delta\hat{H}_{MF}(t_2)\ldots\delta\hat{H}_{MF}(t_k)$$
$$-\alpha^k\left\langle\hat{H}_{SB}(t_1)\ \hat{H}_{SB}(t_2)\ldots\hat{H}_{SB}(t_k)\right\rangle_{\rho_B}\Bigg) = 0, \tag{13.17}$$

where $\langle\cdot\rangle_{\rho_B} = \mathrm{Tr}_B[\,\cdot\,\rho_B]$.

13.3 Mean Force Expansion for Weak Coupling

Now, let us assume that $\alpha \ll 1$, and we expand:

$$\hat{H}_{MF} = \hat{H}_0 + \alpha\hat{H}_{MF}^{(1)} + \alpha^2\hat{H}_{MF}^{(2)} + \ldots, \tag{13.18}$$

so that $\delta\hat{H}_{MF} = \alpha\hat{H}_{MF}^{(1)} + \alpha^2\hat{H}_{MF}^{(2)} + \ldots$

Then, we collect terms in the same order of α appearing in Eq. (13.17). we will obtain the same series as in Eq. (2.12) replacing $i \to 1$. As a reminder for the n^{th} order we have

$$\int_0^\beta dt_1\hat{H}_{MF}^{(n)}(t_1) = \int_0^\beta dt_1\cdots\int_0^{t_{n-1}} dt_n\langle\hat{H}_{SB}(t_1)\ldots\hat{H}_{SB}(t_n)\rangle_B, \tag{13.19}$$

where we assumed we have centralized our interaction (see box 5.1).

13.3.1 First-order correction

Let us first solve the equation for the first-order correction, i.e.,

$$\int_0^\beta dt_1 H_{MF}^{(1)}(t_1) = \int_0^\beta dt_1\langle\hat{H}_{SB}(t_1)\rangle_B \tag{13.20}$$
$$H_{MF}^{(1)}(\beta) = \langle H_{SB}(\beta)\rangle_B = 0, \tag{13.21}$$

as we assume that bath operators are centralized so that $\langle B(\beta)\rangle_B = \langle B\rangle_B = 0$, which implies $H_{MF}^{(1)} = 0$. Where we used the fact that the bath Hamiltonian commutes with the bath's Gibbs state.

13.3.2 Second-order correction

In this section we provide general formula for second-order correction for mean-force Hamiltonian. This is often the one in which the literature is most interested because it is the leading order and that commonly used techniques in open systems cannot reproduce it completely [94]. Remarkably our expression for the correction does not

exhibit any poles, which was unexpected as the Lamb-shift correction does. Yet we also decompose it into bricks that are used to build the Lamb-shift corrections we find in dynamical equations, which do have poles, and require the Cauchy principal value to be well defined.

Let us start with the equation for the second-order correction with centralized bath operators

$$\int_0^\beta dt \hat{H}^{(2)}_{\rm mf}(t) = \int_0^\beta dt \int_0^t ds \langle \hat{H}_{SB}(t)\hat{H}_{SB}(s)\rangle_B. \tag{13.22}$$

Next, we represent the mean force correction as a Lamb-shift Hamiltonian, that is we will write it in the basis of jump operators, using also Eq. (A.15), to write

$$\hat{H}^{(2)}_{\rm mf}(t) = \sum_{\omega,\omega'} \Upsilon^{(\rm mf)}(\omega,\omega') e^{tH_0} A^\dagger(\omega) A(\omega') e^{-tH_0} \tag{13.23}$$

$$= \sum_{\omega,\omega'} \Upsilon^{(\rm mf)}(\omega,\omega') e^{t(\omega-\omega')} A^\dagger(\omega) A(\omega'). \tag{13.24}$$

Then, the LHS of Eq. (13.22) is equal to:

$$\int_0^\beta dt\ \hat{H}^{(2)}_{\rm mf}(t) = \sum_{\omega,\omega'} A^\dagger(\omega)A(\omega') \left(\Upsilon^{(\rm mf)}_{\alpha\beta}(\omega,\omega') \int_0^\beta dt\ e^{t(\omega-\omega')} \right), \tag{13.25}$$

whereas the RHS is given by:

$$\int_0^\beta dt \int_0^t ds \left\langle \hat{H}_{SB}(t)\hat{H}_{SB}(s) \right\rangle_{\gamma_R} = -\int_0^\beta dt \int_0^t ds\ \hat{A}(t)\hat{A}(s)\langle \hat{B}(t)\ \hat{B}(s)\rangle_B \tag{13.26}$$

$$= -\sum_{\omega,\omega'} \int_0^\beta dt \int_0^t ds\ e^{t\omega - s\omega'} A^\dagger(\omega)A(\omega')\langle \hat{B}(t-s)\ \hat{B}\rangle_B \tag{13.27}$$

$$= -\sum_{\omega,\omega'} A^\dagger(\omega)A(\omega') \int_0^\beta dt\ e^{t(\omega-\omega')} \int_0^t ds\ e^{s\omega'} \langle \hat{B}(s)\hat{B}\rangle_B, \tag{13.28}$$

where in the last line we change a variables $s \to \beta - s$. Next, according to Eq. (6.34), let us observe that

$$C(t) = \langle B(t)B\rangle_B = \frac{1}{2\pi}\int_{-\infty}^{+\infty} d\Omega\ e^{-i\Omega t}\ S(\Omega), \tag{13.29}$$

so that in imaginary time

$$\langle \hat{B}(\beta)\hat{B}\rangle = \frac{1}{2\pi}\int_{-\infty}^{+\infty} d\Omega\ e^{-\Omega\beta}\ S(\Omega). \tag{13.30}$$

Finally, the RHS is equal to:

$$\int_0^\beta dt \int_0^t ds \left\langle \hat{H}_{SB}(t)\hat{H}_{SB}(s) \right\rangle_{\rho_B} = \sum_{\omega,\omega'} A^\dagger(\omega)A(\omega') \left(\frac{1}{2\pi}\int_{-\infty}^{+\infty} d\Omega\ S(\Omega) \right.$$

$$\left. \times \int_0^\beta dt\ e^{t(\omega-\omega')} \int_0^t ds\ e^{s(\omega'-\Omega)} \right). \tag{13.31}$$

Equating LHS=RHS we get

$$\sum_{\omega,\omega'} M(\omega,\omega')A^\dagger(\omega)A(\omega') = 0. \tag{13.32}$$

where

$$M(\omega,\omega') = \int_0^\beta dt\ e^{t(\omega-\omega')}\left[\Upsilon^{(\mathrm{mf})}(\omega,\omega') + \frac{1}{2\pi}\int_{-\infty}^{+\infty} d\Omega\ S(\Omega)\int_0^t ds\ e^{s(\omega'-\Omega)}\right] \tag{13.33}$$

Finally, we obtain the second-order correction to the mean force Hamiltonian, which is given by:

$$\Upsilon^{(\mathrm{mf})}(\omega,\omega') = \frac{1}{2\pi}\int_{-\infty}^{+\infty} d\Omega\ S(\Omega)D_{\mathrm{mf}}(\omega,\omega',\Omega), \tag{13.34}$$

where

$$D_{\mathrm{mf}}(\omega,\omega',\Omega) = -\frac{\int_0^\beta dt\int_0^t ds\ e^{t(\omega-\omega')}e^{s(\omega'-\Omega)}}{\int_0^\beta dt\ e^{t(\omega-\omega')}}, \tag{13.35}$$

Performing the integrals, we obtain

$$D_{\mathrm{mf}}(\omega,\omega',\Omega) = \frac{1}{\omega'-\Omega} - \frac{(\omega-\omega')(e^{\beta(\omega-\Omega)}-1)}{(\omega-\Omega)(\omega'-\Omega)(e^{\beta(\omega-\omega')}-1)}, \tag{13.36}$$

Now, at the beginning of the section, we promised no poles. While there seemingly are, all the limits are well defined and we do not require principal value integration [A2], namely

$$\lim_{\omega'\to\Omega} D_{\mathrm{mf}}(\omega,\omega',\Omega) = \frac{e^{\beta(\omega-\Omega)}(\beta(\Omega-\omega)+1)-1}{(\omega-\Omega)\,(e^{\beta(\omega-\Omega)}-1)}, \tag{13.37}$$

$$\lim_{\omega\to\Omega} D_{\mathrm{mf}}(\omega,\omega',\Omega) = \frac{\beta(\omega'-\Omega)+e^{\beta(\Omega-\omega')}-1}{(\omega'-\Omega)\,(e^{\beta(\Omega-\omega')}-1)}, \tag{13.38}$$

$$\lim_{\omega'\to\omega} D_{\mathrm{mf}}(\omega,\omega',\Omega) = \frac{\beta(\omega-\Omega)-e^{\beta(w-\Omega)}+1}{\beta(w-\Omega)^2}. \tag{13.39}$$

The fact that it is well-behaved at these values is what we meant by no poles.

13.4 Quasi Steady-state corrections

Approximate descriptions, such as master equations, have generators whose steady state deviates from the mean force one. In this section, we study how to calculate the Hamiltonian correction due to those methods.

13.4.1 General method

We look for a solution to the equation:

$$\mathcal{L}[\varrho] = 0, \tag{13.40}$$

where $\mathcal{L}$ is the generator of the master equation and ϱ is its stationary state[A2, 94]. We expand the generator and steady-state in the series, i.e.,

$$\mathcal{L}[\rho] = \mathcal{L}_0[\rho] + \alpha^2\mathcal{L}_2[\rho] + \alpha^4\mathcal{L}_4[\rho] + \dots \tag{13.41}$$

$$\varrho = \varrho_0 + \alpha^2\varrho_2 + \alpha^4\varrho_4 + \dots, \tag{13.42}$$

so that we have the following set of equations (for each order in α):

$$\mathcal{L}_0[\varrho_0] = 0 \tag{13.43}$$

$$\mathcal{L}_0[\varrho_2] + \mathcal{L}_2[\varrho_0] = 0 \tag{13.44}$$

$$\mathcal{L}_0[\varrho_4] + \mathcal{L}_2[\varrho_2] + \mathcal{L}_4[\varrho_0] = 0 \tag{13.45}$$

$$\dots. \tag{13.46}$$

Hence we postulate the stationary state to be:

$$\varrho = e^{-\beta(H_0+\alpha^2 H_{\rm st}^{(2)}+\alpha^4 H_{\rm st}^{(4)}} + \dots) = \varrho_0 + \alpha^2\varrho_2 + \alpha^4\varrho_4 + \dots, \tag{13.47}$$

so that

$$\varrho_0 = e^{-\beta H_0} \tag{13.48}$$

$$\varrho_2 = -\, e^{-\beta H_0} \int_0^\beta \mathrm{d}t\, e^{tH_0} H_{\rm st}^{(2)} e^{-tH_0} \tag{13.49}$$

$$\begin{aligned}\varrho_4 = &-\, e^{-\beta H_0} \int_0^\beta \mathrm{d}t\, e^{tH_0} H_{\rm st}^{(4)} e^{-tH_0} \\ &+ e^{-\beta H_0} \int_0^\beta \mathrm{d}t_1 \int_0^{t_1} \mathrm{d}t_2\, e^{t_1 H_0} H_{\rm st}^{(2)} e^{-t_1 H_0} e^{t_2 H_0} H_{\rm st}^{(2)} e^{-t_2 H_0}.\end{aligned} \tag{13.50}$$

We start with representation of the second-order correction in the basis of jump operators:

$$H_{\rm st}^{(2)} = \sum_{\omega,\omega} \Upsilon^{(\rm st)}(\omega,\omega') A_\alpha^\dagger(\omega) A_\beta(\omega'). \tag{13.51}$$

Note that contrary to mean force correction, the above form assumes that Bohr spectrum is nondegenerate. Indeed, then pairs of jump operators span linearly all the space of operators of the system. In accordance, we have the following expression for ϱ_2, i.e.,

$$\varrho_2 = \sum_{\omega,\omega} -e^{-\beta H_0} \Upsilon^{(\rm st)}(\omega,\omega') \int_0^\beta dt\; e^{tH_0} A_\alpha^\dagger(\omega) A_\beta(\omega') e^{-tH_0} \tag{13.52}$$

$$= -\sum_{\omega,\omega} \Upsilon^{(\rm st)}(\omega,\omega')\alpha(\omega'-\omega) e^{-\beta H_0} A_\alpha^\dagger(\omega) A_\beta(\omega'), \tag{13.53}$$

where we define:

$$\alpha(\omega) = \int_0^\beta dt\; e^{-t\omega} = \begin{cases} \frac{1-e^{-\beta\omega}}{\omega}, & \omega \neq 0 \\ \beta, & \omega = 0. \end{cases} \tag{13.54}$$

Higher orders can be obtained in analogous fashion. The 4^{th} order is of particular relevance. It has been shown [A2, 46, 47, 91, 94] that it's the lowest order contribution to the diagonal. The calculations are different for different dynamics considered, explicit expressions for each correction and relationships between them can be seen in [A2]. What we would like to remark here is that master equations at fixed order n have finite α^n while dynamical maps at the same order have many contributions Eq. (11.18). Those contributions may be canceled out. For this reason we call them quasi steady instead of steady state corrections. For example in the cumulant they vanish in the actual dynamics, nevertheless their presence seems to indicate slow relaxation which often helps the cumulant equation have higher fidelity to the exact dynamics [A3].

13.5 Summary of corrections

Both the quasi steady state correction and the Lamb-shift correction can be found in a manner similar to equation Eq. (13.34) (see [A2] for derivations)

$$\Upsilon^{(\mathrm{cor})}(\omega,\omega') = \frac{1}{2\pi}\mathcal{P}\int_{-\infty}^{+\infty} d\Omega\; D_{\mathrm{cor}}(\omega,\omega',\Omega)S(\Omega), \tag{13.55}$$

Where D_{cor} depends on the approach used (either a master equation - GKLS or Bloch-Redfield -, the mean force expansion, or the cumulant equation). The table 13.1 shows the different kernels for different methods.

	GKLS	GKLS (non-secular)	Bloch-Redfield	Cumulant
$D_{\mathrm{LS}}(\omega,\omega,\Omega)$	$\frac{1}{\omega-\Omega}$			
$D_{\mathrm{LS}}(\omega,\omega',\Omega)$	0	$\frac{1}{2}(\frac{1}{\omega-\Omega}+\frac{1}{\omega'-\Omega})+\frac{i}{4}(\delta(\Omega-\omega)-\delta(\Omega-\omega'))$		
$D_{\mathrm{st}}(\omega,\omega,\Omega)$	0	general form not known		
$D_{\mathrm{st}}(\omega,\omega',\Omega)$	0	$D_{\mathrm{LS}}(\omega,\omega',\Omega)$	$D_{\mathrm{mf}}(\omega,\omega',\Omega)$	
$D_{\mathrm{mf}}(\omega,\omega,\Omega)$	$\frac{1-e^{\beta(\omega-\Omega)}+\beta(\omega-\Omega)}{\beta(\omega-\Omega)^2}$			
$D_{\mathrm{mf}}(\omega,\omega',\Omega)$	$\frac{1}{\omega'-\Omega}-\frac{(\omega-\omega')(e^{\beta(\omega-\Omega)}-1)}{(\omega-\Omega)(\omega'-\Omega)(e^{\beta(\omega-\omega')}-1)}$			

Table 13.1: Explicit kernels $D_{\mathrm{cor}}(\omega,\omega',\Omega)$ according to the representation Eq. (13.55) for all Hamiltonian corrections, i.e., cor = LS (Lamb-shift) , cor = mf (mean-force) and cor = st (quasi-steady state).

These corrections summarize results in [A2]. The main difference in this approach with respect to others in the literature [95, 96], is that rather than computing the higher order contributions to the state, we do it at the level of the Hamiltonian, the advantage of doing this instead of considering the state directly, is that one can use it as a "Hamiltonian Dressing" [80, 97, 98] which leads to corrections of the state. While the general expansions for second order corrections in the state are hard to

compare with previous results in the literature directly, in section 13.7, we show that the Gibbs' state of our "Dressed Hamiltonian" corresponds to the formulas in the literature [95, 96] when this state is Taylor expanded to the relevant order.

13.6 Extracting the second order Hamiltonian correction from a density matrix

The methods treated in this thesis, are equations for the density matrix. Once the density matrix for equilibrium is found, we need to extract the second order correction from it, to be able to compare these to the mean force Hamiltonian corrections obtained in this chapter. We start by obtaining the steady state density matrix, which is given by a Gibbs state of the form:

$$\rho_\alpha = \frac{e^{-\beta H}}{\mathcal{Z}}. \tag{13.56}$$

By taking the logarithm, one obtains

$$\log(\mathcal{Z}) + \log(\rho_\alpha) = -\beta H. \tag{13.57}$$

We then expand H

$$H = H_0 + \alpha^2 H_2 + \alpha^4 H_4 + \dots, \tag{13.58}$$

substituting in Eq. (13.57)

$$\log(\mathcal{Z}) + \log(\rho_\alpha) = -\beta(H_0 + \alpha^2 H_2 + \alpha^4 H_4 + \dots). \tag{13.59}$$

We now impose our gauge $\mathrm{Tr}[H] = 0$. Then tracing out both sides we obtain

$$\log(\mathcal{Z}) = -\frac{1}{d}\,\mathrm{Tr}[\log(\rho_\alpha)]. \tag{13.60}$$

By substituting back into Eq.Eq. (13.59) and rearranging terms one obtains

$$H_2 = \frac{1}{\alpha^2}\Big[\frac{1}{\beta}\Big(\frac{1}{d}\,\mathrm{Tr}[\log(\rho_\alpha)] - \log(\rho_\alpha)\Big) - \Big(H_0 + \mathcal{O}(\alpha^4)\Big)\Big]. \tag{13.61}$$

Finally as α approaches zero

$$\lim_{\alpha\to 0} H_2 = \lim_{\alpha\to 0} \frac{1}{\alpha^2}\Big[\frac{1}{\beta}\Big(\frac{1}{d}\,\mathrm{Tr}[\log(\rho_\alpha)] - \log(\rho_\alpha)\Big) - H_0\Big]. \tag{13.62}$$

Higher order corrections to the Hamiltonian can be extracted in a similar fashion. In this section, we use the reaction coordinate mapping as the true solution, similarly to [A2, 81]. The reason to choose reaction coordinate over HEOM or Pseudomodes is that, the reaction coordinate is a Hamiltonian mapping, that depends on the spectral density only and not on temperature. Thus we will have the same accuracy for every temperature, unlike in HEOM and Pseudomodes where we will have to perform different fits. This of course restricts the spectral densities we can study, but it is something we are happy with in this section.

13.7 Comparison with Lamb-shift Hamiltonian and the steady state - qubit case

In this section, we consider the particular case of a qubit coupled to a Bosonic bath given by

$$H = -\frac{\omega_0}{2}\sigma_z + \sum_k \Omega_k a_k^\dagger a_k + S\sum_{k=1}^{\infty} \alpha_k (a_k + a_k^\dagger), \tag{13.63}$$

where we take S to be a general interaction operator in the pauli basis:

$$S = f_1\sigma_x + f_2\sigma_y + f_3\sigma_z, \tag{13.64}$$

Writing the correction in the jump operator basis Eq. (13.51) and this interaction, the second-order correction to the Hamiltonian takes the form:

$$H_{\text{cor}}^{(2)} = \begin{bmatrix} f_3^2\Upsilon_{\text{cor}}(0,0) + |f|^2\Upsilon_{\text{cor}}(\omega,\omega) & f f_3(\Upsilon_{\text{cor}}(0,-\omega) - \Upsilon_{\text{cor}}(\omega,0)) \\ \overline{f} f_3(\Upsilon_{\text{cor}}(0,-\omega) - \Upsilon_{\text{cor}}(\omega,0)) & f_3^2\Upsilon_{\text{cor}}(0,0) + |f|^2\Upsilon_{\text{cor}}(-\omega,-\omega) \end{bmatrix}, \tag{13.65}$$

where cor indicates the Lamb-shift (LS), steady-state (st) or mean-force (mf) correction, and $f = f_1 - if_2$. We can rewrite this correction as a linear combination of the Pauli matrices so that:

$$H_{\text{cor}}^{(2)} = A\mathbb{I} + B\sigma_x + C\sigma_y + D\sigma_z, \tag{13.66}$$

$$A = f_3^2\Upsilon_{\text{cor}}(0,0) + \frac{|f|^2}{2}(\Upsilon_{\text{cor}}(\omega,\omega) + \Upsilon_{\text{cor}}(-\omega,-\omega)), \tag{13.67}$$

$$B = f_1 f_3(\Upsilon_{\text{cor}}(0,-\omega) - \Upsilon_{\text{cor}}(\omega,0)), \tag{13.68}$$

$$C = f_2 f_3(\Upsilon_{\text{cor}}(0,-\omega) - \Upsilon_{\text{cor}}(\omega,0)), \tag{13.69}$$

$$D = \frac{|f|^2}{2}(\Upsilon_{\text{cor}}(\omega,\omega) - \Upsilon_{\text{cor}}(-\omega,-\omega)). \tag{13.70}$$

We can see how the different approaches differ qualitatively by looking at the structure of the different $\Upsilon_{\text{cor}}(\omega,\omega')$ given by each approach. It is important to remark that any approach that performs the secular approximation will have both B and C equal to zero, meaning the correction will be diagonal and as such won't be able to describe the off-diagonal elements of the steady states accordingly. On the other hand, nonsecular approaches such as the Bloch-Redfield equation, will have non-diagonal corrections, leading to a more appropriate description of the off-diagonal elements of the correction as well as steady state coherences. Substituting the results of table 13.1 and using the spectral density

$$J(\omega) = \alpha^2 \frac{4\gamma\omega\omega_{rc}^2}{(\omega_{rc}^2 - \omega^2)^2 + (2\pi\gamma\omega\omega_{rc})^2}. \tag{13.71}$$

we can see from the figure 13.3 that when the coupling is weak, the mean force and reaction coordinate approaches match exactly. A small discrepancy is seen when the width (γ) is augmented, but this is due to the limitations of the reaction coordinate mapping with only one iteration. We can also see that the cumulant equation quasi-steady state correction is in good agreement with the mean force solution, however,

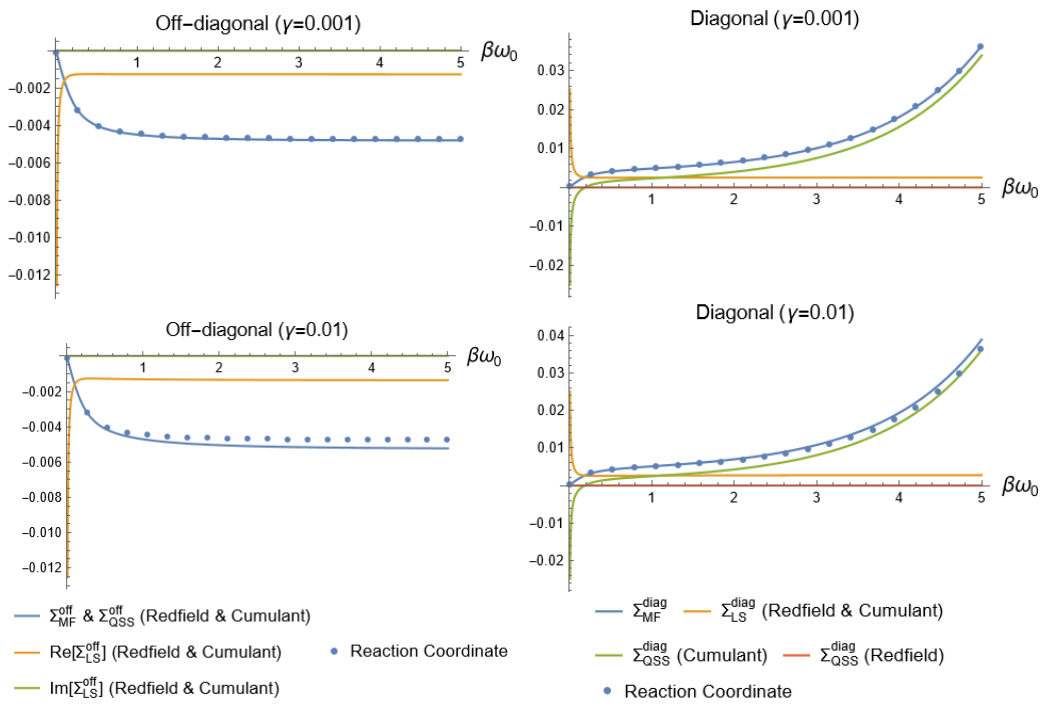

Figure 13.3: In the figure we present the diagonal and off-diagonal corrections, computed for the spin-boson model (Eq. (13.63)) for the spectral density Eq. (13.71) and for $\omega_{rc} = 20\omega_0$. As expected, we observe a very good agreement for $\gamma = 0.001$, whereas some discrepancy is present for $\gamma = 0.01$. showing the limits of the reaction coordinate method. Reproduced from [A2]

as mentioned before the quasisteady state is different from the steady state and the cumulant equation does not exhibit corrections to the diagonal. The steady state was obtained simply from the Gibbs state of the reaction coordinate. We can see how the different approaches differ qualitatively by looking at the structure of the different $\Upsilon_{\rm cor}(\omega,\omega')$ given by each approach.. Let us examine the second order mean force correction, using the information from the table 13.5, and substituting the relevant Bohr frequencies $(-\omega, 0, \omega)$ for the Hamiltonian Eq. (13.63):

$$\Upsilon_{\rm LS}(0,-\omega) - \Upsilon_{\rm LS}(\omega,0) = \frac{S_{LS}(-\omega) - S_{LS}(\omega)}{2} + i\frac{S(0) - (S(\omega) + S(-\omega))}{4}. \quad (13.72)$$

Let us compare this with the mean force correction

$$\Upsilon_{\rm mf}(0,-\omega) - \Upsilon_{\rm mf}(\omega,0) = \frac{1}{2\pi}\int_{-\infty}^{+\infty} d\Omega S(\Omega) C(\omega,\Omega), \quad (13.73)$$

where

$$C(\omega,\Omega) = \left(\frac{\omega^2(1-e^{-\beta\Omega})\coth[\frac{\beta\omega}{2}] + (1+e^{-\beta\Omega})\Omega\omega}{\Omega(\Omega^2-\omega^2)}\right). \quad (13.74)$$

Additionally, our coefficients satisfy detailed balance conditions such that:

$$S(-\Omega) = S(\Omega)e^{-\beta\Omega}, \quad C(\omega,-\Omega) = C(\omega,\Omega)e^{\beta\Omega} \quad (13.75)$$

Using those we see that $S(-\Omega)C(\omega,-\Omega) = S(\Omega)C(\omega,\Omega)$ and

$$\Upsilon_{\rm mf}(0,-\omega) - \Upsilon_{\rm mf}(\omega,0) = \frac{1}{2\pi}\int_0^{+\infty} d\Omega S(\Omega)C(\omega,\Omega). \tag{13.76}$$

Let us now separate $S(\Omega)$ into its symmetric and anti-symmetric parts:

$$S_s(\Omega) = \frac{1}{2}(S(\Omega)+S(-\Omega)) = J(\Omega)\coth\left(\frac{\beta\Omega}{2}\right) \tag{13.77}$$

$$S_a(\Omega) = \frac{1}{2}(S(\Omega)-S(-\Omega)) = J(\Omega) \tag{13.78}$$

Then we may write:

$$K(\omega) = \Upsilon_{\rm mf}(0,-\omega) - \Upsilon_{\rm mf}(\omega,0) \tag{13.79}$$

$$= \frac{2}{\pi}\int_0^{+\infty} d\Omega \left(\frac{\omega^2 S_a(\Omega)\coth[\frac{\beta\omega}{2}] + S_s(\Omega)\Omega\omega}{\Omega(\Omega^2-\omega^2)}\right). \tag{13.80}$$

$$= \frac{2}{\pi}\int_0^{+\infty} d\Omega \left(\frac{\omega^2 J(\Omega)\coth[\frac{\beta\omega}{2}] + J(\Omega)\coth[\frac{\beta\Omega}{2}]\Omega\omega}{\Omega(\Omega^2-\omega^2)}\right). \tag{13.81}$$

Let

$$H_S = -\frac{\omega_0}{2}\sigma_z + H^{(2)}_{mf}, \tag{13.82}$$

where $H^{(2)}_{mf}$ is the second-order mean force correction. To obtain it, one substitutes the coefficients from the table 13.5 into Eq. (13.65). Then we may find that

$$\langle\sigma_x\rangle = \frac{{\rm Tr}\left[\sigma_x e^{-\beta H_S}\right]}{{\rm Tr}[e^{-\beta H_S}]} = -x\frac{\tanh[\sqrt{x^2+(\frac{\omega}{2}+\alpha^2 z)^2}\beta]}{\sqrt{x^2+(\frac{\omega}{2}+\alpha^2 z)^2}}, \tag{13.83}$$

where $x = \alpha^2 f_1 f_3 K(\omega)$, $z = |f|^2(\Upsilon_{\rm cor}(\omega,\omega) - \Upsilon_{\rm cor}(-\omega,-\omega))$, if we expand it up to the second order of α, i.e.,

$$\langle\sigma_x\rangle = -\frac{2x}{\omega}\tanh[\frac{\beta\omega}{2}] + O(\alpha^3), \tag{13.84}$$

and the final result becomes:

$$\langle\sigma_x\rangle = \ -\frac{4\alpha^2 f_1 f_3}{\pi\omega}\tanh\left[\frac{\beta\omega}{2}\right]\int_0^{\infty} d\Omega \left(\frac{J(\Omega)\coth\left(\frac{\beta\Omega}{2}\right)\omega}{\Omega^2-\omega^2} - \frac{\omega^2 J(\Omega)}{\Omega(\Omega^2-\omega^2)}\right), \tag{13.85}$$

which can be rewritten as

$$\langle\sigma_x\rangle = -\frac{4\alpha^2 f_1 f_3}{\omega\pi}\tanh\left[\frac{\beta\omega}{2}\right]\int_0^{\infty} d\Omega J(\Omega)\left(\frac{\coth\left(\frac{\beta\Omega}{2}\right)\omega}{\Omega^2-\omega^2} + \frac{1}{(\Omega^2-\omega^2)} - \frac{1}{\Omega}\right). \tag{13.86}$$

To compare with the literature let $\omega \to -\omega_q$, $f_3 = \cos(\theta)$, $f_1 = \sin(\theta)$ then

$$\langle\sigma_x\rangle = \frac{2\alpha^2\sin(2\theta)}{\pi\omega_q}\tanh\left[\frac{\beta\omega_q}{2}\right]\int_0^{\infty} d\Omega\Bigg(\frac{J(\Omega)\coth\left(\frac{\beta\Omega}{2}\right)\omega_q}{\Omega^2-\omega_q^2} - \frac{J(\Omega)}{(\Omega^2-\omega_q^2)} + \frac{J(\Omega)}{\Omega}\Bigg). \tag{13.87}$$

which is the Eq.(46) in the supplemental material of [95] up to a factor of π^{-1} due to notational differences. The exposition of the mean force correction here in terms of Hamiltonians is equivalent to the section results there for the weak coupling limit on states. On the other hand the diagonal correction is given by

$$\langle\sigma_z\rangle = \frac{\mathrm{Tr}\left[\sigma_z e^{-\beta H_S}\right]}{\mathrm{Tr}[e^{-\beta H_S}]} = \frac{(\frac{\omega}{2}+\alpha^2 z)}{\sqrt{x^2+(\frac{\omega}{2}+\alpha^2 z)^2}}\tanh\left[\beta\sqrt{x^2+(\frac{\omega}{2}+\alpha^2 z)^2}\right] \tag{13.88}$$

Expanding it up to second order in α we get

$$\langle\sigma_z\rangle = \frac{\mathrm{Tr}\left[\sigma_z e^{-\beta H_S}\right]}{\mathrm{Tr}[e^{-\beta H_S}]} = \tanh[\frac{\beta\omega}{2}] + \frac{\alpha^2\beta z}{2}\left(1-\tanh^2[\frac{\beta\omega}{2}]\right) + O(\alpha^3). \tag{13.89}$$

using Eq. (13.55) one can write z as

$$z = \frac{-2f_1^2}{\pi\beta}\int_0^\infty d\Omega \frac{J(\Omega)}{\left(\omega^2-\Omega^2\right)^2}\Bigg[\coth\left(\frac{\beta\Omega}{2}\right)\left(\beta\omega(\Omega^2-\omega^2)+\left(\omega^2+\Omega^2\right)\sinh(\beta\omega)\right) + 2\omega\Omega(1+\cosh(\beta\omega))\Bigg]. \tag{13.90}$$

Using this, we may finally write the diagonal correction as

$$\langle\sigma_z\rangle - \langle\sigma_z\rangle_0 = \int_0^\infty \frac{d\Omega}{2\pi}\frac{2\alpha^2 f_1^2 J(\Omega)}{\left(\omega^2-\Omega^2\right)^2}\Bigg[4\omega\Omega + \coth\left(\frac{\beta\Omega}{2}\right)\left(\beta\omega\,\mathrm{sech}^2\left(\frac{\beta\omega}{2}\right)\left(\omega^2-\Omega^2\right) - 2\left(\omega^2+\Omega^2\right)\tanh\left(\frac{\beta\omega}{2}\right)\right)\Bigg]. \tag{13.91}$$

If again we let $\omega \to -\omega_q$, $f_1 = \sin(\theta)$ then

$$\langle\sigma_z\rangle - \langle\sigma_z\rangle_0 = 2\alpha^2\sin(\theta)^2\left(\beta\omega_q\,\mathrm{sech}^2[\frac{\beta\omega_q}{2}]\int_0^\infty \frac{d\Omega}{2\pi}\frac{J(\Omega)\coth\left(\frac{\beta\Omega}{2}\right)}{\left(\Omega^2-\omega_q^2\right)} + 2\tanh\left(\frac{\beta\omega_q}{2}\right)\int_0^\infty \frac{d\Omega}{2\pi}\frac{J(\Omega)\coth\left(\frac{\beta\Omega}{2}\right)\left(\omega_q^2+\Omega^2\right)}{\left(\omega_q^2-\Omega^2\right)^2} - \int_0^\infty \frac{d\Omega}{2\pi}\frac{4\omega_q\Omega J(\Omega)}{\left(\omega_q^2-\Omega^2\right)^2}\right), \tag{13.92}$$

which is the equation Eq. (42) in the Supplemental Material of [47], and up to a factor of $(\pi)^{-1}$ is the same expression as Eq. (47) in the Supplemental Material of [95]. Those factors are notational differences related to those we mentioned in section 1.1, luckily in this case this notational differences are easy to spot, but this is not always the case.

Part IV

Open Quantum systems III: Applications

Chapter 14

The Spin Boson Model at zero temperature

The spin boson model at zero temperature with the rotating wave approximation (RWA) is one of the few systems to have an exact solution in the field of open quantum systems. This exact description of course is somewhat limited, in the sense that the original system underwent several approximations; nevertheless, this exact master equation provides us with a nice example to test the methods we have developed so far. This chapter loosely follows the descriptions in [B1, 99] with the addition of modern approaches. One thing to keep in mind is that in this chapter, only the exact master equation and the Volterra equation Eq. (14.28) employ the RWA, the other methods agree because the simulations are run with parameters for which the RWA is valid. Consider the Hamiltonian

$$H = \underbrace{H_S + H_B}_{H_0} + H_I, \tag{14.1}$$

$$H_S = \omega_0 \sigma_+ \sigma_-, \tag{14.2}$$

$$H_B = \sum_k \omega_k b_k^\dagger b_k, \tag{14.3}$$

$$H_I = \sigma_+ \otimes B + \sigma_- \otimes B^\dagger, \tag{14.4}$$

$$B = \sum_k g_k b_k. \tag{14.5}$$

Notice we use $H_S = \omega_0 \sigma_+ \sigma_-$ rather than the standard $H_S' = \frac{\omega_0}{2}\sigma_z$, the reason to choose the former is that it makes the algebra in this section a little easier, as we don't need to carry a factor of $\pm\frac{1}{2}$ in some commutation relations.. While we will apply the methods developed in Part II of the thesis, we will briefly review how to obtain an exact master equation for this system in the case of $T = 0$. For methods other than TCL which was derived using the exact master equation, and the exact solution, we will consider the Hamiltonian without the rotating wave approximation. Their agreement will validate the usage of this approximation.

14.1 The exact master equation

Let us introduce the states

$$|\psi_0\rangle = |0\rangle_S \otimes |0\rangle_B , \tag{14.6}$$

$$|\psi_1\rangle = |1\rangle_S \otimes |0\rangle_B , \tag{14.7}$$

$$|\psi_k\rangle = |0\rangle_S \otimes |k\rangle_B , \tag{14.8}$$

where $|k\rangle_B$ denotes the state with a single photon in mode k. This states span all the possibilities of a single excitation in this model. These states will be enough because

$$N = \sigma_+\sigma_- + \sum_k b_k^\dagger b_k, \tag{14.9}$$

$$[H, N] = 0. \tag{14.10}$$

which means that the Hamiltonian conserves the number of particles. If we start with a single excitation in the vacuum, the three states we mentioned before will be the only ones involved in the dynamics. In the interaction picture the state of the full system obeys

$$\dot{\phi}(t) = -iH_I(t)\phi(t), \tag{14.11}$$

with

$$H_I(t) = \sigma_+ B e^{i(\omega_0-\omega_k)t} + \sigma_- B^\dagger e^{-i(\omega_0-\omega_k)t}. \tag{14.12}$$

Consider an initial state of the system of the form

$$\phi(0) = c_0(0)\,|\psi_0\rangle + c_1(0)\,|\psi_1\rangle + \sum_k c_k(0)\,|\psi_k\rangle\,, \tag{14.13}$$

since $|\psi_0\rangle\,, |\psi_1\rangle\,, |\psi_k\rangle$ are the only states involved after time t the state will have evolved to

$$\phi(t) = c_0(t)\,|\psi_0\rangle + c_1(t)\,|\psi_1\rangle + \sum_k c_k(t)\,|\psi_k\rangle\,. \tag{14.14}$$

We then use the equation of motion to find the evolution of c_0, c_1, c_k. But first, consider

$$\begin{aligned}
H_I(t)\,|\psi_0\rangle &= \left(\sigma_+ B e^{i(\omega_0-\omega_k)t} + \sigma_- B^\dagger e^{-i(\omega_0-\omega_k)t}\right)|0\rangle_S \otimes |0\rangle_B && (14.15)\\
&= 0 && (14.16)\\
H_I(t)\,|\psi_1\rangle &= \left(\sigma_+ B e^{i(\omega_0-\omega_k)t} + \sigma_- B^\dagger e^{-i(\omega_0-\omega_k)t}\right)|1\rangle_S \otimes |0\rangle_B && (14.17)\\
&= \sum_k \overline{g_k} e^{-i(\omega_0-\omega_k)t}\,|\psi_k\rangle && (14.18)\\
H_I(t)\,|\psi_k\rangle &= \left(\sigma_+ B e^{i(\omega_0-\omega_k)t} + \sigma_- B^\dagger e^{-i(\omega_0-\omega_k)t}\right)|0\rangle_S \otimes |k\rangle_B && (14.19)\\
&= \sum_k g_k e^{i(\omega_0-\omega_k)t}\,|\psi_1\rangle\,. && (14.20)
\end{aligned}$$

We can then just insert this into the Schrodinger equation in the interaction picture to obtain

$$\begin{aligned}
\dot{c}_0(t)\,|\psi_0\rangle + \dot{c}_1(t)\,|\psi_1\rangle + \sum_k \dot{c}_k(t)\,|\psi_k\rangle &= -ic_1(t)\sum_k \overline{g_k} e^{-i(\omega_0-\omega_k)t}\,|\psi_k\rangle\\
&\quad - i\sum_k c_k(t) g_k e^{i(\omega_0-\omega_k)t}\,|\psi_1\rangle\,. \qquad (14.21)
\end{aligned}$$

By using the fact that the states are orthogonal we find

$$\dot{c_0}(t) = 0, \tag{14.22}$$

$$\dot{c_1}(t) = -i \sum_k c_k(t) g_k e^{i(\omega_0 - \omega_k)t}, \tag{14.23}$$

$$\dot{c_k}(t) = -i c_1(t) \overline{g_k} e^{-i(\omega_0 - \omega_k)t}. \tag{14.24}$$

We then need to solve the set of differential equations, as mentioned before we assumed that we have the oscillators in the vacuum, meaning $c_k(0) = 0$. We then solve the equation for c_k directly which results in

$$\dot{c_k}(t) = -i \int_0^t ds c_1(s) \overline{g_k} e^{-i(\omega_0 - \omega_k)s}. \tag{14.25}$$

We then insert this formal solution into the first equation

$$\dot{c_1}(t) = -\sum_k g_k e^{i(\omega_0 - \omega_k)t} \int_0^t ds c_1(s) \overline{g_k} e^{-i(\omega_0 - \omega_k)s} \tag{14.26}$$

$$= -\int_0^t ds c_1(s) \sum_k |g_k|^2 e^{i(\omega_0 - \omega_k)(t-s)} \tag{14.27}$$

$$= -\int_0^t ds c_1(s) f(t-s), \tag{14.28}$$

where

$$f(t-s) = \sum_k |g_k|^2 e^{i(\omega_0 - \omega_k)(t-s)} = \mathrm{Tr}_B \Big[B(t) B^\dagger(s) \rho_B \Big] e^{i\omega_0 (t-s)}. \tag{14.29}$$

We can identify f as the two time correlation function (see section 1.1) times a phase. Using the equations we derived the density matrix of the qubit which can be written as

$$\rho_s(t) = \mathrm{Tr}_B \Big[\phi(t) \phi^\dagger(t) \Big] = \begin{pmatrix} |c_1(t)|^2 & \overline{c_0} c_1(t) \\ \overline{c_1}(t) c_0 & 1 - |c_1(t)|^2 \end{pmatrix}. \tag{14.30}$$

By taking a time derivative we obtain

$$\dot{\rho}_s(t) = \begin{pmatrix} \frac{d}{dt}|c_1(t)|^2 & \overline{c_0} \dot{c_1}(t) \\ \dot{\overline{c_1}}(t) c_0 & -\frac{d}{dt}|c_1(t)|^2 \end{pmatrix}. \tag{14.31}$$

Notice that

$$\sigma_- \rho_s(t) \sigma_+ = \begin{pmatrix} 0 & 0 \\ 0 & |c_1(t)|^2 \end{pmatrix}, \tag{14.32}$$

$$\frac{1}{2} \{ \sigma_+ \sigma_-, \rho_s(t) \} = \begin{pmatrix} |c_1(t)|^2 & \frac{\overline{c_0} c_1(t)}{2} \\ \frac{\overline{c_1}(t) c_0}{2} & 0 \end{pmatrix}, \tag{14.33}$$

$$[\sigma_+ \sigma_-, \rho_s(t)] = \begin{pmatrix} 0 & \overline{c_0} c_1(t) \\ -\overline{c_1}(t) c_0 & 0 \end{pmatrix}. \tag{14.34}$$

Then let us define the quantities

$$\gamma(t) = -\left(\frac{\dot{c}_1(t)}{c_1(t)} + \frac{\overline{\dot{c}_1(t)}}{c_1(t)}\right), \tag{14.35}$$

$$S(t) = -\left(\frac{\dot{c}_1(t)}{c_1(t)} - \frac{\overline{\dot{c}_1(t)}}{c_1(t)}\right), \tag{14.36}$$

so that

$$\frac{\gamma(t) + iS(t)}{2} = -\frac{\dot{c}_1(t)}{c_1(t)}, \tag{14.37}$$

$$\gamma(t)|c_1(t)|^2 = -\dot{c}_1(t)\overline{c_1}(t) - c_1(t)\dot{\overline{c_1}}(t) \tag{14.38}$$

$$- \frac{d}{dt}|c_1(t)|^2. \tag{14.39}$$

Armed with these definitions we may now write

$$\dot{\rho}_s(t) = \begin{pmatrix} -\gamma(t)|c_1(t)|^2 & -c_1\overline{c_0}S(t) \\ -c_0\overline{c_1}S(t) & \gamma(t)|c_1(t)|^2 \end{pmatrix} \tag{14.40}$$

$$= -i[\frac{S(t)}{2}\sigma_+\sigma_-, \rho_s(t)] + \gamma(t)\left(\sigma_-\rho_s(t)\sigma_+ - \frac{1}{2}\{\sigma_+\sigma_-, \rho_s(t)\}\right). \tag{14.41}$$

The exact master equation Eq. (14.41) is already in TCL form (it is time local). We can now proceed to show that the TCL expansion to any order gives us an equation in this form, we begin by expanding $\gamma(t)$ and $S(t)$ in powers of the coupling strength

$$\gamma(t) = \sum_{n=1}^{\infty} \alpha^{2n}\gamma_{2n}(t), \tag{14.42}$$

$$S(t) = \sum_{n=1}^{\infty} \alpha^{2n}S_{2n}(t). \tag{14.43}$$

Then notice that σ_+ is an eigenoperator, of the generator of the exact master equation

$$\mathcal{K}_{exact}\sigma_+ = -i[\frac{S(t)}{2}\sigma_+\sigma_-, \cdot] + \gamma(t)\left(\sigma_- \cdot \sigma_+ - \frac{1}{2}\{\sigma_+\sigma_-, \cdot\}\right)\sigma_+ \tag{14.44}$$

$$= -\frac{\gamma(t) + iS(t)}{2}\sigma_+. \tag{14.45}$$

The generator of the exact master equation is related to the TCL generator by Eq. (12.17) so we have

$$\mathcal{K}_{exact}\sigma_+ = \sum_{n=1}^{\infty} \alpha^{2n} \int_0^t dt_1 \int_0^{t_1} dt_2 \cdots \int_0^{t_{2n-2}} dt_{2n-1} \langle \mathcal{L}(t)\mathcal{L}(t_1)\mathcal{L}(t_2)\ldots\mathcal{L}(t_{2n-1})\rangle_{oc}\sigma_+. \tag{14.46}$$

Using the fact that $\mathcal{L}(t) = -i[H_I(t), \cdot]$ we can find

$$\mathcal{L}(t)[\sigma_+] = i\sigma_z B^\dagger e^{i(\omega_0-\omega_k)t}, \tag{14.47}$$

$$\mathcal{L}(t_1)\mathcal{L}(t)[\sigma_+] = -\sigma_+ \otimes \left(BB^\dagger + B^\dagger B\right) e^{i(\omega_0-\omega_k)(t-t_1)}. \tag{14.48}$$

By taking the average with respect to the thermal state and using the fact that at zero temperature then mean number of photons in the bath is zero then

$$\langle \mathcal{L}(t_1)\mathcal{L}(t)\rangle[\sigma_+] = -\sigma_+ f(t-t_1). \tag{14.49}$$

Which allows us to write

$$\begin{aligned}\mathcal{K}_{exact}\sigma_+ = \sum_{n=1}^{\infty}(-1)^n\alpha^{2n}\int_0^t dt_1\int_0^{t_1} dt_2\cdots\int_0^{t_{2n-2}} dt_{2n-1} \\ \times\left(f(t-t_1)f(t_1-t_2)\dots f(t_{2n-2}-t_{2n-1})\right)_{oc}\sigma_+,\end{aligned} \tag{14.50}$$

by direct comparison se see that

$$\begin{aligned}\frac{\gamma(t)+iS(t)}{2} = \sum_{n=1}^{\infty}(-1)^n\alpha^{2n}\int_0^t dt_1\int_0^{t_1} dt_2\cdots\int_0^{t_{2n-2}} dt_{2n-1} \\ \times\left(f(t-t_1)f(t_1-t_2)\dots f(t_{2n-2}-t_{2n-1})\right)_{oc}.\end{aligned} \tag{14.51}$$

Where oc stands for ordered cumulant. The TCL_{2n} equation corresponds to truncating the sum to n, $n=1$ corresponds to the Redfield equation we have been studying so far. While $n=2$ yields

$$\frac{\gamma_4(t)+iS_4(t)}{2} = \int_0^t dt_1\int_0^{t_1} dt_2\int_0^{t_2} dt_3\left(f(t-t_1)f(t_1-t_2)f(t_2-t_3)\right)_{oc} \tag{14.52}$$

$$= \int_0^t dt_1\int_0^{t_1} dt_2\int_0^{t_2} dt_3\left(f(t-t_2)f(t_1-t_3)+f(t-t_3)f(t_1-t_2)\right), \tag{14.53}$$

where γ_4 is the $4^{th}-order$ contribution to the decay rate and $S_4(t)$ to the Lamb-shift. We will now show how our method for approximating decay rates can be used in the TCL equation in practice (see section 12.4)

14.2 Using the decaying exponential approximation in TCL

One nice thing about the TCL equation is that in the way we have presented it the correlation functions are always ordered in a way that allows for direct integration as their arguments are always positive, thanks to the ordered cumulants and time ordering. This allows us to use the same approximation we used for second order descriptions (see 6.2 and 7.3) to quickly compute the decay rates and Lamb-shift contribution without the need for high-dimensional integration and for arbitrary spectral densities. While we present it for this simple example, the general case[1] will just include phases due to the jump operators and will remain analogous (see [B1, 18, 89, 90]). This example was chosen because it allows us to concentrate on the decay rates and Lamb-shift without paying the price of the summation over the combinatorics of Bohr frequencies.

[1]We mean the general TCL equation Eq. (12.6)

If we follow the same procedure as in sections 6.2 and 7.3 for the fourth order contribution of the TCL equation, we obtain

$$\begin{aligned}\left(\frac{\gamma(t)+iS(t)}{2}\right)_4 &= \sum_{\substack{k_1,k_2\\k_1\neq k_2}} \frac{c_{k_1}c_{k_2}}{(iv_{k_1}+\omega_0)(iv_{k_2}+\omega_0)} \\ &\times\left[\frac{e^{-t(v_{k_2}-i\omega_0)}}{v_{k_1}-v_{k_2}}+\frac{e^{-t(v_{k_1}+v_{k_2}-2i\omega_0)}}{v_{k_2}-i\omega_0}+\frac{1}{i\omega_0-v_{k_1}}\right. \\ &\left.+\left(t+\frac{1}{v_{k_1}-i\omega_0}-\frac{1}{v_{k_2}-i\omega_0}+\frac{1}{v_{k_2}-v_{k_1}}\right)e^{-tv_{k_1}+it^2\omega_0}\right] \\ &+\sum_k \frac{c_k^2}{(v_k-i\omega_0)^3}\left[1-e^{-2t(v_k-i\omega_0)}-2t(v_k-i\omega_0)e^{-t(v_k-i\omega_0)}\right]. \end{aligned} \tag{14.54}$$

Notice that the decay rates in previous sections, were approximated by a sum of m elements, where m is the number of exponents we used to describe our two time correlation function. As the sum was over only one index is computational cost was $O(m)$. However, from the TCL_{2n} expansion with ordered cumulants, we see that after approximation we will have $O(m^n)$ indices in the summation (as it will be an integral of the product of n correlation functions), increasing the computational cost, thus for higher order master equations, reducing the number of exponents used has a significant impact on the computational cost of the simulation. However the approximation of the high dimensional integrals to this form will remain possible regardless of the order of the truncation.

14.3 Turning the Integro-Differential equation into a system of ODES

For the simple model studied in this chapter, the dynamics is given by Eq. (14.26)

$$\dot{c_1}(t) = -\int_0^t ds c_1(s) f(t-s). \tag{14.55}$$

Now if we assume that we can represent our environment's two time correlation function as a sum of decaying exponentials (See 1.6) then we have[1, 100, 101]

$$f(\tau) = \sum_k^N c_k e^{-\nu_k \tau}, \tag{14.56}$$

hence

$$\dot{c_1}(t) = -\sum_k^N \int_0^t ds c_1(s) c_k e^{-\nu_k(t-s)}. \tag{14.57}$$

If we let

$$y_k(t) = \int_0^t ds c_1(s) c_k e^{-\nu_k(t-s)}, \tag{14.58}$$

then

$$\dot{c_1}(t) = -\sum_k^N y_k(t). \tag{14.59}$$

To find the $y_k(t)$ we simply take the time derivative of Eq. (14.58) resulting in

$$\dot{y_k}(t) = c_1(t) - \nu_k \int_0^t ds c_1(s) c_k e^{-\nu_k(t-s)} \tag{14.60}$$

$$= c_1(t) - \nu_k y_k(t), \tag{14.61}$$

where we used

$$\frac{d}{dx}\left(\int_{a(x)}^{b(x)} f(x,t)dt\right) = f\big(x,b(x)\big)\cdot\frac{db(x)}{dx} - f\big(x,a(x)\big)\cdot\frac{da(x)}{dx} + \int_{a(x)}^{b(x)} \frac{\partial}{\partial_x} f(x,t)dt. \tag{14.62}$$

To obtain the dynamics one then solves the system of ODES

$$\dot{c_1}(t) = -\sum_k^N y_k(t), \tag{14.63}$$

$$\dot{y_k}(t) = c_1(t) - \nu_k y_k(t). \tag{14.64}$$

Subjected to the initial conditions

$$y_k(0) = 0. \tag{14.65}$$

With this change the Volterra equation can be solved as a set of differential equations. We expect this way of solving Volterra equations will be useful in the field beyond this simple example.

14.4 Analytical Example: A Lorentzian Spectral density

Generally, the integro-differential (Volterra) equation Eq. (14.26) cannot be solved analytically, requiring the use of numerical methods. These approaches include directly solving the equation with techniques like the finite element method or converting it into a system of ordinary differential equations (ODEs), as was done in the previous section. In the specific case where the correlation function can be expressed as a single exponent, an exact analytical solution exists [B1, 19]. We will use this solution to validate our proposed numerical scheme.

Let us consider [2]

$$J(\omega) = \frac{1}{2\pi}\frac{\lambda^2\gamma}{(w_0 - w)^2 + \lambda^2}, \tag{14.66}$$

[2]The fact that this spectral density is not zero at zero frequency is rather problematic [29]

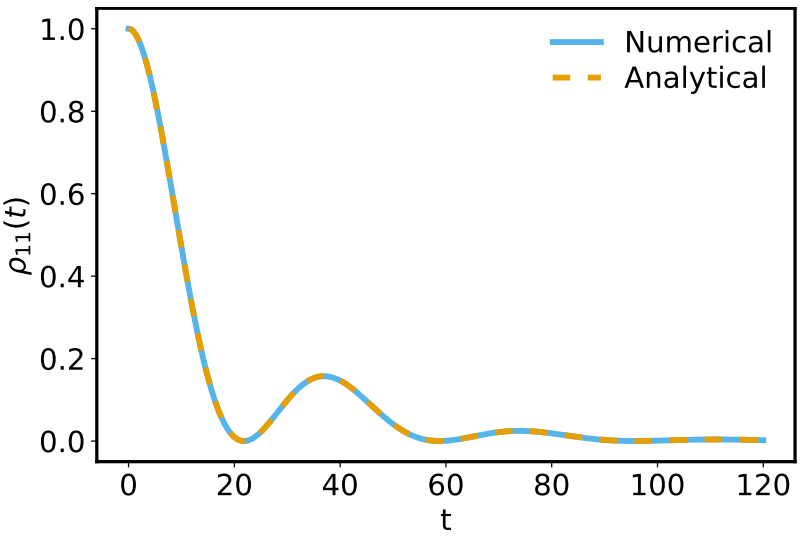

Figure 14.1: The figure shows the result of the simulation using our numerical approach in terms of the system of ODES, and the Analytical solution. The parameters for the simulation are $\lambda = 0.05, \gamma = 0.1\pi$

Then we find that

$$f(\tau) = e^{i\omega_0\tau}\int_0^\infty J(\omega)e^{-i\omega\tau} \approx \frac{1}{2}\lambda\gamma e^{-\lambda t}, \tag{14.67}$$

in this case we can solve the Volterra equation exactly , by using the Laplace transform on Eq. (14.26)

$$\mathcal{L}(\dot{c_1}(t)) = -\mathcal{L}\left(\int_0^t ds c_1(s) f(t-s)\right) \tag{14.68}$$

$$sC_1(s) - C_1(0) = -C_1(s)F(s), \tag{14.69}$$

where $F(s) = \frac{\gamma\lambda}{2(s+\lambda)}$ this allows us to write

$$\left(s + \frac{\gamma\lambda}{2(s+\lambda)}\right) C_1(s) = C_1(0), \tag{14.70}$$

$$C_1(s) = \frac{s+\lambda}{s^2 + s\lambda + \frac{\gamma\lambda}{2}} C_1(0). \tag{14.71}$$

By taking the inverse Laplace transform and using $d = \sqrt{\lambda^2 + 2\gamma\lambda}$ we finally obtain

$$c_1(t) = e^{-\frac{\lambda t}{2}}\left(\cosh\left(\frac{dt}{2}\right) + \frac{\lambda}{d}\sinh\left(\frac{dt}{2}\right)\right). \tag{14.72}$$

Figure 14.1 shows that out way of turning the integro-differential equation to ODEs using an approximation of the correlation function, matches the numerically exact solution Eq. (14.63).

14.5 Beyond Analytical Spectral densities

In this section we will explore the dynamics of our model under two previously unexplored cases. This will also allows to compare the TCL_4 equation with the Redfield

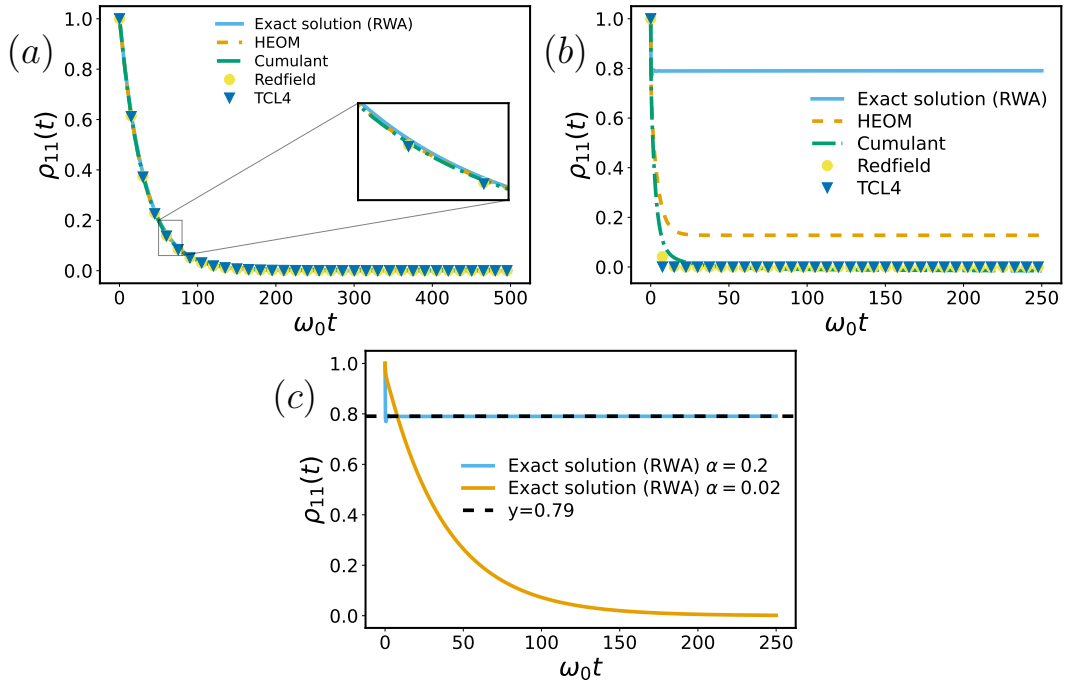

Figure 14.2: Behavior with an Ohmic Spectral density Eq. (1.99) with $s = 1$, $\omega_c = 5$ and $\alpha = 0.01$. a) shows the weak coupling limit where all methods agree. b) shows the strong coupling $\alpha = 0.2$, where we see evidence of the localization-delocalization phase transition even when using the RWA c) shows the localization delocalization transition for strong coupling in the RWA model

and cumulant equations in this simple scenario as well as test our numerically proposed scheme for the Volterra equation by comparing its result to the Hierarchical equations of motion for our model.

As a first example we will explore the dynamics of this model under the influence of a Ohmic spectral density, where we expect all the approximate methods to do fairly good in the weak coupling regime. We also expect those approaches and Eq. (14.26) to break down in the strong coupling regime where the spin boson model has the localization delocalization phase transition [A1, 15, 102]. The figure 14.2 shows the behaviour of the solutions under two sets of parameters, overall we find good agreement in all methods when the coupling is weak, but if we increase either the coupling strength or the cutoff (both increase the value of $S(\omega_0)$) solutions diverge significantly.

An interesting feature of the spin boson model is the localization-delocalization phase transition [A1, 15, 103]. In simple terms that phase transition is a change in the final state of the system from the localized ground state to a delocalized one.[3]. Up until recently it was thought that counter rotating terms were necessary for such a transition, however, using Variational Matrix Product states (VMPS) Wang et al.[104] were able to show that it is possible to have that transition in the rotating wave approximated regime.

Now that we have unlocked the simulation of the exact solution with the Volterra

[3]It is typically studied with a σ_x rather than a σ_z system Hamiltonian. The terms localization and delocalization are not the most appropriate here

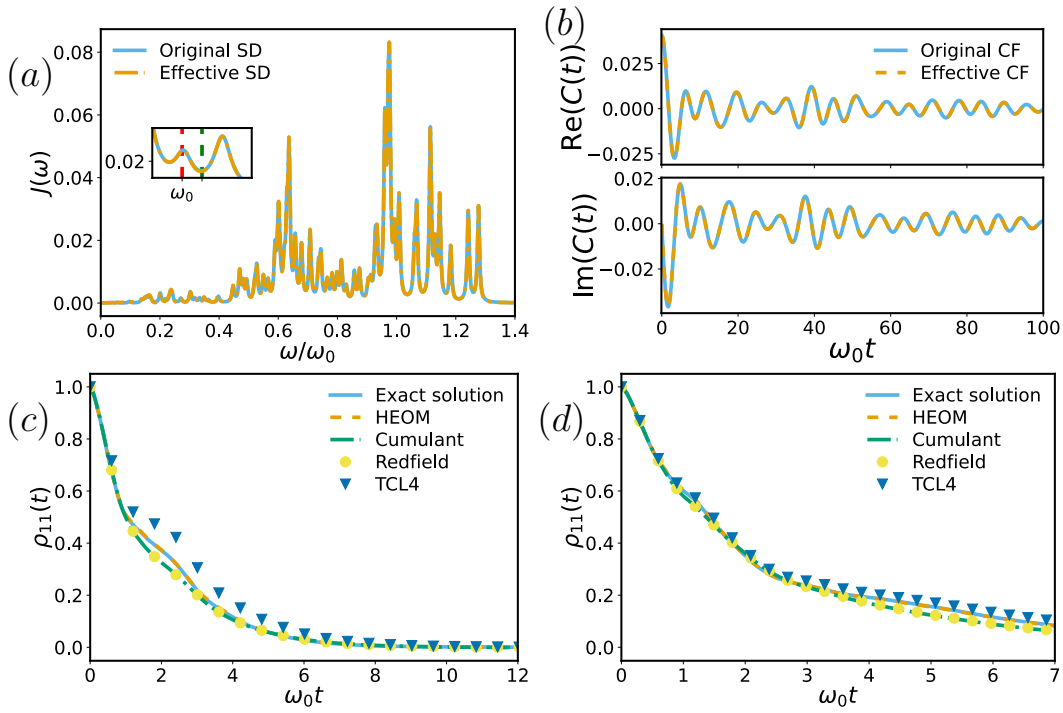

Figure 14.3: a) Spectral density under consideration, the dashed line is the effective spectral density, namely the spectral density that corresponds to the decaying exponential approximation, the inset shows the spectral density near the frequency of the two level system, b) The correlation function under consideration, again the effective one refers to the approximation. c) Decay of the population with all the different methods for the first value of ω_0 (the red line in the inset of subfigure a) d) Decay of the population with all the different methods for the second value of ω_0 (the blue line in the inset of subfigure a)

equation, a natural question is whether this simple model (with the RWA) also sees the phase transition in the same way the full spin boson model does, and how much it differs from a simulation that takes the counter rotating terms into account. The answer is it does as 14.2 shows. while it does show the transition for the same parameters the simulation cost is way less, however the steady states are significantly different, which agrees with the fact that one expects counter rotating terms to become important in the strong coupling regime.

As a second example we consider a structured spectral density taken from [31] where the data for the so called Huang-Rhys factors of experimental data are provided. We rescale the spectral density so that the coupling to our qubit is weak. The data for the spectral density is in the appendix C as well as the rescaling done. In Figure 14.3 a) we can observe the rescaled spectral density in arbitrary units as well as the values of $J(\omega_0)$ for the two values of ω_0 chosen, the two examples c) and d) show that while TCL_4 is better in one of them, the fourth order correction seems to take the dynamics away from the exact solution in the other, which is consistent with the results in [90] where they see that TCL_2 can be better than TCL_4 for a certain regime of parameters.

Finally, Figure 14.3 provides clear evidence against the belief that master equations cannot be used when dealing with structured spectral densities; however, when used within their established regime of validity, Non-Markovian master equations can indeed capture the dynamics of open systems in structured environments with high

fidelity. Furthermore, approximating the decay rates makes these simulations cheap, as the cost of the computation of the decay rates is $O(m)$ where m is the number of exponents needed to represent the environment. We hope this combination of techniques proves useful to others in the future.

Chapter 15

The Spin Boson Model

In the previous chapter we considered a spin-boson model, applied the rotating wave approximation and considered zero temperature. This section considers the spin boson model without the rotating wave approximation and coupled to the environment through an arbitrary operator, which is sometimes called the Non-equilibrium spin-Boson model [98]. For generality we will consider the most general Hamiltonian we can get for a simple Spin-Boson model, which is given by:

$$H = \underbrace{\frac{\omega_0}{2}\sigma_z}_{H_S} + \underbrace{\sum_k w_k a_k^\dagger a_k}_{H_B} + \underbrace{\sum_k g_k(f_1\sigma_x + f_2\sigma_y + f_3\sigma_z)(a_k + a_k^\dagger)}_{H_I}, \tag{15.1}$$

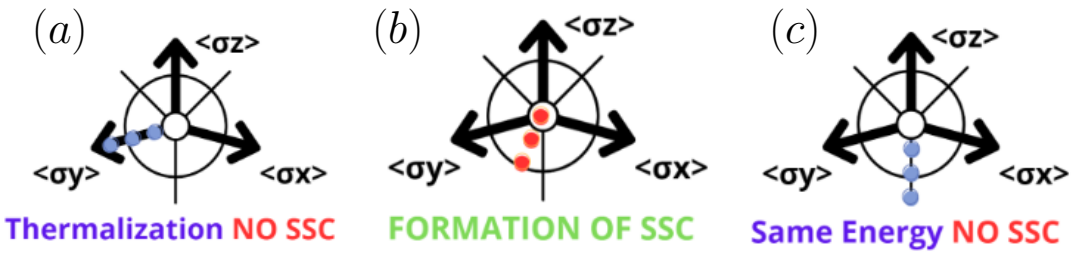

Figure 15.1: a) The interaction Hamiltonian is orthogonal to H_S, in this case the system thermalizes and no steady state coherences are generated. b) The interaction Hamiltonian is neither orthogonal nor parallel to H_S, in this setting steady state coherences are generated. c) The interaction Hamiltonian is parallel to H_S, this is the pure dephasing case.

The system can undergo three types of dynamics, namely thermalization, the formation of Steady State Coherences (SSC)[1], and dephasing. The Steady-state coherences arise when composite interactions are in place, meaning there is an interaction that is both parallel and orthogonal to the system Hamiltonian $H_S = \frac{\omega\sigma_z}{2}$ the figure above illustrates the different cases that rise in a Spin-Boson model depending on the interaction Hamiltonian H_I

- Figure 15.1(a) shows the case in which we have an interaction that is orthogonal to H_S [2], the system is driven to a Gibbs state at the temperature of the bath. No steady state coherences are generated.

[1] Steady state coherences are mean force corrections in the off-diagonal (see 13)

[2] In this context we say an an operator is parallel to another if they commute and orthogonal if the commutator generates a different member of the SU(N) group.

- Figure 15.1(b) shows an interaction that is neither orthogonal nor parallel to H_S but that instead is made of a composition of both orthogonal and parallel components, in this setting steady state coherences are generated
- Figure 15.1(c) illustrates H_S parallel to the interaction. In this case, the populations of the system are not driven towards the Gibbs state at the bath's temperature, only coherences evolve and they go towards zero.

In the reference [A3], we obtain remarkably simple expressions for the dynamics of this system using the cumulant equation. In this section, we will reproduce and extend the results of that paper, by conducting a similar study using all of the methods outlined in the thesis so far, and seeing how a different spectral density affects those results. In particular, in the paper we used an Drude-Lorentz (overdamped) spectral density

$$J(\omega) = \frac{2\lambda_{OD}\omega\gamma}{\gamma^2 + \omega^2}. \tag{15.2}$$

This spectral density is easy to use in practice, due to its pole structure. However, there are several concerns about the physicality of Drude-Lorentz (overdamped) spectral densities at low temperatures [29]. We justify its use because we work in the limit where this is obtained from an underdamped spectral density

$$J_U(\omega) = \frac{\lambda_U^2 \Gamma \omega}{[(\omega_0^2 - \omega^2)^2 + \Gamma^2\omega^2]}, \tag{15.3}$$

in the limit of $\Gamma \gg \omega_0$, where $\gamma = \frac{\omega_0^2}{\Gamma}$, and $\lambda_{OD} = \frac{\lambda_U^2}{2\omega_0^2}$. This regime is free of the issues that make the former unphysical.

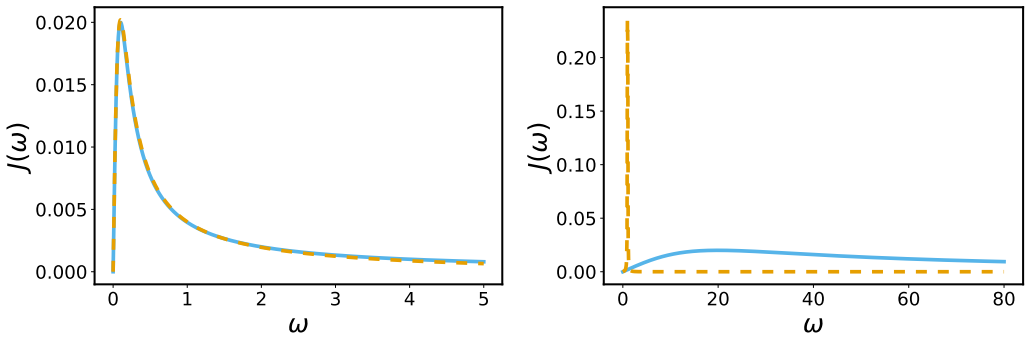

(a) $\Gamma \gg \omega_0$ **(b)** $\Gamma = 0.05\omega_0$

Figure 15.2: Underdamped vs Drude-Lorentz (overdamped) spectral densities. a) Shows parameters where the Drude-Lorentz (overdamped) spectral density is a good approximation of the underdamped case ($\lambda_U = 0.2\omega_0$, $\Gamma = 10\omega_0$) b) Shows parameters for which they differ, all are the same except $\Gamma = 0.05\omega_0$

In this section we will explore a bit the underdamped regime before quoting the results in [A3]. The underdamped spectral density induces underdamped oscillations. As its name suggests, these oscillations can exhibit revivals both in coherence and population in the underdamped regime. This population revivals are not captured by second order master equations even in weak coupling, thus besides coupling we need to consider the width of the spectral density, this fact is usually phrased as "We assume the relaxation time of the environment is much faster than the one of

the system" . This just means our correlation function decays to zero fast compared to the relaxation time of the system, this is broken for correlations that take long to decay, which correspond to narrow spectral densities, which make master equations invalid even in the weak coupling regime (see figure 15.3a) . As an example, consider a spin coupled to a bath at fixed temperature, and coupling constant, but with different widths (Γ). To further illustrate another point the simulation is done at $T = 0$.

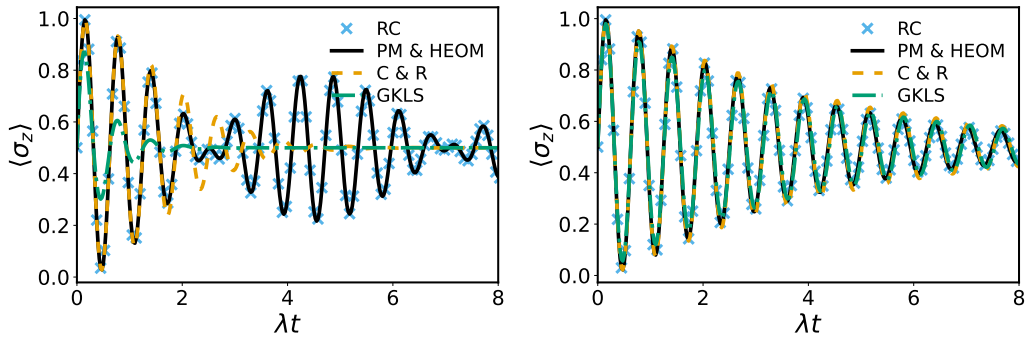

(a) $\Gamma = 0.05\omega_0$ **(b)** $\Gamma = 0.4\omega_0$

Figure 15.3: Spin boson model, with different widths the spectral density parameters correspond to those of figure 15.2, except for Γ, we used $T = 0$ for the simulation. We can see that when Γ is comparable to ω_0 master equations already give good results, similar results are obtained when $\Gamma \gg \omega_0$, but when it is small they deviate significantly. Figure (a) reproduces figure 3 from [12] with the addition of master equation methods. The Hamiltonian used for the simulation corresponds to $\omega_0 = 1$, $f_1 = -1$, $f_2 = f_3 = 0$, after rotating the Hamiltonian Eq. (15.1) with $U = R_y(\frac{\pi}{2})$ where R_y denotes a Bloch-sphere rotation along the $y - axis$. The dynamics shown in both plots correspond to the reaction coordinate with a GKLS master equation (RC), pseudomodes (PM), the hierarchical equations of motion (HEOM), the cumulant equation (C), Redfield (R).

Looking at figures 15.2 and 15.3, notice that even though Fig. 15.3b has the same "coupling strength" (λ_U) to Fig. 15.3a, it yields worse results with respect to the exact solutions. In both the reference and this section, we consider the regime $\Gamma \gg \omega_0$ where master equations work and the Drude-Lorentz (overdamped) spectral density provides a good approximation of the underdamped case. Looking at Fig. 15.2 one can appreciate that the coupling constant alone λ_{UD} is not enough to know the amplitude of the spectral density, that is precisely he point of this discussion, contrary to popular belief, a small coupling constant does not necessarily mean we are in the "weak" coupling regime.

The other issue we want to point out, is that when using an exponential decomposition of an environment, one really needs to be careful about preserving detailed balance, as not using enough exponents may lead to dynamics that is close to the exact one in the transient regime but with an incorrect steady state, which is not always obvious [3]. We make this remark because often it is a good practice to check the final state with more than one method as checking convergence is not always straightforward.

Figure 15.4a shows that detailed balance is violated for many values of ω (where the

[3] This problem is magnified at $T = 0$, but it is present for every T

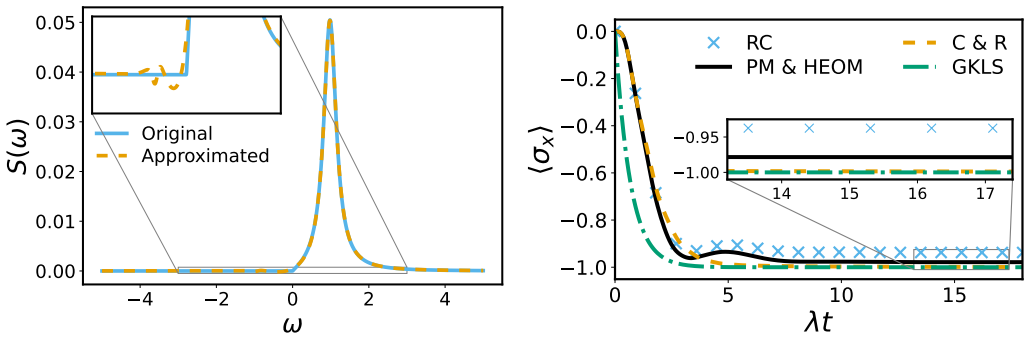

(a) Power spectrum with $\Gamma = 0.4\omega_0$ **(b)** $\Gamma = 0.4\omega_0$

Figure 15.4: a) Power spectrum of the environment used for the calculation of (b), the power spectrum corresponds to $T = 0$, b) Expectation value of σ_x from different methods. Notice the methods predict a different steady state value. Both figures illustrate the loss of detailed balance and the steady state issues associated with it (for a "good environment approximation" Pseudomodes (PM) and HEOM should agree with the reaction coordinate approach (RC)). The parameters are the same as in Figure 15.3.he dynamics shown in both plots correspond to the reaction coordinate with a GKLS master equation (RC), pseudomodes (PM), the hierarchical equations of motion (HEOM), the cumulant equation (C), Redfield (R).

spectrum is negative [4]), this can lead to correct dynamics and an incorrect steady state. This can of course be fixed by better fits. However, it is something one should keep in mind when using methods that rely on this decomposition.

For this model, we obtained a semianalytical solution in terms of $SU(N)$ for the cumulant equation. The dynamics of this system using the cumulant equation reads [A3]

$$e^{\mathcal{K}_2}[\rho] = \frac{\mathbb{I}}{2} + (e^M - \mathbb{I})M^{-1}\vec{r}\cdot\vec{\sigma} + e^M\vec{a}\cdot\vec{\sigma}, \tag{15.4}$$

where $\mathcal{K}_2$ is the cumulant generator from section 7.1 (Eq. (7.20)) and

$$\vec{\sigma} = \begin{pmatrix} \sigma_z \\ \sigma_x \\ \sigma_y \end{pmatrix}, \qquad \vec{a} = \begin{pmatrix} \langle\sigma_z(0)\rangle \\ \langle\sigma_x(0)\rangle \\ \langle\sigma_y(0)\rangle \end{pmatrix}, \tag{15.5}$$

$$M = \begin{pmatrix} -|f|^2\Gamma & 2f_2\xi_z + \mathrm{Re}(\Gamma_z^+) & -2f_1\xi_z - \mathrm{Im}(\Gamma_z^+) \\ \mathrm{Re}(\Gamma_z^+) - 2f_2\xi_z & -(\Gamma_z - \mathrm{Re}(f^2\Gamma_{-+})) & -\left(|f|^2\xi + \mathrm{Im}(f^2\Gamma_{-+})\right) \\ 2f_1\xi_z - \mathrm{Im}(\Gamma_z^+) & \left(|f|^2\xi - \mathrm{Im}(f^2\Gamma_{-+})\right) & -(\Gamma_z + \mathrm{Re}(f^2\Gamma_{-+})) \end{pmatrix} \tag{15.6}$$

[4] This is typically not an issue if $S(\omega_{Hs})$ is well approximated, where ω_{Hs} are the Bohr frequencies of the system Hamiltonian

$$\vec{r} = \begin{pmatrix} |f|^2 \frac{(\Gamma_{++}-\Gamma_{--})}{2} \\ \mathrm{Re}(\Gamma_z^-) \\ -\mathrm{Im}(\Gamma_z^-) \end{pmatrix}. \tag{15.7}$$

where we used the definitions[A3, 55]

$$\xi = \xi_{++} - \xi_{--}, \tag{15.8}$$
$$\Gamma_z^- = f_3 f(\Gamma_{-z} - \Gamma_{z+}), \tag{15.9}$$
$$\Gamma_z^+ = f_3 f(\Gamma_{z-} + \Gamma_{z+}), \tag{15.10}$$
$$\Gamma = \Gamma_{--} + \Gamma_{++}, \tag{15.11}$$
$$\xi_z = f_3(\xi_{z+} - \xi_{z-}), \tag{15.12}$$
$$\Gamma_z = \frac{|f|^2}{2}\Gamma + 2f_3^2\Gamma_{zz}, \tag{15.13}$$
$$f = f_1 - if_2, \tag{15.14}$$

and the explicit frequency dependence was labeled as sub-indices, such that $\Gamma_{\omega,\omega'} = \Gamma(\omega,\omega',t)$ we further simplified the notation by replacing the explicit frequencies as $\omega_0 \to -, -\omega_0 \to +$, $0 \to z$, such that $\Gamma(\omega_0, 0, t) = \Gamma_{-z}$

15.1 Pure dephasing is exact at second order

If we want to recover a pure dephasing model, it suffices to set $f_1 = f_2 = 0$ for which our linear transformation M becomes

$$M = \begin{pmatrix} 0 & 0 & 0 \\ 0 & -2f_3^2\Gamma_{zz} & 0 \\ 0 & 0 & -2f_3^2\Gamma_{zz} \end{pmatrix}. \tag{15.15}$$

In this case, the dynamics are easily solvable as Eq. (15.4) becomes

$$\rho(t) = \frac{\mathbb{I}}{2} + \vec{\sigma}^T e^M \vec{a} \tag{15.16}$$
$$= \begin{pmatrix} \langle\sigma_z(0)\rangle + \frac{1}{2} & e^{-2f_3^2\Gamma_{zz}}(\langle\sigma_x(0)\rangle - i\langle\sigma_y(0)\rangle) \\ e^{-2f_3^2\Gamma_{zz}}(\langle\sigma_x(0)\rangle + i\langle\sigma_y(0)\rangle) & \frac{1}{2} - \langle\sigma_z(0)\rangle \end{pmatrix}. \tag{15.17}$$

Notice the dynamics doesn't induce any change on the diagonal, namely there are no energy exchanges between the system an environment,the interaction simply kills coherences for this sort of evolution as it is expected. For longer times Γ_{zz} increases with t then the steady state is simply given by

$$\rho_{steady} = \begin{pmatrix} \langle\sigma_z(0)\rangle + \frac{1}{2} & 0 \\ 0 & \frac{1}{2} - \langle\sigma_z(0)\rangle \end{pmatrix}. \tag{15.18}$$

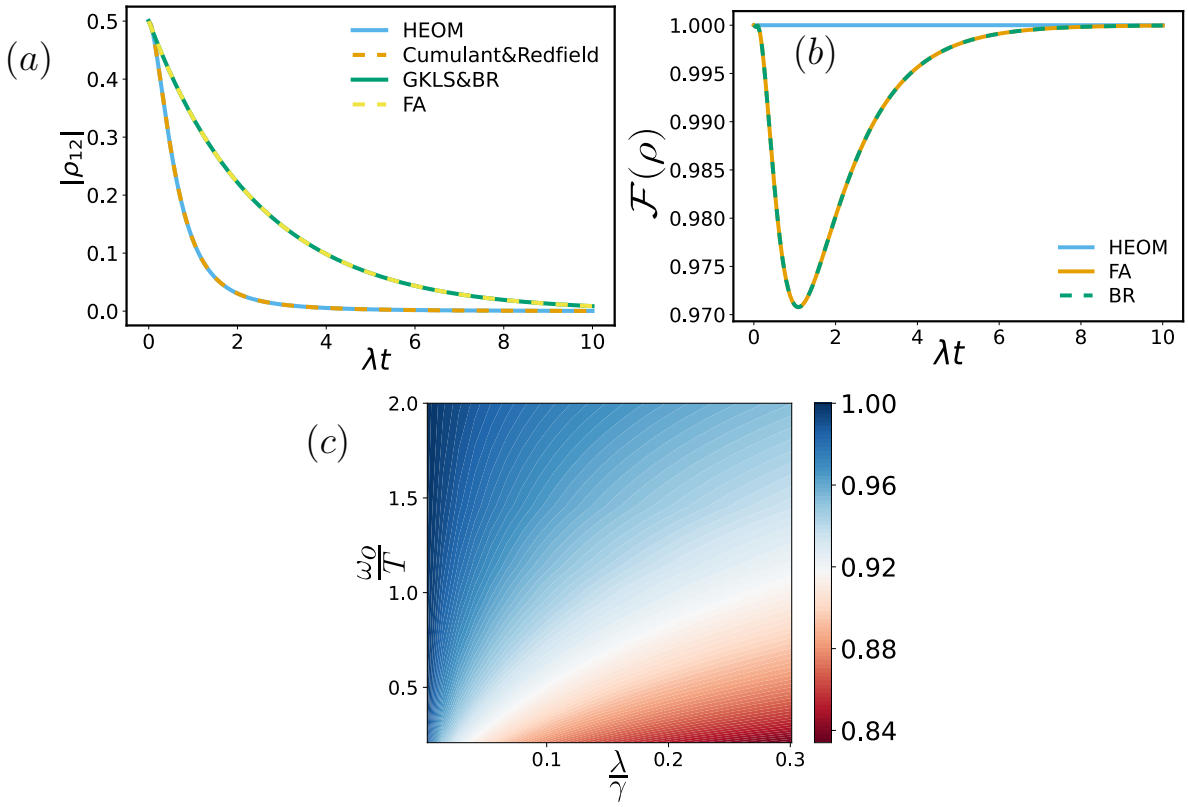

Figure 15.5: (a) Shows the absolute value of the coherence in pure dephasing evolution (b) Shows the fidelity to the exact solution for the different approaches under pure dephasing evolution, cumulant is excluded as it matches the exact solution (c) Shows the Fidelity of the Davies-GKLS and Bloch-Redfield equation for a wide range of parameters. The dynamics for the pure dephasing model are shown, it corresponds to $f_1 = f_2 = 0$ and $f_3 = 1$. For (a) and (b) the parameters used for the simulation were $\frac{\omega_0}{T} = 4, \frac{\lambda}{\gamma} = \frac{\pi}{4}$, $\gamma = 5\omega_0$. We can see HEOM has converged to the analytical exact solution. It should be mentioned the computational effort is significant when compared with the cumulant equation.

A surprising fact is that the cumulant equation is the exact solution in this case [A3, 51, 63]. The cumulant is not the only equation that has this feat. The time convolutionless master equation at second order (Redfield 6.1) is also exact for this model. The fact that we can obtain an exact solution from a second order description was called a conundrum [63]. We see now from section 7.1 that this is simply because $[\mathcal{K}_2(t), \mathcal{K}_2(t')] = 0$, so that the Magnus expansion of the Feynman Vernon Influence functional is complete at second order. To prove this we could construct $\mathcal{K}_2$ normally, or by vectorizing Eq. (15.16) to obtain

$$\vec{\rho}(t) = e^{\mathcal{K}_2(t)}\vec{\rho}(0) \tag{15.19}$$

$$= \begin{pmatrix} 1 & 0 & 0 & 0 \\ 0 & e^{-2f_3^2\Gamma_{zz}} & 0 & 0 \\ 0 & 0 & e^{-2f_3^2\Gamma_{zz}} & 0 \\ 0 & 0 & 0 & 1 \end{pmatrix} \begin{pmatrix} \langle\sigma_z(0)\rangle + \frac{1}{2} \\ (\langle\sigma_x(0)\rangle - i\langle\sigma_y(0)\rangle) \\ (\langle\sigma_x(0)\rangle + i\langle\sigma_y(0)\rangle) \\ \frac{1}{2} - \langle\sigma_z(0)\rangle \end{pmatrix}. \tag{15.20}$$

And from Eq. (15.19) we can see that

$$\mathcal{K}_2(t) = \begin{pmatrix} 0 & 0 & 0 & 0 \\ 0 & -2f_3^2\Gamma_{zz}(t) & 0 & 0 \\ 0 & 0 & -2f_3^2\Gamma_{zz}(t) & 0 \\ 0 & 0 & 0 & 0 \end{pmatrix}. \tag{15.21}$$

In the last equation we made the time dependence of $\Gamma_{z,z}$ explicitr, for the sake of clarity. From there it is straightforward to check that $[\mathcal{K}_2(t), \mathcal{K}_2(t')] = 0$. Similarly using Eq. (5.83) one can show the same holds true for the Redfield generator.

In Fig. 15.5, we can see a contour plot that shows the minimum fidelity the BR equation has for a given set of parameters. We can see that the area where it works with high fidelity is rather restricted, which is understandable given that it is only meant to operate in the weak coupling limit. Still the cumulant equation which was derived in the weak coupling limit, is an exact description, showing a clear advantage to study dephasing scenarios.

In this setting even the simplest equation, namely the GKLS equation is in good agreement with the exact solution, the Redfield and cumulant equation exhibit an advantage as they match the exact solution whereas Bloch-Redfield does not (similarly FA is also not exact in this case).

15.2 The standard Spin-Boson Model

The standard Spin-Boson model [A3, B3] can be recovered from Eq. (15.1) by making $f_3 = f_2 = 0$, the linear transformation giving rise to the cumulant equation dynamics is then given by:

$$M = \begin{pmatrix} -\Gamma & 0 & 0 \\ 0 & -\frac{\Gamma}{2} + \mathrm{Re}(\Gamma_{-+}) & -(\mathrm{Im}(\Gamma_{-+}) + \xi) \\ 0 & \xi - \mathrm{Im}(\Gamma_{-+}) & -\frac{\Gamma}{2} - \mathrm{Re}(\Gamma_{-+}) \end{pmatrix} \tag{15.22}$$

$$\vec{r} = \begin{pmatrix} \frac{(\Gamma_{++} - \Gamma_{--})}{2} \\ 0 \\ 0 \end{pmatrix}. \tag{15.23}$$

The evolution of the system is obtained from Eq. (15.4) easily, in particular one remarkable fact is that since the matrix M rank is 2 this allows us to obtain analytical expressions for its exponential easily, providing a way to get analytical answers for the Spin-Boson model out of this Non-Markovian description.

Another advantage of this form of the evolution is that we may separate the asymptotic dynamics from the memory dependent one, as we know that $e^M \to 0$ as $t \to \infty$ for this model as the real part of its eigenvalues is always negative.

Therefore, if we only aim at knowing the steady state of the system then it suffices to look at the non-vanishing terms of Eq. (15.4) in the long time limit, which results in :

$$\rho_{steady} = \frac{\mathbb{I}}{2} - \vec{\sigma} \cdot M^{-1}\vec{r} = \vec{\sigma} \cdot \begin{pmatrix} \frac{\Gamma_{++}-\Gamma_{--}}{2\Gamma} \\ 0 \\ 0 \end{pmatrix} \tag{15.24}$$

$$= \frac{\mathbb{I}}{2} + \frac{\Gamma_{++} - \Gamma_{--}}{2\Gamma}\sigma_z. \tag{15.25}$$

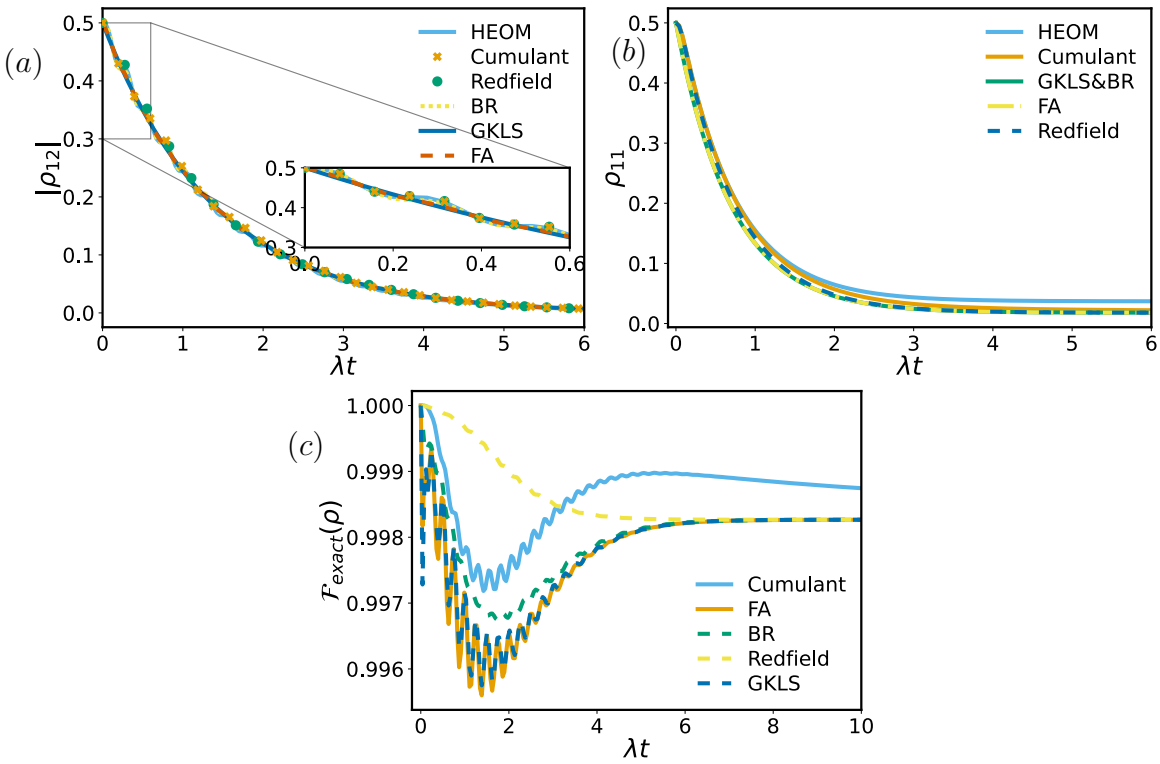

Figure 15.6: (a) Shows the absolute value of coherence for the different approaches, notice in the inset GKLS is the only one with no oscillations (b) Shows the evolution of the population for each of the different approaches (c) Shows the fidelity with respect to the HEOM method. The dynamics for the Spin-Boson shown corresponds to $f_3 = f_2 = 0$ and $f_1 = 1$, The parameters used were $\frac{\omega_0}{T} = 2$, $\frac{\lambda}{\gamma} = 0.01\pi$, $\gamma = 5\omega_0$.

This can be obtained analytically in the long time limit, substituting the adequate time-dependent coefficients into Eq. (7.26):

$$\Gamma_{--} + \Gamma_{++} = \frac{t^2}{\pi}\int_0^\infty d\omega J(\omega) \coth\left(\frac{\omega}{2T}\right) \left(\text{sinc}^2\left(\frac{(\omega-\omega_0)t}{2}\right) + \text{sinc}^2\left(\frac{(\omega+\omega_0)t}{2}\right)\right), \tag{15.26}$$

$$\Gamma_{++} - \Gamma_{--} = \frac{t^2}{\pi}\int_0^\infty d\omega J(w) \left(\text{sinc}^2\left(\frac{(\omega-\omega_0)t}{2}\right) - \text{sinc}^2\left(\frac{(\omega+\omega_0)t}{2}\right)\right). \tag{15.27}$$

Since we only care about the steady state of the system at this point we may take the limit of $t \to \infty$ which greatly simplifies the analysis as the limit of the time-dependent function as :

$$\lim_{t\to\infty} t^2 \operatorname{sinc}^2\left(\frac{(\omega-\omega_0)t}{2}\right) = 2\pi t\delta(\omega-\omega_0). \tag{15.28}$$

Thus we have

$$\rho_{steady} - \frac{\mathbb{I}}{2} = -\frac{\Gamma_{--}-\Gamma_{++}}{2\Gamma}\sigma_z \tag{15.29}$$

$$= \frac{\int_0^\infty d\omega J(\omega)\left(\delta(\omega-\omega_0)-\delta(\omega+\omega_0)\right)\sigma_z}{2\int_0^\infty d\omega J(\omega)\coth\left(\frac{\omega}{2T}\right)\left(\delta(\omega-\omega_0)+\delta(\omega+\omega_0)\right)} \tag{15.30}$$

$$= \frac{1}{2}\left(\frac{J(\omega_0)-J(-\omega_0)}{(J(\omega_0)-J(-\omega_0))\coth\left(\frac{\beta\omega_0}{2}\right)}\right)\sigma_z. \tag{15.31}$$

Which can finally be written down as:

$$\rho_{steady} = \frac{1}{2}\left(\mathbb{I}+\tanh\left(\frac{\beta\omega_0}{2}\right)\sigma_z\right). \tag{15.32}$$

Thus the steady state is just Gibbs state to bare Hamiltonian, in agreement to what is expected for a second order description [A2, 46, 47] as off-diagonal corrections vanish for orthogonal couplings in the Spin-Boson model. Regarding the true evolution, we know that indeed there are no steady state coherences [A2, 46, 47, 97] in this scenario, but there are corrections to populations that are a consequence of $\mathcal{O}(\lambda^4)$ effects, so we see that in this case the cumulant equation does not reach the correct the stationary state, as opposed to what was expected [A2]. The derivation of the cumulant equation in terms of the Feynman-Vernon Influence functional gives some clarity on why this expectation is not met. The Dyson expansion in imaginary time [A2] adds time ordering in terms that are not present in a second order. Magnus expansion. It is no wonder the results of Chapter 13 were so good for the diagonal, as they were more akin to an expansion of the influence functional than an expansion for the dynamics of the cumulant equation.

Since in our representation Eq. (15.4) the dynamics of populations and the dynamics of coherences are decoupled in this case, this allows one to exponentiate the matrix from Eq. (15.22) without making any sort of assumption, which in turn allows us to write the evolution of the population and coherences compactly. We will neglect Lamb-shift to make the equations simpler, we obtain:

$$\langle\sigma_z(t)\rangle = e^{-\Gamma(t)}\langle\sigma_z(0)\rangle + \frac{(e^{-\Gamma(t)}-1)(\Gamma_{++}(t)-\Gamma_{--}(t))}{\Gamma(t)}, \tag{15.33}$$

$$\langle\sigma_+(t)\rangle = \frac{e^{-|\Gamma_{-+}|-\frac{\Gamma}{2}}}{2|\Gamma_{-+}|}\left(\Gamma_{-+}\langle\sigma_-(0)\rangle(e^{2|\Gamma_{-+}|}-1)+|\Gamma_{-+}|\langle\sigma_+(0)\rangle(e^{2|\Gamma_{-+}|}+1)\right), \tag{15.34}$$

$$\langle\sigma_-(t)\rangle = \frac{e^{-|\Gamma_{-+}|-\frac{\Gamma}{2}}}{2|\Gamma_{-+}|}\left(\Gamma_{-+}\langle\sigma_+(0)\rangle(e^{2|\Gamma_{-+}|}-1)+|\Gamma_{-+}|\langle\sigma_-(0)\rangle(e^{2|\Gamma_{-+}|}+1)\right). \tag{15.35}$$

In terms of the dynamics one can see that the cumulant equation is the most favorable approximate description for the parameters chosen in Fig. 15.6. As we are

in the weak coupling regime, we can see a pretty good agreement with the exact dynamics even for the simplest equation, namely, the Davies-GLKS approach. Still the cumulant equation is a better description in early and long times when compared to the other master equations presented here, it is also as good as Bloch-Redfield in intermediate times, which indicates higher orders of the cumulant equation might be worth pursuing in the same way the TCL equation is often written down.

In figure 15.7 we see that the cumulant equation is not only better for our chosen parameters, but that it is a better description for a wide range of parameters. Particularly for the example considered, it is only a worse description in the regime of high "$\frac{\lambda}{\gamma}$" and high temperature, a regime where we expect second order descriptions to fail. Bare in mind that the black line that divides the regime where cumulant is better that Bloch-Redfield may change shape for different values of γ with respect to ω_0 and different spectral densities, here we have chosen $\gamma = \omega_0$. However in general we see that the cumulant equation is a better description at small $\frac{\lambda}{\gamma}$ and low temperature, while Bloch Redfield is better in the opposite regime.

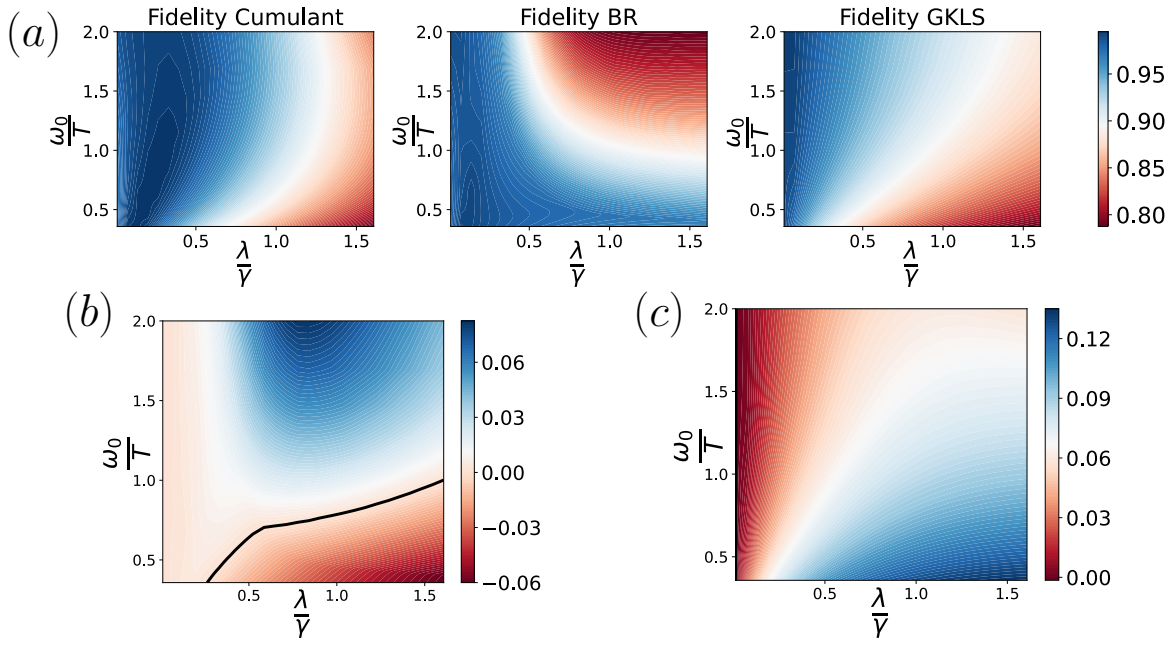

Figure 15.7: a) Shows the minimum fidelity of each of the three approximate descriptions considered with respect to HEOM for a wide range of parameters b)Shows the difference in minimum fidelity between the cumulant equation and the Bloch Redfield equation, the black line divides the region where the difference is positive (cumulant has higher minimum fidelity) and where it is negative. c) Shows the difference in minimum fidelity between the cumulant equation and the GKLS equation, the cumulant equation is a better description for all chosen parameters.

15.3 The Composite interaction case

In the case of composite interactions the matrix M is rank 3, which makes analytical expressions complicated as they depend on a cubic root, and therefore it's hard to get Eq. (15.4) in a compact form unless approximations are done on the integrals.

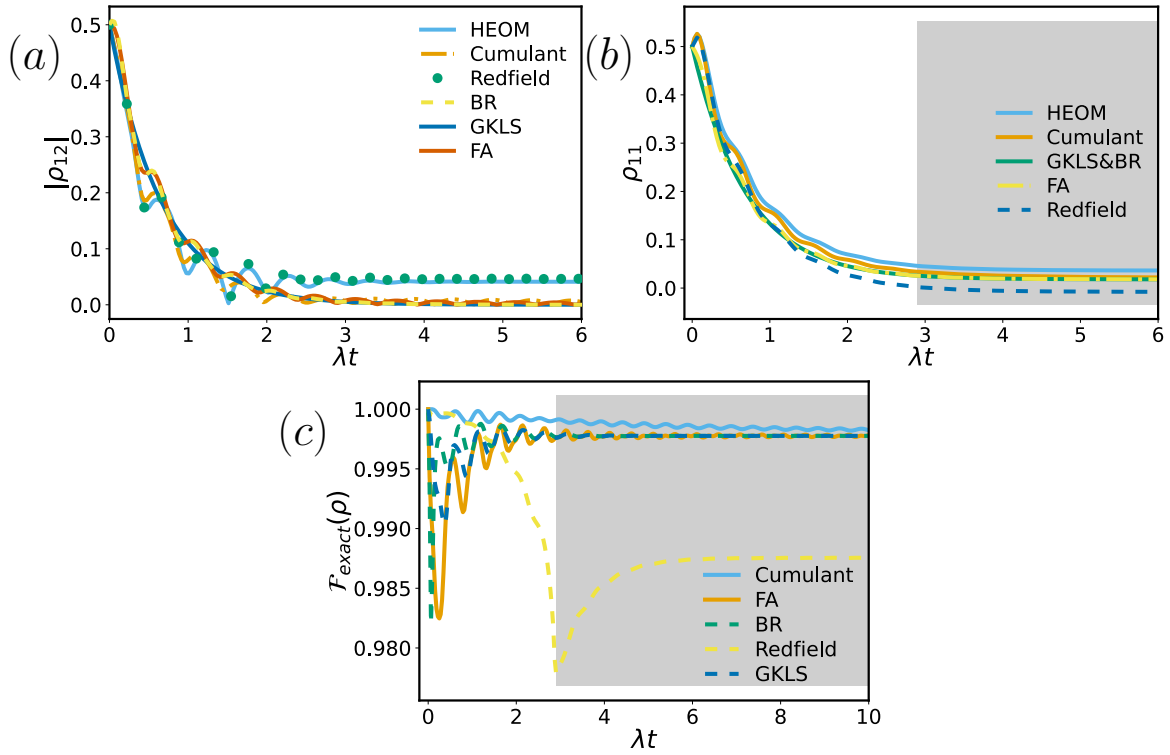

Figure 15.8: (a) Shows the absolute value of the coherence for the different approaches considered (b) Shows the evolution of the population for the different approaches considered (c) Shows the fidelity with respect to HEOM for each of the methods considered. The plots corresponds to $f_2 = 0$ and $f_3 = f_1 = 1$, for the plots shown $\frac{\omega_0}{T} = 2, \frac{\lambda}{\gamma} = 0.01\pi$. The shadowed area marks negativity issues in the Redfield equation.

The result of the dynamics can be observed in the Fig. 15.8. We can see that in this

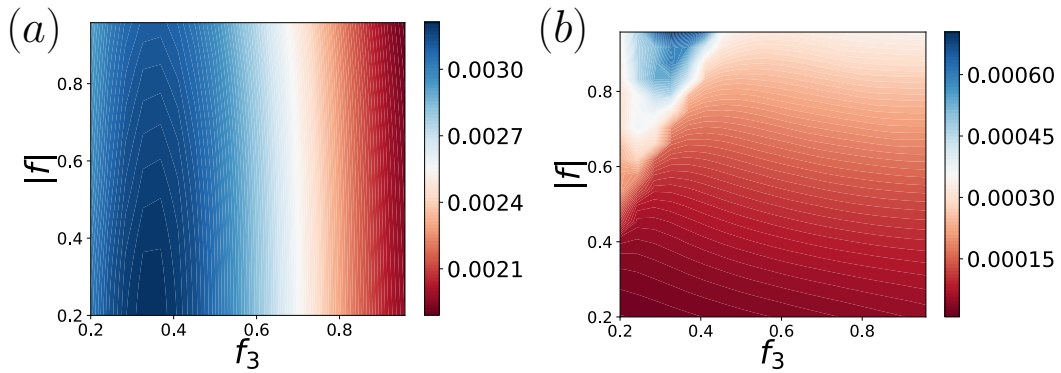

Figure 15.9: (a) The minimum fidelity of the cumulant compared to the Davies-GKLS equation (b) The minimum fidelity of the cumulant compared to the Bloch-Redfield equation. These plots show the different in minimum fidelity between the standard master equations and the cumulant equation, when the couplings between the parallel and orthogonal components of the Hamiltonian are imbalanced. For the simulations we fixed $\frac{\omega_0}{T} = 2$, $\frac{\lambda}{\gamma} = 0.01\pi$

case the cumulant equation has an advantage over the more standard Bloch-Redfield equation. The fact that the cumulant equation can reproduce better the early time populations is the main source of its advantage with respect to the Bloch-Redfield equation. This advantage is lost as $t \to \infty$ because the cumulant equation will go to

the bare Gibbs state in the steady state; however, until then, it has a better fidelity to the true dynamics.

Notice that small oscillations in coherence remain in the cumulant equation while the other master equations have already reached a fixed value. This is due to the slow decay of the cumulant equation to the Davies-GKLS steady state. As we have mentioned this gives a reminiscence of the steady state coherences as they are long lived.

One may wonder if the parameters chosen above namely equal $f_1 = f_3$ played a role in the superiority of the cumulant equation, Fig. 15.9 shows that this is not the case by showing the difference in minimum fidelities over a range of different $|f|$ and f_3.

In this section, we observed that the Bloch-Redfield equation regime of validity seems to be larger than that of the cumulant equation/refined weak coupling as mentioned in [43]. The cumulant equation is a more faithful description when $\frac{\lambda}{\gamma} \ll 1$ which corresponds to the weak coupling regime where master equations are valid descriptions. As Figure 15.10 shows the cumulant description is more faithful in the regime of small "$\frac{\lambda}{\gamma}$" and low temperature, just as in figure 15.7, while for stronger coupling which one is a better description seems model dependent. From these examples, we can conclude that the cumulant equation is a better description at low temperature in the weak coupling regime

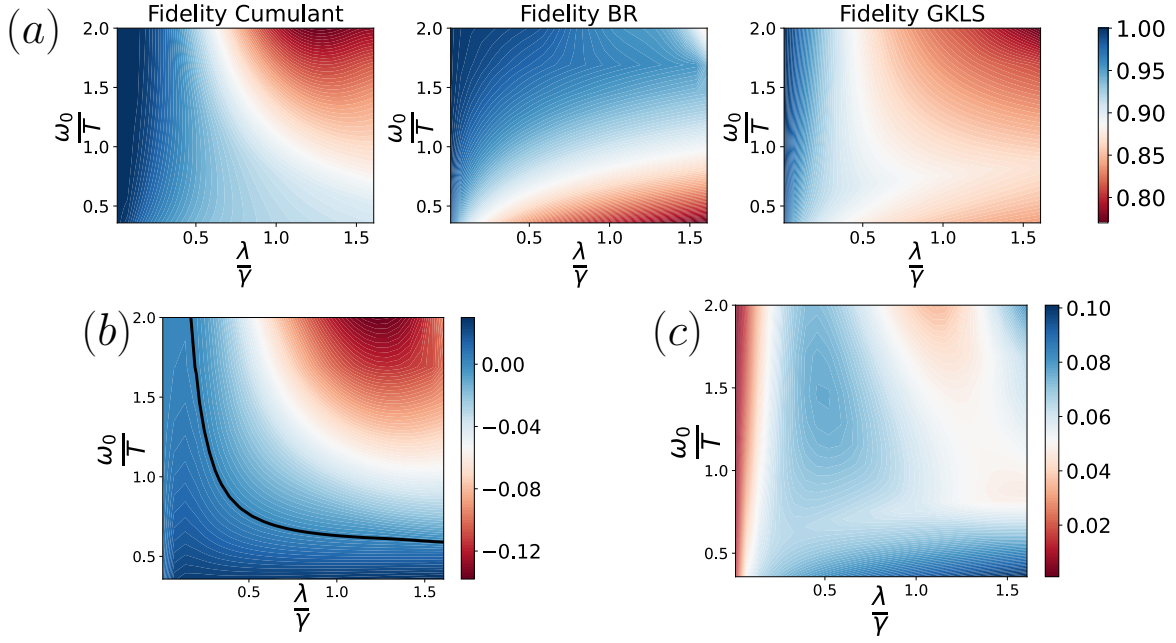

Figure 15.10: a) Shows the minimum fidelity of all master equations against HEOM. Both plot (b) Shows the difference in minimum fidelity between the cumulant equation and the Bloch Redfield equation, the black line divides the region where the difference is positive (cumulant has higher minimum fidelity) and where it is negative. (c) Shows the difference in minimum fidelity between the cumulant equation and the Davies-GKLS equation; the cumulant equation is a better description for all chosen parameters.

In figure 15.8 we see an example of the dynamics of this system, using some of the methods considered in the thesis. The main fact we want to highlight here is that while the Redfield equation does a remarkably better job at keeping track of

coherences in this model, it has negativity issues that render it worse than the other approaches in the long time limit, which is a well known fact [51, 57, 98]. Particularly because of that, and its relatively high computational cost, are some of the reasons we don't see widespread adoption of the Redfield equation. The cumulant being CPTP does not have this problem, and its simulation is less costly.

15.4 Non-Markovianity

The Spin-Boson model has been shown to have Non-Markovian behaviour [A3, A4, 55]. In this section we show the cumulant and Redfield equations exhibit Non-Markovian behaviour whereas their approximations do not. The measure of Non-Markovianity used is the trace distance measure

$$\frac{1}{2}||\rho(t) - \sigma(t)|| = \frac{1}{2}\,\mathrm{Tr}\Big\{\sqrt{(\rho(t) - \sigma(t))^\dagger(\rho(t) - \sigma(t))}\Big\}. \tag{15.36}$$

The initial states for the two evolutions were chosen to be orthogonal specifically

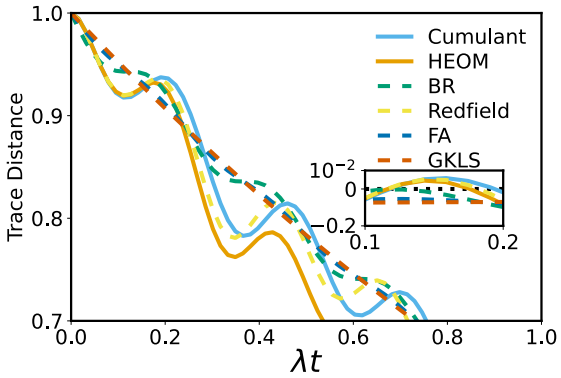

Figure 15.11: (a)Trace distance measure (Eq. (15.36)) of the the different approaches for the Non-equilibrium Spin-Boson model. An inset with the derivative of the trace distance is provided so that increase in trace distance can be observed clearly (values bigger than zero in the inset indicate increase of trace distance). Notice the cumulant equation correctly shows the Non-Markovianity of the model even when overestimating the increase of the trace distance, $f_1 = 1, f_2 = f_3 = 0$ for $\frac{\lambda}{\gamma} = 0.01\pi, \frac{\omega_0}{T} = 1$.

we chose

$$\rho(0) = \begin{pmatrix} 0.5 & 0.5i \\ -0.5i & 0.5 \end{pmatrix} = \overline{\sigma(0)}. \tag{15.37}$$

For Markovian evolutions the trace distance between the states decreases monotonically, while for Non-Markovian evolutions it does not. Usually, the increase in the measure is small [105]. To visualize the increase in the trace distance better, an inset has been placed in Fig. 15.11 the inset contains the derivative of the trace distance, and it is shown in logarithmic scale, a positive value indicates an increase of the trace distance measure and therefore Non-Markovianity

Chapter 16

Heat Transport

The main purpose of this section is to show that Non-Markovian descriptions are necessary to study finite time thermodynamics. An original contribution of this work lies in remarking that Non-Markovian Lamb shift needs to be included to describe heat flows in finite time, as without it the heat flow described by master equations deviates from the exact dynamics. This nonintuitive need for Lamb-shift stems from the fact that Non-Markovian Lamb-shift does not commute with the Hamiltonian (see chapter 11) . We expect this will have impact on the study of finite time thermal machines and the finite time Landauer principle [106–115].

To illustrate the need for Lamb-shift, we will study two simple models, the first one will be a minimal two-qubit engine, and the second one will be a small "Heisenberg spin chain" with XX interaction, with both qubits at the ends of the chain having internal tunneling. We hope Non-Markovian equations as presented in the thesis can help study the dynamics of large open spin chains in the future.

16.1 A two Qubit Machine

In this section, we consider two qubits coupled to two thermal baths according to the Hamiltonian.

$$H = \underbrace{\frac{\omega_c}{2}\sigma_z^{(c)} + \frac{\Delta}{2}\sigma_x^{(c)} + \frac{\omega_h}{2}\sigma_z^{(h)} + g\sigma_x^{(c)}\sigma_x^{(h)}}_{H_S} + \underbrace{\sum_{k,\alpha=h,c} \omega_k^{(\alpha)} a_k^{(\alpha)\dagger} a_k^{(\alpha)}}_{H_B} + \underbrace{\sum_{k,\alpha=h,c} g_k \sigma_z^{(\alpha)}(a_k^{(\alpha)} + a_k^{(\alpha)\dagger})}_{H_{SB}} . \tag{16.1}$$

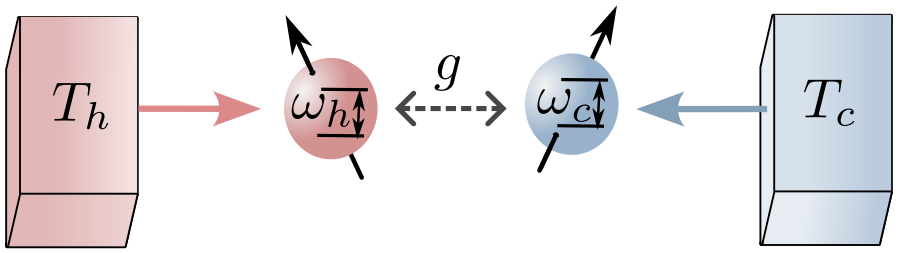

Figure 16.1: A two qubit machine, each qubit is interacting with a different reservoir.

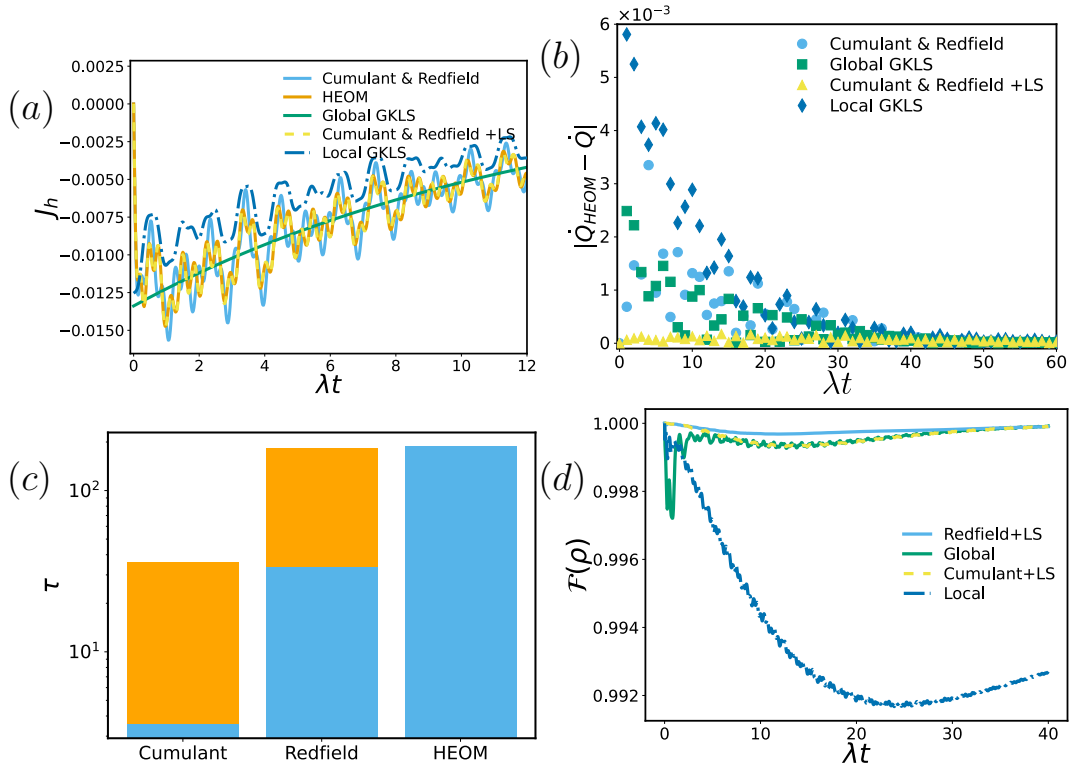

Figure 16.2: Heat transport scenario. Two qubits coupled to two different baths with an underdamped spectral densities. The parameters of the simulation are $T_c = 0.01\omega_c, T_h = 2\omega_c, \Delta = \omega_c = \omega_h = \frac{\omega_0}{2}, \lambda_1 = \lambda_2 = 0.05\pi\omega_0, g = 0.5\omega_0, \Gamma = \omega_0$, a) Shows the heat current from the environment at the hotter temperature. It illustrates that Lamb-shift is necessary to obtain a proper description of heat currents in the transient regime and the failure of GKLS at early times b) Shows the error of the heat generated in this process, c) Shows the time used to obtain the evolution of the density matrix in each approach, the orange block indicates the usage of numerical integration, while blue the usage of decaying exponentials d) Shows the fidelity of the approaches to the exact solution. Notice that even though the global master equation describes the states correctly, the description of heat currents fail as a) and b) show.

Here $\omega_c(\omega_h)$ refers to the frequency of the qubit attached to the cold (hot) environment, g denotes the coupling strength between the qubits and Δ is the cold's qubit tunneling rate between its two levels. The inclusion of a tunelling term in the Hamiltonian of the cold qubit was done to make the Lamb-Shift not commute with the system Hamiltonian[1]. An illustration of the system can be seen in figure 16.1

In Figure 16.2 we can see how a correct description of heat currents in time requires the inclusion of Lamb-shift. This begs for the investigation of Lamb shift corrections to heat currents, a previously unexplored area warranting further research. Furthermore, the question of whether Lamb-shift impacts the description power and work remains open. Consequently, using decaying exponentials to compute Lamb-shift is expected to be instrumental in advancing the understanding of heat and power within non-equilibrium quantum thermodynamics as it makes Lamb-shift inclusion accessible. On the other hand notice from Figure 16.2 that the GKLS master equa-

[1]Similarly we could have considered σ_x coupling to the environment, for the Lamb-shift not to commute with the Hamiltonian

tion both in its global and local forms, fails to capture the behavior of heat currents at early times, predicting non-zero heat at $t = 0$. This is expected as they are meant as a long time approximation. Non-Markovian master equations correctly capture this behaviour, as other methods such as pseudomodes do [4, 116], in contrast with other works exploring heat transport beyond GKLS descriptions [10, 116] . Notice that neither the cumulant nor Redfield equation **increase the size of the Hilbert space of the system** unlike the methods considered in the references mentioned.

16.2 The cumulant equation for weakly interacting subsystems

In reference [43], it was shown for a particular model that Redfield was superior to the cumulant equation. However, in several of our examples, the cumulant equation was better. This sort of puts up a contradiction between the conclusions reached in [43] and ours. The difference in conclusions comes from the fact that in [43] they use a model in which the subsystems do not interact. The cumulant equation goes to the "Global GKLS equation in the long time limit"[2], which is a poor approximation for systems that interact weakly or do not interact. The Redfield equation, on the other hand does not tend to the Global GKLS equation in the long time limit and is usually a better approximation when weakly or non interacting systems are considered. To show this point, we will consider the same example as the previous section but will have the interaction among the qubits to be 10 times weaker.

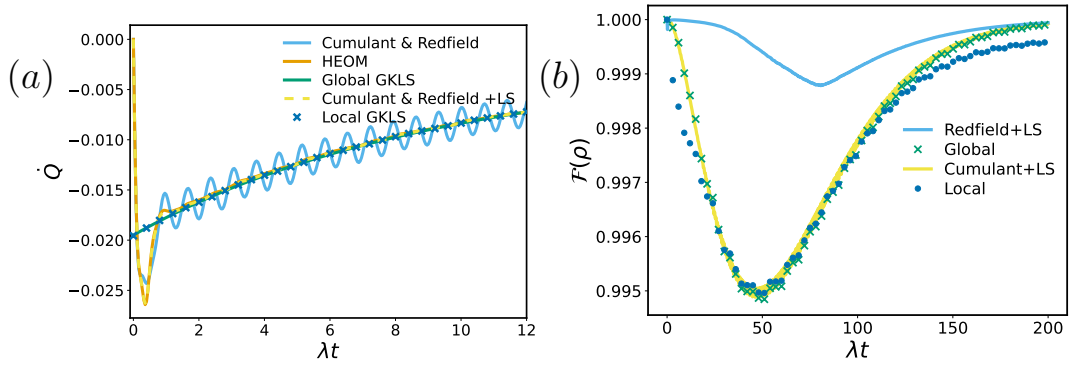

Figure 16.3: Same parameters as figure 16.2 except $g = 0.05\omega_0$ a) Shows the net heat $\dot{Q}$ Eq. (11.5). b) Shows the fidelity of the different approaches with respect to HEOM

Although Redfield is always better than cumulant when the coupling between subsystems is small, as figure 16.3 shows, notice cumulant is still a pretty good description and is also able to describe the heat current as well as Redfield. The cumulant still has the advantage of being CPTP, though negativity issues are less often encountered in transport scenarios. In this particular case, we see Global and cumulant have basically the same fidelity, however the cumulant is still able to adequately predict the behavior of heat currents in early and intermediate times, unlike the former.

[2]It does in the limit of $\mathrm{sinc}(t) \to \delta(t)$, in practice one finds lingering oscillations that make it different from the GKLS equation even in long times

16.2.1 Entanglement

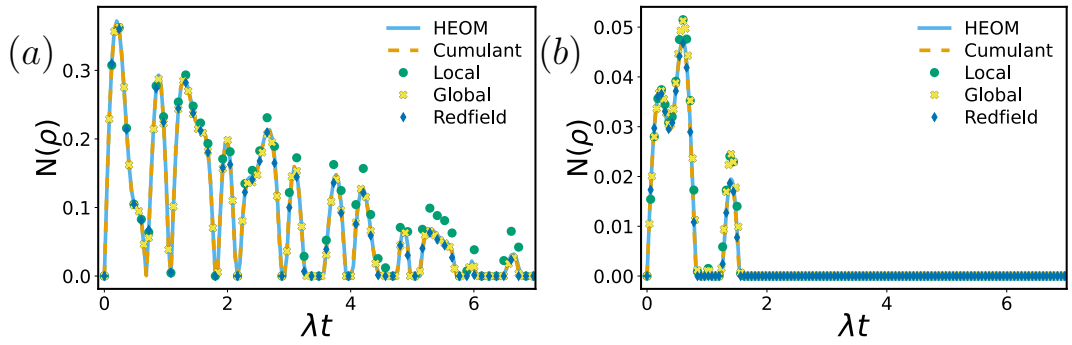

Figure 16.4: Dynamics of the entanglement between qubits. We use negativity as an entanglement measure. The difference between both panels is the coupling between the qubits a) $g = 0.5\omega_0$ b) $g = 0.05\omega_0$. The rest of the parameters are the same as in figure 16.2

The thermal machine considered is sometimes called the entanglement engine [117], in this section, we will not worry about generation of entanglement in the steady state but rather if the entanglement of the states calculated using the different approaches matches the entanglement of the exact solution. We will recycle the calculations of the previous section and calculate the entanglement dynamics for the same parameters. To characterize entanglement we use negativity [118]

$$N(\rho) = \sum_{\lambda_i<0} |\lambda_i|, \tag{16.2}$$

where the λ_is are the eigenvalues of the partial traspose of the density matrix, with respect to one of the qubits. From figure 16.4 we see that in both situations the Markovian approaches tend to overestimate the qubit entanglement, whereas the non-Markovian descriptions follow the entanglement generated by the exact solution closely. We can also appreciate the generation of high entanglement $N(\rho) > 0.3$ in the transient regime. While the transient regime entanglement might not be too useful, we could stabilize them using quantum control later on [A6].

16.3 Cumulant equation for many subsystems

From the previous section, one might wonder whether the cumulant equation is actually a good description to study heat transport scenarios. The fact that it goes to the Global GKLS equation can be seen as a good thing as it ensures obeying the second law of thermodynamics [A4, 119–122]. On the other hand, the same feature becomes an issue as for weakly interacting systems a local master equation is more precise. This seems to put the cumulant equation in a bad spot, as it seems it suffers the same downsides as the global equation in the "local vs global" debate [120, 123]. However, as mentioned in [A4], one of the advantages of the cumulant equation lies in its resolution of small Bohr frequencies. When those Bohr frequencies are too small the sinc functions tend to Dirac deltas slowly. If the Bohr frequencies are small enough, then the cumulant equation deviates from the GKLS global equation for

long times. We will show this using a Heisenberg spin chain whose Hamiltonian is given by

$$H = \underbrace{\sum_{i=1}^{N} \frac{\omega_i}{2}\sigma_z^{(i)} + \frac{\Delta_i}{2}\sigma_x^{(i)} + \sum_{i<j}^{N} g_{ij}\sigma_x^{(i)}\sigma_x^{(j)}}_{H_S} + \underbrace{\sum_{k,\alpha=h,c} \omega_k^{(\alpha)} a_k^{(\alpha)\dagger} a_k^{(\alpha)}}_{H_B} + \underbrace{\sum_{k,\alpha=1,N} g_k \sigma_x^{(\alpha)}(a_k + a_k^\dagger)}_{H_{SB}} . \tag{16.3}$$

For simplicity we will consider $\Delta_1 = \Delta_N = \omega_i = \omega_0$, and all other Δ_i to be zero. In spin chains, as one increases the number of spins in a spin chain of this type, the gap in the Hamiltonian's spectrum diminishes, thus giving rise to smaller Bohr frequencies. We show that even for weak coupling between subsystems as we increase the number of spins the cumulant equation deviates more and more from the Global equation even for long times. This makes the cumulant equation not susceptible to the Global vs local debate [120, 122, 123], as regardless of the coupling, it is an accurate description for systems of many parties.

In figure 16.5, we can observe how the cumulant equation becomes a better description as the number of subsystems grows. Not only it is a good description of the density matrix, but it is also able to reproduce the heat currents faithfully, unlike the local GKLS approach. Thus, it is a perfect candidate for the study of quantum thermal machines in finite time. Remarkably, the cumulant equation fidelity is still high for times for which the system has already reached its Non-equilibrium steady state ($\dot{Q} = 0$), this is because the sinc functions have finite width by the time the system thermalizes, thus not reaching the Global GKLS generators a long time limit [A4, 55]. The possibility of the failure to reach that limit had been mentioned in [A4] and is discussed in [97] in a different context. This example represents the first evidence that the cumulant is not going to the GKLS global generator for long times. In the next chapter we will observe similar behavior due to small frequency spacings in a harmonic oscillator with a Kerr nonlinearity.

Our main point in this section was to show that the cumulant equation tends to the exact solution even for long times when more parties are involved, however, here we would like to discuss an apparent problem which is that the heat currents of the hot bath for $N = 3$ and $N = 4$ matches the local master equation and are negative, which seems to contradict the second law of thermodynamics [84, 122], further study in this direction is needed. Perhaps the definition of heat current for Non-Markovian descriptions needs revisited as figure 16.5 (f) and (e) seem to indicate an apparent violation of the second law [84, 120, 122, 123] .

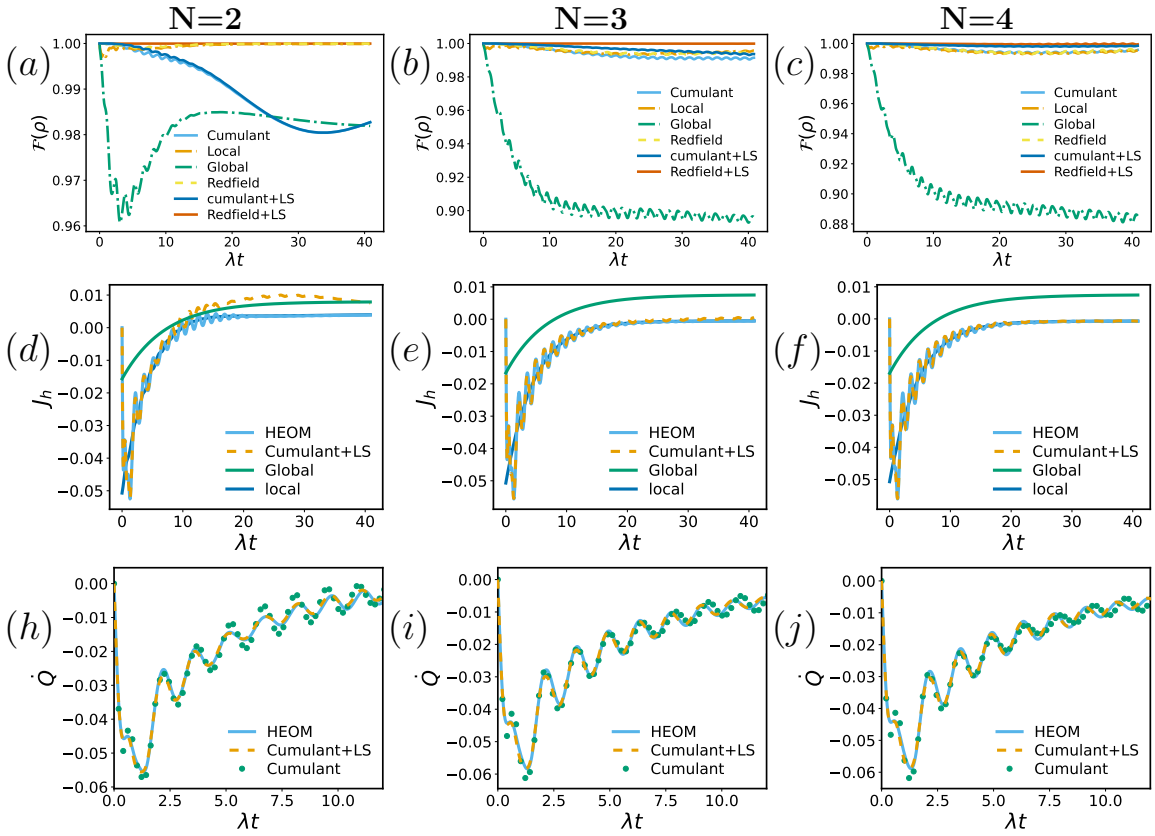

Figure 16.5: This figure shows the fidelity and heat currents of the different approaches for the Hamiltonian Eq. (16.3). The first row corresponds to the fidelity to HEOM for different number of spins in the chain. The second row corresponds to the heat current from the hot bath. Here we can observe how the Markovian approaches are not adequate for finite time descriptions. In the last row, we show the total heat. Notice how, regardless of the number of spins, Lamb-shift is needed for agreement with the exact solution. Remarkably, already for only $N = 4$ spins, the Global and cumulant solutions differ from each other for long times. In these simulations, $\Delta_1 = \Delta_N = \omega_i = \omega_0$ while all other parameters are the same as in the previous figures, except for $\lambda_1 = \lambda_2 = 0.1\pi\omega_0$, $g_{i,j} = 0.05$. Let us remark that regardless of the deviation at long times the cumulant is always a good description at early times.

Chapter 17

The Damped Harmonic Oscillator

The quantum damped harmonic oscillator, characterized by the Hamiltonian

$$H = \underbrace{\frac{p^2}{2} + \Omega^2 \frac{q^2}{2}}_{H_S} + \overbrace{\sum_k \frac{P_k^2}{2} + W_k^2 \frac{Q_k^2}{2}}^{H_B} \underbrace{- q \sum_k C_k Q_k}_{H_I}, \tag{17.1}$$

is one of the few systems that can be solved exactly. The standard method for solving the quantum damped harmonic oscillator in the continuous limit are the Heisenberg-Langevin equations [17, B9, 123]. In recent times, it has served as a guideline to assess the adequacy of different master equations [123] which will be its main purpose in the manuscript. We will closely follow the approach taken in [17].

The first part of this section aims to demonstrate how to use the cumulant equation on infinite-dimensional systems. The second part illustrates how it can be useful to describe nonlinear processes in quantum optics.

17.1 Heisenberg-Langevin Equations

We follow closely the development explained in [17]. Our original contribution in this section is Eq. (17.27) at the end of this segment. We start by deriving the equations of motion for the oscillators in the Heisenberg picture

$$\dot{q} = p, \tag{17.2}$$
$$\dot{p} = -\Omega^2 q + \sum_k C_k Q_k, \tag{17.3}$$
$$\dot{Q}_k = P_k, \tag{17.4}$$
$$\dot{P}_k = -W_k^2 Q_k + q C_k. \tag{17.5}$$

By taking another time derivative and substituting we obtain:

$$\ddot{q} + \Omega^2 q = \sum_k C_k Q_k \tag{17.6}$$
$$\ddot{Q}_k + W_k^2 Q_k = q C_k. \tag{17.7}$$

Notice the equations are those of a driven oscillator, for now let us focus on Eq. (17.7). We might find the solution using the standard Green function method [17, B11], first we obtain the homogeneous solution:

$$Q_k^0 = Q_{homogeneous} = \frac{1}{\sqrt{2W_k}}\left(a_k e^{-iW_k t} + a_k^\dagger e^{iW_k t}\right). \tag{17.8}$$

Where we used the fact that at $t = 0$

$$Q_k(0) = \frac{1}{\sqrt{2W_k}}\left(a_k + a_k^\dagger\right). \tag{17.9}$$

We find the particular solution using the Green function for a driven oscillator [B11]

$$G(t,t') = \theta(t-t')\frac{\sin\left(W_k(t-t')\right)}{W_k}. \tag{17.10}$$

Thus the particular solution is given by

$$Q_p = \int_0^t \frac{C_k \sin\left(W_k(t-t')\right)}{W_k} q(t')dt', \tag{17.11}$$

such that

$$Q_k = Q_k^0 + Q_p. \tag{17.12}$$

Substituting Eq. (17.7) into Eq. (17.6) one obtains

$$\ddot{q} + \Omega^2 q = \sum_k \left(C_k Q_k^0 + \int_0^t \frac{C_k^2 \sin\left(W_k(t-t')\right)}{W_k} q(t')dt' \right). \tag{17.13}$$

At this point it becomes convenient to introduce the following notation

$$\Sigma(t-t') = -\sum_k \frac{C_k}{W_k}\sin\left(W_k(t-t')\right) = \frac{i}{\pi}\int_{-\infty}^{\infty}\sigma(\omega)e^{i\omega(t-t')}d\omega, \tag{17.14}$$

$$\xi(t) = \sum_k C_k Q_k^0, \tag{17.15}$$

$$\sigma(\omega) = \sum_k \frac{\pi}{2}\frac{C_k^2}{W_k}\delta(\omega - W_k). \tag{17.16}$$

In the literature $\Sigma(t-t')$ is known as the self-energy kernel, $\xi(t)$ as the noise term and $\sigma(\omega)$ is the bath's spectral density. Using this one may now rewrite Eq. (17.13) as

$$\ddot{q} + \Omega^2 q + \int_0^t \Sigma(t-t')q(t')dt' = \xi(t). \tag{17.17}$$

We may now use Laplace's transform to solve Eq. (17.17) which results in

$$q(t) = G(t)p(0) + \dot{G(t)}q(0) + \int_0^t G(t-t')\xi(t')dt', \tag{17.18}$$

where we used the spectral density

$$\sigma(\omega) = \gamma\omega^n \frac{\omega_c^2}{\omega_c^2 + \omega^2}, \tag{17.19}$$

and

$$G(t) = \frac{e^{-\frac{\gamma}{2}t}}{2W}\sin\Big(Wt\Big), \tag{17.20}$$

$$W = \sqrt{\Omega_R^2 - \left(\tfrac{\gamma}{2}\right)^2}. \tag{17.21}$$

$$\Omega_R^2 = \Omega^2 - \gamma\omega_c \tag{17.22}$$

Where Ω_R is the re-normalized frequency of the oscillator[1] and γ is a constant that characterizes the strength of the interaction. We now proceed to look at the expectation values. Because the environment operators are centralized $\langle\xi(t)\rangle = 0$ (which can always be done [B1]) we obtain:

$$\langle q(t)\rangle = G(t)\langle p(0)\rangle + \dot{G(t)}\langle q(0)\rangle. \tag{17.23}$$

And we may finally write:

$$\langle q(t)\rangle = \frac{e^{\frac{-\gamma t}{2}}}{W}\sin(Wt)\langle p(0)\rangle + \left(\frac{e^{\frac{-\gamma t}{2}}}{2}\cos(Wt) + \frac{e^{\frac{-\gamma t}{2}}}{2W}\gamma\sin(Wt)\right)\langle q(0)\rangle, \tag{17.24}$$

Similarly, the evolution of the product of the position operator at different times or two point correlations are given by :

$$\begin{aligned}\langle q(t)q(t')\rangle &= G(t)G(t')\langle p^2(0)\rangle_S + \dot{G(t)}\dot{G(t')}\langle q^2(0)\rangle_S \\ &+ \dot{G(t)}G(t')\langle q(0)p(0)\rangle_S + G(t)\dot{G(t')}\langle p(0)q(0)\rangle_S \\ &+ \int_0^t \frac{dt_1}{\pi}\int_0^{t'} dt_2 G(t-t_1)G(t-t_2)\int_{-\infty}^{\infty} dw\sigma(w)n(w)e^{iw(t_1-t_2)},\end{aligned} \tag{17.25}$$

Whenever $t', t \gg \frac{1}{\gamma}$ the only non-negligible term in Eq. (17.25) is the last one, since the first 4 terms are short time effects that vanish for longer times, so that:

$$\langle q(t)q(t')\rangle = \frac{1}{\pi}\int_{-\infty}^{\infty} dw \frac{\sigma(w)n(w)}{[(w^2-\Omega_R^2)^2 + (\gamma w)^2]}e^{iw(t-t')}. \tag{17.26}$$

The first result of this section is an analytical answer for this correlation in the limit of the cutoff going to infinity. We take $\sigma(\omega) = \gamma\omega^n$ and perform contour integration, to obtain

$$\begin{aligned}\langle q(t)q(t')\rangle \approx \frac{2^{2-n}}{\sqrt{4\Omega_R^2-\gamma^2}}\Omega_R \Bigg(&\frac{(D_+)^{n-1}\, e^{\frac{1}{2}i\tau\left(\sqrt{4\Omega_R^2-\gamma^2}+i\gamma\right)}}{-1+e^{\frac{\sqrt{4\Omega_R^2-\gamma^2}+i\gamma}{2T}}} \\ &- \frac{(D_-)^{n-1}\, e^{\frac{1}{2}\left(-\gamma\tau+\frac{(1-i\tau T)\sqrt{4\Omega_R^2-\gamma^2}}{T}\right)}}{-e^{\frac{\sqrt{4\Omega_R^2-\gamma^2}}{2T}}+e^{\frac{i\gamma}{2T}}}\Bigg),\end{aligned} \tag{17.27}$$

[1]Typically, one takes Ω_R from the experiment and do not work with Ω

where $D_\pm = \pm\sqrt{4\Omega_R^2 - \gamma^2} + i\gamma$ and $\tau = t - t'$. Remarkably the result is finite ,taking an Ohmic bath with $\tau = 0, n = 1, \Omega_R \gg \gamma$ we obtain

$$\lim_{t\to\infty} \langle q^2(t)\rangle = \coth \frac{\Omega_R}{2T}, \tag{17.28}$$

which is what we expect after the system has thermalized. One may check the consistency of Eq. (17.27) by numerically integrating Eq. (17.26) for some set of parameters, this comparison is shown in Fig. 17.1

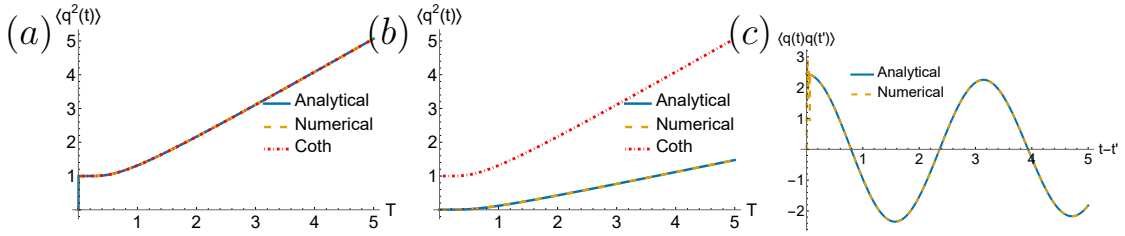

Figure 17.1: Two point correlations with a)$\gamma = 0.025\Omega_R, \tau = 0, n = 1$b)$\gamma = 0.025\Omega_R, \tau = 0, n = \frac{1}{2}$,c)$\gamma = 0.025\Omega_R, n = 1, T = 1.5\Omega_R$

17.2 The cumulant equation for systems of infinite dimension

We start from the Hamiltonian Eq. (17.1). We decompose H_I into the bath and system operators:

$$H_I = \sum_k A_k \otimes B_k. \tag{17.29}$$

In this case we only need one system and bath operators, namely:

$$A_1 = (a^\dagger + a) \tag{17.30}$$

$$B_1 = \int_0^\infty g(w)(a_w^\dagger + a_w)dw. \tag{17.31}$$

From there, we get:

$$A_1(\Omega) = a, \tag{17.32}$$

$$A_1(-\Omega) = a^\dagger, \tag{17.33}$$

$$B_1(w) = g(w)b_\omega. \tag{17.34}$$

Using these definitions let us see that Eq. (7.20) will look like for this particular case. We first calculate the dissipative part of our evolution:

$$D = \sum_{w,w'} \Gamma(\omega, \omega', t)\mathcal{L}(w, w'), \tag{17.35}$$

where D is shorthand notation for the dissipative part and:

$$\mathcal{L}(w, w') = \mathcal{L}_{w,w'} = A(w')\rho_S A^\dagger(w) - \frac{\{A^\dagger(w)A(w'), \rho_s\}}{2}, \tag{17.36}$$

so that:

$$\mathcal{L}_{++} = a\rho_S a^\dagger - \frac{\{a^\dagger a, \rho_s\}}{2}, \tag{17.37}$$

$$\mathcal{L}_{--} = a^\dagger \rho_S a - \frac{\{aa^\dagger, \rho_s\}}{2}, \tag{17.38}$$

$$\mathcal{L}_{-+} = a\rho_S a - \frac{\{aa, \rho_s\}}{2}, \tag{17.39}$$

$$\mathcal{L}_{+-} = a^\dagger \rho_S a^\dagger - \frac{\{a^\dagger a^\dagger, \rho_s\}}{2}. \tag{17.40}$$

where the subindices follow the same notation as in chapter 15 ($\Omega \to -, -\Omega \to +$). We now compute the Hamiltonian part [2]:

$$\Lambda(t) = \sum_{w,w'} \xi(\omega, \omega', t) A^\dagger(w) A(w'). \tag{17.41}$$

Expanding $\Lambda(t)$ and considering that $A_1(\Omega) = A_1^\dagger(-\Omega) = a$ and $A_1(-\Omega) = A_1^\dagger(\Omega) = a^\dagger$:

$$\Lambda(t) = \xi_{++} a^\dagger a + \xi_{--} aa^\dagger + \xi_{+-} a^\dagger a^\dagger + \xi_{-+} aa \tag{17.42}$$

$$= (\xi_{++} + \xi_{--})\, a^\dagger a + \xi_{+-} (a^\dagger)^2 + \xi_{-+} a^2. \tag{17.43}$$

where we dropped the constant term as any operator commutes with it, then by defining

$$\alpha = (\xi_{++} + \xi_{--}), \tag{17.44}$$

$$\beta = \xi_{+-} = \xi_{-+}. \tag{17.45}$$

we write our superoperator as:

$$\begin{aligned}\mathcal{K}_2(t)[\rho_s] = &-i[\alpha a^\dagger a + \beta (a^\dagger)^2 + \beta a^2, \rho_s] + \Gamma_{++}\left(a\rho_S a^\dagger - \frac{\{a^\dagger a, \rho_s\}}{2}\right) \\ &+ \Gamma_{--}\left(a^\dagger \rho_S a - \frac{\{aa^\dagger, \rho_s\}}{2}\right) + \Gamma_{+-}\left(a^\dagger \rho_S a^\dagger - \frac{\{a^\dagger a^\dagger, \rho_s\}}{2}\right) \\ &+ \Gamma_{-+}\left(a\rho_S a - \frac{\{aa, \rho_s\}}{2}\right),\end{aligned} \tag{17.46}$$

Now, our aim is to compute expected values of the form:

$$\langle aa^\dagger \rangle(t) = \mathrm{Tr}\{aa^\dagger e^{\mathcal{K}_2(t)} \rho(0)\}, \tag{17.47}$$

To do that, we find the adjoint of $\mathcal{K}_2$ so that we can apply it to our operator of interest. To do that, we use:

$$\mathrm{Tr}\{A\mathcal{K}_2[\rho]\} = \mathrm{Tr}\Big\{\mathcal{K}_2^\dagger[A]\rho\Big\}, \tag{17.48}$$

[2] We don't use this in the actual comparison, due to the Heisenberg-Langevin equations being renormalized

To find $\mathcal{K}_2^\dagger$ let us note the following identities:

$$\begin{aligned} \mathrm{Tr}\{A\{BC,\rho\}\} &= \mathrm{Tr}\{\{BC,A\}\rho\}, && (17.49)\\ \mathrm{Tr}\{A[B,\rho]\} &= \mathrm{Tr}\{[A,B]\rho\}. && (17.50) \end{aligned}$$

Using those and cyclic property of the trace one may write

$$\begin{aligned} \mathcal{K}_2^\dagger(t)[O] = &-i[O,\alpha a^\dagger a+\beta(a^\dagger)^2+\beta a^2]\\ &+\Gamma_{++}\left(a^\dagger O a-\frac{\{a^\dagger a,O\}}{2}\right)+\Gamma_{--}\left(aOa^\dagger-\frac{\{aa^\dagger,O\}}{2}\right)\\ &+\Gamma_{+-}\left(a^\dagger O a^\dagger-\frac{\{a^\dagger a^\dagger,O\}}{2}\right)+\Gamma_{-+}\left(aOa-\frac{\{aa,O\}}{2}\right). \end{aligned} \tag{17.51}$$

Now, we finally aim to compute $e^{\mathcal{K}_2^\dagger(t)}a^\dagger a$, for that we note that:

$$\mathcal{K}_2^\dagger(t)[\mathbb{I}] = 0, \tag{17.52}$$

$$\mathcal{K}_2^\dagger(t)[a] = \frac{\Gamma_{--}-\Gamma_{++}-2i\alpha}{2}a-2i\beta a^\dagger, \tag{17.53}$$

$$\mathcal{K}_2^\dagger(t)[a^\dagger] = \frac{\Gamma_{--}-\Gamma_{++}+2i\alpha}{2}a^\dagger+2i\beta a, \tag{17.54}$$

$$\mathcal{K}_2^\dagger(t)[a^\dagger a] = \mathcal{K}_2^\dagger(t)[aa^\dagger] = -2i\beta(a^\dagger)^2+2i\beta a^2+(\Gamma_{--}-\Gamma_{++})a^\dagger a+\Gamma_{--}, \tag{17.55}$$

$$\mathcal{K}_2^\dagger(t)[a^2] = (-2i\alpha+(\Gamma_{--}-\Gamma_{++}))a^2-4\beta i a^\dagger a-\Gamma_{+-}-2i\beta, \tag{17.56}$$

$$\mathcal{K}_2^\dagger(t)[(a^\dagger)^2] = (2i\alpha+(\Gamma_{--}-\Gamma_{++}))(a^\dagger)^2+4\beta i a^\dagger a-\Gamma_{-+}+2i\beta. \tag{17.57}$$

Since the superoperator is linear, we can write the evolution of linear combinations of the operators, for example

$$\begin{aligned} \mathcal{K}_2^\dagger(t)[ea^\dagger a+ba^2+c(a^\dagger)^2] = &\,e\left(-2i\beta(a^\dagger)^2+2i\beta a^2+(\Gamma_{--}-\Gamma_{++})a^\dagger a+\Gamma_{--}\right)\\ &+b\left((-2i\alpha+(\Gamma_{--}-\Gamma_{++}))a^2-4\beta i a^\dagger a-\Gamma_{+-}-2i\beta\right)\\ &+c\left((2i\alpha+(\Gamma_{--}-\Gamma_{++}))(a^\dagger)^2+4\beta i a^\dagger a-\Gamma_{-+}+2i\beta\right), \end{aligned} \tag{17.58}$$

$$\begin{aligned} \mathcal{K}_2^\dagger(t)[la^\dagger+ma] = &\,l\left(\frac{\Gamma_{--}-\Gamma_{++}+2i\alpha}{2}a^\dagger+2i\beta a\right)\\ &+m\left(\frac{\Gamma_{--}-\Gamma_{++}-2i\alpha}{2}a-2i\beta a^\dagger\right). \end{aligned} \tag{17.59}$$

Using $\Gamma=(\Gamma_{++}-\Gamma_{--})$, these can then be seen as a linear transformation on the coefficients [A3]

$$\begin{pmatrix} e'\\ b'\\ c' \end{pmatrix} = \begin{pmatrix} -\Gamma & -4i\beta & 4i\beta\\ 2i\beta & -2i\alpha-\Gamma & 0\\ -2i\beta & 0 & 2i\alpha-\Gamma \end{pmatrix}\begin{pmatrix} e\\ b\\ c \end{pmatrix}+\begin{pmatrix} \Gamma_{--}\\ -2i\beta-\Gamma_{+-}\\ (2i\beta+\Gamma_{-+}) \end{pmatrix}, \tag{17.60}$$

and

$$\begin{pmatrix} l'\\ m' \end{pmatrix} = \begin{pmatrix} \frac{2i\alpha-\Gamma}{2} & -2i\beta\\ 2i\beta & -\frac{\Gamma+2i\alpha}{2} \end{pmatrix}\begin{pmatrix} l\\ m \end{pmatrix}. \tag{17.61}$$

Then the evolution of the observables can be written as the exponential of a linear map Eq. (15.4). Using the equations above and going back from the interaction picture[17] [3], one obtains

$$\langle q(t)\rangle = e^{\frac{\Gamma_{--}-\Gamma_{++}}{2}}\left(\cos(\Omega t+\delta)\langle q(0)\rangle + \frac{\sin(\Omega t+\delta)(\alpha+2\beta)}{\delta\Omega}\langle p(0)\rangle\right). \quad (17.62)$$

Unfortunately, the procedure is not always possible, as the number of variables that need to participate in the linear transformation for the evolution may not be finite. In such cases, one may perform a mean field approximation or truncation of the Fock space. Figure 17.2 shows the dynamics of position for the damped harmonic oscillator.

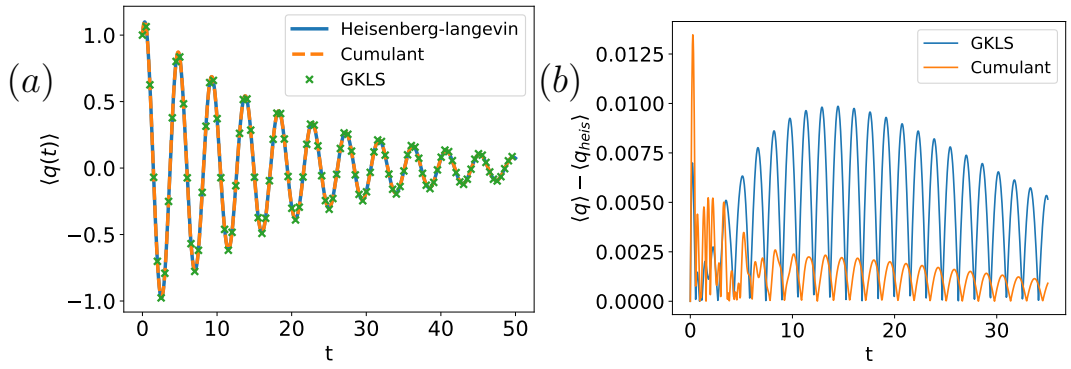

Figure 17.2: Dynamics of the damped harmonic oscillator, a) shows position, b) the error with respect to the Heisenberg-Langevin equation. The parameters are $\Omega_R = 2, \gamma = 0.15, T = 0$

17.3 Harmonic Oscillator with Kerr non-linearity

Nonlinear processes are important in quantum optics [B6, B7]. One of the most studied processes are Kerr Nonlinearities. Modeling their interaction with the environment is the reason for the cumulant/refined weak coupling equation was first proposed [54]. The idea behind proposing this equation was that it can handle small spacing in Bohr frequencies, which are important for transient dynamics, and has the GKLS master equation as a limit when $t \to \infty$ [A4, 54, 55] (see [A4] for an in-depth discussion). In this section, we consider the Hamiltonian

$$H = \omega_0 a^\dagger a + \underbrace{\frac{\chi}{2}a^\dagger a^\dagger a a}_{H_S} + \underbrace{\sum_k w_k a_k^\dagger a_k}_{H_B} + \underbrace{(a+a^\dagger)\sum_k g_k(a_k+a_k^\dagger)}_{H_I}. \quad (17.63)$$

with an Ohmic Spectral density Eq. (1.99). We show how the master equation is almost exact but cheaper than the numerically exact approach. To perform the

[3] We simply rotate back to the Schrodinger picture because our equations here are in the interaction-Heisenberg i.e. (interaction picture evolution of observables with respect to the free Hamiltonian) picture rather than the normal Heisenberg picture

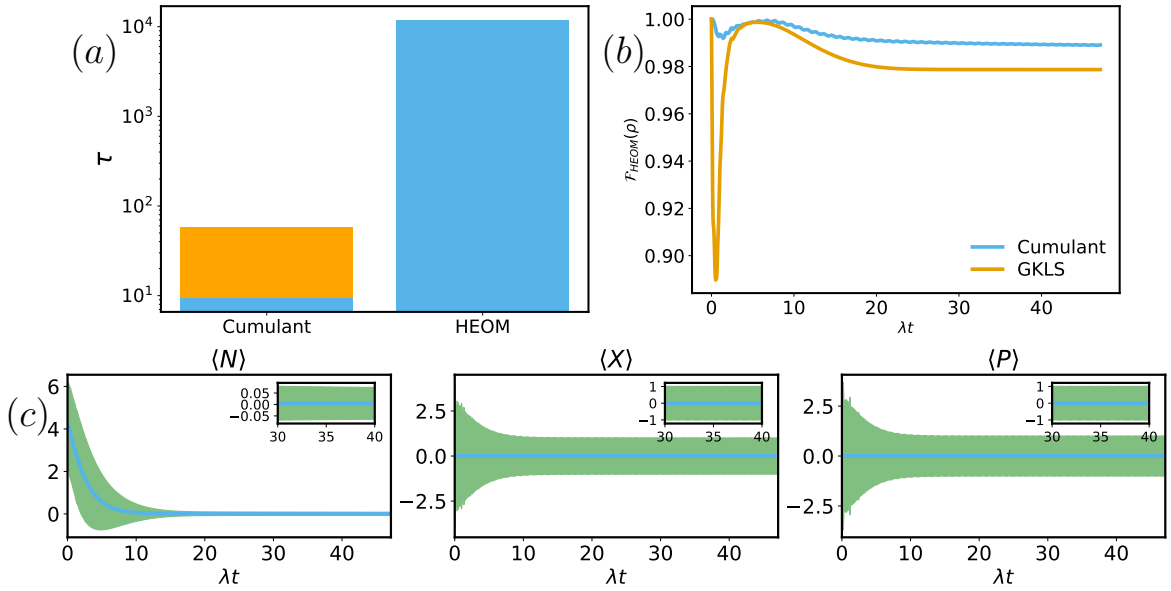

Figure 17.3: a)Shows the computation time required for the cumulant and HEOM,b) Shows the fidelity of the cumulant and GKLS master equation to HEOM , c) Shows the evolution of the average population, position and momentum which are represented by the solid line, while the shadow represents their variance. The parameters used for the simulation are , $T = 0.1\omega_0, \lambda = \frac{\omega_0}{8}, s = 1, \omega_c = \omega_0, \xi = \frac{\omega_0}{2}$

simulation We truncated the Hilbert space of the oscillator such that it contains $N = 10$ excitations. This number is chosen to keep HEOM feasible, but as we see from the figure it is enough as the mean population of photons is never high. We can also appreciate the difference in simulation time and precision of the different approaches.

Notice from Figure 17.3 b) and c) that the cumulant equation has not converged to the GKLS equation. Similarly to the results in chapter 15, the oscillation of the coherence dies out slower than the exact solution. The presence of those oscillations are what keep the cumulant equation more faithful than the GKLS master equation, even when in Figure 17.3 it looks like the steady state was achieved for the observables.

Conclusions

In this thesis, specifically in chapters 1-12, we have provided an exhaustive and comprehensive overview of techniques used to simulate open quantum systems beyond the Markovian regime, including HEOM, TCL, the cumulant equation, pseudomodes, etc. Chapter 1 presents the correlation function and its approximation by decaying exponentials, a key ingredient in many numerical methods, such as HEOM and Pseudomodes. We present modern methods to obtain such a decomposition and propose our own, which borrows the idea from [33, 34] but ensures that one does not depend on the Matsubara decomposition and is therefore not limited by temperature. All the methods were also made available for Bosonic environments in the open-source package QuTiP [A1], and this chapter was mainly based on [1].

In Chapter 5, we provided a derivation of the Feynman-Vernon influence functional for open systems in a Gaussian environment and with linear coupling. We used this derivation to obtain both the Redfield (TCL2) and the cumulant equation as particular limits in chapters 6 and 7, respectively. This unconventional derivation allows us to understand the relationship between the cumulant and Redfield generators we first obtained in [A2]. In these chapters, we also show how one can use the approximations described in Chapter 1 to obtain the decay rates and Lamb shift required in master equations, accelerating their simulation.

In chapters 8 and 9, we discuss two numerically exact methods, pseudomodes and HEOM. We end chapter 9 with a discussion of the many methods based on these two that are closely related. We then discuss the Reaction Coordinate mapping in Chapter 10, where we derive the mapping and show how to relate the old and new spectral densities. Chapter 11 shows how to calculate heat using some of the methods we explored before; special emphasis is given to the fact that, in Non-Markovian master equations, there is a coherent contribution to the heat currents. Finally, we conclude this overview of the literature with a brief discussion of projection operator techniques, in which we again propose using the approximations of Chapter 1 to accelerate their simulation.

In chapter 13, we discussed the results in [A2], which include a discussion of the steady state of open quantum systems and an application of the reaction-coordinate mapping. We also briefly discuss how the quasi-steady state differs from the steady state and explain it in terms of the relationship between the cumulant equation and the Feynman-Vernon influence functional.

In chapter 14, we analyze a simple open quantum system with an exact solution. We show how the approximations of chapter 1 may be used to solve integro-differential equations, and extend this model to arbitrary spectral densities. We study an Ohmic spectral density and confirm the presence of the localization-delocalization phase transition in this model. We then show how master equations can be precise even when dealing with highly structured spectral densities.

In chapter 15, we study the spin boson model with composite interactions [A3]. In this section, we added the filtered approximation to the cumulant equation FA [A4],

and compare with other methods such as the Bloch-Redfield master equation and HEOM. In this section, we introduce a method for solving the cumulant equation via linear maps and show that it is exact in the pure dephasing case.

In chapter 16, we showed that the cumulant equation can accurately describe heat transport in open quantum systems. We also showed that including the Lamb shift is necessary to adequately describe currents in this regime. We also explained the discrepancy between [43] and [A3], which stems from the fact that the former uses non-interacting qubits. We also showed that the cumulant equation may fail when the local master equation is adequate in bipartite systems, but that as we include more parties, the cumulant equation takes longer to reach the global GKLS state, and becomes faithful even till reaching the steady state. We remark that this chapter casts doubt on the definition of the heat current for Non-Markovian equations, as it appears to contradict the second law in one of the scenarios studied.

Finally, in Chapter 17, we showed how to use the cumulant equation for infinite-dimensional systems, provided the exact solution using the Heisenberg-Langevin equations, and also provided an analytical solution for the Heisenberg-Langevin equations in the infinite cutoff limit. As the last example, we used a damped oscillator with a Kerr nonlinearity, and we observed the same behavior: the cumulant does not tend to the Global master equation prior to equilibration time due to the small Bohr frequencies.

Appendix A

Jump operators

Let us express our interaction Hamiltonian as

$$H_{SB}(t) = \sum_{\alpha} S_\alpha \otimes B_\alpha. \tag{A.1}$$

Here both S_α and B_α are Hermitian operators. If the spectrum of our system of interest is discrete, and we denote the eigenvalues of H_S by epsilon one may write

$$A_\alpha = \underbrace{\sum_{\epsilon} |\epsilon\rangle\langle\epsilon|}_{\mathbb{I}} A \underbrace{\sum_{\epsilon'} |\epsilon'\rangle\langle\epsilon'|}_{\mathbb{I}} = \sum_{\epsilon,\epsilon'} |\epsilon\rangle\langle\epsilon| A |\epsilon'\rangle\langle\epsilon'|. \tag{A.2}$$

In consecutive levels $\epsilon - \epsilon' = \omega$, so we may write this as

$$A_\alpha = \sum_{\omega} \overbrace{\sum_{\epsilon'-\epsilon=\omega} |\epsilon\rangle\langle\epsilon| A |\epsilon'\rangle\langle\epsilon'|}^{A(\omega)} = \sum_{\omega} A(\omega). \tag{A.3}$$

An immediate (and useful) consequence of this way of expressing the operators is that

$$[H_S, A_\alpha(\omega)] = H_S \sum_{\epsilon'-\epsilon=\omega} |\epsilon\rangle\langle\epsilon| A |\epsilon'\rangle\langle\epsilon'| - \sum_{\epsilon'-\epsilon=\omega} |\epsilon\rangle\langle\epsilon| A |\epsilon'\rangle\langle\epsilon'| H_S \tag{A.4}$$

$$= \sum_{\epsilon'-\epsilon=\omega} \underbrace{(\epsilon - \epsilon')}_{-\omega} |\epsilon\rangle\langle\epsilon| A |\epsilon'\rangle\langle\epsilon'| \tag{A.5}$$

$$= -\omega \sum_{\epsilon'-\epsilon=\omega} |\epsilon\rangle\langle\epsilon| A |\epsilon'\rangle\langle\epsilon'| \tag{A.6}$$

$$= -\omega A_\alpha(\omega). \tag{A.7}$$

In the same way one can see that

$$[H_S, A_\alpha^\dagger(\omega)] = \omega A_\alpha^\dagger(\omega). \tag{A.8}$$

Because of the expressions above $A_\alpha^\dagger(\omega)$ and $A_\alpha(\omega)$ are said to be Eigenoperators of $[H_S, \bullet]$ belonging to the frequencies $\pm\omega$ respectively. This representation is convenient because the operators in the interaction picture take the form:

$$A_I(\omega) = e^{IH_S t} A(\omega) e^{-IH_S t} = A(\omega) + (it)[H_S, A(\omega)] + \frac{(it)^2}{2!}[H_S, [H_S, A(\omega)]] + \frac{(it)^3}{3!}[H_S, [H_S, [H_S, A(\omega)]]] + \cdots + \frac{(it)^n}{n!}[H_S, [H_S, \ldots, [H_S, A(\omega)], \ldots]] \tag{A.9}$$

$$= e^{-i\omega t} A(\omega). \tag{A.10}$$

Similarly one obtains

$$A_I^\dagger(\omega) = e^{i\omega t} A^\dagger(\omega). \tag{A.11}$$

From these definitions we can notice that:

1. Positive and negative frequencies are related via $A_\alpha^\dagger(\omega) = A_\alpha(-\omega)$
2. The product of the jump operators of a given frequency is a conserved quantity under free evolution

$$[H_S, A_\alpha^\dagger(\omega)A_\alpha(\omega)] = [H_S, A_\alpha^\dagger(\omega)]A_\alpha(\omega) + A_\alpha^\dagger(\omega)[H_S, A_\alpha(\omega)] \tag{A.12}$$

$$= \omega A_\alpha^\dagger(\omega)A_\alpha(\omega) - \omega A_\alpha^\dagger(\omega)A_\alpha(\omega) = 0. \tag{A.13}$$

We may now write our interaction Hamiltonian as

$$H_{SB}(t) = \sum_{\alpha,\omega} A_\alpha(\omega) \otimes B_\alpha = \sum_{\alpha,\omega} A_\alpha^\dagger(\omega) \otimes B_\alpha. \tag{A.14}$$

Both sides are the same since the sum over frequencies runs for both positive and negative. This notation allows us to have a simple representation in the interaction picture, namely

$$H_{SB}^I(t) = \sum_{\alpha,\omega} e^{-i\omega t} A_\alpha(\omega) \otimes B_\alpha(t) = \sum_{\alpha,\omega} e^{i\omega t} A_\alpha^\dagger(\omega) \otimes B_\alpha^\dagger(t). \tag{A.15}$$

where $B_\alpha(t) = e^{IH_B t} B_\alpha e^{-IH_B t} = B_\alpha^\dagger(t)$. The expectation value remains zero as

$$\langle B_\alpha \rangle_B = \langle B_\alpha(t) \rangle_B = 0. \tag{A.16}$$

this indicates that the first moments of the bath are always zero. The procedure of the box 5.1.1 is usually called centralization for this reason. In particular, notice that this is satisfied for thermal environments, and that in this notation the procedure of 5.1.1 becomes apparent.

Appendix B

Projection Operator Techniques

B.1 Evolution of projected density matrices

We start from the standard Von Neumann equation Eq. (2.27)

$$\frac{d}{dt}\rho(t) = \mathcal{L}(t)\rho(t). \tag{B.1}$$

Then

$$\frac{d}{dt}\mathcal{P}\rho(t) = \mathcal{P}\frac{d}{dt}\rho(t) = \mathcal{P}\mathcal{L}(t)\rho(t), \tag{B.2}$$

$$\frac{d}{dt}\mathcal{Q}\rho(t) = \mathcal{Q}\frac{d}{dt}\rho(t) = \mathcal{Q}\mathcal{L}(t)\rho(t). \tag{B.3}$$

Since we do not want to deal with the full ρ, we use the fact that $\mathcal{P}+\mathcal{Q} = \mathbb{I}$ to write has

$$\frac{d}{dt}\mathcal{P}\rho(t) = \mathcal{P}\mathcal{L}(t)\mathcal{P}\rho(t) + \mathcal{P}\mathcal{L}(t)\mathcal{Q}\rho(t), \tag{B.4}$$

$$\frac{d}{dt}\mathcal{Q}\rho(t) = \mathcal{Q}\mathcal{L}(t)\mathcal{Q}\rho(t) + \mathcal{P}\mathcal{Q}(t)\mathcal{P}\rho(t). \tag{B.5}$$

Once in this form, we can solve the second equation by Green functions [B11] to obtain

$$Q\rho(t) = G(t,0)Q\rho(0) + \int_0^t dt_1 G(t,t_1)Q\mathcal{L}(t_1)\mathcal{P}\rho(t_1). \tag{B.6}$$

The Green function satisfies the homogeneous equation, which has the formal solution Eq. (2.31)

$$G(t,t_1) = \mathcal{T}e^{\int_{t_1}^{t} dt_2 Q\mathcal{L}(t_2)}. \tag{B.7}$$

where $\mathcal{T}$ is the time ordering operator, it is typical to perform some extra simplifications at this stage. The first one we call centralization. Namely $\mathcal{P}\mathcal{L}(t_1)\mathcal{L}(t_2)\dots\mathcal{L}(t_{2n+1})\mathcal{P} = 0$, while this assumption may seem strange we have been doing it all along, this is nothing more than 5.1 in a more general form (the form in 5.1 corrresponds to $n = 0$). To see this clearly let us expand this

$$\mathcal{P}\mathcal{L}(t_1)\mathcal{L}(t_2)\dots\mathcal{L}(t_{2n+1})\mathcal{P} = 0, \tag{B.8}$$

$$\mathrm{Tr}_{IR}[\mathcal{L}(t_1)\mathcal{L}(t_2)\dots\mathcal{L}(t_{2n+1})\rho]\otimes\rho_{IR}\mathcal{P} = 0. \tag{B.9}$$

This is a chain of commutators, however for simplicity let us just look at one of the terms involved

$$\mathrm{Tr}_{IR}[H(t_1)H(t_2)\dots H(t_{2n+1})\rho]\otimes\rho_{IR}\mathcal{P}=0, \tag{B.10}$$
$$\mathrm{Tr}_{IR}[H(t_1)H(t_2)\dots H(t_{2n+1})Q\rho+P\rho]\otimes\rho_{IR}\mathcal{P}=0. \tag{B.11}$$

Essentially, what we are asking for is that the expectation value of the product of the interation hamiltonians at different times is zero. Meaning

$$\mathrm{Tr}_{IR}[H(t_1)H(t_2)\dots H(t_{2n+1})\rho_{IR}]=0. \tag{B.12}$$

While this seems like a big ask, it is true for the typical applications where we consider the irrelevant part of our system to be in a thermal state, and be large enough so that it is not affected by our system such that it remains on a thermal state, and thus the state is time independent (This can also be justified from the point of view that the time scale of evolution of the system is short compared to the changes in the environment). This technical assumption is not required for the derivation of the equations to follow but makes the math way easier, also bare in mind that so far we have not asked for any special initial conditions [1]. Substituting Eq. (B.4) into Eq. (B.6) yields

$$\frac{d}{dt}\mathcal{P}\rho(t)=\mathcal{P}\mathcal{L}(t)\mathcal{P}\rho(t)+\mathcal{P}\mathcal{L}(t)G(t,0)Q\rho(0)+\int_0^t dt_1\mathcal{P}\mathcal{L}(t)G(t,t_1)Q\mathcal{L}(t_1)\mathcal{P}\rho(t_1). \tag{B.13}$$

Equation Eq. (B.13) is known in the literature as the Nakajima-Zwanzig equation. It is an exact equation for the dynamics of the system of interest. If we now assume we can centralize this equation simplifies to

$$\frac{d}{dt}\mathcal{P}\rho(t)=\mathcal{P}\mathcal{L}(t)G(t,0)Q\rho(0)+\int_0^t dt_1\mathcal{K}_S(t,t_1)\mathcal{P}\rho(t_1), \tag{B.14}$$

where $\mathcal{K}_S(t,t_1)$ is the memory kernel superoperator given by

$$\mathcal{K}_S(t,t_1)=\mathcal{P}\mathcal{L}(t)G(t,t_1)Q\mathcal{L}(t_1). \tag{B.15}$$

Even with the assumption of centralization, in practice the Nakajima-Zwanzig equation while exact is hard to work with. So further approximations are typically taken into account.

B.2 The Redfield equation from the Nakajima-Zwanzig equation

In this section, we will briefly show how the second order expansion of the Nakajima-Zwanzig equation yields the Redfield equation when we consider an initial product

[1] There could be an interesting discussion regarding how feasible is the time independence of the environment, however that is beyond the scope of this thesis

state. If we consider an initial product stat,e we have

$$\begin{aligned}\mathcal{Q}\rho(0) &= (\mathbb{I}-\mathcal{P})\rho(0) && \text{(B.16)}\\ &= \rho(0)-\mathcal{P}\rho(0) && \text{(B.17)}\\ &= \rho_S(0)\otimes\rho_{IR}(0)-\rho_S(0)\otimes\rho_{IR} && \text{(B.18)}\\ &= 0. && \text{(B.19)}\end{aligned}$$

Then Eq. (B.13) simplifies to

$$\frac{d}{dt}\mathcal{P}\rho(t)=\int_0^t dt_1\mathcal{K}_S(t,t_1)\mathcal{P}\rho(t_1). \tag{B.20}$$

We then expand the memory kernel in powers of the coupling strength. Since $\mathcal{L}$ is linear in the coupling strength, the first non-trivial term is given by the second order in coupling strength, which effectively means we approximate $G(t,t_1)\approx 1$ [2] so that

$$\begin{aligned}\mathcal{K}_S(t,t_1) &\approx \mathcal{P}\mathcal{L}(t)Q\mathcal{L}(t_1) && \text{(B.21)}\\ &\approx \mathcal{P}\mathcal{L}(t)\mathcal{L}(t_1)-\underbrace{\mathcal{P}\mathcal{L}(t)\mathcal{P}}_{0}\mathcal{L}(t_1) && \text{(B.22)}\\ &\approx \mathcal{P}\mathcal{L}(t)\mathcal{L}(t_1). && \text{(B.23)}\end{aligned}$$

So then we can rewrite the evolution of the system as

$$\frac{d}{dt}\mathcal{P}\rho(t)=\int_0^t dt_1\mathcal{P}\mathcal{L}(t)\mathcal{L}(t_1)\mathcal{P}\rho(t_1), \tag{B.24}$$

using the fact that

$$\frac{d}{dt}\mathcal{P}\rho(t)=\frac{d}{dt}\rho_S(t)\otimes\rho_B. \tag{B.25}$$

If we now reintroduce the definition of $\mathcal{L}(t)$ as in Eq. (2.31) we finally obtain

$$\frac{d}{dt}\rho_S(t)\otimes\rho_B=-\int_0^t ds\mathrm{Tr}_B\Big[[H(t),[H(s),\rho_S(s)\otimes\rho_B]]\Big]\otimes\rho_B, \tag{B.26}$$

which we can recast as

$$\frac{d}{dt}\rho_S(t)=-\int_0^t ds\mathrm{Tr}_B\Big[[H(t),[H(s),\rho_S(s)\otimes\rho_B]]\Big]. \tag{B.27}$$

Notice this is the same as Eq. (6.12), namely the Redfield equation. (Up to the Markov approximation). While approximating the memory kernel helped to simplify the equations the resulting equation is still time non-local and integro-differential, making it hard to work with. In the next section we will take a look at an alternate approximation approach that yields equations that are time local, and thus easier to work with.

[2] Notice this is exactly the same we did when deriving Redfield from the Feynman Vernon influence functional

B.3 The Time Convolutionless (TCL) equation

As mentioned at the end of the previous section, it is desirable to come up with an approximation scheme that yields time local equations. The first step to realize this is to notice that we can write

$$\rho(s) = G_R(t,s)\rho(t) = G_R(t,s)(\mathcal{P}+\mathcal{Q})\rho(t), \tag{B.28}$$

where $G_R(t,s)$ is the backward propagator of the full evolution

$$G_R(t,s) = \mathcal{T}_{\leftarrow} e^{-\int_s^t dt_2 \mathcal{L}(t_2)}. \tag{B.29}$$

where $\mathcal{T}_{\leftarrow}$ is the anti-chronological time ordering operator. Then substituting in Eq. (B.6) one can write

$$Q\rho(t) = G(t,0)Q\rho(0) + \int_0^t dt_1 G(t,t_1)Q\mathcal{L}(t_1)\mathcal{P}G_R(t,t_1)(\mathcal{P}+\mathcal{Q})\rho(t), \tag{B.30}$$

we then introduce the superoperator Σ

$$\Sigma(t) = \int_{t_0}^t ds G(t,s)Q\mathcal{L}(s)\mathcal{P}G_R(t,s). \tag{B.31}$$

The superoperator Σ contains both the chronological and anti-chronological time ordering, thus computing it is a challenge. However, it allows us to express the irrelevant part of the density matrix as

$$Q\rho(t) = G(t,0)Q\rho(0) + \Sigma(t)(\mathcal{P}+\mathcal{Q})\rho(t), \tag{B.32}$$

$$(\mathbb{I}-\Sigma(t))\,Q\rho(t) = G(t,0)Q\rho(0) + \Sigma(t)\mathcal{P}\rho(t). \tag{B.33}$$

The superoperator Σ has two obvious properties

- $\Sigma(t_0) = 0$.
- $\Sigma(t)|_{\alpha=0} = 0$.

Asumming the superoperator can be inverted we can write [3].

$$Q\rho(t) = (\mathbb{I}-\Sigma(t))^{-1} G(t,0)Q\rho(0) + (\mathbb{I}-\Sigma(t))^{-1}\Sigma(t)\mathcal{P}\rho(t) \tag{B.34}$$

$$= (\mathbb{I}-\Sigma(t))^{-1} G(t,0)Q\rho(0) + (\mathbb{I}-\Sigma(t))^{-1}\mathcal{P}\rho(t) - \mathcal{P}\rho(t). \tag{B.35}$$

where we used

$$\frac{\Sigma(t)}{\mathbb{I}-\Sigma(t)} = \frac{\mathbb{I}-\mathbb{I}+\Sigma(t)}{\mathbb{I}-\Sigma(t)} = (\mathbb{I}-\Sigma(t))^{-1} - \mathbb{I}. \tag{B.36}$$

This means that the relevant part of the density matrix can in principle be obtained from minimal knowledge of the irrelevant part and the initial condition. The history kernel in the Nakajima-Zwanzig equation Eq. (B.13), has been removed at the expense of using the exact backwards propagator. Of course, this may not always

[3] This may not always be the case, and it happens in many circunstances that it is only invertible for weak coupling or short times

be reasonable as it might not be possible to invert $\mathbb{I} - \Sigma(t)$. By inserting this into Eq. (B.4) we get

$$\frac{d}{dt}\mathcal{P}\rho(t) = \mathcal{P}\mathcal{L}(t)\mathcal{P}\rho(t) + \mathcal{P}\mathcal{L}(t)\Big((\mathbb{I} - \Sigma(t))^{-1} G(t,0)Q\rho(0) + (\mathbb{I} - \Sigma(t))^{-1} \mathcal{P}\rho(t) - \mathcal{P}\rho(t)\Big). \tag{B.37}$$

We then define the superoperators

$$I(t) = \mathcal{P}\mathcal{L}(t) (\mathbb{I} - \Sigma(t))^{-1} G(t,0), \tag{B.38}$$

$$\mathcal{K}(t) = \mathcal{P}\mathcal{L}(t) (\mathbb{I} - \Sigma(t))^{-1}. \tag{B.39}$$

Then the evolution can be rewritten as

$$\frac{d}{dt}\mathcal{P}\rho(t) = \mathcal{K}(t)\mathcal{P}\rho(t) + I(t)\mathcal{Q}\rho(0). \tag{B.40}$$

This equation, while time local still involves the calculation of intractable objects, comprised of both chronological and anti-chronological time ordering. In order to be able to compute actual dynamics, we need to approximate the superoperator $\Sigma(t)$ to be tractable.

B.3.1 Perturbative expansions of the TCL generator

On top of the assumption that $(\mathbb{I} - \Sigma(t))$ is invertible, we also now assume the following Taylor expansion is admissible

$$(\mathbb{I} - \Sigma(t))^{-1} = \sum_{n=0}^{\infty} \Sigma(t)^n, \tag{B.41}$$

so that

$$\mathcal{K}(t) = \alpha \sum_{n=0}^{\infty} \mathcal{P}\mathcal{L}(t)\Sigma(t)^n = \sum_{n=1}^{\infty} \alpha^n \mathcal{K}_n(t). \tag{B.42}$$

Here we introduced the parameter α (the coupling constant) explicitly for the sake of bookkeeping. In order to find the contribution $\mathcal{K}_n(t)$ of the n^{th} order expansion in coupling strenght, we also need to expand $\Sigma(t)$ in powers of the coupling strenght

$$\Sigma(t) = \sum_{n=0}^{\infty} \alpha^n \Sigma_n(t). \tag{B.43}$$

Inserting Eq. (B.43) into Eq. (B.42), and then sorting the terms of the same power in coupling strength, up to the fourth order, one obtains for $n = 1$:

$$\alpha\mathcal{K}_1(t) = \alpha \sum_{n=0}^{\infty} \mathcal{P}\mathcal{L}(t)\Sigma(t)^n. \tag{B.44}$$

Thus, the same power of the coupling strength is obtained for $n = 0$ in the sum which yields

$$\alpha\mathcal{K}_1(t) = \alpha\mathcal{P}\mathcal{L}(t). \tag{B.45}$$

For $n = 2$ we have

$$\alpha^2\mathcal{K}_2(t) = \alpha\sum_{n=0}^{\infty}\mathcal{PL}(t)\Sigma(t)^n = \alpha\sum_{n=0}^{\infty}\mathcal{PL}(t)\left(\sum_{k=0}^{\infty}\alpha^k\Sigma_k(t)\right)^n, \tag{B.46}$$

this is satisfied when $n = k = 1$, thus we obtain

$$\alpha^2\mathcal{K}_2(t) = \alpha^2\mathcal{PL}(t)\Sigma_1(t). \tag{B.47}$$

For $n = 3$:

$$\alpha^3\mathcal{K}_3(t) = \alpha\sum_{n=0}^{\infty}\mathcal{PL}(t)\Sigma(t)^n = \alpha\sum_{n=0}^{\infty}\mathcal{PL}(t)\left(\sum_{k=0}^{\infty}\alpha^k\Sigma_k(t)\right)^n, \tag{B.48}$$

In this case, there are two instances where the sum generates a second order expression in coupling strength, those are $n = 2, k = 1$ and $n = 1, k = 2$. All different terms generate other couplings, thus we have

$$\alpha^3\mathcal{K}_3(t) = \alpha^3\mathcal{PL}(t)\left(\Sigma_1^2(t) + \Sigma_2(t)\right). \tag{B.49}$$

The last term we will consider is $n = 4$. In this case there are more combinations that give rise to a third order power, the obvious ones are $n = 1, k = 3$,$n = 3, k = 1$, to understand where the others come from consider:

$$(\alpha\Sigma_1(t) + \alpha^2\Sigma_2(t))^2 = (\alpha\Sigma_1(t))^2 + \left(\alpha^2\Sigma_2(t)\right)^2 + \alpha^3\{\Sigma_2(t), \Sigma_1(t)\}, \tag{B.50}$$

there we see that the n^{th} of many ks can generate terms of a given power, in this case the non-obvious terms are those with $n = 2, k = (1, 2)$. Then we have

$$\alpha^4\mathcal{K}_4(t) = \alpha^4\mathcal{PL}(t)\left(\Sigma_1^3(t) + \Sigma_3(t) + \{\Sigma_2(t), \Sigma_1(t)\}\right). \tag{B.51}$$

The contributions of the first four orders can then be written as

$$\mathcal{K}_1(t) = \mathcal{PL}(t), \tag{B.52}$$
$$\mathcal{K}_2(t) = \mathcal{PL}(t)\Sigma_1(t), \tag{B.53}$$
$$\mathcal{K}_3(t) = \mathcal{PL}(t)\left(\Sigma_1^2(t) + \Sigma_2(t)\right), \tag{B.54}$$
$$\mathcal{K}_4(t) = \mathcal{PL}(t)\left(\Sigma_1^3(t) + \Sigma_2(t)\Sigma_1(t) + \Sigma_1(t)\Sigma_2(t) + \Sigma_3(t)\right). \tag{B.55}$$

In order to write down the final contributions we need to find the expressions for Σ_i using Eq. (B.43). This simply boils down to expanding the Green function. For completeness let us find more concrete expressions for these contributions in the case where we use box 5.1.

Since $\mathcal{K}(t)$ acts on $\mathcal{P}\rho$ and because we have centralized, then

$$\mathcal{K}_1(t) = 0. \tag{B.56}$$

Now to get Σ_1 let us consider Eq. (B.31)

$$\Sigma(t) = \alpha\int_{t_0}^{t} dsG(t, s)Q\mathcal{L}(s)\mathcal{P}G_R(t, s). \tag{B.57}$$

The idea now is to approximate both $G(t,s)$ and $G_R(t,s)$ which contain all powers of α. In order to get first order in coupling strength, both superoperators need to be approximated to the identity superoperator namely

$$\Sigma_1(t) = \alpha \int_{t_0}^{t} ds Q\mathcal{L}(s)\mathcal{P}, \tag{B.58}$$

so then the second order contribution of the memory kernel is

$$\mathcal{K}_2(t) = \alpha \int_{t_0}^{t} ds \mathcal{P}\mathcal{L}(t)Q\mathcal{L}(s)\mathcal{P} \tag{B.59}$$

$$= \alpha \int_{t_0}^{t} ds \mathcal{P}\mathcal{L}(t)\mathcal{L}(s)\mathcal{P}. \tag{B.60}$$

Here in the last line we used the fact that $\mathcal{Q} = \mathbb{I} - \mathcal{P}$ and 5.1. At this stage notice what the equation of motion generated at this order is (considering an initial product state):

$$\frac{d}{dt}\mathcal{P}\rho(t) = \mathcal{K}_2(t)\mathcal{P}\rho(t). \tag{B.61}$$

Notice the similarity to Eq. (B.24). Expanding this expression in the same way one obtains:

$$\frac{d}{dt}\rho_S(t) = \alpha \int_{t_0}^{t} ds \mathcal{P}\mathcal{L}(t)\mathcal{L}(s)\mathcal{P}\rho(t) \tag{B.62}$$

$$= -\int_{0}^{t} ds \mathrm{Tr}_B\Big[[H(t),[H(s),\rho_S(t)\otimes\rho_B]]\Big]. \tag{B.63}$$

which is the Redfield equation Eq. (6.12). Notice the locality in time **did not involve the Markov approximation**. To find the next contribution we need to find $\Sigma_2(t)$. To do it we approximate the Green functions by $G(t,s) = \mathbb{I}+\alpha\mathcal{Q}A(s)$, and $G_R(t,s) = \mathbb{I}-\alpha A(s)$, where $A(s) = \int_s^t ds'\mathcal{L}(s')$ and consider only the contributions proportional to the coupling strength. Using this we find

$$\Sigma(t) = \Sigma_1(t) + \underbrace{\int_0^t ds\left(\mathcal{Q}A(s)Q\mathcal{L}(s)\mathcal{P} - Q\mathcal{L}(s)\mathcal{P}A(s)\right)}_{\Sigma_2} + \mathcal{O}(\alpha^2). \tag{B.64}$$

We then have

$$\Sigma_2(t) = \int_0^t ds\left(\mathcal{Q}A(s)Q\mathcal{L}(s)\mathcal{P} - Q\mathcal{L}(s)\mathcal{P}A(s)\right) \tag{B.65}$$

$$= \int_0^t ds \int_s^t ds'\left(\mathcal{Q}\mathcal{L}(s')Q\mathcal{L}(s)\mathcal{P} - Q\mathcal{L}(s)\mathcal{P}\mathcal{L}(s')\right), \tag{B.66}$$

by making the same change of variable as in Fig. 2.1 we obtain

$$\Sigma_2(t) = \int_0^t ds' \int_0^{s'} ds\left(\mathcal{Q}\mathcal{L}(s')Q\mathcal{L}(s)\mathcal{P} - Q\mathcal{L}(s)\mathcal{P}\mathcal{L}(s')\right). \tag{B.67}$$

Substituting this into Eq. (B.54)

$$\mathcal{K}_3(t) = \int_0^t ds' \int_0^{s'} ds \mathcal{P}\mathcal{L}(t) \left(\mathcal{Q}\mathcal{L}(s')Q\mathcal{L}(s)\mathcal{P} - Q\mathcal{L}(s)\mathcal{P}\mathcal{L}(s')\right) \tag{B.68}$$

$$= 0. \tag{B.69}$$

On the last line we replaced $\mathcal{Q} = \mathbb{I} - \mathcal{P}$ in all instances and used 5.1. From what we have derived so far we know that $\Sigma_1(t)\Sigma_2(t) = 0$ (becase $\mathcal{P}\mathcal{Q} = 0$) and the contribution of $\Sigma_1(t)^3$ is null. Thus

$$\mathcal{K}_4(t) = \mathcal{P}\mathcal{L}(t) \left(\Sigma_2(t)\Sigma_1(t) + \Sigma_3(t)\right). \tag{B.70}$$

Lastly we need to find Σ_3 whose calculation is a bit more troublesome and not included here, but yields

$$\Sigma_3 = \int_0^t dt_1 \int_0^{t_1} dt_2 \int_0^{t_2} dt_3 \left(\mathcal{L}(t_1)\mathcal{L}(t_2)\mathcal{L}(t_3) - \mathcal{L}(t_1)\mathcal{P}\mathcal{L}(t_2)\mathcal{L}(t_3) + \mathcal{L}(t_3)\mathcal{P}\mathcal{L}(t_2)\mathcal{L}(t_1)\right) \tag{B.71}$$

Finally, Eq. (B.55) is given by

$$\mathcal{K}_4(t) = \int_0^t dt_1 \int_0^{t_1} dt_2 \int_0^{t_2} dt_3 \left(\mathcal{P}\mathcal{L}(t)\mathcal{L}(t_1)\mathcal{L}(t_2)\mathcal{L}(t_3)\mathcal{P}\right. \tag{B.72}$$

$$- \mathcal{P}\mathcal{L}(t)\mathcal{L}(t_1)\mathcal{P}\mathcal{L}(t_2)\mathcal{L}(t_3)\mathcal{P} - \mathcal{P}\mathcal{L}(t)\mathcal{L}(t_2)\mathcal{P}\mathcal{L}(t_1)\mathcal{L}(t_3)\mathcal{P} \tag{B.73}$$

$$\left. - \mathcal{P}\mathcal{L}(t)\mathcal{L}(t_3)\mathcal{P}\mathcal{L}(t_1)\mathcal{L}(t_2)\mathcal{P}\right). \tag{B.74}$$

The general expression for higher order contributions can be obtained in the same way or by using ordered cumulants [B1, 42]

$$\mathcal{K}_n(t) = \int_0^t dt_1 \int_0^{t_1} dt_2 \cdots \int_0^{t_{n-2}} dt_{n-1} \langle \mathcal{L}(t)\mathcal{L}(t_1)\mathcal{L}(t_2)\ldots\mathcal{L}(t_{n-1})\rangle_{oc}, \tag{B.75}$$

where

$$\langle \mathcal{L}(t)\mathcal{L}(t_1)\mathcal{L}(t_2)\ldots\mathcal{L}(t_{n-1})\rangle_{\text{oc}} = \sum (-1)^q \mathcal{P}\mathcal{L}(t)\ldots\mathcal{L}(t_i)\mathcal{P}\mathcal{L}(t_j)\ldots\mathcal{L}(t_k)\mathcal{P}, \tag{B.76}$$

where *oc* stands for *ordered cumulants*. Here q refers to the number of $\mathcal{P}$ we insert between the first and the last to partition the n elements, in such a way that each partition is time ordered. The sum is over all possible partitions. Luckily if we centralize $\mathcal{P}\mathcal{L}(t)\mathcal{P} = 0$ the number of partitions decreases greatly, basically, boiling down to the different partitions of pairs, similar to the ones we had in 5.5. This formula allows us to obtain higher order terms, or the ones shown here, without going through all the hassle of equating terms of different powers.

Appendix C

Data for the structured Spectral density

The structured spectral density considered corresponds to an experimentally estimated phonon spectral density of the FMO complex. It was taken from [11, 31] . The low-frequency part is modeled by the Adolphs-Renger (AR) spectral density

$$J_{AR}(\omega) = \frac{S}{s_1 + s_2} \sum_{i=1}^{2} \frac{s_i}{7!2\omega_i^4} \omega^5 e^{-(\omega/\omega_i)^{1/2}}, \tag{C.1}$$

where $S = 0.29$, $s_1 = 0.8$, $s_2 = 0.5$, $\omega_1 = 0.069\,\text{meV}$ and $\omega_2 = 0.24\,\text{meV}$. The intra-pigment vibrational modes are modeled

$$J_h(\omega) = \sum_{k=1}^{62} \frac{4\omega_k s_k \gamma_k (\omega_k^2 + \gamma_k^2)\omega}{\pi((\omega + \omega_k)^2 + \gamma_k^2)((\omega - \omega_k)^2 + \gamma_k^2)}, \tag{C.2}$$

where ω_k is the vibrational frequency and s_k the Huang-Rhys factor. whose values are summarized in Table C.1. The parameter γ_k is taken to be $1\,\text{ps}^{-1} \approx 5\,\text{cm}^{-1}$[31]. The total phonon spectral density of the FMO complex is given by $J(\omega) = J_{\text{AR}}(\omega) + J_h(\omega)$.

Table C.1: Vibrational frequencies ω_k and Huang-Rhys factors s_k [11, 31]

k	1	2	3	4	5	6	7	8	9	10
$\omega_k\,[\text{cm}^{-1}]$	46	68	117	167	180	191	202	243	263	284
s_k	0.011	0.011	0.009	0.009	0.010	0.011	0.011	0.012	0.003	0.008
k	11	12	13	14	15	16	17	18	19	20
$\omega_k\,[\text{cm}^{-1}]$	291	327	366	385	404	423	440	481	541	568
s_k	0.008	0.003	0.006	0.002	0.002	0.002	0.001	0.002	0.004	0.007
k	21	22	23	24	25	26	27	28	29	30
$\omega_k\,[\text{cm}^{-1}]$	582	597	630	638	665	684	713	726	731	750
s_k	0.004	0.004	0.003	0.006	0.004	0.003	0.007	0.010	0.005	0.004
k	31	32	33	34	35	36	37	38	39	40
$\omega_k\,[\text{cm}^{-1}]$	761	770	795	821	856	891	900	924	929	946
s_k	0.009	0.018	0.007	0.006	0.007	0.003	0.004	0.001	0.001	0.002
k	41	42	43	44	45	46	47	48	49	50
$\omega_k\,[\text{cm}^{-1}]$	966	984	1004	1037	1058	1094	1104	1123	1130	1162
s_k	0.002	0.003	0.001	0.002	0.002	0.001	0.001	0.003	0.003	0.009
k	51	52	53	54	55	56	57	58	59	60
$\omega_k\,[\text{cm}^{-1}]$	1175	1181	1201	1220	1283	1292	1348	1367	1386	1431
s_k	0.007	0.010	0.003	0.005	0.002	0.004	0.007	0.002	0.004	0.002
k	61	62								
$\omega_k\,[\text{cm}^{-1}]$	1503	1545								
s_k	0.003	0.003								

The spectral density is defined in terms of these factors as

$$J(\omega) = \pi \sum_k \omega_k^2 \frac{s_k}{\pi} \delta(\omega - \omega_k). \tag{C.3}$$

Notice there is a factor π with respect to [11, 31] to agree with the definitions in the Thesis Eq. (1.21). We will rescale the coupling strength to the experimentally measured factors via a constant g (which already includes the factor π)

$$J_{new}(\omega) = g \sum_k \omega_k^2 s_k \delta(\omega - \omega_k) = \sum_k \omega_k^2 s'_k \delta(\omega - \omega_k). \tag{C.4}$$

For the simulations shown we choose $g = \frac{1}{15}$.

Appendix D

Matsubara Expansion

Let us consider the correlation function using an underdamped spectral density, by substitution of Eq. (1.78) into Eq. (1.23) we get

$$C(t) = \frac{1}{\pi}\int_0^\infty d\omega \frac{\alpha^2\Gamma\omega}{[(\omega_c^2-\omega^2)^2+\Gamma^2\omega^2]}\left(\cos(\omega t)\coth\left(\frac{\beta\omega}{2}\right) - i\sin(\omega t)\right) \tag{D.1}$$

We will perform Contour integration here, however notice that there's two contributions to the poles, the poles coming from the spectral density and the poles coming from the temperature (those in the cotangent). We will first deal with the former, which are (in the upper half of the complex plane):

$$\omega_1 = \frac{i\Gamma}{2} + \Omega, \tag{D.2}$$

$$\omega_2 = \frac{i\Gamma}{2} - \Omega, \tag{D.3}$$

where $\Omega = \sqrt{\omega_c - (\frac{\Gamma}{2})^2}$. Using Contour integration over the upper half with a semicircle, with obtain the contribution of these spectral poles to be

$$\begin{aligned}
&\frac{1}{2\Omega}\alpha^2\left(\coth\left(\frac{\beta}{2}\,(\Omega - i\frac{\Gamma}{2})\right)\cos\left(\left(\Omega - \frac{i\Gamma}{2}\right)t\right)\right.\\
&+\coth\left(\frac{\beta}{42}(\Omega + i\frac{\Gamma}{2})\right)\cos\left(\left(\Omega + \frac{i\Gamma}{2}\right)t\right)\\
&\left.+\,i\sin\left(\left(\Omega + \frac{i\Gamma}{2}\right)t\right) + i\sin\left(\left(\Omega - \frac{i\Gamma}{2}\right)t\right)\right).
\end{aligned} \tag{D.4}$$

we can now split this part into a sum of decaying exponentials, taking into account Eq. (7.41), we can write this contribution as

$$C(\tau) = \sum_{k=0}^{\infty} c_k e^{-\nu_k\tau} \tag{D.5}$$

where

$$c_k = \begin{cases} \left(\alpha^2\coth(\beta(\Omega + i\Gamma/2)/2) + i\alpha^2\right)/4\Omega & k = 0, \\ \left(\alpha^2\coth(\beta(\Omega - i\Gamma/2)/2) - i\alpha^2\right)/4\Omega & k = 1, \end{cases} \tag{D.6}$$

$$\nu_k = \begin{cases} -i\Omega + \Gamma/2 & k = 0, \\ i\Omega + \Gamma/2 & k = 1. \end{cases} \tag{D.7}$$

However, to complete the expansion we are missing the poles of the cotangent, which are infinitely many and are known as Matsubara poles [27, 28]. We will consider the series expansion of the cotangent, namely

$$\coth(x) = \sum_{k=-\infty}^{\infty} \frac{x}{(k\pi)^2 + x^2}, \tag{D.8}$$

such that our thermal part gives us the poles (again on the upper half plane)

$$\omega_k = i\frac{2\pi k}{\beta}. \tag{D.9}$$

The contribution of each of these poles to the contour is

$$-\frac{4\pi\alpha^2\beta^2\Gamma k\cosh\left(\frac{2\pi kt}{\beta}\right)}{\left(\beta^2\left(\frac{\Gamma^2}{4}+\Omega^2\right)+4\pi^2k^2\right)^2-4\pi^2\beta^2\Gamma^2k^2} \tag{D.10}$$

$$=-\frac{4\pi\alpha^2\beta^2\Gamma k\cosh\left(\frac{2\pi kt}{\beta}\right)}{\beta^4[(\Omega+i\Gamma/2)^2+(\frac{2\pi k}{\beta})^2)][(\Omega-i\Gamma/2)^2+(\frac{2\pi k}{\beta})^2]}, \tag{D.11}$$

which can be rewritten as

$$c_k = \frac{-4\alpha^2\Gamma\pi k}{\beta^2[(\Omega+i\Gamma/2)^2+(\frac{2\pi k}{\beta})^2)][(\Omega-i\Gamma/2)^2+(\frac{2\pi k}{\beta})^2]}. \tag{D.12}$$

$$\nu_k = \frac{2\pi k}{\beta}. \tag{D.13}$$

The Padé expansion works similarly, but we integrate over the poles of the Padé approximation of the Bose-Einstein distribution instead of the Matsubara poles.

Appendix E

Software and Hardware used for the simulations

For the simulation of GKLS master equations and HEOM the optimizations performed for this methods see [A1, 20]. The versions and configuration of the software used was

- **QuTiP Version:** 5.0.4
- **Numpy Version:** 2.1.1
- **Scipy Version:** 1.14.1
- **Cython Version:** None
- **Python Version:** 3.12.6
- **Number of CPUs:** 16
- **BLAS Info:** openblas64

For the simulation of Redfield and cumulant we used [124] which we built on top of QuTiP. For the simulations here we used the QuTiP backend in [124] no optimizations were used, even though the usage of GPU (via the jax backend or qutip-jax), just in time compilation and parallelization is available for the cumulant equation, we did not use the optimizations available because we did not produce equivalent code for the Redfield equation. Which was at a disadvantage with respect to GKLS and HEOM as QuTiP's internal ODE routines are faster than the one we used for Redfield. Both equations would benefit greatly from caching which will be available in future versions of [124]

Simulations were run on the Windows subsystem for linux a lenovo Thinkpad X1 with the following specifications

- **Processor:** 12th Gen Intel(R) Core(TM) i7-1260PR
- **RAM:** 16GB
- **RAM accessible by WSL:** 11GB

References

Articles by the author

A1 Neill Lambert, Eric Giguère, Paul Menczel, Boxi Li, Patrick Hopf, **Gerardo Suárez**, Marc Gali, Jake Lishman, Rushiraj Gadhvi, Rochisha Agarwal, Asier Galicia, Nathan Shammah, Paul Nation, J.R. Johansson, Shahnawaz Ahmed, Simon Cross, Alexander Pitchford, and Franco Nori. "QuTiP 5: The Quantum Toolbox in Python". In: *Physics Reports* 1153 (2026), pp. 1–62. ISSN: 0370-1573. DOI: https://doi.org/10.1016/j.physrep.2025.10.001.

A2 Marcin Łobejko, Marek Winczewski, **Suárez, Gerardo**, Robert Alicki, and Michał Horodecki. "Corrections to the Hamiltonian induced by finite-strength coupling to the environment". In: *Phys. Rev. E* 110 (1 2024), p. 014144. DOI: 10.1103/PhysRevE.110.014144.

A3 **Suárez, Gerardo**, Marcin Łobejko, and Michał Horodecki. "Dynamics of the nonequilibrium spin-boson model: A benchmark of master equations and their validity". In: *Phys. Rev. A* 110 (4 2024), p. 042428. DOI: 10.1103/PhysRevA.110.042428.

A4 Marek Winczewski, Antonio Mandarino, **Suárez, Gerardo**, Robert Alicki, and Michał Horodecki. "Intermediate-times dilemma for open quantum system: Filtered approximation to the refined weak-coupling limit". In: *Phys. Rev. E* 110 (2 2024), p. 024110. DOI: 10.1103/PhysRevE.110.024110.

A5 Robert Alicki, Michał Horodecki, Alejandro Jenkins, Marcin Łobejko, and **Suárez, Gerardo**. "The Josephson junction as a quantum engine". en. In: *New J. Phys.* 25.11 (2023). Publisher: IOP Publishing, p. 113013. ISSN: 1367-2630. DOI: 10.1088/1367-2630/ad06d8.

A6 R. R. Rodríguez, B. Ahmadi, **Suárez, G.**, P. Mazurek, S. Barzanjeh, and P. Horodecki. "Optimal quantum control of charging quantum batteries". en. In: *New J. Phys.* 26.4 (2024). Publisher: IOP Publishing, p. 043004. ISSN: 1367-2630. DOI: 10.1088/1367-2630/ad3843.

Books

B1 Heinz-Peter Breuer and Francesco Petruccione. *The Theory of Open Quantum Systems*. eng. Oxford: Oxford University Press, 2007. ISBN: 978-0-19-921390-0. DOI: 10.1093/acprof:oso/9780199213900.001.0001.

B2 Ulrich Weiss. *Quantum Dissipative Systems*. 2nd. World Scientific, 1999.

B3 Ángel Rivas and Susana F. Huelga. *Open Quantum Systems: An Introduction*. SpringerBriefs in Physics. Springer Berlin Heidelberg, 2011. ISBN: 978-3-642-23353-1.

B4 Barandiarán, Zoila and Joos, Jonas and Seijo, Luis. *Luminescent materials : a quantum chemical approach for computer-aided discovery and design*. eng. Vol. 322. Springer, 2022, p. 372. ISBN: 9783030949839.

B5 James Stewart. *Calculus*. 8th. Cengage Learning, 2016.

B6 H. J. Carmichael. *Statistical Methods in Quantum Optics 1: Master Equations and Fokker-Planck Equations*. Springer-Verlag, Berlin, 1999.

B7 H. J. Carmichael. *An open systems approach to quantum optics*. Berlin Heidelberg: Springer-Verlag, 1993.

B8 Michael Edward Peskin and Daniel V. Schroeder. *An Introduction to Quantum Field Theory*. Reading, USA: Addison-Wesley (1995) 842 p. Westview Press, 1995.

B9 Ulrich Weiss. *Quantum Dissipative Systems*. 4th ed. WORLD SCIENTIFIC, 2012. ISBN: 978-981-4374-91-0 978-981-4374-92-7. DOI: 10.1142/8334.

B10 David W. Kammler. *A First Course in Fourier Analysis*. 2nd ed. Cambridge University Press, 2008. ISBN: 978-0521709798. DOI: 10.1017/CBO9781139185596.

B11 Tom Rother. *Green's Functions in Classical Physics*. en. Lecture Notes in Physics. Springer International Publishing, 2017. ISBN: 978-3-319-52436-8. DOI: 10.1007/978-3-319-52437-5.

Articles, proceedings and theses

1 **Suárez, Gerardo** and Michał Horodecki. *Making Non-Markovian master equations accessible with approximate environments*. 2025.

2 Tatsushi Ikeda and Gregory D. Scholes. "Generalization of the hierarchical equations of motion theory for efficient calculations with arbitrary correlation functions". In: *The Journal of Chemical Physics* 152.20 (2020), p. 204101. ISSN: 0021-9606. DOI: 10.1063/5.0007327.

3 Hasan Rahman and Ulrich Kleinekathöfer. "Chebyshev hierarchical equations of motion for systems with arbitrary spectral densities and temperatures". In: *The Journal of Chemical Physics* 150.24 (2019), p. 244104. ISSN: 0021-9606. DOI: 10.1063/1.5100102.

4 Paul Menczel, Ken Funo, Mauro Cirio, Neill Lambert, and Franco Nori. *Non-Hermitian Pseudomodes for Strongly Coupled Open Quantum Systems: Unravelings, Correlations and Thermodynamics*. arXiv:2401.11830 [cond-mat, physics:quant-ph]. 2024. DOI: 10.48550/arXiv.2401.11830.

5 A. O. Caldeira and A. J. Leggett. "Path integral approach to quantum Brownian motion". In: *Physica A: Statistical Mechanics and its Applications* 121.3 (1983), pp. 587–616. ISSN: 0378-4371. DOI: https://doi.org/10.1016/0378-4371(83)90013-4.

6 A. J. Leggett, S. Chakravarty, A. T. Dorsey, Matthew P. A. Fisher, Anupam Garg, and W. Zwerger. "Dynamics of the dissipative two-state system". In: *Rev. Mod. Phys.* 59 (1 1987), pp. 1–85. DOI: 10.1103/RevModPhys.59.1.

7 Ángel Rivas, A. Douglas K. Plato, Susana F. Huelga, and Martin B. Plenio. "Markovian Master Equations: A Critical Study". In: *New J. Phys.* 12.11 (2010). arXiv: 1006.4666, p. 113032. ISSN: 1367-2630. DOI: 10.1088/1367-2630/12/11/113032.

8 Po-Chen Kuo, Neill Lambert, Mauro Cirio, Yi-Te Huang, Franco Nori, and Yueh-Nan Chen. *Kondo QED: The Kondo effect and photon trapping in a two-impurity Anderson model ultra-strongly coupled to light*. arXiv:2302.01044 [cond-mat, physics:quant-ph]. 2023.

9 Ahsan Nazir and Gernot Schaller. "The Reaction Coordinate Mapping in Quantum Thermodynamics". In: *Thermodynamics in the Quantum Regime*. Springer International Publishing, 2018, pp. 551–577. ISBN: 9783319990460. DOI: 10.1007/978-3-319-99046-0_23.

10 Nicholas Anto-Sztrikacs, Felix Ivander, and Dvira Segal. "Quantum thermal transport beyond second order with the reaction coordinate mapping". In: *The Journal of Chemical Physics* 156.21 (2022), p. 214107. ISSN: 0021-9606. DOI: 10.1063/5.0091133.

11 Margus Rätsep and Arvi Freiberg. "Electron–phonon and vibronic couplings in the FMO bacteriochlorophyll a antenna complex studied by difference fluorescence line narrowing". In: *Journal of Luminescence* 127.1 (2007). Proceedings of the Ninth International Meeting on Hole Burning, Single Molecule, and Related Spectroscopies: Science and Applications, pp. 251–259. ISSN: 0022-2313. DOI: https://doi.org/10.1016/j.jlumin.2007.02.053.

12 Neill Lambert, Shahnawaz Ahmed, Mauro Cirio, and Franco Nori. "Modelling the ultra-strongly coupled spin-boson model with unphysical modes". en. In: *Nat Commun* 10.1 (2019). Publisher: Nature Publishing Group, p. 3721. ISSN: 2041-1723. DOI: 10.1038/s41467-019-11656-1.

13 Neill Lambert, Mauro Cirio, Jhen-dong Lin, Paul Menczel, Pengfei Liang, and Franco Nori. *Fixing detailed balance in ancilla-based dissipative state engineering.* arXiv:2310.12539 [quant-ph]. 2023.

14 Mauro Cirio, Po-Chen Kuo, Yueh-Nan Chen, Franco Nori, and Neill Lambert. "Canonical derivation of the Fermionic influence superoperator". en. In: *Phys. Rev. B* 105.3 (2022), p. 035121. ISSN: 2469-9950, 2469-9969. DOI: 10.1103/PhysRevB.105.035121.

15 Meng Xu, Yaming Yan, Qiang Shi, J. Ankerhold, and J. T. Stockburger. "Taming Quantum Noise for Efficient Low Temperature Simulations of Open Quantum Systems". en. In: *Phys. Rev. Lett.* 129.23 (2022), p. 230601. ISSN: 0031-9007, 1079-7114. DOI: 10.1103/PhysRevLett.129.230601.

16 Hideaki Takahashi, Samuel Rudge, Christoph Kaspar, Michael Thoss, and Raffaele Borrelli. "High accuracy exponential decomposition of bath correlation functions for arbitrary and structured spectral densities: Emerging methodologies and new approaches". In: *The Journal of Chemical Physics* 160.20 (2024), p. 204105. ISSN: 0021-9606. DOI: 10.1063/5.0209348.

17 Daniel Boyanovsky and David Jasnow. "Heisenberg-Langevin versus quantum master equation". In: *Physical Review A* 96.6 (2017). DOI: 10.1103/physreva.96.062108.

18 Elyana Crowder, Lance Lampert, Grihith Manchanda, Brian Shoffeitt, Srikar Gadamsetty, Yiting Pei, Shantanu Chaudhary, and Dragomir Davidović. "Invalidation of the Bloch-Redfield equation in the sub-Ohmic regime via a practical time-convolutionless fourth-order master equation". In: *Physical Review A* 109.5 (2024). ISSN: 2469-9934. DOI: 10.1103/physreva.109.052205.

19 Andrea Smirne and Bassano Vacchini. "Nakajima-Zwanzig versus time-convolutionless master equation for the non-Markovian dynamics of a two-level system". In: *Phys. Rev. A* 82 (2 2010), p. 022110. DOI: 10.1103/PhysRevA.82.022110.

20 Neill Lambert, Tarun Raheja, Simon Cross, Paul Menczel, Shahnawaz Ahmed, Alexander Pitchford, Daniel Burgarth, and Franco Nori. "QuTiP-BoFiN: A Bosonic and Fermionic numerical hierarchical-equations-of-motion library with applications in light-harvesting, quantum control, and single-molecule electronics". In: *Phys. Rev. Res.* 5 (1 2023), p. 013181. DOI: 10.1103/PhysRevResearch.5.013181.

21 Yoshitaka Tanimura. "Numerically "exact" approach to open quantum dynamics: The hierarchical equations of motion (HEOM)". In: *The Journal of Chemical Physics* 153.2 (2020), p. 020901. ISSN: 0021-9606. DOI: 10.1063/5.0011599.

22 *Time Evolution of a Quantum System in Contact with a Nearly Gaussian-Markoffian Noise Bath.* en. DOI: 10.1143/JPSJ.58.101.

23 B. M. Garraway. "Decay of an atom coupled strongly to a reservoir". In: *Phys. Rev. A* 55 (6 1997), pp. 4636–4639. DOI: 10.1103/PhysRevA.55.4636.

24 Jian Ma, Zhe Sun, Xiaoguang Wang, and Franco Nori. "Entanglement dynamics of two qubits in a common bath". In: *Phys. Rev. A* 85 (6 2012), p. 062323. DOI: 10.1103/PhysRevA.85.062323.

25 Alejandro D. Somoza, Oliver Marty, James Lim, Susana F. Huelga, and Martin B. Plenio. "Dissipation-Assisted Matrix Product Factorization". In: *Phys. Rev. Lett.* 123 (10 2019), p. 100502. DOI: 10.1103/PhysRevLett.123.100502.

26 Robert Rosenbach, Javier Cerrillo, Susana F Huelga, Jianshu Cao, and Martin B Plenio. "Efficient simulation of non-Markovian system-environment interaction". In: *New Journal of Physics* 18.2 (2016), p. 023035. ISSN: 1367-2630. DOI: 10.1088/1367-2630/18/2/023035.

27 Munshi G. Mustafa. "An introduction to thermal field theory and some of its application". In: *The European Physical Journal Special Topics* 232.9 (2023), pp. 1369–1457. ISSN: 1951-6401. DOI: 10.1140/epjs/s11734-023-00868-8.

28 Alberto Salvio. "Introduction to Thermal Field Theory: From First Principles to Applications". In: *Universe* 11.1 (2025), p. 16. ISSN: 2218-1997. DOI: 10.3390/universe11010016.

29 Akihito Ishizaki. "Prerequisites for Relevant Spectral Density and Convergence of Reduced Density Matrices at Low Temperatures". In: *Journal of the Physical Society of Japan* 89.1 (2020), p. 015001. ISSN: 1347-4073. DOI: 10.7566/jpsj.89.015001.

30 Zi-Hao Chen, Yao Wang, Xiao Zheng, Rui-Xue Xu, and YiJing Yan. "Universal time-domain Prony fitting decomposition for optimized hierarchical quantum master equations". In: *The Journal of Chemical Physics* 156.22 (2022). ISSN: 1089-7690. DOI: 10.1063/5.0095961.

31 Nicola Lorenzoni, Namgee Cho, James Lim, Dario Tamascelli, Susana F. Huelga, and Martin B. Plenio. "Systematic Coarse Graining of Environments for the Nonperturbative Simulation of Open Quantum Systems". In: *Phys. Rev. Lett.* 132 (10 2024), p. 100403. DOI: 10.1103/PhysRevLett.132.100403.

32 Pauli Virtanen, Ralf Gommers, Travis E. Oliphant, Matt Haberland, Tyler Reddy, David Cournapeau, Evgeni Burovski, Pearu Peterson, Warren Weckesser, Jonathan Bright, Stéfan J. van der Walt, Matthew Brett, Joshua Wilson, K. Jarrod Millman, Nikolay Mayorov, Andrew R. J. Nelson, Eric Jones, Robert Kern, Eric Larson, C J Carey, İlhan Polat, Yu Feng, Eric W. Moore, Jake VanderPlas, Denis Laxalde, Josef Perktold, Robert Cimrman, Ian Henriksen, E. A. Quintero, Charles R. Harris, Anne M. Archibald, Antônio H. Ribeiro, Fabian Pedregosa, Paul van Mulbregt, and SciPy 1.0 Contributors. "SciPy 1.0: Fundamental Algorithms for Scientific Computing in Python". In: *Nature Methods* 17 (2020), pp. 261–272. DOI: 10.1038/s41592-019-0686-2.

33 Christoph Meier and David J. Tannor. "Non-Markovian evolution of the density operator in the presence of strong laser fields". In: *The Journal of Chemical Physics* 111.8 (1999), pp. 3365–3376. ISSN: 0021-9606. DOI: 10.1063/1.479669.

34 Zhoufei Tang, Xiaolong Ouyang, Zhihao Gong, Haobin Wang, and Jianlan Wu. "Extended hierarchy equation of motion for the spin-boson model". In: *The Journal of Chemical Physics* 143.22 (2015), p. 224112. ISSN: 0021-9606. DOI: 10.1063/1.4936924.

35 Yuji Nakatsukasa, Olivier Sète, and Lloyd N. Trefethen. "The AAA algorithm for rational approximation". In: *SIAM J. Sci. Comput.* 40.3 (2018). arXiv:1612.00337 [math], A1494–A1522. ISSN: 1064-8275, 1095-7197. DOI: 10.1137/16M1106122.

36 Xiaohan Dan, Meng Xu, J. T. Stockburger, J. Ankerhold, and Qiang Shi. "Efficient low-temperature simulations for Fermionic reservoirs with the hierarchical equations of motion method: Application to the Anderson impurity model". In: *Phys. Rev. B* 107 (19 2023), p. 195429. DOI: 10.1103/PhysRevB.107.195429.

37 Nadiia Derevianko, Gerlind Plonka, and Markus Petz. "From ESPRIT to ESPIRA: estimation of signal parameters by iterative rational approximation". In: *IMA Journal of Numerical Analysis* 43.2 (2022), pp. 789–827. ISSN: 0272-4979. DOI: 10.1093/imanum/drab108.

38 L. S. Schulman. "Note on the quantum recurrence theorem". In: *Phys. Rev. A* 18 (5 1978), pp. 2379–2380. DOI: 10.1103/PhysRevA.18.2379.

39 P. Bocchieri and A. Loinger. "Quantum Recurrence Theorem". In: *Phys. Rev.* 107 (2 1957), pp. 337–338. DOI: 10.1103/PhysRev.107.337.

40 Akihito Ishizaki and Graham R. Fleming. "Unified treatment of quantum coherent and incoherent hopping dynamics in electronic energy transfer: Reduced hierarchy equation approach". en. In: *The Journal of Chemical Physics* 130.23 (2009), p. 234111. ISSN: 0021-9606, 1089-7690. DOI: 10.1063/1.3155372.

41 Ryogo Kubo. "Generalized Cumulant Expansion Method". In: *Journal of the Physical Society of Japan* 17.7 (1962), pp. 1100–1120. DOI: 10.1143/JPSJ.17.1100.

42 N.G. Van Kampen. "A cumulant expansion for stochastic linear differential equations. II". In: *Physica* 74.2 (1974), pp. 239–247. ISSN: 0031-8914. DOI: https://doi.org/10.1016/0031-8914(74)90122-0.

43 Richard Hartmann and Walter T. Strunz. "Accuracy Assessment of Perturbative Master Equations – Embracing Non-Positivity". In: *Physical Review A* 101.1 (2020). arXiv:1906.02583 [quant-ph], p. 012103. ISSN: 2469-9926, 2469-9934. DOI: 10.1103/PhysRevA.101.012103.

44 Meng Xu and Joachim Ankerhold. *About the performance of perturbative treatments of the spin-boson dynamics within the hierarchical equations of motion approach*. 2023.

45 Meng Xu, J. T. Stockburger, and J. Ankerhold. "Heat transport through a superconducting artificial atom". In: *Phys. Rev. B* 103 (10 2021), p. 104304. DOI: 10.1103/PhysRevB.103.104304.

46 Giacomo Guarnieri, Michal Kolá ř, and Radim Filip. "Steady-State Coherences by Composite System-Bath Interactions". In: *Phys. Rev. Lett.* 121 (7 2018), p. 070401. DOI: 10.1103/PhysRevLett.121.070401.

47 Archak Purkayastha, Giacomo Guarnieri, Mark T. Mitchison, Radim Filip, and John Goold. "Tunable phonon-induced steady-state coherence in a double-quantum-dot charge qubit". In: *npj Quantum Information* 6.1 (2020), p. 27. ISSN: 2056-6387. DOI: 10.1038/s41534-020-0256-6.

48 Konstantin P. Lovetskiy, Leonid A. Sevastianov, Michal Hnatič, and Dmitry S. Kulyabov. "Numerical Integration of Highly Oscillatory Functions with and without Stationary Points". In: *Mathematics* 12.2 (2024). ISSN: 2227-7390. DOI: 10.3390/math12020307.

49 David Levin. "Fast integration of rapidly oscillatory functions". In: *Journal of Computational and Applied Mathematics* 67.1 (1996), pp. 95–101. ISSN: 0377-0427. DOI: https://doi.org/10.1016/0377-0427(94)00118-9.

50 Gunhee Park, Zhen Huang, Yuanran Zhu, Chao Yang, Garnet Kin-Lic Chan, and Lin Lin. "Quasi-Lindblad pseudomode theory for open quantum systems". In: *Physical Review B* 110.19 (2024). ISSN: 2469-9969. DOI: 10.1103/physrevb.110.195148.

51 Daniel A. Lidar. *Lecture Notes on the Theory of Open Quantum Systems*. arXiv:1902.00967 [quant-ph]. 2020. DOI: 10.48550/arXiv.1902.00967.

52 Jan Jeske, David Ing, Martin B. Plenio, Susana F. Huelga, and Jared H. Cole. "Bloch-Redfield equations for modeling light-harvesting complexes". In: *The Journal of Chemical Physics* 142.6 (2015). arXiv:1408.2726 [physics, physics:quant-ph], p. 064104. ISSN: 0021-9606, 1089-7690. DOI: 10.1063/1.4907370.

53 W. Thomas Pollard and Richard A. Friesner. "Solution of the Redfield equation for the dissipative quantum dynamics of multilevel systems". In: *The Journal of Chemical Physics* 100.7 (1994), pp. 5054–5065. ISSN: 0021-9606. DOI: 10.1063/1.467222.

54 Robert Alicki. "Master equations for a damped nonlinear oscillator and the validity of the Markovian approximation". en. In: *Phys. Rev. A* 40.7 (1989), pp. 4077–4081. ISSN: 0556-2791. DOI: 10.1103/PhysRevA.40.4077.

55 Ángel Rivas. "Refined Weak Coupling Limit: Coherence, Entanglement and Non-Markovianity". In: *Phys. Rev. A* 95.4 (2017). arXiv: 1611.01483, p. 042104. ISSN: 2469-9926, 2469-9934. DOI: 10.1103/PhysRevA.95.042104.

56 Christian Majenz, Tameem Albash, Heinz-Peter Breuer, and Daniel A. Lidar. "Coarse graining can beat the rotating-wave approximation in quantum Markovian master equations". In: *Phys. Rev. A* 88.1 (2013). Publisher: American Physical Society, p. 012103. DOI: 10.1103/PhysRevA.88.012103.

57 Evgeny Mozgunov and Daniel Lidar. "Completely positive master equation for arbitrary driving and small level spacing". In: *Quantum* 4 (2020), p. 227. ISSN: 2521-327X. DOI: 10.22331/q-2020-02-06-227.

58 Zihan Xia, Juan Garcia-Nila, and Daniel Lidar. *Markovian and non-Markovian master equations versus an exactly solvable model of a qubit in a cavity*. 2024.

59 Gernot Schaller and Tobias Brandes. "Preservation of positivity by dynamical coarse graining". en. In: *Physical Review A* 78.2 (2008), p. 022106. ISSN: 1050-2947, 1094-1622. DOI: 10.1103/PhysRevA.78.022106.

60 Marco Bianucci and Mauro Bologna. "About the foundation of the Kubo generalized cumulants theory: a revisited and corrected approach". In: *Journal of Statistical Mechanics: Theory and Experiment* 2020.4 (2020), p. 043405. DOI: 10.1088/1742-5468/ab7755.

61 S. Blanes, F. Casas, J.A. Oteo, and J. Ros. "The Magnus expansion and some of its applications". In: *Physics Reports* 470.5–6 (2009), pp. 151–238. ISSN: 0370-1573. DOI: 10.1016/j.physrep.2008.11.001.

62 Kurusch Ebrahimi-Fard, Igor Mencattini, and Alexandre Quesney. "What is the Magnus expansion?" In: *Journal of Computational Dynamics* 12.1 (2025), pp. 115–159. ISSN: 2158-2505. DOI: 10.3934/jcd.2024028.

63 Roland Doll, David Zueco, Martijn Wubs, Sigmund Kohler, and Peter Hänggi. "On the conundrum of deriving exact solutions from approximate master equations". In: *Chemical Physics* 347.1–3 (2008), pp. 243–249. ISSN: 0301-0104. DOI: 10.1016/j.chemphys.2007.09.003.

64 Ángel Rivas. "Quantum Thermodynamics in the Refined Weak Coupling Limit". In: *Entropy* 21.8 (2019), p. 725. ISSN: 1099-4300. DOI: 10.3390/e21080725.

65 Ángel Rivas. "Refined weak-coupling limit: Coherence, entanglement, and non-Markovianity". In: *Physical Review A* 95.4 (2017). ISSN: 2469-9934. DOI: 10.1103/physreva.95.042104.

66 Valery Serov. "Tempered Distributions". In: *Fourier Series, Fourier Transform and Their Applications to Mathematical Physics*. Cham: Springer International Publishing, 2017, pp. 153–165. ISBN: 978-3-319-65262-7. DOI: 10.1007/978-3-319-65262-7_18.

67 Paweł Keller and Iwona Wróbel. "Computing Cauchy principal value integrals using a standard adaptive quadrature". In: *Journal of Computational and Applied Mathematics* 294 (2016), pp. 323–341. ISSN: 0377-0427. DOI: https://doi.org/10.1016/j.cam.2015.08.021.

68 Jin Li and Yongling Cheng. "Extrapolation Algorithm for Computing Multiple Cauchy Principal Value Integrals". In: *Mathematical Problems in Engineering* 2020.1 (2020), p. 6340231. DOI: https://doi.org/10.1155/2020/6340231.

69 Akihito Kato and Yoshitaka Tanimura. "Hierarchical Equations of Motion Approach to Quantum Thermodynamics". In: *Thermodynamics in the Quantum Regime*. Springer International Publishing, 2018, pp. 579–595. ISBN: 9783319990460. DOI: 10.1007/978-3-319-99046-0_24.

70 D. Tamascelli, A. Smirne, S. F. Huelga, and M. B. Plenio. "Nonperturbative Treatment of non-Markovian Dynamics of Open Quantum Systems". In: *Physical Review Letters* 120.3 (2018). ISSN: 1079-7114. DOI: 10.1103/physrevlett.120.030402.

71 Xiang Li, Su-Xiang Lyu, Yao Wang, Rui-Xue Xu, Xiao Zheng, and YiJing Yan. "Toward quantum simulation of non-Markovian open quantum dynamics: A universal and compact theory". In: *Physical Review A* 110.3 (2024). ISSN: 2469-9934. DOI: 10.1103/physreva.110.032620.

72 Artur M. Lacerda, Michael J. Kewming, Marlon Brenes, Conor Jackson, Stephen R. Clark, Mark T. Mitchison, and John Goold. "Entropy production in the mesoscopic-leads formulation of quantum thermodynamics". In: *Physical Review E* 110.1 (2024). ISSN: 2470-0053. DOI: 10.1103/physreve.110.014125.

73 Meng Xu, Vasilii Vadimov, Malte Krug, J. T. Stockburger, and J. Ankerhold. *A Universal Framework for Quantum Dissipation:Minimally Extended State Space and Exact Time-Local Dynamics*. 2023.

74 Mauro Cirio, Neill Lambert, Pengfei Liang, Po-Chen Kuo, Yueh-Nan Chen, Paul Menczel, Ken Funo, and Franco Nori. "Pseudofermion method for the exact description of Fermionic environments: From single-molecule electronics to the Kondo resonance". In: *Phys. Rev. Res.* 5 (3 2023), p. 033011. DOI: 10.1103/PhysRevResearch.5.033011.

75 Maksim Lednev, Francisco J. García-Vidal, and Johannes Feist. "Lindblad Master Equation Capable of Describing Hybrid Quantum Systems in the Ultrastrong Coupling Regime". In: *Phys. Rev. Lett.* 132 (10 2024), p. 106902. DOI: 10.1103/PhysRevLett.132.106902.

76 Richard Hartmann and Walter T. Strunz. "Exact Open Quantum System Dynamics Using the Hierarchy of Pure States (HOPS)". In: *Journal of Chemical Theory and Computation* 13.12 (2017), pp. 5834–5845. ISSN: 1549-9626. DOI: 10.1021/acs.jctc.7b00751.

77 Nicholas Anto-Sztrikacs, Ahsan Nazir, and Dvira Segal. "Effective-Hamiltonian Theory of Open Quantum Systems at Strong Coupling". en. In: *PRX Quantum* 4.2 (2023), p. 020307. ISSN: 2691-3399. DOI: 10.1103/PRXQuantum.4.020307.

78 Philipp Strasberg, Gernot Schaller, Neill Lambert, and Tobias Brandes. "Nonequilibrium thermodynamics in the strong coupling and non-Markovian regime based on a reaction coordinate mapping". In: *New Journal of Physics* 18.7 (2016), p. 073007. ISSN: 1367-2630. DOI: 10.1088/1367-2630/18/7/073007.

79 R. Martinazzo, B. Vacchini, K. H. Hughes, and I. Burghardt. "Communication: Universal Markovian reduction of Brownian particle dynamics". en. In: *The Journal of Chemical Physics* 134.1 (2011), p. 011101. ISSN: 0021-9606, 1089-7690. DOI: 10.1063/1.3532408.

80 Jonas Glatthard, Guillem Aznar-Menargues, José P. Palao, Daniel Alonso, and Luis A. Correa. *Accurate heat currents via reorganised master equation*. 2025.

81 Camille L. Latune. "Steady state in strong system-bath coupling regime: Reaction coordinate versus perturbative expansion". In: *Phys. Rev. E* 105 (2 2022), p. 024126. DOI: 10.1103/PhysRevE.105.024126.

82 Yoshitaka Tanimura and Ryogo Kubo. "Time Evolution of a Quantum System in Contact with a Nearly Gaussian-Markoffian Noise Bath". In: *Journal of the Physical Society of Japan* 58.1 (1989), pp. 101–114. DOI: 10.1143/jpsj.58.101.

83 R Alicki. "The quantum open system as a model of the heat engine". In: *Journal of Physics A: Mathematical and General* 12.5 (1979), p. L103. DOI: 10.1088/0305-4470/12/5/007.

84 Robert Alicki and Ronnie Kosloff. "Introduction to Quantum Thermodynamics: History and Prospects". In: *Thermodynamics in the Quantum Regime: Fundamental Aspects and New Directions*. Ed. by Felix Binder, Luis A. Correa, Christian Gogolin, Janet Anders, and Gerardo Adesso. Cham: Springer International Publishing, 2018, pp. 1–33. ISBN: 978-3-319-99046-0. DOI: 10.1007/978-3-319-99046-0_1.

85 R. E. Wengert. "A simple automatic derivative evaluation program". In: *Commun. ACM* 7.8 (1964), pp. 463–464. ISSN: 0001-0782. DOI: 10.1145/355586.364791.

86 Charles C. Margossian. "A review of automatic differentiation and its efficient implementation". In: *WIREs Data Mining and Knowledge Discovery* 9.4 (2019), e1305. DOI: https://doi.org/10.1002/widm.1305.

87 Sergei Izvekov. "Mori-Zwanzig projection operator formalism: Generalized Langevin equation dynamics of a classical system perturbed by an external generalized potential and far from equilibrium". In: *Phys. Rev. E* 111 (3 2025), p. 034130. DOI: 10.1103/PhysRevE.111.034130.

88 Michael te Vrugt and Raphael Wittkowski. "Projection operators in statistical mechanics: a pedagogical approach". In: *European Journal of Physics* 41.4 (2020), p. 045101. DOI: 10.1088/1361-6404/ab8e28.

89 Lance Lampert, Srikar Gadamsetty, Shantanu Chaudhary, Yiting Pei, Jiahao Chen, Elyana Crowder, and Dragomir Davidović. *TCL6 and Beyond: Late-Time Resummations, Asymptotic Inflation and Time Limit*. 2025.

90 Jiahao Chen, Elyana Crowder, Lian Xiang, and Dragomir Davidovic. *Benchmarking TCL4: Assessing the Usability and Reliability of Fourth-Order Approximations*. 2025.

91 A. S. Trushechkin, M. Merkli, J. D. Cresser, and J. Anders. "Open quantum system dynamics and the mean force Gibbs state". In: *AVS Quantum Science* 4.1 (2022). DOI: 10.1116/5.0073853.

92 Takashi Mori and Seiji Miyashita. "Dynamics of the Density Matrix in Contact with a Thermal Bath and the Quantum Master Equation". In: *Journal of the Physical Society of Japan* 77.12 (2008), p. 124005. ISSN: 1347-4073. DOI: 10.1143/jpsj.77.124005.

93 Mingjie Xin, Wui Seng Leong, Zilong Chen, Yu Wang, and Shau-Yu Lan. "Rapid Quantum Squeezing by Jumping the Harmonic Oscillator Frequency". In: *Phys. Rev. Lett.* 127 (18 2021), p. 183602. DOI: 10.1103/PhysRevLett.127.183602.

94 Devashish Tupkary, Abhishek Dhar, Manas Kulkarni, and Archak Purkayastha. "Fundamental limitations in Lindblad descriptions of systems weakly coupled to baths". In: *Physical Review A* 105.3 (2022). ISSN: 2469-9934. DOI: 10.1103/physreva.105.032208.

95 J. D. Cresser and J. Anders. "Weak and Ultrastrong Coupling Limits of the Quantum Mean Force Gibbs State". In: *Phys. Rev. Lett.* 127 (25 2021), p. 250601. DOI: 10.1103/PhysRevLett.127.250601.

96 F Cerisola, M Berritta, S Scali, S A R Horsley, J D Cresser, and J Anders. "Quantum–classical correspondence in spin–boson equilibrium states at arbitrary coupling". In: *New Journal of Physics* 26.5 (2024), p. 053032. DOI: 10.1088/1367-2630/ad4818.

97 Marek Winczewski and Robert Alicki. "Renormalization in the theory of open quantum systems via the self-consistency condition". In: (2021).

98 Dazhi Xu and Jianshu Cao. "Non-canonical distribution and non-equilibrium transport beyond weak system-bath coupling regime: A polaron transformation approach". en. In: *Frontiers of Physics* 11.4 (2016), p. 110308. ISSN: 2095-0470. DOI: 10.1007/s11467-016-0540-2.

99 B. M. Garraway. "Nonperturbative decay of an atomic system in a cavity". In: *Phys. Rev. A* 55 (3 1997), pp. 2290–2303. DOI: 10.1103/PhysRevA.55.2290.

100 P.N. Vabishchevich. "Numerical solution of the Cauchy problem for Volterra integrodifferential equations with difference kernels". In: *Applied Numerical Mathematics* 174 (2022), pp. 177–190. ISSN: 0168-9274. DOI: https://doi.org/10.1016/j.apnum.2022.01.013.

101 Zixuan Gao, Jiuyang Liang, and Zhenli Xu. "A Kernel-Independent Sum-of-Exponentials Method". In: *Journal of Scientific Computing* 93.2 (2022), p. 40. ISSN: 1573-7691. DOI: 10.1007/s10915-022-01999-1.

102 S. Wenderoth, H.-P. Breuer, and M. Thoss. "Non-Markovian effects in the spin-boson model at zero temperature". en. In: *Physical Review A* 104.1 (2021), p. 012213.

103 Zach Blunden-Codd, Soumya Bera, Benedikt Bruognolo, Nils-Oliver Linden, Alex W. Chin, Jan von Delft, Ahsan Nazir, and Serge Florens. "Anatomy of quantum critical wave functions in dissipative impurity problems". In: *Phys. Rev. B* 95 (8 2017), p. 085104. DOI: 10.1103/PhysRevB.95.085104.

104 Yan-Zhi Wang, Shu He, Liwei Duan, and Qing-Hu Chen. "Quantum phase transitions in the spin-boson model without the counterrotating terms". In: *Physical Review B* 100.11 (2019). ISSN: 2469-9969. DOI: 10.1103/physrevb.100.115106.

105 Dariusz Chru ści ński, Andrzej Kossakowski, and Ángel Rivas. "Measures of non-Markovianity: Divisibility versus backflow of information". In: *Phys. Rev. A* 83 (5 2011), p. 052128. DOI: 10.1103/PhysRevA.83.052128.

106 Alberto Rolandi and Martí Perarnau-Llobet. "Finite-time Landauer principle beyond weak coupling". In: *Quantum* 7 (2023), p. 1161. ISSN: 2521-327X. DOI: 10.22331/q-2023-11-03-1161.

107 Yang Xiao, Dehua Liu, Jizhou He, Lin Zhuang, Wu-Ming Liu, L.-L Yan, and Jianhui Wang. "Thermodynamics and fluctuations in finite-time quantum heat engines under reservoir squeezing". In: *Phys. Rev. Res.* 5 (4 2023), p. 043185. DOI: 10.1103/PhysRevResearch.5.043185.

108 S Hamedani Raja, S Maniscalco, G S Paraoanu, J P Pekola, and N Lo Gullo. "Finite-time quantum Stirling heat engine". In: *New Journal of Physics* 23.3 (2021), p. 033034. ISSN: 1367-2630. DOI: 10.1088/1367-2630/abe9d7.

109 Jeanne Bourgeois, Gianmichele Blasi, Shishir Khandelwal, and Géraldine Haack. "Finite-Time Dynamics of an Entanglement Engine: Current, Fluctuations and Kinetic Uncertainty Relations". In: *Entropy* 26.6 (2024). ISSN: 1099-4300. DOI: 10.3390/e26060497.

110 Tan Van Vu and Keiji Saito. "Finite-Time Quantum Landauer Principle and Quantum Coherence". In: *Physical Review Letters* 128.1 (2022). ISSN: 1079-7114. DOI: 10.1103/physrevlett.128.010602.

111 Alberto Rolandi, Paolo Abiuso, and Martí Perarnau-Llobet. "Collective Advantages in Finite-Time Thermodynamics". In: *Physical Review Letters* 131.21 (2023). ISSN: 1079-7114. DOI: 10.1103/physrevlett.131.210401.

112 Paolo A. Erdman, Alberto Rolandi, Paolo Abiuso, Martí Perarnau-Llobet, and Frank Noé. "Pareto-optimal cycles for power, efficiency and fluctuations of quantum heat engines using reinforcement learning". In: *Phys. Rev. Res.* 5 (2 2023), p. L022017. DOI: 10.1103/PhysRevResearch.5.L022017.

113 Revathy B. S, Victor Mukherjee, Uma Divakaran, and Adolfo del Campo. "Universal finite-time thermodynamics of many-body quantum machines from Kibble-Zurek scaling". In: *Phys. Rev. Res.* 2 (4 2020), p. 043247. DOI: 10.1103/PhysRevResearch.2.043247.

114 P A Erdman, V Cavina, R Fazio, F Taddei, and V Giovannetti. "Maximum power and corresponding efficiency for two-level heat engines and refrigerators: optimality of fast cycles". In: *New Journal of Physics* 21.10 (2019), p. 103049. ISSN: 1367-2630. DOI: 10.1088/1367-2630/ab4dca.

115 Paolo Abiuso and Martí Perarnau-Llobet. "Optimal Cycles for Low-Dissipation Heat Engines". In: *Phys. Rev. Lett.* 124 (11 2020), p. 110606. DOI: 10.1103/PhysRevLett.124.110606.

116 Maria Popovic, Mark T. Mitchison, Aidan Strathearn, Brendon W. Lovett, John Goold, and Paul R. Eastham. "Quantum Heat Statistics with Time-Evolving Matrix Product Operators". In: *PRX Quantum* 2 (2 2021), p. 020338. DOI: 10.1103/PRXQuantum.2.020338.

117 Shishir Khandelwal, Nicolas Palazzo, Nicolas Brunner, and Géraldine Haack. "Critical heat current for operating an entanglement engine". In: *New Journal of Physics* 22.7 (2020), p. 073039. ISSN: 1367-2630. DOI: 10.1088/1367-2630/ab9983.

118 Ryszard Horodecki, Paweł Horodecki, Michał Horodecki, and Karol Horodecki. "Quantum entanglement". In: *Rev. Mod. Phys.* 81 (2 2009), pp. 865–942. DOI: 10.1103/RevModPhys.81.865.

119 Marco Cattaneo, Gian Luca Giorgi, Sabrina Maniscalco, and Roberta Zambrini. "Local versus global master equation with common and separate baths: superiority of the global approach in partial secular approximation". In: *New J. Phys.* 21.11 (2019), p. 113045.

120 Patrick P. Hofer, Martí Perarnau-Llobet, L. David M. Miranda, Géraldine Haack, Ralph Silva, Jonatan Bohr Brask, and Nicolas Brunner. "Markovian master equations for quantum thermal machines: local versus global approach". en. In: *New J. Phys.* 19.12 (2017). Publisher: IOP Publishing, p. 123037. ISSN: 1367-2630. DOI: 10.1088/1367-2630/aa964f.

121 Stefano Scali, Janet Anders, and Luis A. Correa. "Local master equations bypass the secular approximation". In: *Quantum* 5 (2021). arXiv:2009.11324 [cond-mat, physics:quant-ph], p. 451. ISSN: 2521-327X. DOI: 10.22331/q-2021-05-01-451.

122 Amikam Levy and Ronnie Kosloff. "The local approach to quantum transport may violate the second law of thermodynamics". In: *EPL (Europhysics Letters)* 107.2 (2014), p. 20004. ISSN: 1286-4854. DOI: 10.1209/0295-5075/107/20004.

123 J. Onam González, Luis A. Correa, Giorgio Nocerino, José P. Palao, Daniel Alonso, and Gerardo Adesso. "Testing the Validity of the 'Local' and 'Global' GKLS Master Equations on an Exactly Solvable Model". In: *Open Systems & Information Dynamics* 24.04 (2017), p. 1740010. DOI: 10.1142/S1230161217400108.

124 Gerardo Suarez. *Non Markovian Methods https://github.com/gsuarezr/NonMarkovianMethods.*